UNIVERSITÉ DE STRASBOURG

EDSC
Ecole Doctorale des
Sciences Chimiques

ÉCOLE DOCTORALE DES SCIENCES CHIMIQUES

Institut de chimie de Strasbourg – UMR 7177

THÈSE

présentée par

Wenjun Liu

soutenue le : **22 Janvier 2013**

pour obtenir le grade de

Docteur de l'Université de Strasbourg

Discipline / Spécialité : Chimie

Triterpénoïdes bactériens en C_{35} de série hopane: biosynthèse de la chaîne latérale

---

THÈSE dirigée par :
   M. Michel ROHMER   Professeur, Université de Strasbourg.

RAPPORTEURS :
   M. Erwan POUPON   Professeur, Université de Paris-Sud, Châtenay-Malabry.
   M. Stéphane VINCENT   Professeur, Facultés Universitaires Notre-Dame de la Paix, Namur.

MEMBRES DU JURY :
   M. Michel ROHMER   Professeur, Université de Strasbourg.
   M. Philippe SCHAEFFER   Directeur de recherche au CNRS, Université de Strasbourg.

MEMBRE INVITÉE:
   Mme. Anne BODLENNER   Maître de Conférences, Université de Strasbourg.

ACKNOWLEDGEMENTS

I am grateful to the following people:

To my director Prof. Michel Rohmer who made me a better scientist, thank you for all of the guidance and support during these years. I appreciate your generous sharing your deep knowledge in not only science but also humanities.

To the members of the committee, Prof. Poupon, Rohmer and Vincent and Dr. Schaeffer, thanks for the valuable comments.

To my master advisor Prof. Pei-Qiang Huang without whose help I would not have the opportunity to pursue my Ph. D study in France.

To my coworkers Drs. E. Takano, E. Kannenberg, T. Härtner, P. Schaeffer, H. Talbot and E. Sakr for the collaboration.

To Dr. Anne Bodlenner, thank you for the numerous discussions and valuable advices for my research work. I appreciate your encouragement and friendship which make me faithful.

To E. Motsch, thanks for GC/MS and MS analysis

To M. Lebreton and H. Nierengarten, thanks for (HR)MS measurements.

To the NMR service (L. Allouche, B. Vincent, J-D. Sauer and M. Coope), thanks for the NMR measurements.

To the rest lovely members in our lab: thanks Catherine G-B for the help on NMR; thanks Denis T. for all the biological questions; thanks Agata L., Anh-Thu N., Clément G., Fanny K., Jeanne T., Mathilde M. and Nader M. for making my life easier; thanks Huguette D., Magalie P., Myriam S., and Philippe C. for your support.

To my parents, my boyfriennd and all my dear friends, many thanks for your generous love and support!

Content

Hemisynthesis of adenosylhopane and of a deuteriated isotopomer

Incorporation of deuteriated adenosylhopane into bacteriohopanetetrol by a cell-free system from *Methylobacterium organophilum*

Attempts of identification of the origin of the terminal amino group of 35-aminobacteriohopanetriol in *Rhodopseudomonas palustris*

Abbreviations

Ac	Acetyl
AcOH	Acetic acid
Ade	Adenosyl
Ala	Alanine
APCI-LC/MS^n	Atmospheric pressure chemical ionization liquid chromatography/ion trap mass spectrometry
Asp	Aspartate
9-BBN	9-Borabicyclo[3.3.1]nonane
BHP	Bacteriohopanepolyol
BHT	Bacteriohopanetetrol
^{n}BuLi	^{n}Butyl lithium
Bn	Benzyl
Bz	Benzoyl
Cat.	Catalyst
CM	Cross metathesis
CoA	Coenzyme A
Cy	Cyclohexyl
DCC	*N,N'*-Dicyclohexylcarbodiimide
DCM	Dichloromethane
DMAPP	Dimethyl allyldiphosphate
DMSO	Dimethyl sulfoxide
EI	Electron ionization
ESI	Electrospray ionization
EtOH	Ethanol
FCC	Flash column chromatography
G I	Grubbs' catalyst 1st generation
G II	Grubbs' catalyst 2nd generation
GC	Gas chromatography
Gln	Glutamine
Glu	Glutamate
H II	Hoveyda-Grubbs catalyst 2nd generation
HPLC	High performance liquid chromatography

HRMS	High resolution mass spectrometry
IPP	Isopentenyl diphosphate
Me	Methyl
MeOH	Methanol
MEP	Metylerythritol phosphate
Mes	2,4,-Trimethylphenyl
MW	Microwave
NADH	Nicotinamide dinucleotide hydride
NADPH	Nicotinamide adenine dinucleotide phosphate
NMR	Nuclear magnetic resonance
OAT	Ornithine Aminotransferase
ORF	Open reading frames
P	Phosphate
PADA	Potassium azodicarboxylate
Ph	Phenyl
PLP	Pyridoxal phosphate
PMP	Pyridoxamine-5'-phosphate
PNP	Purine nucleoside phosphorylase
PP	Diphosphate
^{i}Pr	Isopropyl
Py.	Pyridine
R_f	Retention of solute
SAM	*S*-Adenosyl methionine
S_N1	Unimolecular nucleophilic substitution
TEA	Triethylamine
TFA	Trifluoroacetic acid
THF	Tetrahydrofuran
TLC	Thin layer chromatography
TMS	Trimethylsilyl

Résumé

Introduction

Les hopanoïdes sont des triterpénoïdes pentacycliques présents chez de nombreux procaryotes de groupes taxonomiques variés, notamment chez les méthanotrophes, certains méthylotrophes, les cyanobactéries, certaines bactéries fixatrices d'azote et les bactéries pourpres non-sulfureuses (Rohmer et al, 1984; Talbot et Farrimond, 2007). Les hopanoïdes sont également considérés comme des biomarqueurs des populations et des processus bactériens dans les environnements modernes et anciens (Rohmer *et al.*, 1979 ; Talbot et Farrimond, 2007). Les hopanoïdes sont les équivalents biologiques des stérols dans les membranes bactériennes (Ourisson et al, 1987;. Kannenberg et Poralla, 1999): ils modulent la fluidité des membranes phospholipidiques et permettent de renforcer la stabilité et l'imperméabilité de ces membranes afin de protéger les organismes de facteurs de stress externes comme la chaleur, le pH, la dessiccation, l'éthanol... (Poralla *et al.*, 1984; Poralla *et al*, 2000;. Joyeux et al, 2004; Welander *et al.*, 2009).

Les bactériohopanepolyols (BHPs) en C_{35} sont les principaux hopanoïdes trouvés chez les bactéries. Ces composés présentent une chaîne latérale polyhydroxylée en C_5 liée par une liaison carbone/carbone au groupement isopropyle du squelette hopane. Le bactériohopanetétrol (BHT) **6** et l'aminobactériohopanetriol **7** sont les composés majoritaires. Ils sont généralement accompagnés de diploptène **3** et de diploptérol **2**. Les hopanoïdes bactériens présentent, cependant, de nombreuses variations structurales, au niveau du squelette pentacyclique, du centre asymétrique en position C-17, C-22 ou C-34 et au niveau de la chaîne latérale (position et nature des groupes fonctionnels) (Rohmer, 1993; Talbot et Farrimond, 2007). La biochimie des hopanoïdes s'est révélée être très intéressante (Rohmer *et al.,* 1993; Duvold *et al.*, 1997b; Rohmer, 1999, 2008), puisqu'elle a permis la découverte d'une nouvelle voie de biosynthèse pour les unités isopréniques, la voie du méthylérythritol phosphate (MEP). Cette voie est présente dans la plupart des eubactéries et dans les chloroplastes de tous les organismes phototrophes. De plus, les travaux sur la biosynthèse des hopanoïdes ont permis de mettre en évidence de nouvelles enzymes impliquées dans la formation des hopanoïdes en C_{35}. Les expériences déjà effectuées et certains travaux en cours ont mis en évidence les informations suivantes.

- La chaîne latérale polyhydroxylée est dérivée du D-ribose lié par son carbone C-5 au squelette triterpénique (Flesch et Rohmer, 1988b; Neunlist *et al.*, 1988; Rohmer *et al.*, 1989)

- Le groupement méthyle terminal Z du squalène, correspondant au méthylène oléfinique du diploptène, est engagé dans la liaison avec le pentose.
- Le diploptène est le précurseur putatif de la partie triterpénique.
- L'adénosylhopane fréquemment rencontré chez les bactéries est un intermédiaire présumé (Neunlist *et al.* 1985b; Stampf, 1992 ; Rohmer, 1993).
- Le passage du squalène, du diploptène ou du bactériohopanetétrol s'accompagne d'une réaction de réduction. Cette réduction ne correspond pas à un transfert d'hydrure dérivé du NAD(P)H, mais s'accompagne du transfert d'un hydrogène échangeable (Toulouse, 2012).

A partir de ces données, un schéma biogénétique hypothétique a été proposé pour la biosynthèse des hopanoïdes bactériens en C_{35} (Rohmer, 1993). L'adénosylhopane **25** serait dérivé du couplage entre le diploptène **3** et le radical 5'-déoxyadénosyle catalysé par une enzyme à radical et à cluster Fe_4S_4 (Schéma 1, réaction I). Le clivage consécutif de l'adénine conduirait au ribosylhopane **23** (Schéma 1, réaction II), intermédiaire putatif qui serait considéré comme un précurseur commun possible pour le BHT **6** et le 35-aminobactériohopanetriol **7** (Rohmer, 1993). La réduction (Schéma 1, réaction III) ou l'amination réductrice (Schéma 1, réaction IV) du ribosylhopane mèneraient alors respectivement au BHT **6** ou au 35-aminobactériohopanetriol **7** (Rohmer, 1993).

Au cours de ce travail, nous nous sommes intéressés aux bactériohopanepolyols et plus particulièrement à leur biosynthèse. Un premier projet à été mené sur des souches mutantes de *Streptomyces coelicolor*. Il nous a permis d'une part de caractériser deux gènes impliqués dans la formation de la chaîne latérale chez cette bactérie, et d'autre part d'isoler le ribosylhopane. Dans un deuxième projet, nous avons décrit la synthèse de l'adénosylhopane et d'un isotopomère bisdeutérié. L'analogue marqué a par la suite été incorporé dans le BHT dans un troisième projet, et le suivi du marquage nous a permis de démontrer l'implication de l'adénosylhopane dans la biosynthèse des hopanoïdes en C_{35}. Enfin, dans un dernier projet, nous avons mené des études sur l'origine du groupement amino présent dans l'aminobactériohopanetriol.
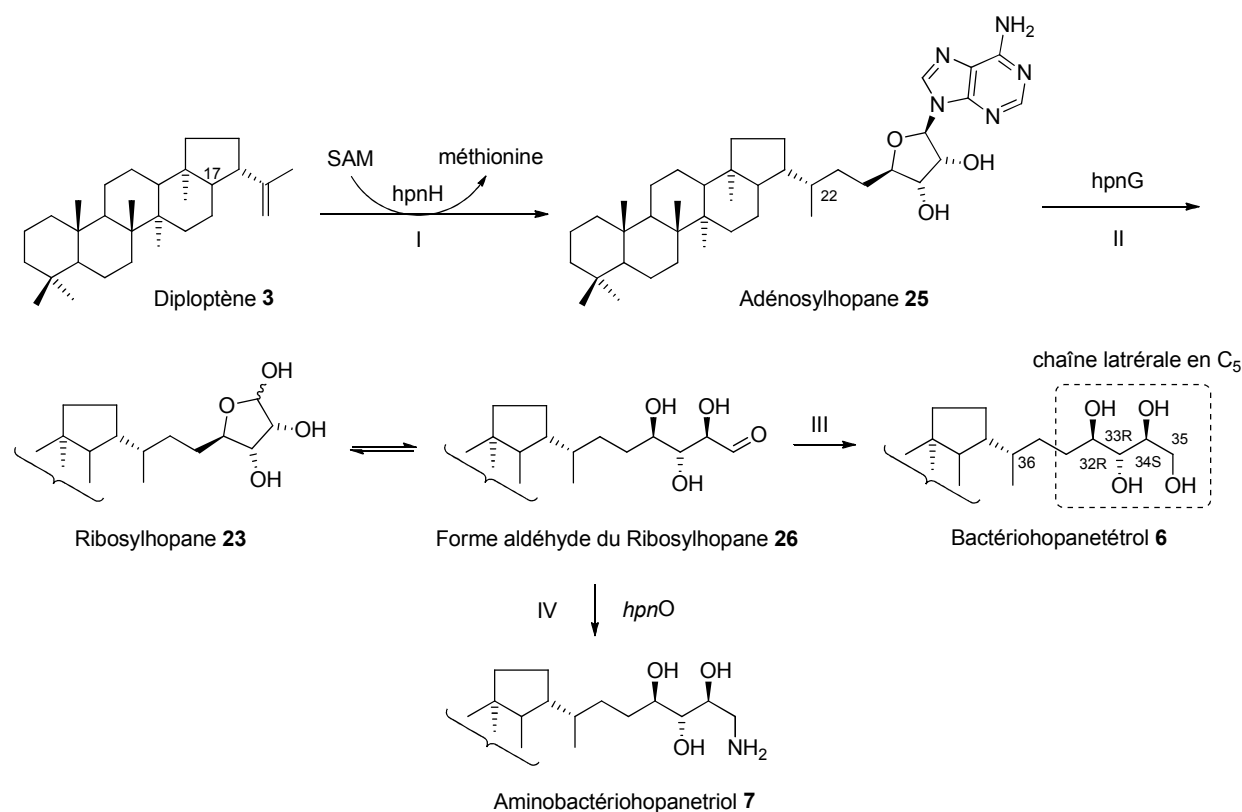
Schéma 1. Voie de biosynthèse hypothétique pour la biosynthèse des hopanoïdes en C_{35}. Les gènes *hpnH* et *hpnG* sont annotés chez *Methylobacterium extorquens* et *Rhodopseudomonas palustris* TIE-1, le gène *hpnO* chez *R. palustris*.

La biosynthèse des hopanoïdes chez *Streptomyces coelicolor* A3(2) : l'identification du ribosylhopane comme un intermédiaire (Chapitre I)

Les *Streptomyces* sont des eubactéries filamenteuses, aérobies et Gram positives. Elles appartiennent à la classe des actinomycètes et vivent dans les sols. Sur le plan de la génétique, *Streptomyces coelicolor* A3(2) est le représentant le mieux connu de ces bactéries qui produisent nombre d'antibiotiques utilisés en médecine humaine et vétérinaire. Le premier génome de *Streptomyces* entièrement séquencé est celui de *S.coelicolor* A3(2), publié à partir d'une bibliothèque ordonnée de cosmides (Bentley *et al.*, 2002). Un cluster de gènes (SCO6759-6771) a été détecté sur le cosmide SC6A5 annoté et a été supposé impliqué dans la biosynthèse des hopanoïdes (Poralla *et al.*, 2000). Parmi ces 13 cadres de lecture ouverts (en anglais *open reading frame*, ou ORF), le gène *orf14* (SCO6765) présente une similarité significative avec le gène *hpnG* (27,7% d'identité, 31,5% de similarité avec des écarts de

35%), ce dernier codant pour la protéine responsable du clivage de l'adénine à partir d'adénosylhopane chez *M. extorquens* et *R. palustris* TIE-1 (Bradley *et al*., 2010; Welander *et al*., 2012). Selon l'analyse bio-informatique, le gène *orf18* (SCO6769) code une enzyme appartenant à la famille des aminotransférases de classe III qui nécessitent la présence de phosphate de pyridoxal. Il est l'homologue du gène *hpnO* qui est indispensable pour la biosynthèse de l'aminobactériohopanetriol chez *R. palustris* TIE-1 (Welander *et al*., 2012) (Schéma 1, réaction IV). Dans ce projet, la production des hopanoïdes chez des mutants caractérisés par la délétion des gènes *orf14* ou *orf18* a été étudiée. La partie génétique de ce travail sur *S. coelicolor* A3(2) et la construction des mutants obtenus par insertion du gène de résistance à l'apramycine dans le gène dont on veut supprimer l'expression ont été effectuées par E. Kannenberg (Université de Tübingen et Athens, Université of Georgia), E. Takano. (Université de Groningen) et T. Härtner (Université de Tübingen). L'analyse des hopanoïdes a été réalisée en collaboration avec P. Schaeffer (Université de Strasbourg) et H. Talbot (Université de Newcastle).

Le type sauvage de *S. coelicolor* et les mutants avec une délétion des gènes *orf14* ou *orf18* ont été cultivés sur un milieu solide dans des boîtes de Petri emballées (Poralla *et al.*, 2000). Après extraction et purification (Neunlist *et al*., 1985;. Renoux et Rohmer, 1985), les hopanoïdes ont été identifiés par différentes techniques analytiques (GC, GC-MS, HPLC, APCI-MS^n et RMN).

Le type sauvage de *S. coelicolor* n'accumule que l'aminobactériohopanetriol **7** comme hopanoïde en C_{35}. Le phénotype au niveau des hopanoïdes des souches mutantes *Δorf14* et *Δorf18* a suggéré les fonctions de ces gènes mutés.

L'absence du gène *orf14* dans *S. coelicolor* induit l'accumulation du seul adénosylhopane **25** comme hopanoïde en C_{35}, ce qui indique que le couplage du diploptène **3** avec un groupe adénosyle est toujours possible, mais que la transformation de l'adénosylhopane en d'autres hopanoïdes en C_{35}, en particulier en aminobactériohopanetriol **7,** est bloquée. Ces résultats sont en accord avec la fonction postulée du gène *orf14*: le codage de l'enzyme de désadénylation pour produire le ribosylhopane **23** à partir d'adénosylhopane **25**. En outre, l'absence de quantités détectables d'adénosylhopane **25** chez le type sauvage de *S. Coelicolor* indique que dans cette souche l'adénosylhopane se comporte comme un intermédiaire, à renouvellement rapide subissant les modifications supplémentaires catalysées par la protéine codée par le gène *orf14*.

La délétion du gène *orf18* conduit à une disparition complète de l'aminobactériohopanetriol **7** et à la formation de petites quantités de BHT **6**. La biosynthèse

de l'aminobactériohopanetriol a été restaurée lorsque le gène silencieux a été réintroduit. A coté du BHT, des traces de ribosylhopane ont été détectées pour la première fois dans une bactérie. La structure de son triacétate a été confirmée par spectrométrie de masse et spectroscopie RMN et par comparaison avec un échantillon synthétique (Duvold et Rohmer, 1999). Cette découverte est une preuve solide confirmant le rôle du ribosylhopane comme intermédiaire dans la biosynthèse des hopanoïdes. En l'absence d'aminotransférase fonctionnelle dans le mutant *Δorf18*, la biosynthèse de l'aminobactériohopanetriol est bloquée. Ainsi, on peut supposer que le ribosylhopane, au lieu d'être converti par une aminotransférase en aminobactériohopanetriol, peut être réduit par une aldose réductase non spécifique au BHT, qui n'est normalement pas détectable dans le type sauvage de *S. coelicolor*. D'après sa séquence, la protéine codée par le gène *orf18* serait une aminotransférase appartenant à la famille des *N*-acétylornithine aminotransférases. Elle est donc censée agir sur un aldéhyde. Par conséquent, cette protéine codée par le gène *orf18* est supposée catalyser l'amination réductrice du ribosylhopane (sous sa forme aldéhyde et non sous sa forme hémicétal cyclique) en aminobactériohopanetriol. Cette conclusion est conforme à la voie de biosynthèse des hopanoïdes postulée (Schéma 1) et à la découverte récente du mutant *ΔhpnO* de *R. palustris* TIE-1, dans lequel le gène *hpnO* a été annoté comme une ornithine:oxo-acide aminotransférase putative (Welander *et al.*, 2012). Il est possible que ce gène soit impliqué dans la formation d'aminobactériohopanetriol. Il présente des homologies avec la *N*-acétylornithine aminotransférase (ArgD) qui agit uniquement sur un aldéhyde. Par conséquent, le ribosylhopane sous forme d'aldéhyde libre **26** (Schéma 1) semble être le substrat approprié pour une telle aminotransférase codée par le gène *hpnO* (Rohmer *et al.*, 1993; Welander *et al.*, 2012).

Hémisynthèse d'adénosylhopane et d'un isotopomère bisdeutérié (Chapitre II)

L'élucidation de la biosynthèse des BHPs nécessite la caractérisation des gènes et la purification des enzymes impliquées. D'importantes quantités de hopanoïdes sont nécessaires pour pouvoir mener à bien les essais enzymatiques. Les hopanoïdes naturels sont cependant très difficiles à isoler et généralement obtenus en quantités infimes à partir de sources natuelles. C'est pourquoi la synthèse chimique apparaît comme un moyen approprié pour

produire ces molécules. De plus, le recours à la synthèse chimique est nécessaire afin d'obtenir des isotopomères marqués, qui représentent l'outil indispensable pour tester les systèmes enzymatiques impliqués dans une biosynthèse.

Nous avons développé une méthode de synthèse permettant d'obtenir pour la première fois l'adénosylhopane déprotégé en 14 étapes, avec tous les centres asymétriques correspondant à ceux du composé naturel (Schéma 2). Cette méthode consiste en une élongation de la chaîne latérale du diploptène **3**, facilement accessible à partir de l'hydroxyhopanone **56** extraite de la résine de Dammar. La stratégie la plus évidente serait d'effectuer un couplage entre un dérivé hopanique en C_{30} et un dérivé de l'adénosine. Cependant, d'après la littérature, des réactions de couplage de type Wittig (Stampf, 1992) ou des réactions assistées impliquant un hopanyllithien (Pan *et al.*, 2007) n'ont pas permis d'obtenir le composé désiré avec des rendements satisfaisants. Nous avons donc choisi de synthétiser l'adénosylhopane via une réaction de métathèse croisée, car cette méthode, en plus de son efficacité remarquable, présente une grande tolérance envers les groupes fonctionnels et les structures volumineuses.

Les réactions de métathèse croisée ont été testées avec plusieurs catalyseurs (Schéma 3) dans diverses conditions. En effet, en présence d'un excès de homohop-30-ène **55** (Stampf, 1992; Duvold et Rohmer, 1999) par rapport à la 6-*N*-benzoyl-5'-désoxy-5'-méthylène-2',3'-*O*-isopropylidène adénosine **62** (Ranganathan *et al.*, 1974; McLaughlin *et al.*, 1985; Eppacher *et al.*, 2004) le rendement de la réaction s'est nettement amélioré. Le meilleur résultat a été obtenu avec le catalyseur de deuxième génération de Hoveyda-Grubbs H II, sous irradiation micro-ondes. Nous avons ainsi obtenu l'adénosylhopène **38** et le dimère du dérivé d'adénosine **64** avec des rendements respectifs de 59% et 40%. La dimérisation du homohop-30-ène **55** n'a pas été observée, probablement à cause d'un fort encombrement stérique dû à la position α de la chaîne latérale du squelette hopane et à l'encombrement stérique introduit par les cycle D et E.
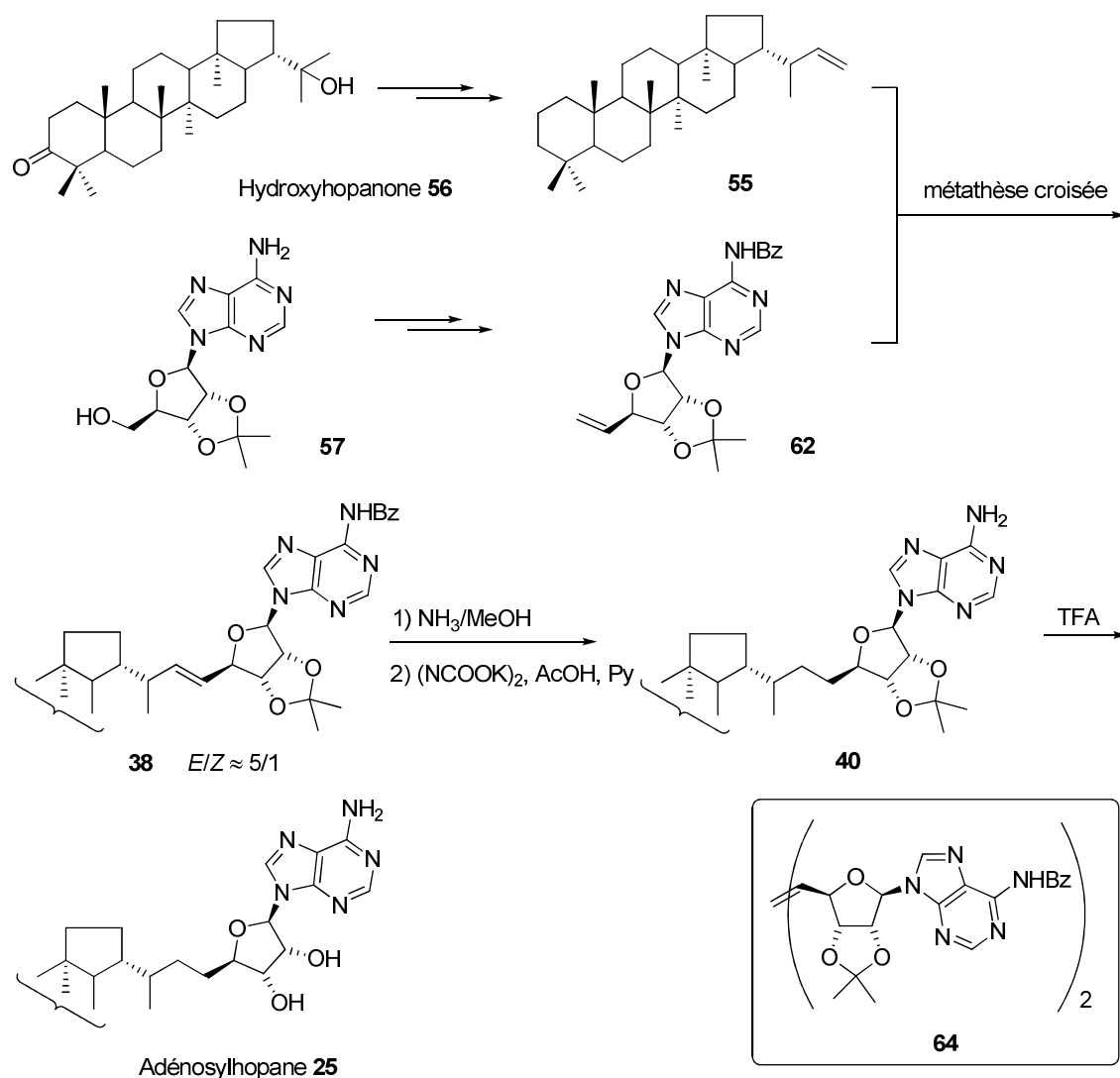
Schéma 2. Hémisynthèse de l'adénosylhopane **25**.
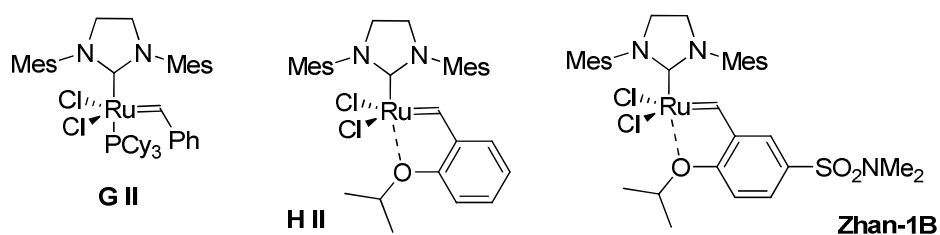
Schéma 3. Catalyseurs pour la métathèse croisée

L'hydrogénation catalytique [Pd/C, PtO$_2$, Rh(PPh$_3$)$_3$Cl, catalyseur de Crabtree] de la double liaison carbone/carbone de l'adénosylhopène **38** a été obtenue avec des rendements décevants, et cela même sous pression. Ce problème a été résolu par l'utilisation de diimide, une petite molécule ayant facilement accès à la double liaison. Nous avons donc obtenu le

produit désiré **40** avec un rendement de 73%. La déprotection du groupement acétonide dans l'acide trifluoroacétique aqueux a fourni l'adénosylhopane libre **25** (Schéma 2).

Pour la synthèse de l'analogue bisdeutérié nécessaire pour les tests biologiques, nous avons essentiellement suivi la même stratégie que celle utilisée pour l'adénosylhopane **25** (Schéma 4). L'acide acétique deutérié (abondance isotopique 98%) a été utilisé en tant que source de deutérium pour engendrer le diimide bisdeutérié utilisé lors de l'étape de réduction. Malgré les précautions prises pour éviter la contamination par l'eau, l'abondance isotopique $^2H/^1H$ de l'adénosylhopane **25** était modérée: [30,31-$^2H_2$] adénosylhopane **25-D** avec une abondance isotopique de 60% en C-30 et C-31, [30-^2H]- et [31-^2H]adénosylhopane **25-D** avec une abondance isotopique de 32% en C-30 ou C-31. Ces résultats sont probablement dus à l'utilisation de CH_3CO_2D (abundance isotopique 98%) en large excès (60 éq.) qui est une source de proton et à un effet cinétique primaire en faveur de l'incorporation des protons minoritaires à la place des deutérium majoritaires. L'excès de CH_3CO_2D est cependant nécessaire pour obtenir une réaction complète. Le rapport de marquage serait probablement amélioré en utilisant un CH_3CO_2D avec un enrichissement en deutérium supérieur à celui du produit utilisé.
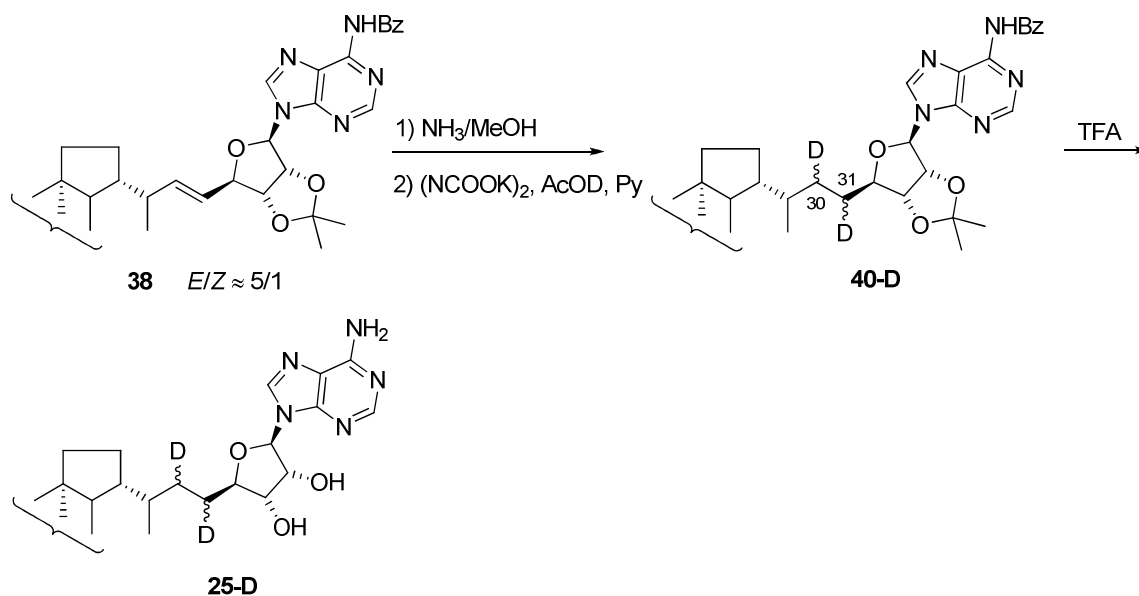
Schéma 4. Synthèse de l'adénosylhopane deutérié **25-D**.

Afin de vérifier la structure du composé, l'adénosylhopane **25** a été acétylé. Les spectres RMN du dérivé acétylé ont été comparés avec ceux de l'adénosylhopane naturel acétylé.

Toutes les données analytiques se sont révélées être conformes à celles décrites dans la littérature. La structure de l'adénosylhopane bisdeuterié **25-D** a été validée en comparant ses spectres ^{1}H-RMN et ^{13}C-RMN des son acétates (di- et triacétates) avec ceux des acétates du composé **25** en abondance naturelle (Neunlist et Rohmer, 1985b; Neunlist *et al.*, 1988).

Incorporation de [²H]adénosylhopane dans le bactériohopanetétrol par un système acellulaire de *Methylobacterium organophilum* (Chapitre III)

L'adénosylhopane a été proposé comme précurseur putatif des hopanoïdes bactériens en C_{35} dans notre schéma biogénétique initial (Schéma 1). Une recherche dans le génome de *Methylobacterium extorquens* a suggéré que l'adénosylhopane serait dérivé du couplage entre le diploptène **3** et un radical 5'-déoxyadénosyl produit par une enzyme à radical SAM codée par le gène *hpnH* (Schéma 1, réaction I) (Bradley *et al.*, 2010). Ces auteurs ont supposé que pendant la biosynthèse, l'adénosylhopane conduirait à l'adénine et au ribosylhopane phorphorylé, en raison de l'accumulation d'adénosylhopane et de la production bloquée de BHT dans le mutant *ΔhpnG* de *M. extorquens* (Schéma 5). L'hypothèse d'un dérivé du ribosylhopane comme d'intermédiaire putatif a été renforcée par la détection de ribosylhopane dans un mutant de *Streptomyces coelicolor*. Par ailleurs, nous avons démontré que le ribosylhopane est réduit en BHT par un système acellulaire brut de *M. organophilum*. Une réductase nécessitant le NAD(P)H comme cofacteur (Charon, 2000; Bodlenner, travaux non publiés) serait impliquée dans la transformation ultérieure du ribosylhopane en BHT de *Methylobacterium* spp. (Schéma 5). En outre, la forme aldéhyde du ribosylhopane est en équilibre avec deux autres anomères furanoses (35α- et 35β-ribosylhopane) et est probablement le substrat approprié pour la réductase inconnue. Bien que les gènes *hpnG* et *hpnH* aient été caractérisés dans *M. extorquens* et que l'adénosylhopane ait été suggéré comme intermédiaire essentiel dans la biosynthèse de hopanoïdes fonctionnalisés, aucune preuve moléculaire directe n'a permis de prouver que l'adénosylhopane serait converti en BHPs (par exemple en BHT). Par conséquent, il serait intéressant d'incorporer de l'adénosylhopane deutérié dans les hopanoïdes en C_{35} dans un système acellulaire brut.
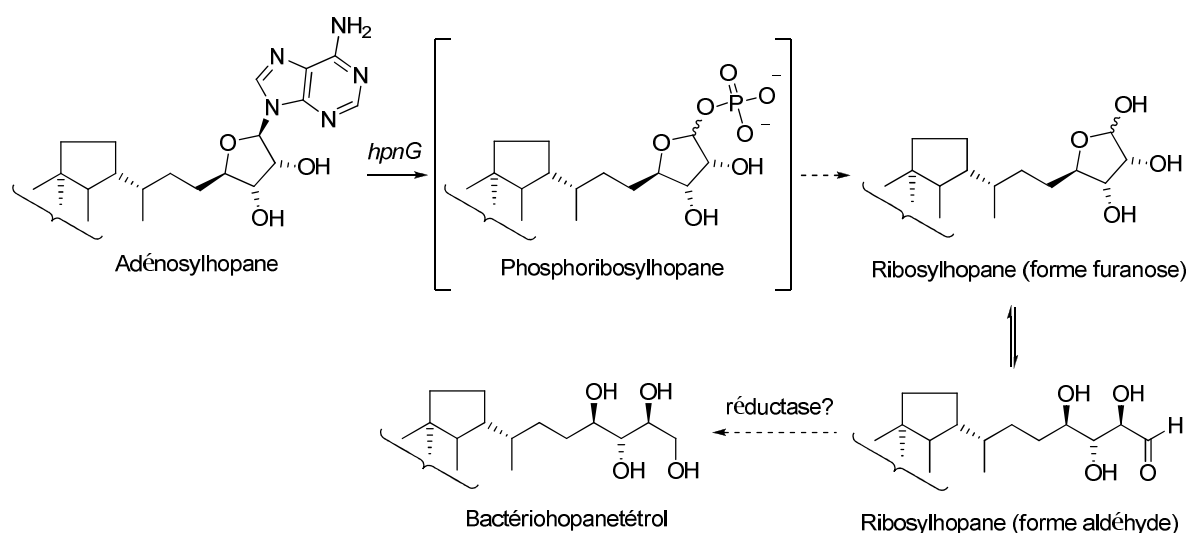
Schéma 5. Schéma biogénétique présumé pour la biosynthèse des chaînes latérales des hopanoïdes bactériens en C_{35} chez *Methylobacterium* spp. (Bradley *et al.*, 2010). Les flèches pleines indiquent les étapes pour lesquelles des données génétiques ont été obtenues. Les flèches en pointillées sont utilisées pour les réactions hypothétiques.

Methylobacterium organophilum DSM 760 a été choisi comme microorganisme modèle, car il est facile à cultiver et produit du BHT et d'autres hopanoïdes complexes dérivés du BHT (éther et glycoside de BHT) en quantités suffisantes dans un temps relativement court. Aucun cofacteur n'est utilisé pour hydrolyser l'adénosine, mais du phosphate inorganique serait nécessaire au cas où une purine nucléoside phosphorylase serait exigée. Le système acellulaire contenant les enzymes a été incubé avec NADPH et une solution d'adénosylhopane dans THF.

Le BHT acétylé a été analysé par GC/MS pour mesurer l'abondance isotopique des fragments contenant la chaîne latérale. L'intensité des signaux M+2*/z* des fragments de BHT acétylé contenant la chaîne latérale a augmenté, ce qui prouve que l'acétate de BHT est marqué. Cela indique également que le marquage au ^{2}H est uniquement présent sur la chaîne latérale en C_5. La contribution des adénosylhopanes mono- et bisdeutérié au BHT marqué est cohérente avec leur composition originale de deutérium (d_2 60%, d_1 32%). Afin de prouver que la conversion d'adénosylhopane en BHT est enzymatique, le [^{2}H]adénosylhopane a été incubé avec des extraits cellulaires inactivés bouillis. Aucun marquage au deutérium n'a été détecté dans le BHT.

Bien que ni le ribosylhopane, ni le phosphoribosylhopane n'aient été isolés comme intermédiaires présumés, il ne fait aucun doute que l'adénosylhopane est l'un des précurseurs de la biosynthèse du BHT chez *M. organophilum*. Récemment, la biosynthèse de la chaîne

latérale des hopanoïdes a été partiellement révélée chez *Rhodopseudomonas palustris* TIE-1 (Welander *et al.*, 2012). De plus, le gène *hpnH* a été caractérisé pour la biosynthèse d'adénosylhopane de la même manière que chez *M. extorquens*. Cependant, le gène *hpnG* était défini comme étant une hydrolase de nucléotides conduisant ainsi directement au ribosylhopane à partir d'adénosylhopane. Ce désaccord ne met pas en doute le rôle de l'adénosylhopane comme premier intermédiaire dans la biosynthèse de la chaîne latérale des hopanoïdes, mais il requiert pour être levé l'identification du gène *hpnG* et la purification de la protéine correspondante (travaux actuellement en cours dans notre laboratoire).

Tentative d'identification de l'origine du groupe amino terminal de l'aminobactériohopanetriol (Chapitre IV)

Le gène *hpnO* a été annoté chez *R. palustris* TIE-1 comme une ornithine:oxo-acide aminotransférase putative et impliquée dans la formation de l'aminobactériohopanetriol (Schéma 1, réaction **IV**). Sa délétion induit l'absence de ce hopanoïde. Vingt-huit autres bactéries possédant un gène homologue de ce gène *hpnO* contiennent également des copies du gène *shc* de la squalène/hopène cyclase, et certaines d'entre elles sont capables de produire le 35-aminobactériohopanetriol (Welander *et al.*, 2012). Par exemple, le gène SCO6769 chez *S. Coelicolor*, un autre producteur d'aminobactériohopanetriol, est supposé coder pour une aminotransférase appartenant à la famille des *N*-acétylornithine aminotransférases, dont tous les membres agissent sur des acides aminés basiques. Le test enzymatique de cette aminotransférase nécessite l'identification du donneur du groupement amino. Plusieurs candidats (aspartate, glutamate, glutamine, ornithine et alanine) sont possibles et ont été testés chez le type sauvage de *R. palustris* qui ne produit que de l'aminobactériohopantriol comme hopanoïde en C_{35}.

L'incorporation *in vitro* des acides aminés précédents marqués au ^{15}N a donné des résultats positifs quel que soit l'amino acide testé: le triacetate du [^{15}N]aminobactériohopanetriol a été détecté par spectrométrie de masse dans tous les cas. Cela est probablement dû à un métabolisme rapide des acides aminés marqués au ^{15}N et au transfert du groupement amino marqué vers le bon donneur, ou à une aminotransférase peu sélective.

Afin de tenter d'éclaircir ce point, des expériences d'incorporation de ribosylhopane et

d'acides aminés marqués au ^{15}N dans l'aminobactériohopanetriol ont été tentées avec un système acellulaire de *R. palustris*. Dans ces conditions, la biosynthèse des acides aminés serait largement bloquée, ce qui entraînerait moins d'interférences lors de l'expérience. D'après l'analyse de l'aminobactériohopanetriol acétylé par SM, aucun marquage n'a été détecté. Cela indique que soit la protéine n'est pas activée, soit que le taux de conversion du ribosylhopane en aminobactériohopanetriol est trop faible pour permettre une détection de l'enrichissement isotopique de l'aminobactériohopanetriol par spectrométrie de masse. L'expression du(des) gène(s) et la purification de la protéine correspondant sont nécessaires afin de poursuivre ces investigations.

General introduction

1. Hopanoids are spread in sediments, eukaryotes and prokaryotes

Hopanoids are pentacyclic triterpenes of the hopane series that represent the most abundant family of complex organic substances on Earth (Ourisson *et al.*, 1987). They are widespread in some eukaryotes, in many prokaryotes as well as in the organic matter of sediments.

Eukaryotic hopanoids can be divided into two types. Those with an oxygenated function at C-3 (*e.g.* 3-hydroxy and 3-oxohopanoids) are derived from the cyclization of oxidosqualene. They have been occasionally discovered in scattered taxa of higher plants. For instance, hydroxyhopanone, the first known hopanoid, was isolated from the dammar resin obtained from *Hopea* species. To date, it is still the most easily accessible starting material for hopanoid hemisynthesis (Mills and Werner, 1955). Other hopanoids produced by eukaryotes are known as 3-deoxyhopanoids (*e.g.* diplopterol **2**, Fig. 2). They derive from squalene cyclization and are distributed in a few species of ferns, mosses, lichens and fungi (Ourisson *et al.*, 1987 and references cited therein) (Fig. 1). Hopanoids in eukaryotes remain, however, rare and few, and constitute only one of the many minor families of plant triterpenes. Therefore, any deep mining for the biochemistry of eukaryotic hopanoids is denied due to the data paucity.

Since the 1970's, the presence of hopanoids has been gradually reported from crude oils and the organic matter of all sediments: marine or terrestrial, young or old (from soils or muds only a few years old to shales at least 1.5×10^9 yrs old), rich or poor in organic matter (in crude oils or coals, in oil shales, in dry shales, in peats, in limestones, *etc.*). The hopanoids found in geological sediments are called geohopanoids. Their total amount was estimated on the order of 10^{12} tons, which happens to be the order of magnitude estimated for the total mass of organic carbon in all presently living organisms (Ourisson and Albrecht, 1992)! So far, more than 200 individual structures of geohopanoids have been fully identified. Due to their saturated polycyclic structures that are resistant to biodegradation and to diagenesis, the rigid backbone was preserved with only small structural changes (Fig. 1).

(A) Typical structures of eukaryotic hopanoids

Hydroxyhopanone
isolated from dammar resin

Zeorine
isolated from lichens

Diploptene
isolated from ferns
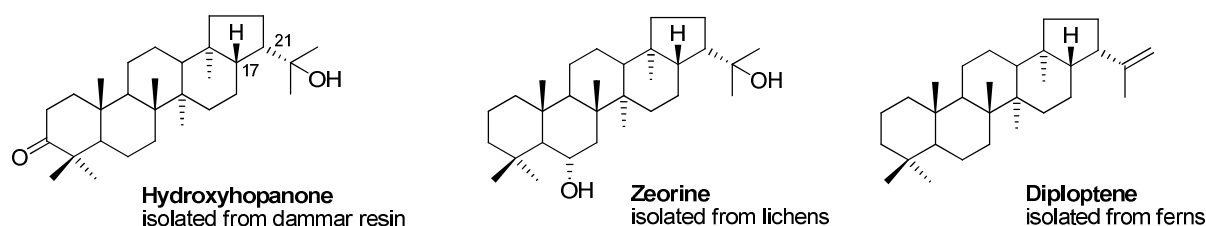
(B) Typical structures of geohopanoids
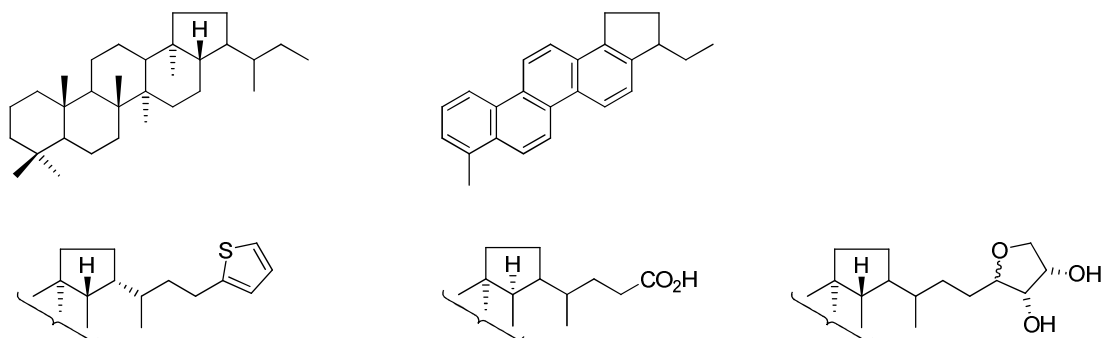
Fig. 1. Typical hopanoids found in eukaryotes (A) and sediments (B).

The ubiquitous presence and the huge amounts of geohopanoids, together with their extremely varied structures, make them very useful geochemical markers and, more importantly, the attractive "molecular fossils" of bacteria. This argument was supported, on the one hand, by the fact that diploptene **3** was detected in the early 1970's in a few prokaryotes (Gelpi *et al.*, 1970; Bird *et al.*, 1971; De Rosa *et al.*, 1971). It was then consequently interpreted as the precursor of some of the C_{30} or smaller geohopanoids (Bird *et al.*, 1971). On the other hand, isolation of the highly amphiphilic bacteriohopanetetrol **6** (BHT) from *Acetobacter xylinum* shed light on the origin of complex geohopanoids containing up to 35 carbons (Förster *et al.*, 1973; Haigh *et al.*, 1973). However, BHT was not proven as a precursor of geohopanoids until its correct structure was identified as a C_{35} bacteriohopanoid that possesses an additional linear polyhydroxylated C_5 side chain linked to the C-30 carbon atom of the hopane side-chain (Rohmer and Ourisson, 1976b). To date, numerous diverse hopanoid structures have been elucidated from a wide range of bacteria from different taxonomic groups. Moreover, the transformation of these bacterial hopanoids into their geological analogues is accomplished by mostly well known maturation reactions taking place in sediments (Ourisson *et al.*, 1979; Bisseret and Rohmer, 1993; Schaeffer *et al.*, 2008). According to these results, hopanoids derived from bacteria are widely considered as the precursor of the geohopanoids (Ourisson *et al.*, 1979).

2. Bacteriohopanoids present huge structural diversity from a wide range of bacteria

Hopanoids produced by bacteria present an impressive structural diversity (Fig. 2). The most readily detected hopanoids, diplopterol **2** and diploptene **3** with the usual C_{30} skeleton, are present, at least in trace amount, in all hopanoid synthesizing bacteria (Rohmer *et al.*, 1984). Tetrahymanol **5** (Fig. 2) derivatives with the quasi-hopanoid gammacerane skeleton are characteristic of *Rhodopseudomonas palustris* and the related *Bradyrhizobium* spp. (Bravo *et al.*, 2001). The majority of bacterial triterpenoids are the C_{35} bacteriohopanepolyols (BHPs), called here bacteriohopanoids, that bear an additional C_5 side chain linked by a carbon/carbon bond to the isopropyl group of the hopane skeleton.

Structures of BHPs differ in modifications of the pentacyclic ring system and also in the number, position and nature of functional groups of the side chains (Rohmer, 1993; Talbot and Farrimond, 2007). The most commonly occurring side chain structures contain three hydroxyl groups at C-32, C-33 and C-34 positions with another hydroxyl (bacteriohopanetetrol, BHT **6**) or amino group at C-35 (aminobacteriohopanetriol **7**). These two compounds represent the most common C_{35} bacteriohopanoids, and are usually found in a diverse suite of organisms (Ourisson *et al.*, 1987; Rohmer, 1993). The structural variations of bacteriohopanoids and their source microorganisms are listed below (Fig. 2 and table 1):

- Methylation at C-2, C-3, C-12 or C-31 and presence of double bonds at C-6 and/or C-11.

Presence of a methyl group at C-2β on ring A was first found in the BHPs from the cyanobacterium *Nostoc muscorum* and in diplopterol from *Methylobacterium organophilum* (Bisseret *et al.*, 1985). In the latter bacterium, it was even accompanied by trace amounts of 2α-methyldiplopterol (Stampf *et al.*, 1991). 2β-Methyldiplopterol was later found in all *Methylobacterium* spp. (Knani *et al.*, 1994) and also in *Bradyrhizobium japonicum* with the accompanition of 2β-methyltetrahymanol (Bravo *et al.*, 2001). 2β-MethylBHT has been discovered in trace amounts in *Methylobacterium organophilum* and is considered as characteristic feature of cyanobacteria (Zhao *et al.*, 1996; Summons *et al.*, 1999). A tentative structural assignment for 2β-methyladenosylhopane according to an APCI-LC/MS^n spectrum, was reported from *Bradyrhizobium japonicum* (Talbot *et al.*, 2007a).

Methylation at C-3β positions occurs in the BHPs in all acetic acid bacteria (Rohmer and Ourisson, 1976a; Zundel and Rohmer, 1985a; Peiseler and Rohmer, 1992) and also in most

Type I methanotrophs (Neunlist and Rohmer, 1985c; Cvejic *et al.*, 2000a). In acetic acid bacteria, *e.g. Acetobacter aceti* ssp. *xylinum* (Rohmer and Ourisson, 1986) and *Acetobacter europaeus* (Simonin *et al.*, 1994), this feature is usually accompanied by unsaturation of the ring system at C-6 and/or C-11.

Complex bacteriohopanoids possessing an additional methyl group at C-31 were reported from *Acetobacter europaeus* (Simonin *et al.*, 1994). The unsual 12α-Methyl BHT has been identified from the marine sponge *Plakortis simplex* (Costantino *et al.*, 2000).

- The presence of hydroxyl group(s) at C-30 and/or C-31 of the side chain.

Hopanoids **8** and **9** with five functional groups, containing an additional hydroxyl group at C-30 or C-31, were reported in cyanobacteria (Bisseret *et al.*, 1985; Zhao *et al.*, 1996) and methanotrophic bacteria (Neunlist and Rohmer, 1985c; Cvejic *et al.*, 2000a; Talbot *et al.*, 2001). A unique hexafunctionalized side chain structure **10**, containing five hydroxyl groups and a terminal amino group, is only present in Type I methanotrophs (Neunlist and Rohmer, 1985a; Cvejic *et al.*, 2000a; Talbot *et al.*, 2001).

- Addition of functional moieties to the terminal functional group of C_{35} bacteriohopanoids on the side chain.

Bacteriohopanoids bearing an aminohexose (*e.g.* **16**), *N*-acylaminohexoses (*e.g.* **17**) or a hexosuronic acid (*e.g.* **15**) linked to the C-35 hydroxy group of BHT **6** via a glycosidic bond were discovered in the thermoacidophile *Alicyclobacillus acidocaldarius* (Langworthy *et al.*, 1976) and the purple non-sulfur bacterium *Rhodospirillum rubrum* (Llopiz *et al.*, 1992).

A carbapseudopentose **18** linked to the terminal hydroxyl group of BHT via an ether bond is frequently present in numerous bacteria (Renoux and Rohmer, 1985; Flesch and Rohmer, 1988b; Neunlist *et al.*, 1988; Flesch and Rohmer, 1989; Knani *et al.*, 1994; Simonin *et al.*, 1994; Vilcheze *et al.*, 1994; Herrmann *et al.*, 1996; Cvejic *et al.*, 2000b; Talbot *et al.*, 2003b; Joyeux *et al.*, 2004; Talbot *et al.*, 2007a). Production of the guanidine substituted BHT cyclitol ether **19** is, however, restricted to *Methylobacterium* spp. (Renoux and Rohmer, 1985; Knani *et al.*, 1994). Tentative assignment of new structures, solely based on APCI-LC/MS[n] of the aceylated derivatives, was reported by Talbot *et al.* from cyanobacteria from sedimentary samples (*e.g.* BHT ether **20** possessing a carbapseudopentose moiety with a hydroxy group at C-2' instead of an amino group) (Talbot and Farrimond, 2007).

Other functional groups linked to BHT or aminobacteriohopanetriol include carbamoyl groups to C-35 and/or C-34 hydroxyl groups of BHT (*e.g.* **21** and **22**) (Renoux and Rohmer,

1985; Neunlist *et al.*, 1988), amino-acids (*e.g.* **13** and **14**) (Neunlist *et al.*, 1985) or fatty acids (*e.g.* **11** and **12**) (Seemann *et al.*, 1999) to the terminal amino group of aminobacteriohopanetriol **7** via an amide bond.

- Side-chain modification of C_{35} bacteriohopanoids with 5'-deoxy adenosyl moiety (*e.g.* **25**) linked to the hopane skeleton via carbon/carbon bond at C-30 was reported in *Rhodopseudomonas acidophila* (Neunlist and Rohmer, 1985b; Flesch and Rohmer, 1988b; Neunlist *et al.*, 1988; Talbot *et al.*, 2007a). Another unique hopanoid side-chain structure **24** containing a ribonolactone moiety was found in *Nitrosomonas europaea* (Seemann *et al.*, 1999).

- Presence of the two diastereoisomers at C-34 in BHTs has been only observed in the *Acetobacter* spp. (Peiseler and Rohmer, 1992) or at C-22 in the saturated BHTs of the *Acetobacter* spp. (Rohmer and Ourisson, 1976b, 1986) and in adenosylhopane **25** of *Rhodopseudomonas acidophila* (Neunlist *et al.*, 1988). Moreover, 32,35-anhydro-BHT **67** has not only been found as a geohopanoid, but is also produced by the sponge *P. simplex* (Costantino *et al.*, 2012).

- The unexpected discovery of 17α-BHT in a few Gram-positive bacteria such as *Frankia* spp. and related species (Rosa-Putra *et al.*, 2001).

Table. 1. Examples of source microorganisms of functionalized bacteriohopanoids.

		BHT 6	2-Me BHT	3-Me BHT	8 and 2-Me 8	7	9 & 3-Me 9	10 & 3-Me 10	11 & 12	13 & 14	18	Derivatives of 18 31-Me 18	3-Me 18	2-Me 18	19	20	16	17	21 & 22	15	25	2-Me 25	24
Methanotrophs	Type I[4,15,18,31,35,38,39]	√				√	√	√			√												
	Type II[16,35,38]	√				√	√																
	Methylocella palustris[35] (Type II)	√				√																√	
	Methylacidiphilum spp.[35] (*Verrucomicrobia*)					√	√																
Cyanobacteria[1,8,23,28,30,32,37]		√	√		√									√		√							
Purple non-sulfur bacteria[6,10,13,14,17,19,23,33,38]		√				√				√	√								√	√	√		
Nitromonas europaea[27,33]						√			√												√		√
Nitrogen-fixing bacteria	*Beijerinckia* spp.[36]	√				√																	
	Frankia spp.[26]	√																					
	Bradyrhizobium japonium[3,33]	√				√															√	√	
	Azotobacter vinelandii[36]										√												
Methylobacterium[1,6,11,22,29,33,40]		√	√								√				√			√					

Acetic acid bacteria[20,24,25,28,34,40]	√		√								√	√	√										
Burkholderia spp.[5,33]	√										√						√						
Alicyclobacillus acidocaldarius[12,21,33]	√																						
Frateuria aurantia[9]	√										√												
Zymomonas mobilis[7,8]	√										√						√						
Desulfovibrio[2]	√				√	√																	

[1]Bisseret *et al.* (1985); [2]Blumenberg *et al.* (2006); [3]Bravo *et al.* (2001); [4]Cvejic *et al.* (2000a); [5]Cvejic *et al.* (2000b); [6]Flesch and Rohmer (1988); [7]Flesch and Rohmer (1989); [8]Herrmann *et al.* (1996); [9]Joyeux *et al.* (2004); [10]Kleemann *et al.* (1990); [11]Knani *et al.* (1994); [12]Langworthy and Mayberry; (1976); [13]Llopiz *et al.* (1992); [14]Neunlist *et al.* (1985); [15]Neunlist and Rohmer (1985c); [16]Neunlist and Rohmer (1985a); [17]Neunlist and Rohmer (1985b); [18]Neunlist and Rohmer (1985c); [19]Neunlist *et al.* (1988); [20]Peiseler and Rohmer (1992); [21]Poralla *et al.* (1980); [22]Renoux and Rohmer (1985) ; [23]Rohmer *et al.* (1984); [24]Rohmer and Ourisson (1976b) ; [25]Rohmer and Ourisson (1986); [26]Rosa-Putra *et al.* (2001); [27]Seemann *et al.* (1999); [28]Simonin *et al.* (1994); [29]Stampf *et al.* (1991); [30]Summons *et al.* (1999); [31]Talbot *et al.* (2001); [32]Talbot *et al.* (2003); [33]Talbot *et al.* (2007a); [34]Talbot *et al.* (2007b); [35]van Winden *et al.* (2012); [36]Vilcheze *et al.* (1994); [37]Zhao *et al.* (1996); [38]Zhou *et al.* (1991); [39]Zundel and Rohmer (1985a); [40]Zundel and Rohmer (1985b)
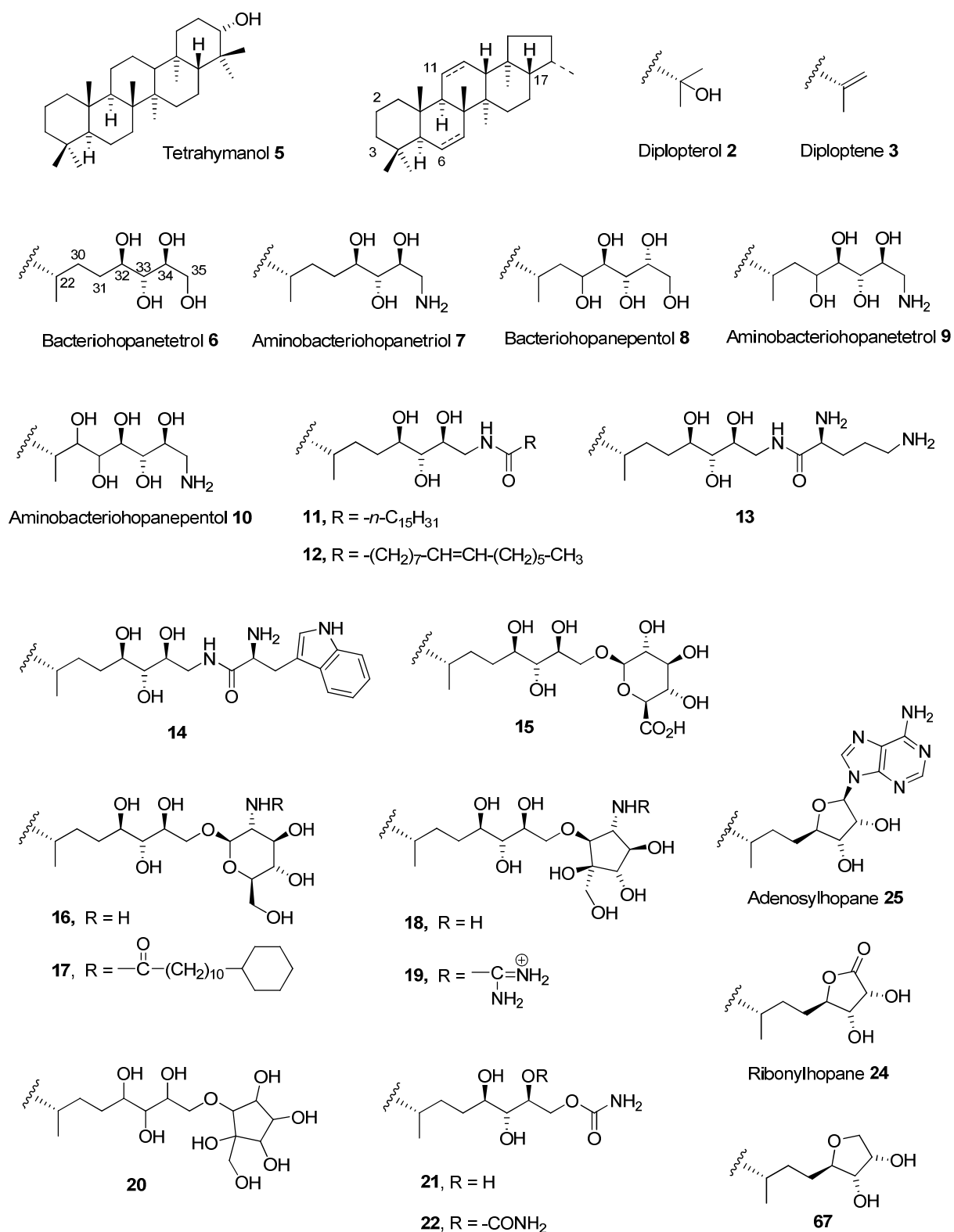
Fig. 2. Examples of triterpenes of the hopane series produced by bacteria.

Bacteriohopanoids are characterized by a huge structural diversity, a high polarity and a

strong amphiphilic character. Therefore, no general method has been developed so far for the screening of intact hopanoids. Furthermore, isolation of the BHPs, which are highly functionalized and amphiphilic, proved difficult, because they can hardly dissolve in most of the usual solvents. The structure elucidation for intact hopanoids is hence generally performed on their peracetylated derivatives, which allow the purification by chromatographic methods and the detection in the resulting fractions by the fingerprints of methyl groups of hopane skeleton and by the acetyl groups observed on ^{1}H-NMR spectra. The widely used method for detection of bacteriohopanoids was developed by Rohmer: the crude extracts were treated by periodic acid (H_5IO_6) to cleave the polyhydroxylated side chain, followed by sodium borohydride ($NaBH_4$) to reduce the resulting aldehydes to a mixture of primary alcohols which were then acetylated for the convenient purification process and the easy analysis by GC-MS (Rohmer and Ourisson, 1976b; Rohmer *et al.*, 1984) (Fig. 3). Although the derivatization results in the loss of information for the side chain structural diversity, this methodology is still the most general way to detect the presenc of bacteriohopanoids. Among the bacteriohopanoids discovered so far, only adenosylhopane **25** escapes from this derivatization method.
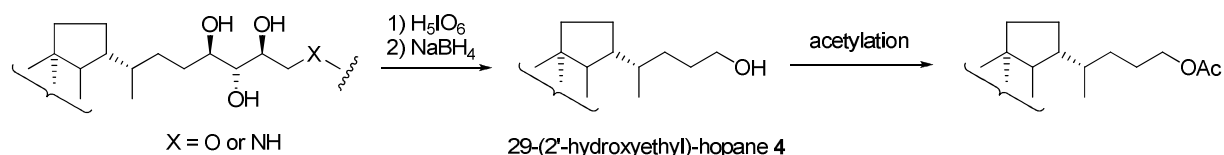
Fig. 3. H_5IO_6/ $NaBH_4$ derivatization on the polyhydroxylated side chain of bacteriohopanoids.

A procedure requiring no further derivatization of hopanoids was also developed for hopanoid analysis. This method employs a solid-phase extraction followed by semi-preparative HPLC purification of complex bacterial hopanoids, and it has been proved efficient for the isolation and quantification of individual hopanoids (Moreau *et al.*, 1995; Roth *et al.*, 1995). A novel method using atmospheric pressure chemical ionization liquid chromatography/ion trap mass spectrometry (APCI-LC/MS[n]) allows rapid screening of intact BHP peracetates that are not suitable for conventional GC/MS techniques, such as the aminobacteriohopanetriol **7**, adenosylhopane **25** and many other complex BHPs. This feature makes APCI-LC/MS[n] an interesting alternative for the rapid detection of hopanoids in diverse biological and in environmental samples (Talbot *et al.*, 2001; Talbot *et al.*, 2003a; Talbot *et al.*, 2003b; Talbot *et al.*, 2007a, b). This method requires reference samples for the

identification, thus it is better suited for the detection of known hopanoids.

Thanks to these analytical methods, a wide range of bacteriohopanoids has been detected and their distribution has been elucidated. The first report concerning hopanoid distributions in prokaryotes in 1984 pointed out the absence of hopanoids in Archaea as well as their ubiquitous presence in vast bacteria, including many methanotrophs, methylotrophs, cyanobacteria, nitrogen fixing bacteria and purple non-sulfur bacteria (Rohmer *et al.*, 1984). Although hopanoid biosynthesis does not require dioxygen (Rohmer *et al.*, 1979) and their presence has been reported in facultative anaerobic bacteria grown in strictly anaerobic conditions, *e.g. Rhodopseudomonas vannielii* (Neunlist *et al.*, 1985), *Rhodopseudomonas palustris* (Neunlist et al., 1988), *Rhodopseudomonas acidophila* (Neunlist *et al.*, 1988) and *Zymomonas moblis* (Flesch and Rohmer, 1989; Herrmann *et al.*, 1996), hopanoids have traditionally been regarded as being derived mainly from aerobic organisms. In the last years, hopanoids have been observed in a range of facultative or obligate anaerobes, such as anaerobic ammonium oxidazing and sulfate reducing bacteria (Thiel *et al.*, 2003; Sinninghe Damsté *et al.*, 2004; Härtner *et al.*, 2005; Blumenberg *et al.*, 2006; Fischer and Pearson, 2007; Rattray *et al.*, 2008). Besides aminobacteriohopanetetrol from *Desulfovibrio* (Blumenberg *et al.*, 2006), a genus of sulfate reducing bacteria, the only other intact structure reported from anaerobes is BHT. No unsaturated ring system or methylated BHPs structures have been found in the investigated anaerobes.

More recently, genome analysis was engaged in the studies concerning hopanoid biosynthesis, and allowed a more accurate overview of hopanoid distribution among eubacteria. The successfully characterized *squalene-hopene cyclase* (*shc*) gene is widely considered as an indicator of the potential hopanoid producers as it is required to produce all hopanoids. Analysis of the genome sequences of more than 600 bacteria revealed that only 10% contained *shc* genes and suggested an abundance of hopanoid biosynthesis in bacteria lower than expected (Fischer and Pearson, 2007). Studies including non-cultivable organisms, using polymerase chain reaction (PCR) and metagenomic data from different ecosystems, confirmed that the true fraction of hopanoid producers in most environmental samples (*e.g.* diverse farm soils and mine drainage) may be no more than 10% and in aquatic systems it could be less than 5% (Pearson *et al.*, 2007). Recently, a new and apparently ubiquitous group of hopanoid producers, the members of which also possess the *shc* genes but have no identifiable close relatives, was identified by metagenomic analyses (Pearson *et al.*, 2009; Pearson and Rusch, 2009). If we take into consideration that the majority of bacterial species remains uncultivable, this reflects how little is known about the phenotypes of

hopanoid-producing bacteria (Hugenholtz and Pace, 1996; Rappe and Giovannoni, 2003).

3. Bacteriohopanepolyols serve as biomarkers for bacterial environments

Triterpenic biomarkers in hopane series are widely used in organic geochemistry. Many studies have employed BHP fingerprinting in an attempt to elucidate present bacterial community composition, according to their limited production in specific individual, or classes and groups of organisms (Talbot and Farrimond, 2007). Moreover, as most BHPs appear to be relatively resilient to degradation, their potential is highlighted as sedimentary tracers for past bacterial population distributions. Aminopentol **10** and its 3-methylated analogue serve as markers for type I methanotrophs (Neunlist and Rohmer, 1985c; Cvejic *et al.*, 2000a; Talbot *et al.*, 2001); the occurrence of methylation at C-3 and unsaturation at C-6 and/or C-11 at the same time is an important structural character of the BHPs produced by acetic acid bacteria (Peiseler and Rohmer, 1992). 2β-Methylhopanoids are used as biomarkers for cyanobacteria, although their finding in a *Rhodopseudomonas palustris* strain challenges this possibly too narrow interpretation (Rashby *et al.*, 2007). Even the widespread BHT **6** and BHT cyclitol ether **18**, which are thus not diagnostic for any particular group of organisms or processes, help to indicate the bacterial activity/bacterially derived organic matter according to their presence and relative abundance.

Production of BHPs is also related to different environments. Their distribution in sedimentary organic matters can reflect certain ecosystem changes. For example, adenosylhopane **25**, the tentatively identified 2-methyladenosylhopane and structurally related compounds were recently proposed by Cooke *et al.* (Cooke *et al.*, 2008) as synthesized exclusively by soil bacteria, thereby possibly constituting a novel tracer for tracking soil derived organic matter (OM) input into aquatic sediments (Talbot and Farrimond, 2007; Cooke *et al.*, 2008, 2009). The presence of the tentatively identified unsaturated BHT cyclitol ethers (Δ^6 or Δ^{11}) and structurally related Δ^{11}-BHT in high concentration between 500 and 600 ka in the Congo deep see fan, which were proposed as possible biomarkers for nitrogen-fixing *Trichodesmium* cyanobacteria, was interpreted by a decrease in nutrient supply to surface waters, resulting in more intense pelagic N fixation (Handley *et al.*, 2010).

In summary, BHPs offer great potential as molecular markers of bacterial populations and processes due to the taxonomic variation expressed by the producer organisms, which could

provide a valuable record of bacterial community structures in modern or ancient environments. However, very little is known about the diagenetic processes implied in the conversion of a bacterial biohopanoid into the geohopanoids found in sediment; on the other hand, the interpretation of hopanoids as indicators of certain bacterial groups ultimately relies on the understanding of their physiological role in modern bacteria.

4. Biological function of bacteriohopanoids

Hopanoids are regarded as surrogates to sterols not only because of their amphiphilic nature, a characteristic feature of membrane lipids, but also because of their flat, rigid skeleton resulting from the all *trans* ring junctions of the pentacyclic triterpene ring system and of a length corresponding to the half of the thickness of a phospholipid bilayer (Rohmer *et al.*, 1979; Ourisson *et al.*, 1987). They have been shown to be localized in the cytoplasmic and outer membranes of certain bacteria (Jahnke *et al.*, 1992; Jürgens *et al.*, 1992; Simonin *et al.*, 1996) and *in vitro* experiments have shown that these molecules are efficient in condensing artificial membranes and enhancing the viscosity of liposomes.

The condensing effect of hopanoids on phospholipid layers was proved by Kannenberg *et al.*(1994). Hopanoids are able to regulate membrane fluidity and induce order in the phospholipid matrix of membranes, thus reducing molecular permeability and increasing liposome membrane stability (Fig. 4).
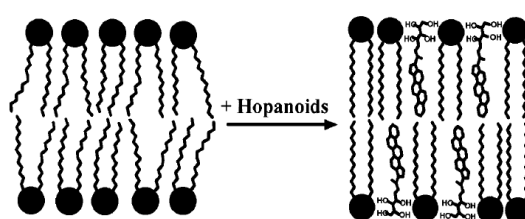
Fig. 4. Schematic representation of the condensing action imposed by elongated hopanoids (BHT) on phospholipids in bilayer membranes (Kannenberg and Poralla, 1999). *Black circles*, polar phospholipid heads; *zigzag lines*, attached fatty acids.

The sterol-surrogate function of hopanoids was also supported by their increased concentration in membranes of *Alicyclobacillus acidocaldarius* at high temperatures and at acidic conditions (Poralla *et al.*, 1984). Deletion of the *shc* gene in *Rhodopseudomonas palustris* resulted in the lack of hopanoid production and consequently caused the increase of

membrane permeability. In addition, a severe growth defect, as well as significant morphological damage, was observed in this *R. palustris* mutant when cells were grown under acidic and alkaline conditions. Putative role of hopanoids in membrane integrity and pH homeostasis was thus suggested according to this physiological study (Welander *et al.*, 2009).

Hopanoids have also been proposed to be a response to extreme alcohol concentrations. In the alcohol-tolerant *Zymomonas mobilis,* the bacteria are rendered sensitive to ethanol in the presence of inhibitors preventing hopanoid biosynthesis (Sahm *et al.*, 1993). However, the correlation between ethanol concentration in medium and hopanoid content in *Z. mobilis* membranes was found controversial in later studies. Only minor changes were observed in hopanoids concentration and composition over a wide range of ethanol concentrations (Hermans *et al.*, 1991; Moreau *et al.*, 1997).

Another example of a biological function of hopanoids was described for *Streptomyces coelicolor*, in which hopanoid production is strongly linked to aerial growth and sporulation: these triterpenoids may alleviate stress in aerial mycelium by diminishing water permeability across the membrane (Poralla *et al.*, 2000). A recent physiological study on hopanoids in *Rhodopseudomonas palustris* demonstrated that unmethylated and C_{30} hopanoids are sufficient to maintain cytoplasmic but not outer membrane integrity (Welander *et al.*, 2012). These results imply that hopanoid modifications, including methylation of the A-ring and the addition of a polar head group, may have biologic functions beyond playing a role in membrane permeability

Hopanoid function is not restricted to membrane-related activities alone. For example, hopanoids were reported to be capable of aligning cellulose microfibrils excreted by *Acetobacteria. xylinum* (Haigh *et al.*, 1973). An extracellular function for hopanoids has been observed as well. Nitrogen-fixing Actinomycetes of the genus *Frankia* form nitrogenase-containing vesicles that are surrounded by multilamellate lipid envelopes containing hopanoids. It is assumed that the lipid envelope serves as an oxygen barrier to protect nitrogenase from exposure to oxygen (Kleemann *et al.*, 1994; Nalin *et al.*, 2000; Abe, 2007). However, the absence of hopanoids in heterocysts, which are formed by *Nostoc punctiforme* and express nitrogenase that supplies adjacent vegetative cells with fixed N, suggests that there is no functional link between N-fixation and hopanoid in *Nostoc punctiforme* (Doughty *et al.*, 2009).

In conclusion, hopanoids certainly have a strong impact on the barrier properties of biological membranes in different culture conditions but apparently can have several other specific functions in many bacteria, most of which probably have not been identified yet.

Construction of deletion mutants and phenotype analysis will be necessary to identify specific functions in selected species.

5. Biosynthesis of bacteriohopanoids

Numerous efforts have been dedicated in order to elucidate the biosynthesis of bacterial hopanoids. Pioneer work was done by Rohmer and co-workers, utilizing isotopic labeled substrates as tracers to elucidate hopanoids formation in selected bacteria. The possible enzymatic reactions and putative precursors involved in bacteriohopanoid biosynthesis could thus be deduced according to the labeling results. Interesting features have been revealed thanks to the labeling experiments, as well as the genetic studies being carried out in recent years.

5.1. Synthesis of the C_5 precursors isopentenyl diphosphate and dimethylallyl diphosphate

Bacterial hopanoids are derived from isopentenyl units via the mevalonate-independent methylerythritol phosphate (MEP) pathway that is used by most prokaryotes, green algae as well as some higher plants (Rohmer *et al*., 1996; Rohmer, 1999) (Fig. 5b). The MEP pathway was unexpectly discovered by the labeling experiments that intended to elucidate the origin of C_5 side chain (Flesch and Rohmer, 1988b). The labeling patterns found in the isoprene units after introduction of [1-^{13}C]- and [2-^{13}C]acetates differed completely from those expected from the mevalonate pathway (Fig. 5a), which was unanimously admitted as the sole biosynthetic pathway towards isopentenyl diphosphate (IPP) and dimethylallyl diphosphate (DMAPP), the universal precursors of isoprenoids in living organisms.
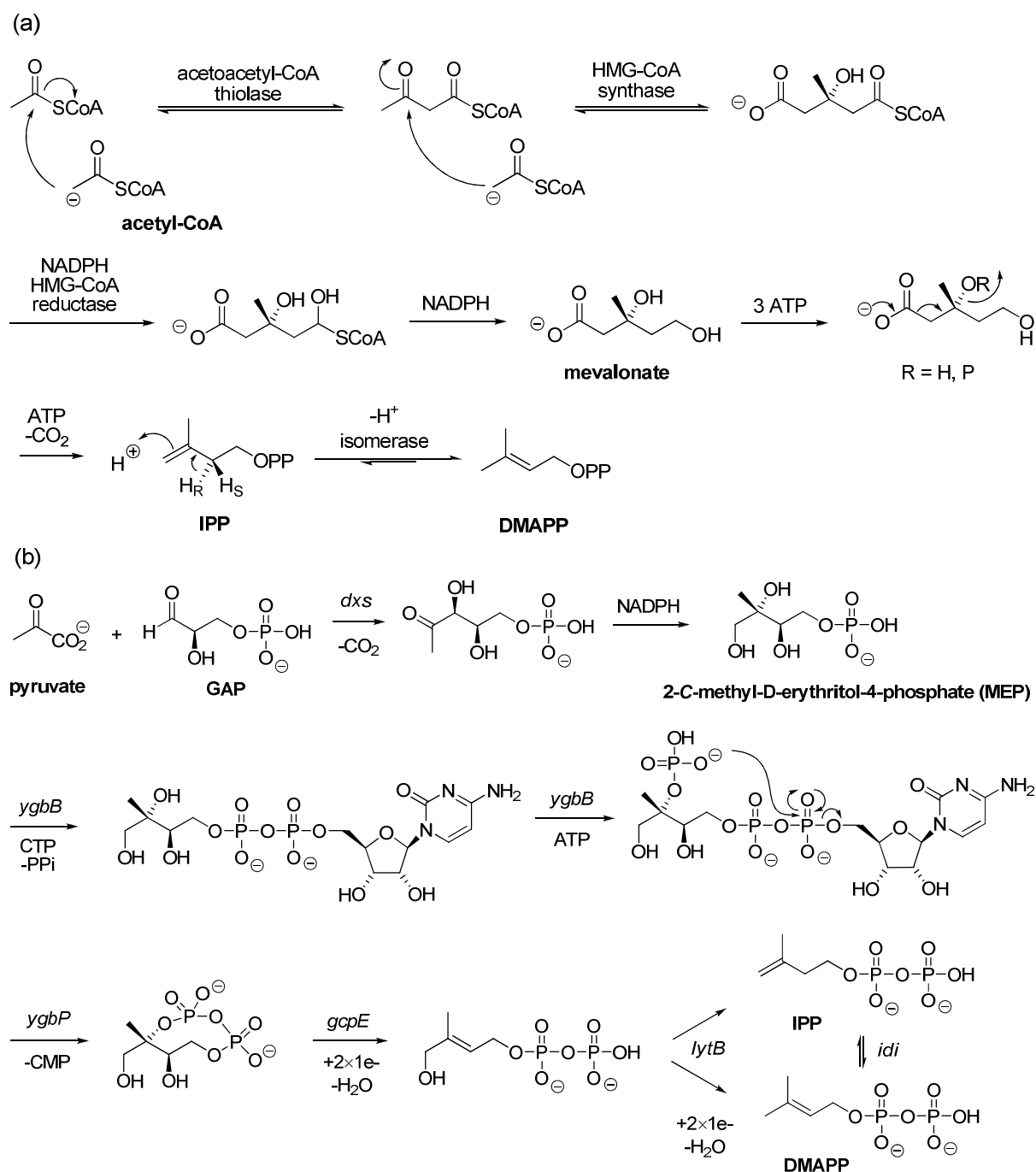
Fig. 5. Biosynthesis of isoprene units via the mevalonate pathway (a) and via the MEP pathway (b).

Further incorporation experiments using ^{13}C-labeled precursors (glucose, erythrose, pyruvate) as well as deuterium labeled glucose and 2-*C*-methylerythritol unveiled the mysteries of MEP pathway: IPP and DMAPP are derived from pyruvate and glyceraldehyde 3-phosphate (GAP) via 2-*C*-methyl-D-erythritol-4-phosphate (Rohmer *et al.*, 1993; Duvold *et al.*, 1997a; Duvold *et al.*, 1997b; Rohmer, 1996, 2007).

5.2. Synthesis of triterpenes of hopane series from IPP and DMAPP

Stepwise head-to-tail additions of IPP to DMAPP and further to other derived allyldiphosphorate under catalysis of prenyltransferases result in geranyl diphosphate (C_{10}), farnesyl diphosphate (C_{15}), and geranylgeranyl diphosphate (C_{20}). Two farnesyl diphosphate units can be condensed tail-to-tail by squalene synthases to yield squalene (Fig. 6).

Fig. 6. Formation of squalene from IPP and DMAPP.

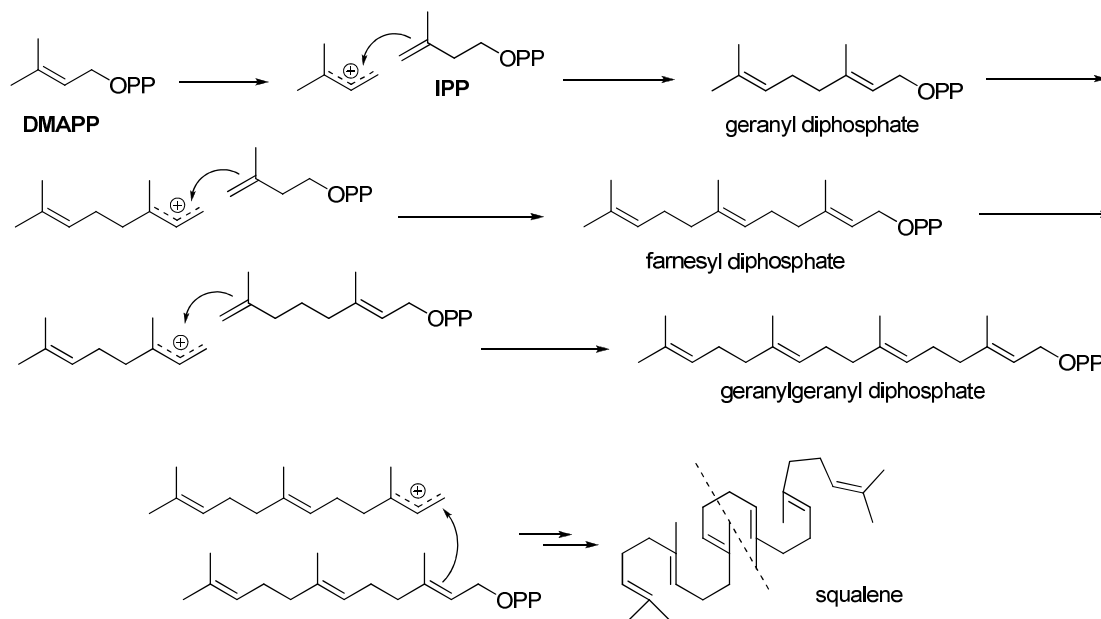Squalene is then cyclized to hopene by the key enzyme of hopanoid biosynthesis, squalene-hopene cyclase (SHC; EC 5.4.99.17) (Seckler and Poralla, 1986; Ochs *et al.*, 1990; Ochs *et al.*, 1992). This SHC reaction involves formation of five ring structures, 13 covalent bonds, and nine stereocenters and therefore is one of the most complex one-step enzymatic reactions (Fig. 7). Only a few SHCs have been purified and biochemically studied so far including *Alicyclobacillus acidocaldarius* SHC, *Methylococcus capsulatus* SHC, *Zymomonas mobilis* SHC, *Bradyrhizobium japonicum* SHC, *Streptomyces peucetius SHC, Tetrahymena thermophila* SHC and *Rhodopseudomonas palustris* SHC (Siedenburg and Jendrossek, 2011 and references cited therein). SHC enzymes present a low degree of substrate selectivity but a high degree of product specificity (Anding *et al.*, 1976), and they are capable of accepting a wide variety of squalene analogues (C_{25}–C_{31}) and efficiently perform sequential ring-forming reactions to produce a series of unnatural cyclic polyprenoids. By utilizing such properties of

the enzyme, unnatural novel polycyclic polyprenoids have been generated by enzymatic conversion of chemically synthesized substrate analogues (Hoshino *et al.*, 1999 and references cited therein).
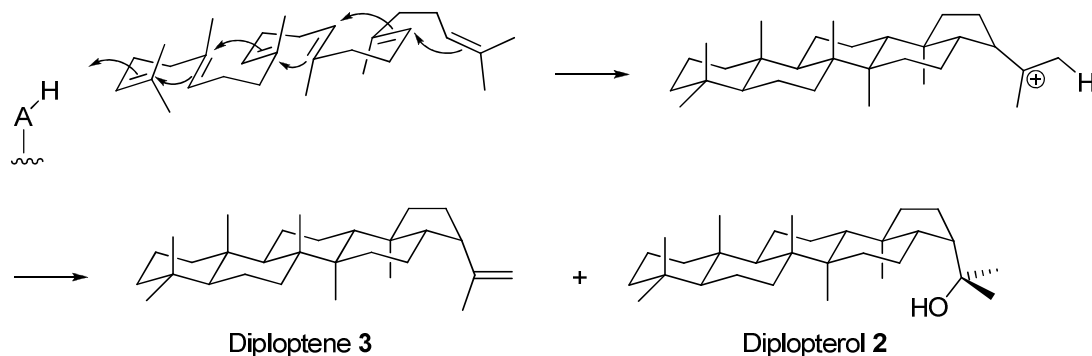

Fig. 7. The polycyclization reaction of squalene to hopene by SHCs

5.3. Origin of additional methyl groups on hopane skeleton from methionine

The last biosynthetic step corresponding to the modification of the hopane skeleton concerns the introduction of additional methyl groups, which are found on saturated carbon atoms of the hopane skeleton. Methionine is the initial methyl donor for the additional methyl groups of 3β-methyl BHTs of *Acetobacter pasteurianus (*Zundel and Rohmer, 1985b), 2β-methyldiplopterol of *Methylobacterium organophilum* (Zundel and Rohmer, 1985b) or 31-methyl BHT of *Acetobacter europaeus* (Simonin *et al.*, 1994). The additional methyl groups were all labeled by an unspecified methylation process upon feeding with [CD$_3$]methionine with retention of all three deuterium atoms.

Recently, a *hpnP* gene was characterized from a *Rhodopseudomonas palustris* strain (Welander *et al.*, 2010). It was annotated as a radical *S*-adenosylmethionine (SAM) methylase and was indicated to be necessary for the methylation at C-2 of bacteriohopanoids. At present, the *hpnP* gene appears to be a potent predictor of the capacity to produce 2-methylhopanoids, for it is identified so far as the only gene engaged in the methylation process among the tested bacteria.

An additional gene, *hpnR*, was identified very recently for the methylation of hopanoids

at C-3 in the obligate methanotroph *Methylococcus capsulatus* strain Bath (Welander and Summons, 2012). Like the *hpnP* gene, *hpnR* gene was also annotated as a radical SAM protein possibly containing a B-12 binding domain. Bioinformatic analysis revealed that the taxonomic distribution of *hpnR* extends beyond methanotrophic and acetic acid bacteria. The distribution of the C-3 methylase in oxygen-demanding bacteria seems robust for now and can be seen as further evidence for the use of 3-methylhopanes as proxies for the occurrence of aerobic metabolisms in ancient environments.

5.4. Polyhydroxylated C_5 side chains of bacteriohopanoids are derived from a D-ribose derivative.

Feeding experiments using $[1-^{13}C]$acetate on *Rhodopseudomonas palustris*, *Rhodopseudomonas acidophila* and *Methylobacterium organophilum* (Flesch and Rohmer, 1988b), as well as $[1-^{13}C]$-, $[2-^{13}C]$-, $[3-^{13}C]$-, $[5-^{13}C]$- or $[6-^{13}C]$glucose into *Zymomonas mobilis* (Rohmer *et al.*, 1989) indicated that the side chain of C_{35} bacteriohopanoids (BHT **6** and aminobacteriohopanetriol **7**) was derived from a D-pentose derivative, xylulose 5-phosphate, via the non-oxidative pentose phosphate pathway (Fig. 8), because the distribution of isotopic enrichment observed in the supplementary C_5 unit was in total agreement with that derived from this metabolic process (Fig. 9). Moreover, the labeling result also pointed out that the C-5 carbon atom of the D-pentose derivative, which corresponds to the C-6 carbon atom of glucose, was linked to the C-30 position of the hopane skeleton.
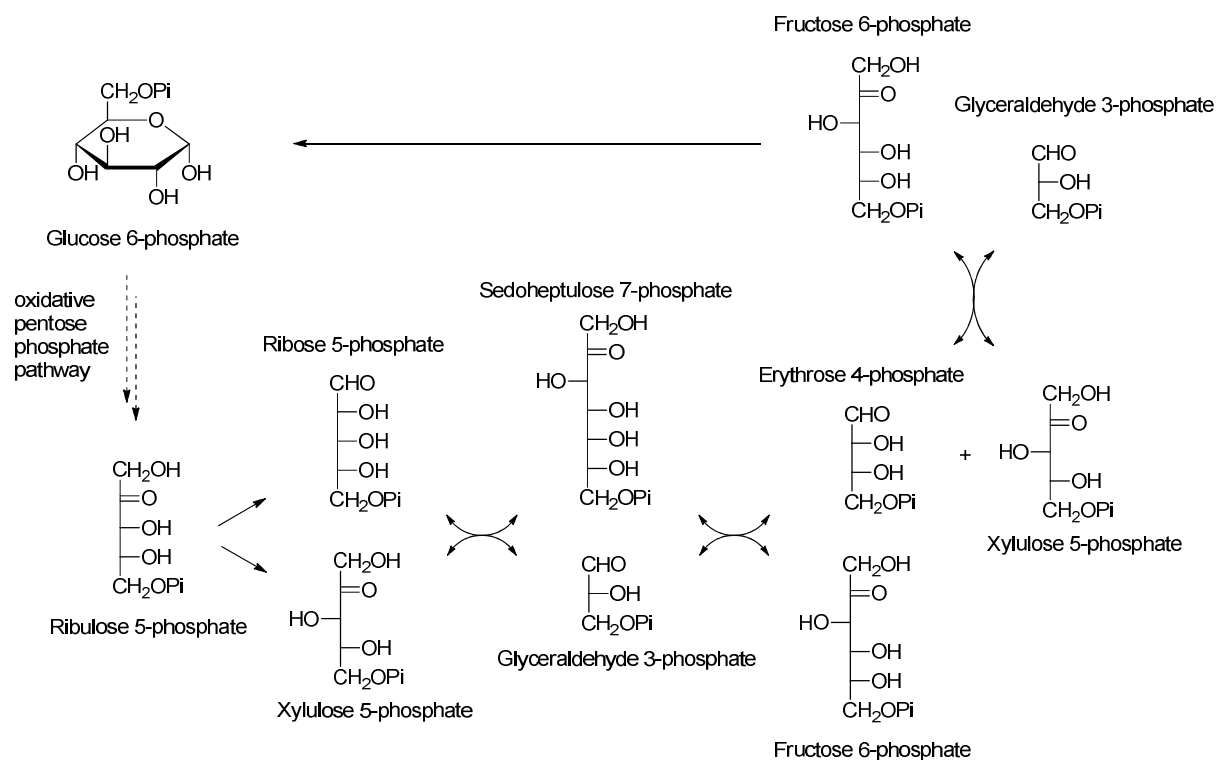
Fig. 8. Non-oxidative pentose phosphate pathway. Ribulose-5-phosphate generated from glucose 6-phosphate via oxidative pentose phosphate pathway is converted into ribose-5-phosphate and xylulose-5-phosphate in the non-oxidative phase of pentose phosphate pathway. Further conversion of these pentose derivatives leads to the formation of fructose 6-phosphate which regenerates glucose 6-phosphate via enolization.
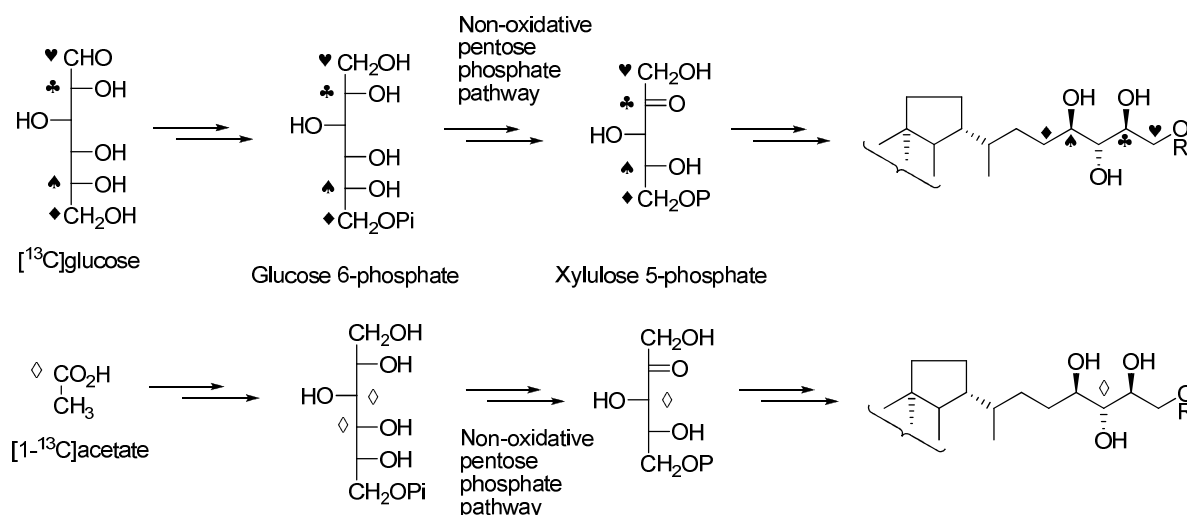
Fig. 9. Side-chain labeling pattern of BHT from ^{13}C-labeled glucose or [1-^{13}C]acetate via non-oxidative pentose phosphate pathway.

The stereochemistry of this side-chain was unambiguously determined as 32*R*, 33*R* and 34*S* by the comparison of the natural BHT with eight possible synthetic diastereomers with

varied stereochemistry at C-32, C-33 and C-34 (Bisseret and Rohmer, 1989) and also by the chemical correlation with adenosylhopane **25** of known absolute configuration (Neunlist *et al.* 1988). The consistent side-chain configuration observed in nearly all elongated bacteriohopanoids indicates that a D-ribose derivative is a likely precursor for the additional C_5 unit that it is attached to the C-30 carbon atom of the hopane framework via its C-5 carbon atom.

Labeling experiments not only revealed the origin of the C_5 side chain of C_{35} bacteriohopanoids, but also allowed verifying the non-equivalence of the two carbons from the isopropyl group of the hopane skeleton. Indeed, the C-30 position was always labeled whereas the C-29 position was never labeled in all the bacteriohopane derivatives when they were derived from the labeled precursors, [1-^{13}C]acetate which is converted *in vivo* into [3,4-^{13}C$_2$]glucose (Flesch and Rohmer, 1988a), and [3-^{13}C]- or [6-^{13}C]glucose (Sutter, 1991; Rohmer *et al.*, 1993); on the other hand, C-29 could be labeled only when [4-^{13}C]glucose was incorporated (Toulouse, 2011) (Fig. 10). This showed that there was no free rotation around the C-21–C-22 bond in the cationic intermediate with a positive charge at C-22 arising from squalene cyclization. The carbon atom C-30 that is coupled to C_5 side chain corresponds only to the terminal *Z*-methyl group of squalene. Cyclization of [25,30-^{13}C$_2$]squalene, where the two terminal *Z*-methyl groups are labeled, by *Alicyclobacillus acidocaldarius* SHC protein showed that the *Z*- or *E*-methyl groups of squalene corresponds respectively to the methylene (C-29) or the methyl group (C-30) of the diploptene side chain (Hirsch, 2004).
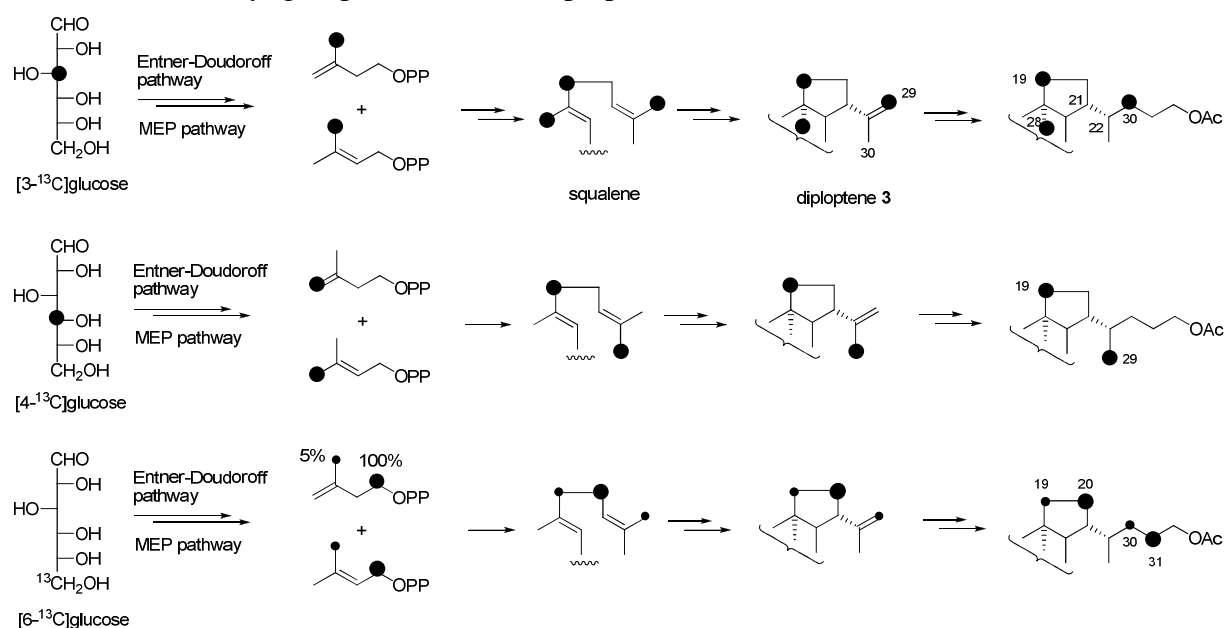

Fig. 10. Partial labeling results of hopanoids arising from [3-^{13}C]-, [4-^{13}C] and [6-^{13}C]glucose (Toulouse, 2011).

5.5. Coupling between a triterpene moiety and a D-ribose derivative

The nature of the reaction, which permits the coupling between the triterpene moiety and a D-ribose derivative, was first proposed by Rohmer *et al.* according to few already known enzymatic reactions that probably had similar characters (e.g. the biosynthesis of *S*-adenosylmethionine) (Neunlist and Rohmer, 1985b; Flesch and Rohmer, 1988b; Rohmer, 1993) (Fig. 11). It was presumed to involve a nucleophilic hopane derivative, such as diploptene **3**, and an electrophilic D-ribose derivative possessing a good leaving group at C-5 (*e.g.* ribose 5-phosphate, ribose 5-diphosphate or *S*-adenosylmethionine) yielding 30-(5'-ribosyl)hopane **23** or adenosylhopane **25** via a cationic intermediate with a positive charge at C-22, hence interpreting the simultaneous presence of the two C-22 diastereoisomers of BHT in acetic acid bacteria (Rohmer and Ourisson, 1976b, 1986) and of adenosylhopane in *Rhodopseudomonas acidophila* (Neunlist *et al.*, 1988).
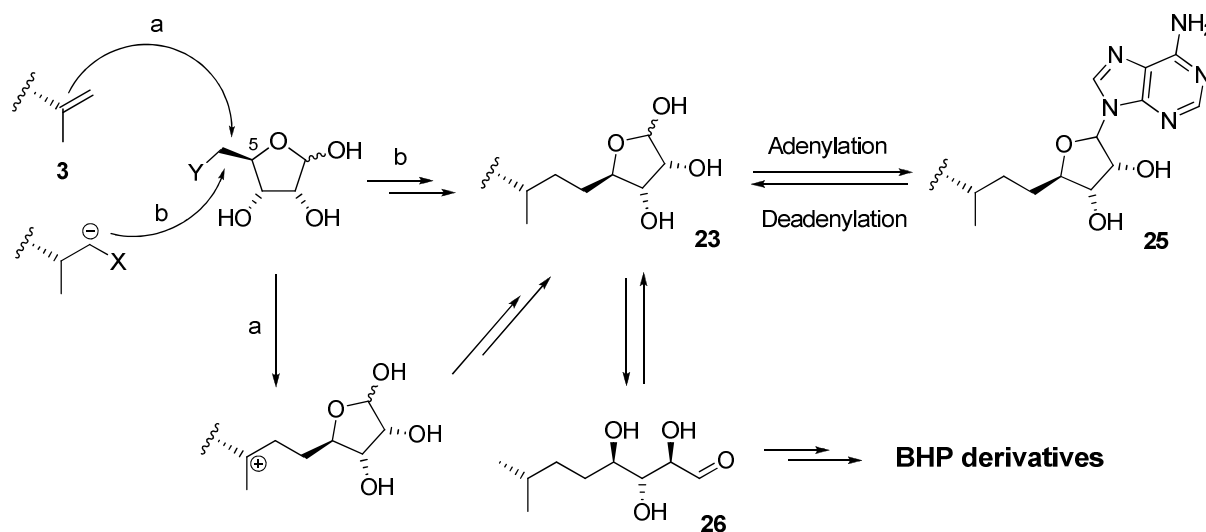
Fig. 11. Proposed substitution reaction for the coupling between a triterpene moiety and a D-ribose derivative (Rohmer, 1993).

The incorporation experiment of $[6,6-^2H_2]$glucose into the hopanoids of *Zymomonas. mobilis* also shed light on the essence of the coupling reaction (Duvold, 1997). $[5,5-^2H_2]$Xylulose 5-phosphate is synthesized *in vivo* from $[6,6-^2H_2]$glucose, and both of the two deuterium atoms were retained on the C-31 position of complex bacteriohopanoids (Fig. 12). Accordingly, an oxidation of the C-5 position of xylulose 5-phosphate and a subsequent

addition reaction between the hopanoid derivative and the pentose precursor are definitely excluded for the formation of the side chains of bacteriohopanoids. The coupling reaction was supposed to be a substitution.

Fig. 12. Labeling patterns of the C_5 side-chain after the incorporation with $[6,6-^2H_2]$glucose into the hopanoids of *Zymomonas mobilis*.

According to the mechanism suggested for the coupling reaction, a cationic intermediate with a positive charge at C-22 would be involved as well as a consequently reduction leading to 30-(5'-ribosyl)hopane derivative. Therefore, it is *not necessarily unexpected that* an hydrid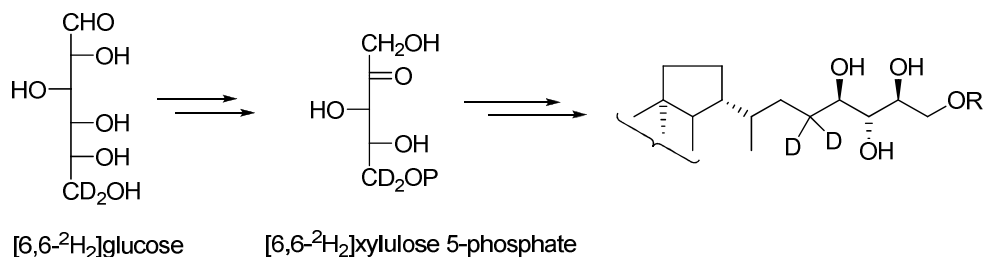e would be introduced from NAD(P)H, which is a general cofactor for enzymatic reductions, such as the DXR or LytB catalyzed reactions in the MEP pathway (Fig. 5). However, deuterium labeling at C-22 has never been observed in the presence of a diastereomeric mixture of NADP^{2}H synthesized *in vivo* from $[1-^2H]$glucose in *Zymomonas mobilis*, whereas all other reduction depending directly (reduction catalyzed by the DXR) or indirectly (reduction catalyzed by lytB) on NADPH were characterized by a deuterium atom on the carbon atom corresponding to the site of reduction (Charon, 2000; Toulouse, 2011). This result showed that the hydrogen atom on C-22 position does not correspond to a hydride transfer from NADPH, but to the transfer of an exchangeable hydrogen atom (H$^•$ or H$^+$) originating from water of the environment.

Since this non-labeling of C-22 position was in contradiction with the proposed substitution mechanism, an alternative hypothesis was proposed for the formation of bacteriohopanoid side chain: an adenosyl radical would be involved in the coupling reaction (Charon, 2000). It was suggested to be generated from *S*-adenosylmethionine by a reduced iron-sulfur cluster, yielding the well known 5'-deoxyadenosyl radical, thus giving adenosylhopane **25** as a putative intermediate.

This hypothesis is consistent with the results obtained from already performed

experiments. Firstly, feeding experiments with [1-^{13}C]acetate in *R. acidophila* has shown that the labeling patterns of the D-ribose moiety of adenosylhopane were quantitively identical with those of the side chains of all the other BHP derivatives (Flesch and Rohmer, 1988b), indicating that they were derived from the same origin. Moreover, adenosylhopane is frequently isolated in various hopanoid-producing bacteria (Neunlist and Rohmer, 1985b; Seemann *et al.*, 1999; Bravo *et al.*, 2001; Talbot *et al.*, 2007a). The small amounts of adenosylhopane usually found in many hopanoid producers is in agreement with the role of an intermediate in a biosynthetic process, being constantly converted with a high turnover into the major bacteriohopanoids with linear side chains (*e.g.* BHT **6** or 35-aminobacteriohopantriol **7**). Last but not least, although the adenosyl radical could either arise from homolytic cleavage of adenosylcobalamin (coenzyme B$_{12}$) or from single-electron reduction of *S*-adenosylmethionine (coenzyme iron-sulfur cluster), the latter is more often consumed as a co-substrate rather than a true cofactor in various enzymatic processes (Marsh *et al.*, 2010).

A possible mechanism shown in Fig. 13 would generate an intermediate having a radical at C-22 position. The radical would first accept an electron from [4Fe-4S]$^{1+}$. The resulting anion may be protonated by an acid residue of the enzyme active site, and then provide adenosylhopane **25** (Fig. 13, mechanism A). Alternatively, the radical intermediate would accept a radical H$^{\bullet}$ from a cysteine thiol in the enzyme active site to afford adenosylhopane **25**. The resulting radical from deprotonated cysteine thiol might then transfer an electron to oxidized iron-sulfur cluster [4Fe-4S]$^{2+}$ and form a new disulfide bond. The cysteine thiol residue is then restored to its deprotonated form by the reduction promoted by cofactor NAD(P)H (Fig. 13, mechanism B). This mechanism is inspired by the mechanism of ribonuleotide reductase, which catalyzes the formation of 2-deoxyribonucleotides in *Escherichia coli* (Eklund *et al.*, 1997; Mulliez *et al.*, 2001). The two hypothetical mechanisms for the protonation process on C-22 position are in agreement with the fact that the conversion of squalene or diploptene **3** into elongated bacteriohopanoids is accompanied with a reduction involving the transfer of an exchangeable hydrogen atom, which could be either in the form of H^{+} or in the form of H$^{\bullet}$.
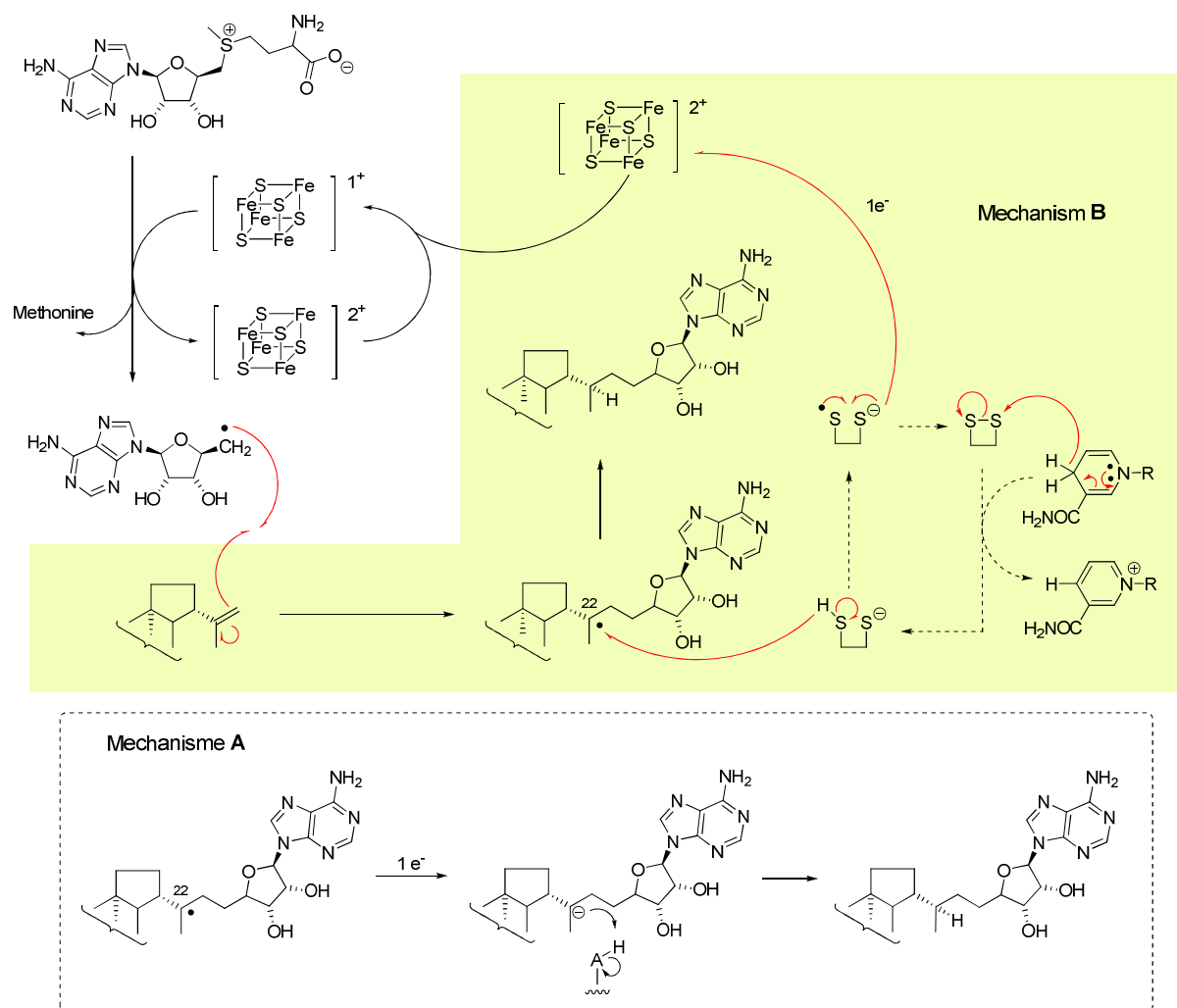
Fig. 13. Hypothetical mechanisms for the coupling between diploptene **3** and a radical SAM enzyme as the donor of an adenosyl group.

Recent genetic study on hopanoid biosynthesis in *Methylobacterium* further confirmed this idea (Bradley *et al.*, 2010). The gene required for adenosylhopane formation is annotated as a radical SAM enzyme complexed to a reduced Fe-S cluster. Deletion of this gene in *Methylobacterium* resulted in the deficiency of elongated bacteriohopanoids but the accumulation of a C_{30} hopanoid, diploptene **3**. The authors thus proposed that adenosylhopane was the first precursor in the side chain biosynthesis of C_{35} bacteriohopanoid derivatives.

Although diploptene was suggested as the possible precursor for the hopane moiety, the incorporation of tritium labeled diploptene into C_{35} bacteriohopanoid derivatives was only achieved once from the cell-free system of *Acetobacter pasteurianus*. Tritium labeled 29-(2'-hydroxyethyl)-hopane **4** acetate was isolated after $H_5IO_6/NaBH_4$ derivatization on the side chain, therefore indicating the formation of tritium labeled elongated bacteriohopanoids

(Rohmer, unpublished work). However, most incorporation experiments in other cell-free systems of different bacteria using isotope labeled diploptene failed (Rohmer, 1993). This could be interpreted by the nature of the enzymatic coupling reaction between the triterpene moiety and a radical SAM enzyme, which is definitely sensitive to the presence of oxygen.

5.6.   Ribosylhopane as a putative intermediate of C_{35} bacteriohopanoids

Ribosylhopane **23** is a rather likely hypothetical intermediate in the side chain biosynthesis of C_{35} bacteriohopane derivatives (Rohmer, 1993). It is easily derived from adenosylhopane **25** by hydrolysis. Although it has never been detected before from any bacterium, its role as a key intermediate in the side-chain formation of hopanoids was supported by convincing arguments.

Incorporation experiments of [1-^{2}H]glucose into the complex hopanoids of *Zymomonas mobilis* indicated that a reduction step was engaged in the biosynthesis of the polyhydroxylated linear side-chains of BHT derivatives (Sutter, 1991; Charon, 2000). The C-35 position of the BHT glycoside, corresponding to the C-1 hemiketal of D-glucose, was found to be labeled with two deuterium atoms after incorporation. The first deuterium atom corresponds to the originally labeled [1-^{2}H]glucose, whereas the second one can only be derived from NADP^{2}H, which is synthesized *de novo* in *Z. mobilis* in the presence of [1-^{2}H]glucose. This NADP^{2}H-dependent reduction pointed out that the right substrate probably possesses a functional aldehyde carbonyl group, and this carbonyl group can only be located on the C-35 carbon atom, since no deuterium labeling has been observed on the C-32, C-33 or C-34 positions of the BHT glycoside. In fact, the possible candidate is the open aldehyde form of 30-(5'-ribosyl)hopane **26**, which is normally present as a minor isomer in equilibrium with ribosylhopane **23**. The open aldehyde form **26** may explain the presence of two diastereoisomers at C-34 position of BHTs in *Acetobacter* species (Peiseler and Rohmer, 1992): this isomerization of the C-34 chiral centre in α position of the terminal carbonyl group occurs via enolization, directly giving the (34*R*)-BHT series (Charon, 2000) (Fig. 14). Although ribosylhopane **23** has not been isolated, the lactone **24** (Fig. 2) bearing a unique carbon/carbon bond between hopane and ribonolactone was isolated from *Nitrosomonas europaea* (Seemann *et al.*, 1999). It would directly result from the oxidation of ribosylhopane **23**, thus strengthening the hypothesis of the presence of ribosylhopane in bacteria.
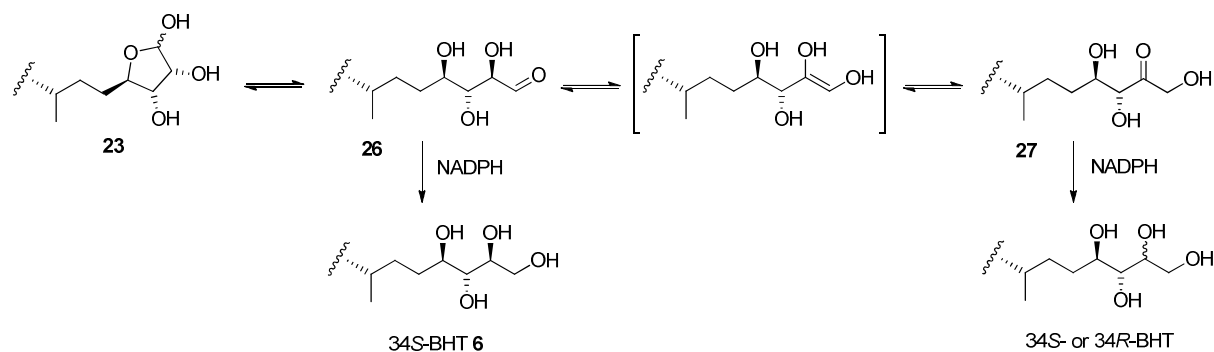
Fig. 14. The reduction step leading to the (*34R*)- and (*34S*)-BHT epimers from ribosylhopane **23**.

For the biosynthesis of 35-aminobacteriohopanetriol **7**, we can assume that it is directly derived from ribosylhopane **23** via a reductive amination or, alternatively, from BHTs that are generated from ribosylhopane. However, the latter interpretation seems unlikely given that all the known enzymatic reactions involving the transfer of an amino group usually occur on some electrophilic fragment (*e. g.* an acyl or oxo group or phosphorylated furanose), which is attacked by a nucleophilic N atom and then followed by a reduction. It is obviously not the case when BHT **6** is the substrate. Therefore, it is plausible to presume that ribosylhopane **23** is the branching point between the biosynthesis of BHT **6** and 35-aminobacteriohopanetriol **7**. Similar to the bioconversion leading to BHT from ribosylhopane, the open form **26** of ribosylhopane **23** possessing the aldehyde carbonyl group at C-35 is more likely the precursor of aminobacteriohopanetriol **7**, and an aminotransferase would be required for the reductive amination as it is fairly well known for the transfer of an amino group to an oxoacid.

With all these data, a reasonable hypothetical biosynthetic pathway leading to BHT **6** or aminobacteriohopanetriol **7** could be proposed as shown in Fig. 15. Adenosylhopane **25**, as the first precursor for side chain biosynthesis, is derived from diploptene **3** under catalysis of a radical SAM enzyme. Subsequent cleavage of adenine group of adenosylhopane **25** affords ribosylhopane **23** as a key intermediate. This hemiketal is in equilibrium with the open aldehyde form **26**. Further reduction or reductive amination of the aldehyde **26** leads to the formation of the two major C_{35} bacteriohopanoids, BHT **6** or 35-aminobacteriohopanetriol **7**, respectively.
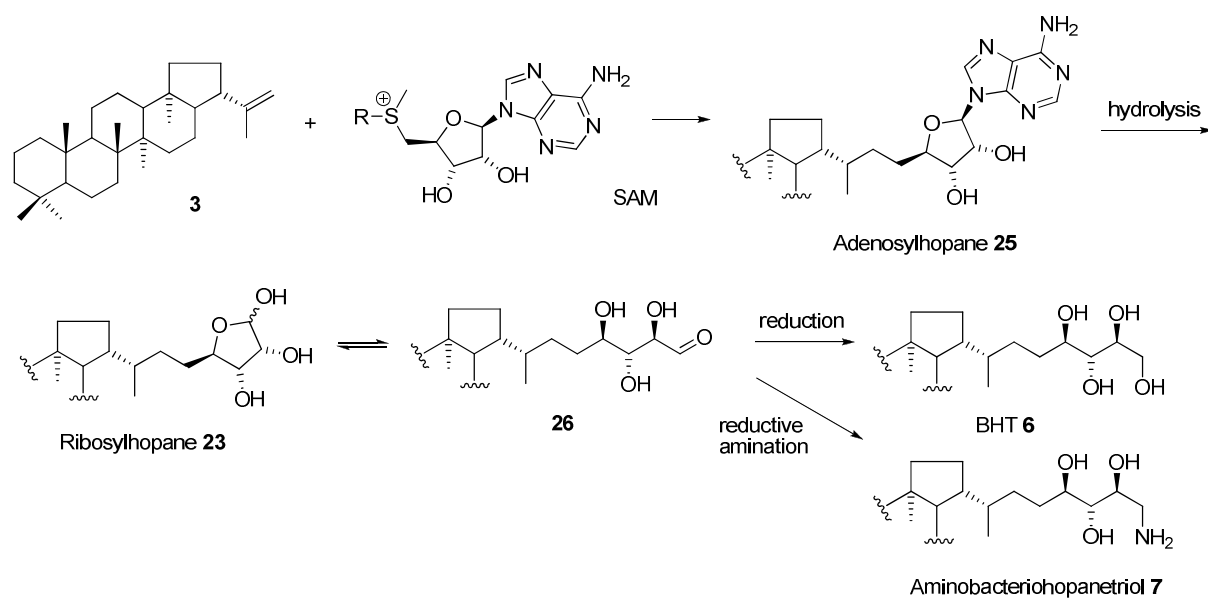
Fig. 15. Hypothetical biosynthetic scheme for side chain formation of C_{35} bacteriohopanoids **6** and **7**.

6. Objectives of this thesis

To date, there are more than 200 hopanoids having been reported, presenting an impressive structural diversity. Most of the modification on hopanoid structures happened on the polyhydroxylated side chains, and it was proposed that hopanoid side chain structures carry taxonomic and/or physiological information. Indeed, most bacteriohopanepolyols are more specific to certain organisms or environments, offering thus great potential as biomarkers for bacterial communities. A robust interpretation of hopanoids in modern and ancient settings relies on the better understanding of their phylogenetic distribution. However, only limited knowledge has been obtained so far in this area. Genome analysis recently serves as a valuable tool to predict hopanoid production by bacteria, especially for those that may not be cultivable or only produce hopanoids under certain environmental conditions (Poralla *et al.*, 2000). Full characterization of the genes involved in bacteriohopanoid biosynthesis would allow scientists to decipher how the structural diversity of hopanoids is linked to their sources. Therefore, deeper understanding of hopanoid biosynthesis is absolutely indispensable and would provide a better basis for interpreting the meaning of these geologically important molecules.

Compared to the well-established biosynthetic pathway for the pentacyclic skeleton of triterpenoids in hopane series, very little is known concerning the formation of their polyhydroxylated side-chains. The main interest of this thesis is thus to investigate the side chain biosynthesis of C_{35} bacteriohopanoids (BHT and aminobacteriohopanetriol). Four projects concerning hopanoid side-chain formation in selected bacteria were performed.

The first project is engaged in the characterization of the genes required for hopanoid production in *Streptomyces coelicolor* A3(2). Identifying the genes responsible for various hopanoid modifications will provide robust tools to illustrate the possibly involved enzymatic reactions in hopanoid synthesis and predict the hopanoid structure based on genomic or metagenomic sequence information.

Considering that sufficient amounts of hopanoid substrates are required for enzyme assays and the difficulties for the isolation of natural hopanoids and their tiny amounts in the nature, the second project is focused on the chemical synthesis of natural adenosylhopane as well as its deuteriated isotopomer, which represents the critical tool for testing the viability of the biosynthetic scheme.

Incorporation of synthesized adenosylhopane into C_{35} bacteriohopanoids was performed

in *Methylobacterium organophilum* to verify the role of adenosylhopane as a key intermediate in the biosynthesis of hopanoid side chain.

In the last part, primary investigation was carried out concerning aminobacteriohopanetriol biosynthesis. Attempts were made to identify the possible donor for the terminal amino group of 35-aminobacteriohopanetriol, which will promote better understanding of the relative enzymatic reaction involved in the side chain formation of aminobacteriohopanetriol.

Chapter I

Hopanoid biosynthesis in *Streptomyces coelicolor* A3(2): identification of ribosylhopane as an intermediate

I.1. The gene cluster associated with hopanoid biosynthesis in *Streptomyces coelicolor* A3(2)

Streptomyces coelicolor A3(2) is the genetically best known representative of the group of soil-dwelling, filamentous bacteria with a complex lifecycle involving mycelial growth and spore formation. The A3(2) strain has one linear chromosome and two plasmids. The single chromosome was sequenced and annotated in 2002 from an ordered cosmid library (Bentley *et al.*, 2002). It was considered to be grouped into three regions: the core and two arms. On the one hand, the core region comprises about half of the chromosome and contains the essential genes for the survival of the organism. The two arms regions, on the other hand, code for nonessential functions like the biosynthesis of "secondary metabolites", hydrolytic exoenzymes and so on. A cluster of genes (SCO6759-6771) has been detected on the annotated cosmid SC6A5 located on one arm region and were supposed to be implied in isoprenoid biosynthesis (Bentley *et al.*, 2002). This gene cluster comprises 13 open reading frames (ORFs), seven of which by their similarity are connected to hopanoid biosynthesis (Poralla *et al.*, 2000) (Fig. I-1).
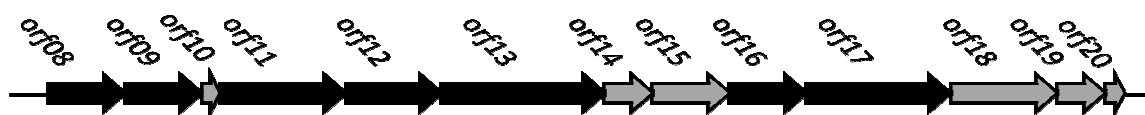

Fig. I-1. Isoprenoid/hopanoid biosynthetic genes on cosmid SC6A5 from *S. coelicolor* A3(2). Black arrows indicate the genes probably involved in hopanoid biosynthesis. 08, phytoene or squalene synthase; 09, phytoene or squalene synthase; 10, unknown function; 11, phytoene dehydrogenase; 12, polyprenyl diphosphate synthase or farnesyl diphosphate synthase; 13, significant similarity also in the conserved motifs to other squalene-hopene cyclases; 14, lipoprotein; 15, hypothetical protein; 16, putative 4-hydroxy-3-methylbut-2-en-1-yl diphosphate synthase; 17, putative 1-deoxy-D-xylulose 5-phosphate synthase; 18, putative aminotransferase; 19, DNA-binding protein; 20, unknown function.

The gene *orf13* is annotated as a putative ortholog to squalene-hopene/tetraprenyl-β-curcumene cyclase [EC:5.4.99.17, EC:4.2.1.129]. In the so far invested genomes, the hopanoid biosynthetic genes always surround the *squalene-hopene cyclase* (*shc)* locus. Upstream of the *orf13* gene, a group of genes (*orf8, 9* and *11*) that probably encode for two phytoene/squalene synthases and a corresponding dehydrogenase are

present in the same order as those in *Rhizobium* NGR 234, *Bradyrhizobium japonicum* and *Zymomonas mobilis* (Perzl *et al.*, 1998), pointing out the possibly retained functional relationships among these groups of genes. Moreover, the putative genes *orf8, 9, 12* and *13* are sufficient to explain the synthesis of hopene from farnesyl diphosphate.

The two genes, *orf16* and *orf17*, located downstream of the *orf13* gene are annotated as 4-hydroxy-3-methylbut-2-en-1-yl diphosphate synthase (*ispG*) (EC:1.17.7.1) and 1-deoxy-D-xylulose 5-phosphate synthase (*dxs*) (EC:2.2.1.7) respectively. The latter protein was discovered to be required in the non-mevalonate pathway for isoprenoids biosynthesis (Rohmer, 1999), suggesting that hopanoid biosynthesis may depend on the alternative pathway.

The *orf14* gene is predicted to encode for a putative lipoprotein, on which the conserved domain belongs to the phosphorylase superfamily (Marchler-Bauer *et al.*, 2009). Members of this family include: purine nucleoside phosphorylase (PNP), Uridine phosphorylase and 5'-methylthioadenosine phosphorylase (MTA phosphorylase). These proteins catalyze the cleavage of a nucleoside to its corresponding base and sugar-1-phosphate (or sugar).

The genome annotation of *S. coelicolor* A3(2) classifies the *orf18* gene as encoding for an aminotransferase. A Basic Local Alignment Search Tool (BLAST) search of ORF18 protein shows that it possesses a putative conserved domain (OAT_like) corresponding to the *N*-acetyl ornithine aminotransferase family. This family belongs to a pyridoxal phosphate (PLP)-dependent aspartate aminotransferase superfamily. The major groups in this CD include: ornithine aminotransferase, acetylornithine aminotransferase, alanine-glyoxylate aminotransferase, dialkylglycine decarboxylase, 4-aminobutyrate aminotransferase, β-alanine-pyruvate aminotransferase, adenosylmethionine-8-amino-7-oxononanoate aminotransferase, and glutamate-1-semialdehyde 2,1-aminomutase. All these enzymes belonging to this family act on basic amino acids and their derivatives are involved in transamination or decarboxylation.

As a possible member of acetyl ornithine aminotransferase family, ORF18 is expected to catalyze the replacement of the keto group of an α-oxo acid by the α-amino group (or 5-amino group in the case of ornithine) from a basic amino acid. Otherwise, it could act on an aldehyde group instead of a α-keto group, as acetylornithine aminotransferase (ArgD) [EC:2.6.1.11] in the metabolism of arginine and proline. The proposed function fits the requirement of the reductive amination leading to aminobacteriohopanetriol from ribosylhopane.

Indeed, besides minor amount of diploptene, aminobacteriohopanetriol is the only elongated bacteriohopanoid detected in wild-type *S. coelicolor* A3(2) (Poralla *et al.*, 2000). Hopanoid biosynthesis in *S. coelicolor* A3(2) is severely affected by growth conditions. The strain does not produce hopanoids, or only minor amounts (a few μg/g, dry weight) in liquid culture but produces them on solid medium when sporulating. Mutants defective in the formation of aerial mycelium and unable to sporulate generally do not synthesize hopanoids, whereas mutants, which form aerial mycelium but no spores, do (Poralla *et al.*, 2000). This observation suggests that hopanoids may protect the cells against water loss through the plasma membrane in the aerial mycelium.

In this study, the putative function of the two *S. coelicolor* genes, *orf14* and *orf18,* were investigated. The hopanoid phenotypes were analyzed in the mutants respectively defective in the *orf14* and *orf18* genes, and allowed to deduce the role of the corresponding genes by comparison with the homologous genes of known functions.

Construction of the Δ*orf14* and Δ*orf18* mutants, as well as complementation of Δ*orf18* deletion mutant was carried out by E. Kannenberg (University of Tübingen and Athens, University of Georgia), E. Takano (University of Groningen) and T. Härtner (University of Tübingen). Analysis of hopanoid profiles was performed in collaboration with P. Schaeffer (University of Strasbourg) for GC and GC/EI-MS analysis and H. Talbot (University of Newcastle) for APCI-LC/MS[n].

I.2. Characterization of the *orf14* and *orf 18* genes

I.2.1. Hopanoid production in Δ*orf18* strain of *S. coelicolor* mutant

Δ*orf18* strain of *S. coelicolor* mutant were grown on a solid medium R2YE in Petri dishes with cellophane films applied on the top to facilitate harvesting of lipids (Poralla *et al.*, 2000). Formation of the ash gray aerial myceliums was observed. The extracts from lyophilized cells were first treated by H_5IO_6 and then $NaBH_4$ to cleave the polyhydroxylated side chains of hopanoids (Rohmer and Ourisson, 1976b; Rohmer *et al.*, 1984) and acetylated with Ac_2O/Py. 29-(2'-Hydroxyethyl)-hopane **4** acetate and diploptene **3** were present, indicating that the Δ*orf18* strain was capable of producing elongated C_{35} hopanoids.

In order to identify the hopanoid composition, the freeze-dried cell extracts were directly acetylated and then analyzed by gas chromatography/electron impact ionization mass spectrometry (GC/EI-MS) and atmospheric pressure chemical ionization liquid chromatography/ion trap mass spectrometry (APCI-LC/MS[n]).

BHT tetraacetate was identified by comparison of retention times and mass spectra with that of acetylated BHT of *Methylobacterium organophilum* (Renoux and Rhomer, 1985) by using GC/MS and with the reported data by using APCI-LC/MS[n] (Talbot *et al.* 2003a) (Fig. I-5). The presence of BHT tetraacetate in *S. coelicolor* was further confirmed by NMR spectroscopy.

More interestingly, ribosylhopane triacetate was detected by GC/MS and APCI-LC/MS[n] for the first time from a bacterium. The GC result shows the retention time of acetylated ribosylhopane of *S. coelicolor* is identical to that of the synthesized compound (Duvold and Rohmer, 1999; Bodlenner, unpublished work). It is worth to mention that the 35β-ribosylhopane decomposes during GC/MS analysis, giving rise to a degradation product with a molecular ion at m/z 550, and having a shorter retention time in GC (Fig. I-2A). Ion *m/z* 550 is also a characteristic fragment of ribosylhopane triacetate in EI-MS spectra by losing two molecules of AcOH (Fig. I-3). The EI-MS spectrum of this fragment gives ion *m/z* 191, the typical fragment of hopanoids produced by ring C cleavage, and *m/z* 287, probably resulted from the loss of one molecule of ethenone from fragment *m/z* 329 (Fig. I-2B and Fig. I-3). The 35α-ribosylhopane was however stable under the same GC/MS conditions, and showed all the important fragments in MS spectrometry as those observed from the

synthesized compounds, which are a mixture of 35α- and 35β-anomer [for the mass spectra of natural and chemically synthesized ribosylhopane (35α and 35β), see Appendix 2-6].
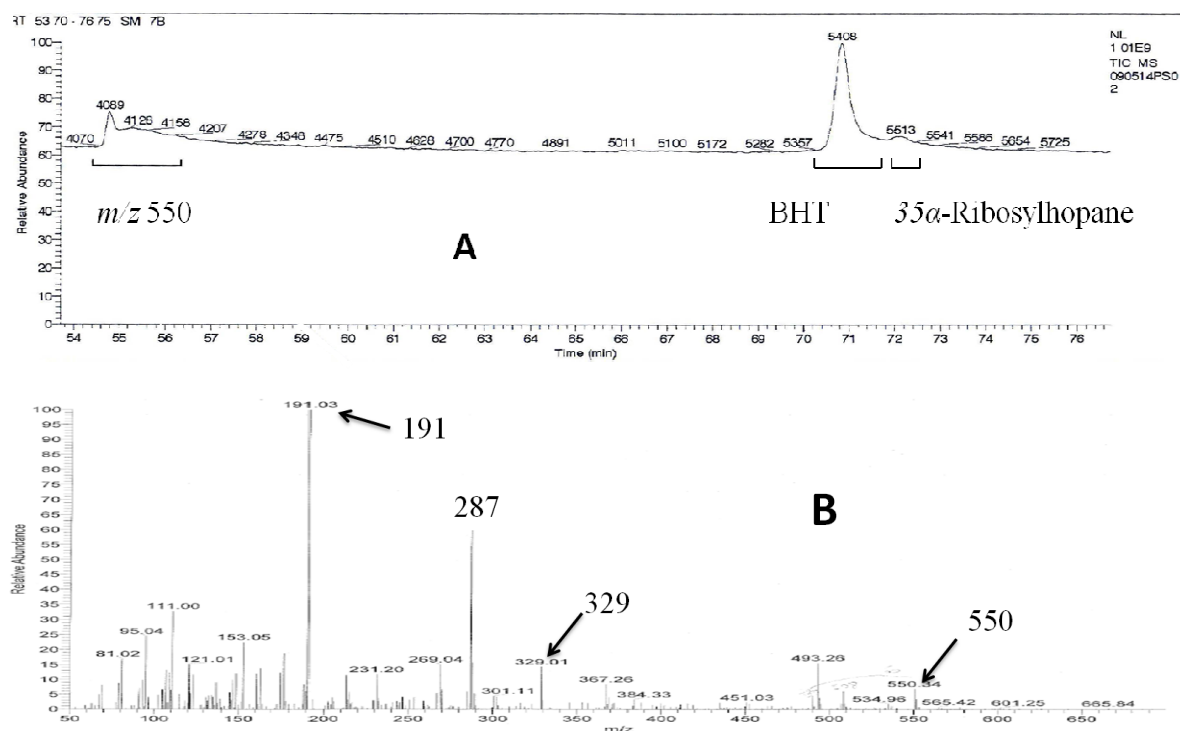

Fig. I-2. (A) Partial GC chromatogram showing the presence of BHT tetraacetate, ribosylhopan triacetate and the degradation product *m/z* 550. (B) EI-MS spectrum of the degradation product *m/z* 550.
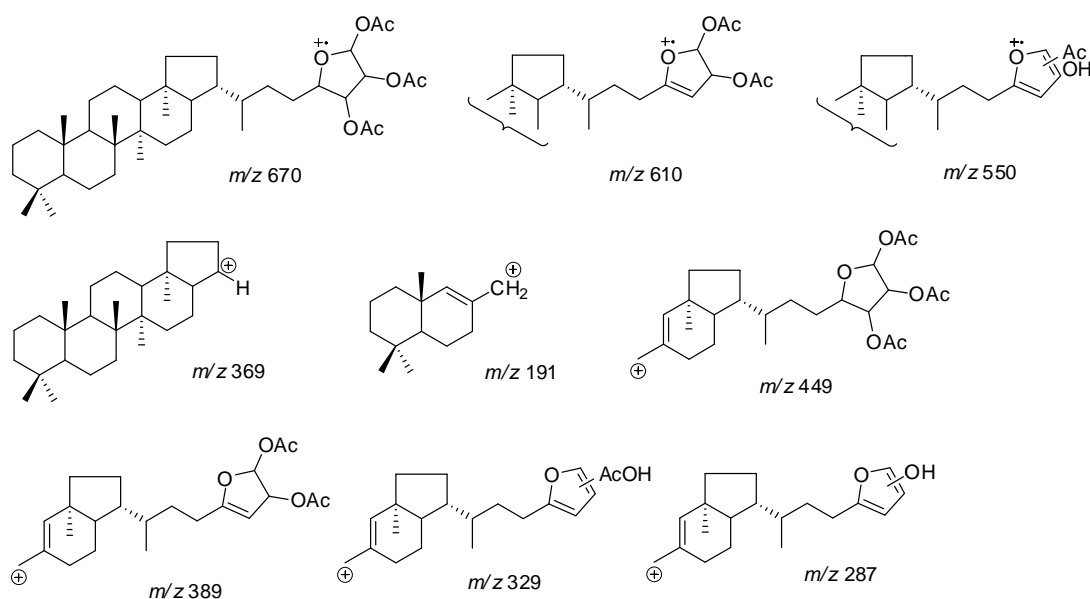

Fig. I-3. Possible fragmentations of ribosylhopane triacetate by EI-MS.

Presence of the two anomers of ribosylhopane triacetates was also confirmed by APCI-LC/MS[n] (Fig. I-4). For each anomer, both [M+H]+ 671 and [M+H-AcOH]+ 611 were found in the full mass spectrum in similar abundance. Fragmentation of [M+H-AcOH]+ 611 resulted in the ions more characteristic for ribosylhopane peracetate (Table I-1). The MS[2] spectra of acetylated ribosylhopane are in accordance with the MS[3] spectrum of adenosylhopane after initial loss of the adenine (Talbot *et al.*, 2007a).

Table I-1. Ribosylhopane triacetate fragments derived from APCI-LC/MS[n]

[M+H]+	[M+H-AcOH]+	[M+H -2AcOH]+	[M+H -3AcOH]+	ring C cleavage -AcOH	ring C cleavage -2AcOH	ring C cleavage -3AcOH	ring C cleavage
671	611	551	491	419	359	299	191
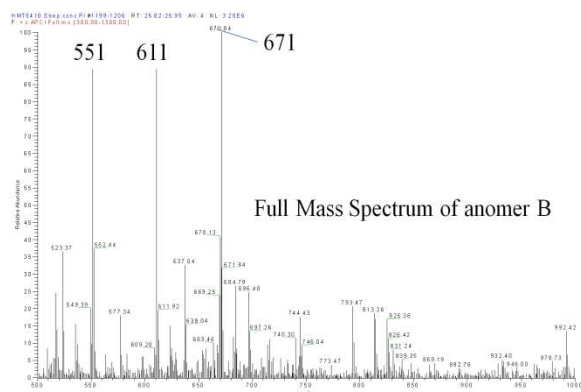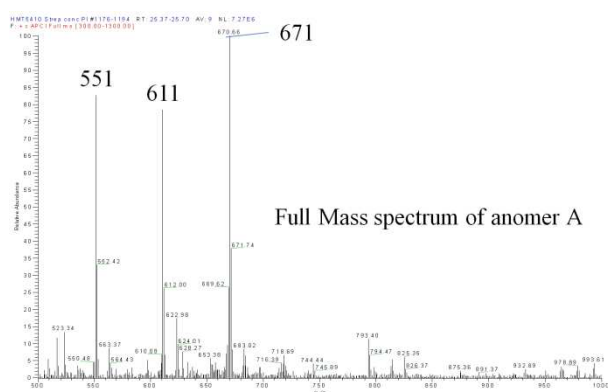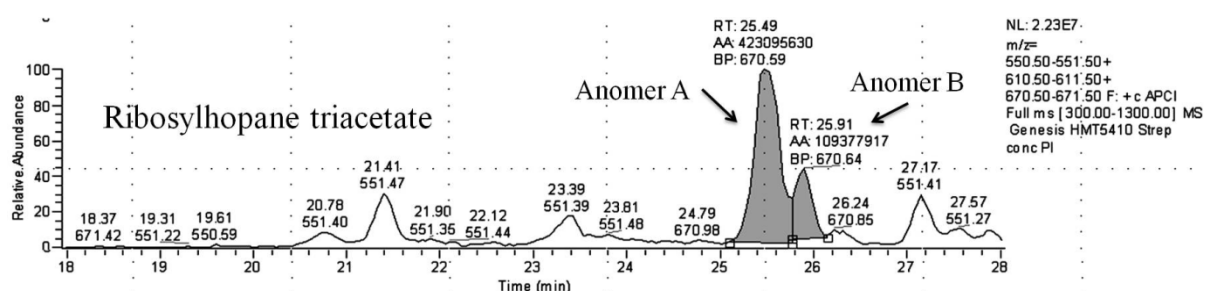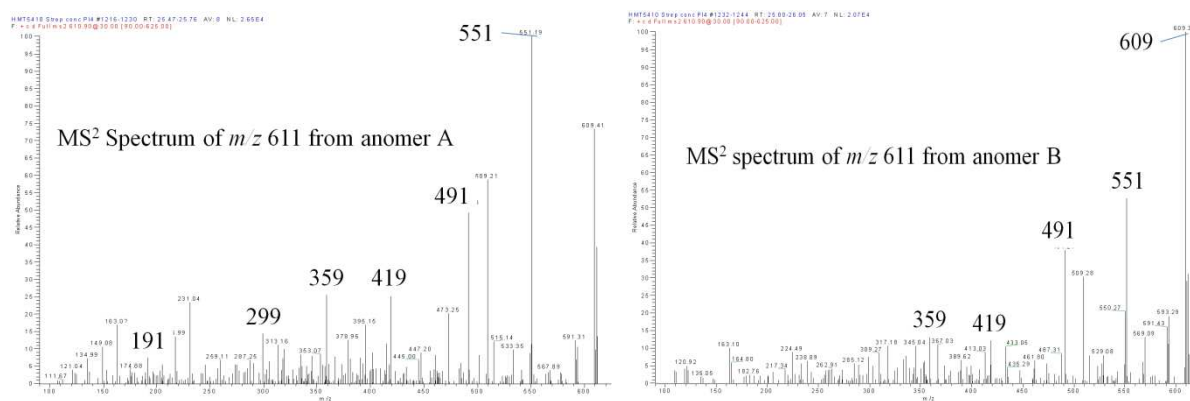
Fig. I-4. Mass chromatograms, full mass and MS^2 spectrums of ribosylhopane triacetate by APCI-LC/MS^n.

These two anomers of ribosylhopane (35α and 35β) were further isolated from the Δ*orf18* mutant of *S. coelicolor* and separated by RP-HPLC. Their structures were identified respectively by NMR spectroscopy. The derived NMR spectra are consistent with the reported data of the chemically synthetic ribosylhopane (Duvold and Rohmer, 1999; Françis *et al.* 1991; Neunlist *et al.* 1988; Stampf, 1992; Pan, 2005).

As adenosylhopane triacetate and aminobacteriohopanetriol tetraacetate are not amenable to GC/EI-MS due to their highly functionalized amphiphilic nature and/or larger molecular weight, the crude acetylated cell extracts were directly analyzed by APCI-LC/MS^n (Talbot *et al.*, 2003a; Talbot *et al.*, 2007a). The signature of aminobacteriohopanetriol tetraacetate has not been detected, but the characteristic fragments from adenosylhopane triacetate were observed (Fig. I-5).
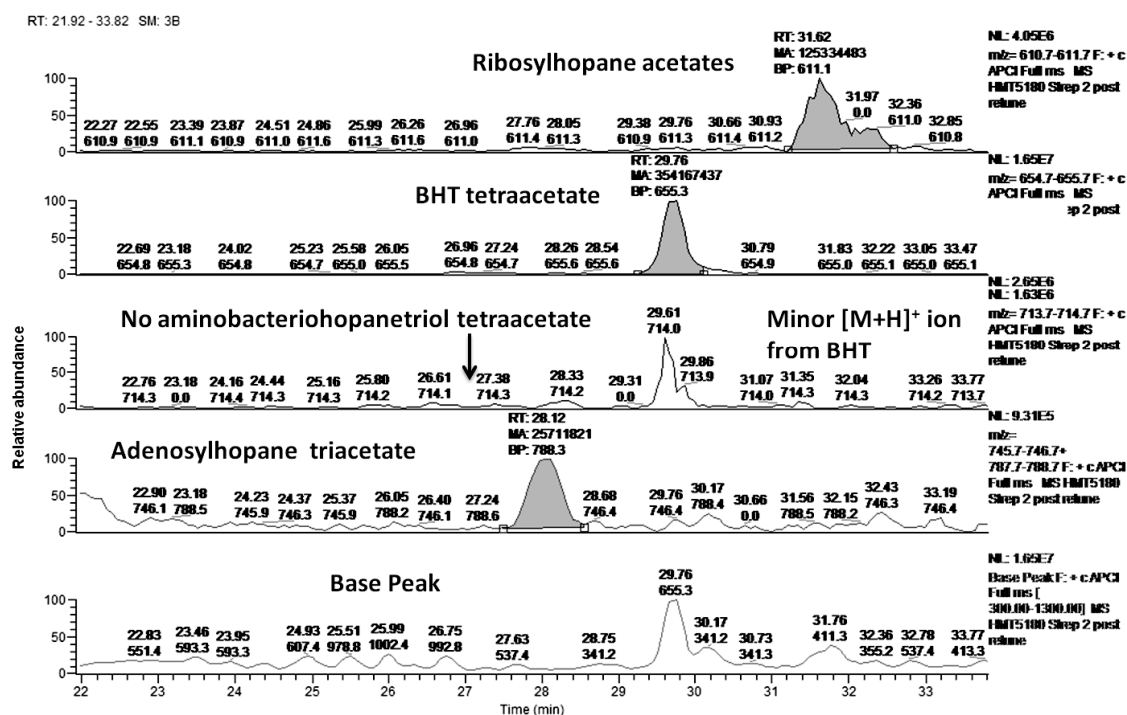
Fig. I-5. Partial APCI-MS base peak and mass chromatograms showing tetraacetate BHT, ribosylhopane triacetate and adenosylhopane triacetate.

The deletion of the *orf18* gene resulted in the absence of aminobacteriohopanetriol in *S. coelicolor*. In order to confirm the role of *orf18*, this silenced gene was reintroduced via a hygromycine-selective plasmid. This construct synthesized again aminobacteriohopanetriol like the wild-type strain (Table I-2, entry 3), whereas, in the construct bearing the plasmid alone without *orf18* gene, aminobacteriohopanetriol was not detected (Table I-2, entry 4).

Table I-2. Identification of the activity of the *orf18* gene produced in *S. coelicolor*.

	Strains	diploptene	adenosylhopane	ribosylhopane	BHT	aminobacteriohopanetriol
1	Wild-type	+	-	-	-	+
2	Δ*orf18*	+	+	+	+	-
3	*orf18* reintroduced	+	-	-	-	+
4	Empty plasmid	+	-	+	+	-

I.2.2. ORF18 protein is essential in the biosynthesis of aminobacteriohopanetriol

Deletion of the *orf18* gene in *S. coelicolor* resulted in the absence of aminobacteriohopanetriol as the only enlongated C_{35} hopanoid. In whilst, BHT, which is normally absent in the wild-type strain, was accumulated as a major product. Small amounts of ribosylhopane and trace amounts of adenosylhopane were also detected. Aminobacteriohopanetriol biosynthesis was restored when a copy of the *orf18* gene was re-introduced. These results indicate that the *orf18* gene is required in the biosynthesis of aminobacteriohopanetriol in *S. coelicolor*.

This is the first report of ribosylhopane as a natural product in a bacterium. Isolation of ribosylhopane in tiny quantity from Δ*orf18* mutant is in agreement with its hypothetical role as a precursor of bacteriohopanepolyols (BHPs), instead of a final product, in hopanoid biosynthesis. Serving as an intermediate, ribosylhopane is supposed to have a high turn-over and to be consumed in further transformation into final hopanoids, such as aminobacteriohopanetriol in the wild-type strain and BHT in the Δ*orf18* strain where it is present in a significant amount. In addition, the accumulation of small amounts of ribosylhopane may result from the relatively low efficiency of the enzyme(s) involved in the biosynthesis of BHT, which is not a normal intermediate of *S. coelicolor*. According to the hypothetical biosynthetic scheme for hopanoid side-chain biosynthesis in bacterium (Fig. I-6), ribosylhopane is supposed to be converted to BHT or aminobacteriohopanetriol respectively via two independent pathways. When the *orf18* gene is expressed in the wild-type *S. coelicolor*, ribosylhopane is completely converted into aminobacteriohopanetriol, and no other C_{35} bacteriohopanoids are detected. However, when this main route is blocked as in the Δ*orf18* strain, intermediates like adenosylhopane and ribosylhopane can be accumulated to some extent. The reduction of ribosylhopane into BHT may be performed by a non-specific aldose reductase. This unusual biosynthetic process in *S. coelicolor* is suggested by the rather low BHT concentration in the Δ*orf18* mutant as compared to the aminobacteriohopanetriol content in the wild-type strain. Last but not least, the trace amount of adenosylhopane, which has not been detected from wild-type *S. coelicolor*, is in accordance with the fact that it might also act as an intermediate in the formation of C_{35} bacteriohopanoids. However, its

relationship with ribosylhopane can not be proved by the hopanoid-production pattern of the Δ*orf18* mutant. Adenosylhopane may be the precursor of ribosylhopane, as presumed from the hypothetical hopanoid biosynthesis pathway, or it may be derived from ribosylhopane via adenylation.
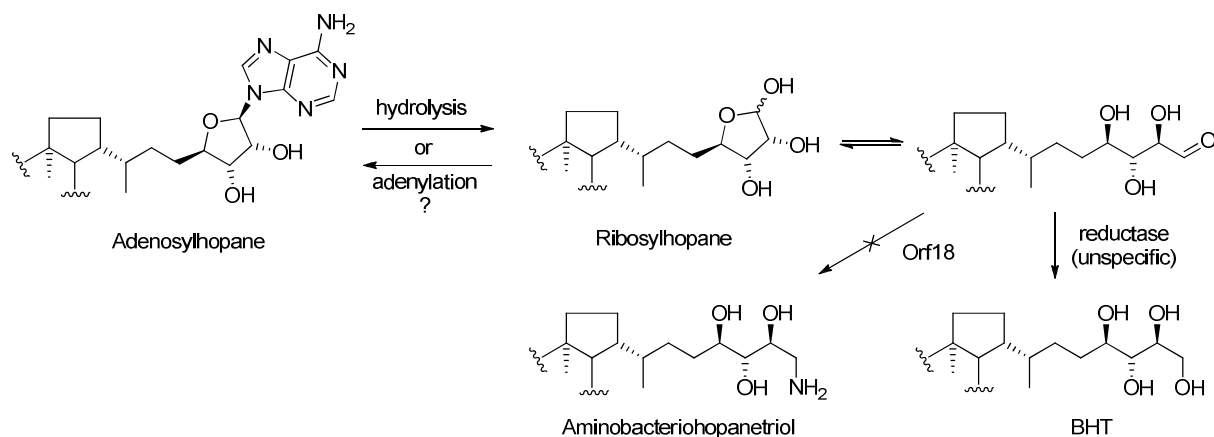

Fig. I-6. Hypothetical pathway for the side-chain biosynthethis of bacteriohopanoids in *S. coelicolor* deduced from the hopanoid phenotype of Δ*orf18* mutant.

I.2.3. Hopanoid production in Δ*orf14* strain of *S. coelicolor* mutant

The Δ*orf14* strain was grown under the same conditions as those utilized for the Δ*orf18* strain of *S. coelicolor*. The strain did not lose the ability to produce hopanoids since diploptene was still present. No C_{32} hopanoid has been observed after H_5IO_6/$NaBH_4$ degradation (Rohmer and Ourisson, 1976b; Rohmer *et al.*, 1984). This fact indicated the absence of elongated hopanoids, such as BHT or aminobacteriohopanetriol. However, the hopanoids with no free vicinal hydroxyl groups at C-32 and C-33, like adenosylhopane, escape from this derivatization method and thus not give the C_{32} bishomohopanol 4 after derivatization. APCI-LC/MS[n] analysis was therefore performed on the acetylated crude extracts for the directed search of adenosylhopane, which was found as the only functionalized C_{35} bacteriohopanoid in significant amount (Fig. I-7).
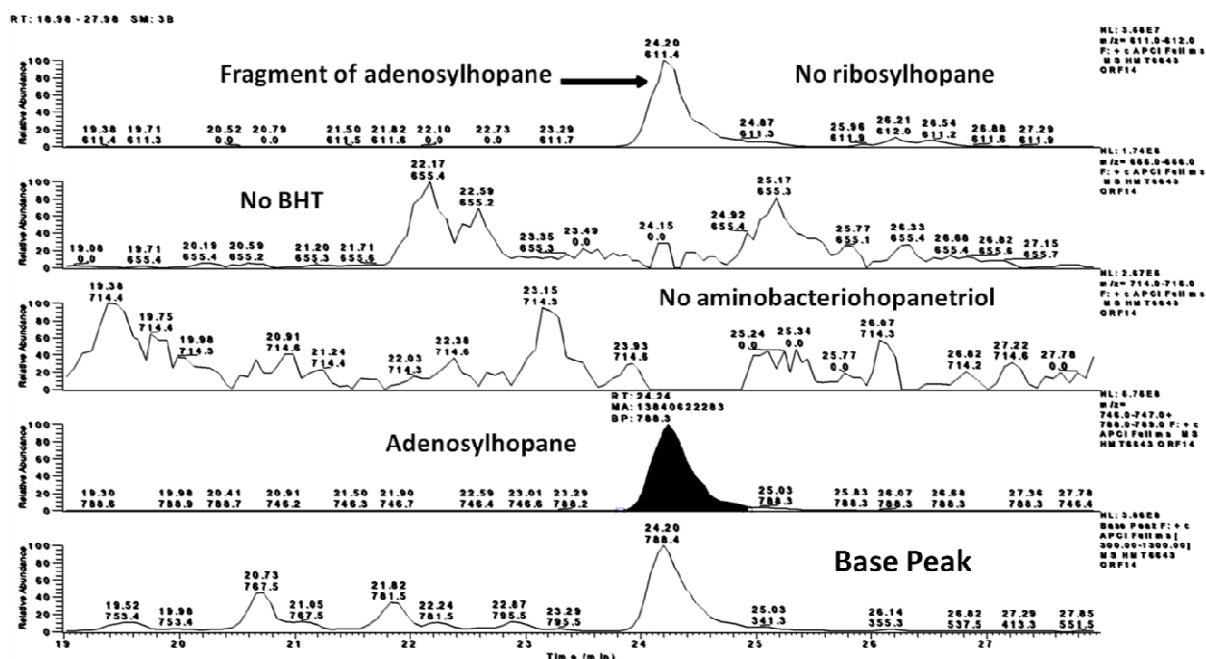
Fig. I-7. Partial APCI-MS base peak and mass chromatograms showing the presence of adenosylhopane triacetate in *S. coelicolor* Δ*orf14* mutant.

I.2.4.   ORF14 protein is required to produce both bacteriohopanetetrol and bacteriohopanetriol

The strain lacking the *orf14* gene failed to produce aminobacteriohopanetriol, but accumulated adenosylhopane. This mutant still contains a functional copy of the putative aminotransferase ORF18 and the unknown enzyme(s) for BHT production, which means it is capable of converting ribosylhopane, if there is any, into aminobacteriohopanetriol or BHT. However, no trace of ribosylhopane, BHT or aminobacteriohopanetriol has been detected, but adenosylhopane was observed as the only C_{35} hopanoid identified by ACPI-LC/MS^n method. This fact suggests that the biosynthesis of ribosylhopane is blocked, and that adenosylhopane serves as a possible precursor of ribosylhopane. This argument is consistent with the presumed function of the deleted gene. The conserved domain in ORF14 suggested that it might act like a nucleosidase or phosphorylase belonging to the phosphorylase superfamily, cleaving the adenosyl group from adenosylhopane and affording ribosylhopane consequently. In the wild-type *S. coelicolor*, adenosylhopane is supposed to be transformed into ribosylhopane. However, when the *orf14* gene is removed from *S. coelicolor*, the deadenylation is apparently blocked. Adenosylhopane, the substrate of the encoded enzyme, is

accumulated, and the corresponding product, ribosylhopane or any further derivatives, are not produced.

Alternatively, the hopanoid profile of the Δorf14 strain may be differently interpreted. Adenosylhopane and ribosylhopane are derived from a common precursor via separated pathways, as the supposed biosynthesis of BHT and aminobacteriohopanetriol from ribosylhopane. This argument is, however, probably untenable, because no novel hopanoid was detected in this study. Diploptene can not serve as a direct precursor either, since the delected gene *orf14* is supposed to encode for a hydrolysis/phosphorolysis reaction instead of an addition/substitution reaction which would probably be required for the conversion of diploptene into ribosylhopane.

I.2.5. Bioinformatic exploration of hopanoid biosynthesis associated genes in *S. coelicolor*

Recently, it was shown in *Methylobacterium extorquens* and *Rhodopseudomonas palustris* that the *hpnG* gene, a putative nucleoside phosphorylase or nucleosidase, and the *hpnH* gene, a radical SAM protein, are required for the addition of the bacteriohopanoid C_5 side chain (Bradley *et al.*, 2010; Welander *et al.*, 2012). The *hpnG* and *hpnH* genes are frequently found in the same locus as *shc* and other genes associated with the biosynthesis of hopanoids, indicating that those genes are closely related to hopanoid production. For example, a hopanoid biosynthesis locus was described in *Zymomonas mobilis* consisting of the genes *hpnA-E* and *shc* (*hpnF*) (Perzl *et al.*, 1998). Continuing past *shc* are found the genes *hpnG* and *hpnH*. Granted, in *Z. mobilis*, *hpnH* is in a convergent orientation with respect to *hpnA-G*, but one gene beyond *hpnH* and running in the same convergent direction is *IspH*, an essential enzyme of IPP biosynthesis and therefore essential for the biosynthesis of hopanoids. Extending the gene symbol sequence, the symbol *hpnG* and *hpnH* are suggested for these genes in NCBI databank. Annotation for the <u>hopan</u>oid-associated *hpn* genes is listed in appendix 1. According to the putative function, protein HpnH is supposed to utilize an iron-sulfur redox cluster and *S*-adenosylmethionine to carry out the conversion of diploptene to adenosylhopane, which was suggested as the first intermediate in hopanoid side-chain biosynthesis (Bradley *et al.*, 2010); protein HpnG may be engaged in the subsequent cleavage

of the adenosyl group from adenosylhopane, affording ribosylhopane 35-phosphate or ribosylhopane as an intermediate (Bradley *et al.*, 2010; Welander *et al.*, 2012). Ribosylhopane or phosphorilated ribosylhopane was, however, never detected in these studies.

Comparison of the conserved domain on ORF14 protein with those on HpnG proteins in NCBI data bank shows significant similarity (Cd Length: 212; Bit Score: 67.75; E-value: 2.04e-14). A BLAST analysis suggested that the *S. coelicolor* ORF14 protein may be a homolog to the two recently reported HpnGs in *M. extorquens* and *R. palustris* (Bradley *et al.* 2010; Welander *et al.* 2012). The identity of ORF14 towards *M. extorquens* HpnG is 67% (E-value: 2e-07; query cover: 40%) and 40% (E-value: 7e-10; query cover: 50%) towards *R. palustris* HpnG. Analysis on co-occurring proteins based on the STRING database showing that up to 96% bacterial genomes, which encode for apparent SHCs, also have ORF14 homologs. Based on the strong linkage of ORF14 protein with HpnGs and SHCs, as well as the altered hopanoid phenotype of Δ*orf14* mutant of *S. coelicolor*, protein ORF14 is consequently suggested as a HpnG protein.

To further explore the nature of the HpnG proteins as a purine nucleoside phosphorylase or as a nucleosidase, protein sequences of ORF14 and the other nine HpnG proteins from diverse species of bacteria were aligned together with 5'-methylthioadenosine/*S*-adenosylhomocysteine (MTA/AdoHcy) nucleosidase from *Escherichia coli* (Fig. I-8). MTA/AdoHcy nucleosidase is a key enzyme in a number of critical biological processes in many microbes. This nucleosidase catalyzes the irreversible hydrolysis of the N^9–$C^{1'}$ bond of MTA or AdoHcy to form adenine and the corresponding thioribose (Lee *et al.*, 2003). Alignment of these protein sequences shows that 4.6% amino acid residues were identical, and important amino acid residues of the active sites are fairly conserved from MTA/AdoHcy nucleosidase (Fig. I-9). The catalytic residues (E12 and D197) are invariant as are the residues involved in coordinating the catalytic water (M9, E174 and R193). Moreover, M173 is also strictly conserved, whose role is to stabilizing and orienting the ribose moiety of the substrate.

Fig. I-8. Sequence alignment of various species of HpnG proteins with the ORF14 protein and MTA/AdoHcy nucleosidase.

Fig. I-9. Active sites of MTA/AdoHcy nucleosidase of *E. coli* (Lee *et al.*, 2003). A schematic representation of the interactions made between the nucleosidase and formycin A. *Dotted lines* represent protein-protein or protein-ligand hydrogen bonds with distances in angstroms (Å). Residues donated from a neighboring subunit are shown in *shaded boxes*.

Lower identity (1.7%) is found for the alignment of the sequences of the ORF14 and the same HpnG proteins with *E. coli*. PNP. Conservation of the phosphate binding sites (G20, R24, R87 or S90) is not observed (Erion *et al.*, 1997; Bennett *et al.*, 2003, Štefanić *et al.*, 2012). However, a few residues coordinated with the ribose (V178, E179 and M180) and base (V178, E179, M180 and D204) retain.

Based on the conserved domain of ORF14, we presume that it may more likely encode for a nucleosidase. Therefore, the activity of ORF14 is supposed to cleave the adenine moiety from the adenosylhopane, resulting ribosylhopane instead of ribosylhopane 35-phosphate.

The HpnO protein, a homolog of ornithine-oxo-acid aminotransferase, was shown to be required in the biosynthesis of aminobacteriohopanetriol in *R. palustris* (Welander *et al.*, 2012). All the tested bacteria with the genes homologous to the *hpnO* gene of *R. palustris* have been shown to produce terminal aminoBHPs (Welander *et al.*, 2012). This fact matches with the role of the HpnO protein as an aminotransferase associated with hopanoid biosynthesis. The protein sequences of *R. palustris* HpnO and ORF18 were compared and

resulted in 52% of identity (E value: 5e-167; query cover; 98%), indicating that the *orf18* gene may be a homolog to *hpnO* genes.

The genes on cosmid SC6A5 were queried to the genomes that were predicted to contain a copy of *hpnO*. A synteny map representing the distribution of *S. coelicolor* genome homologs in other genomes based on NCBI databank is showed in Fig. I-10. Each row on the map corresponds to one genome replicon (chromosome or plasmid).

Great resemblance is found not only for the homologous genes but also for the preserved co-localization of genes on chromosomes of different species. Conserved DXS homologs in these genomes suggest that the biosynthesis of isoprene in these microbes may depend on the MEP pathway. SHCs and putative aminotransferases are present in all the analyzed genomes. This is consistent with their predicted ability to produce aminoBHPs. Another group of conserved genes is *orf15* homologs, some of which are classified as the *hpnH* gene as in *R. palustris* and *Catenulispora acidiphila*. Sequence of ORF15 was further compared to those of the documented HpnH proteins (159 hits) in NCBI database. Significant identities were shown from 100% to 49% with the maximal e-value of $1e^{-91}$. This indicates that *orf15* gene may be associated with hopanoid biosynthesis in *S. coelicolor*, catalyzing the first step in the side-chain formation to produce adenosylhopane.

An apparently conserved genomic region, including two putative squalene synthases, one dehydrogenase, SHC, the SAM radical protein and nucleotide phosphorylase, was observed on chromosomes of the aminoBHP-producing bacteria. The relative position of these genes in the genomes is consistent (an example is given in Fig. I-11). Exceptional conservation of the synteny group not only points out the orthologous genes with similar functions, but may also reflect important functional relationships between the genes: these hopanoid-associated genes may interact one with each other in critical ways.
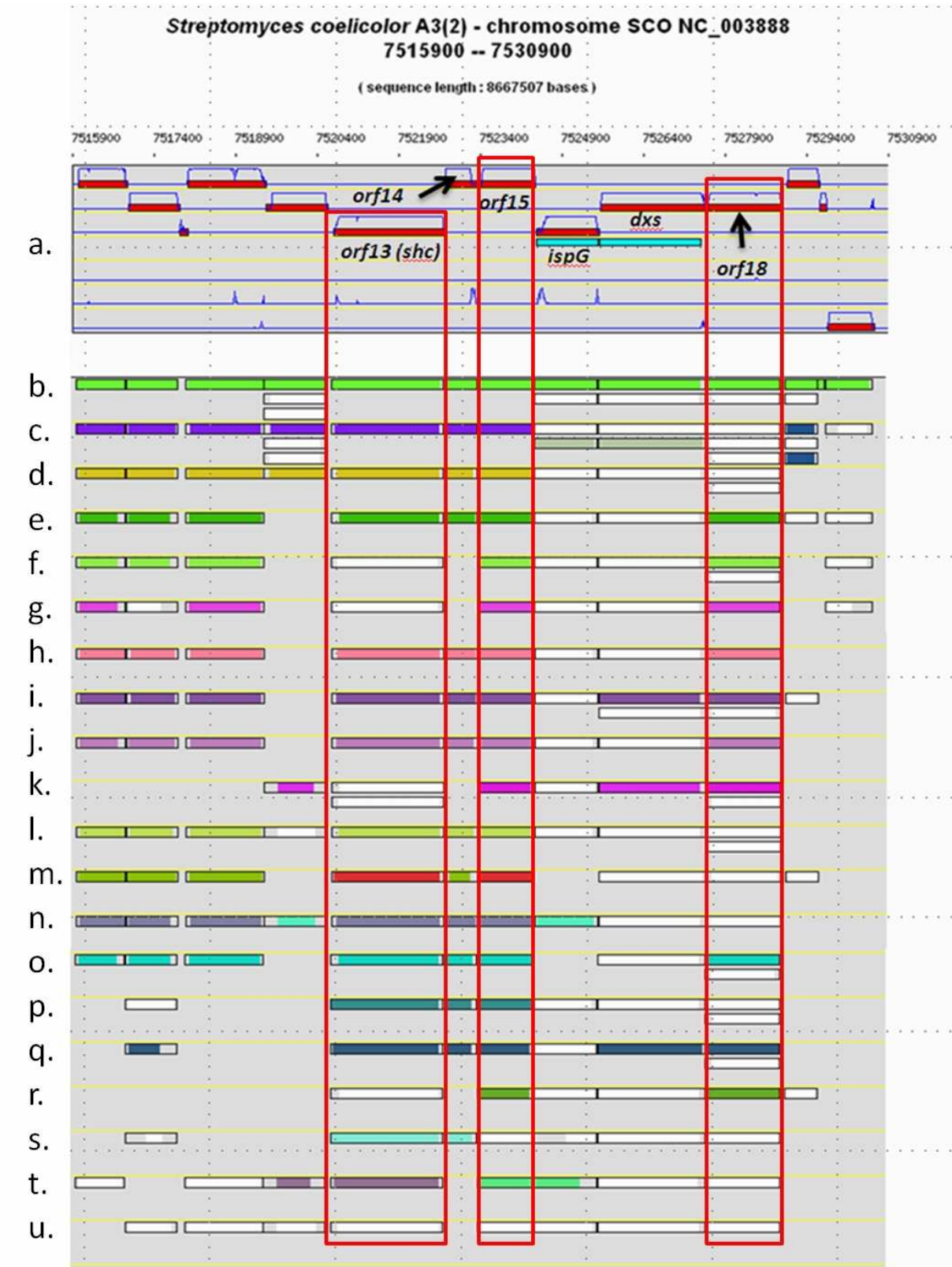
Fig. I-10. Synteny map with representation by pairs of genomes calculated from NCBI databank. (1) Sequence similarity is valued by BlastP bidirectional best hit or at least 30% identity on 80% of the shortest sequence (minLrap 0.8). (2) A rectangle has the same size as the CDS to which it is homolog. (3) The color of the rectangles reflects synteny conservation,

with the exception of the white color; a group of rectangles which share a common color shows that there is a conservation of the synteny between the current genome and the genome of the synteny map; rectangles filled with white color indicate homologs that don't belong to a synteny group. The color code has to be interpreted by replicon, i.e. by row. The same color on two synteny map rows doesn't indicate any synteny relationship. (4) The filling of a rectangle reflects the alignment quality between the two proteins. (5) a. *Streptomyces. coelicolor*; b. *Streptomyces avermitilis*; c. *Catenulispora acidiphila*; d. *Acidothemus cellulolyticus*; e. *Bradyrhizobium japonicum*; f. *Bradyrhizobium* sp. BTAi1; g. *Bradyrhizobium* sp. ORS278; h. *Rhodopseudomonas palustris*; i. *Oligotropha carboxidovorans*; j. *Nitrobacter hamburgensis*; k. *Pelobacter carbinolicus*; l. *Beijerinckia indica*; m. *Acidobacterium capsulatum*; n. *Methylocella silvestris*; o. *Nitrobacter winogradskyi*; p. *Nitrosospira multiformis*; q. *Methylococcus capsulatus*; r. *Desulfovibrio salexigens*; s. *Nitrosomonas europaea*; t. *Methylacidiphilum infernorum*; u. *Microcystis aeruginosa.*
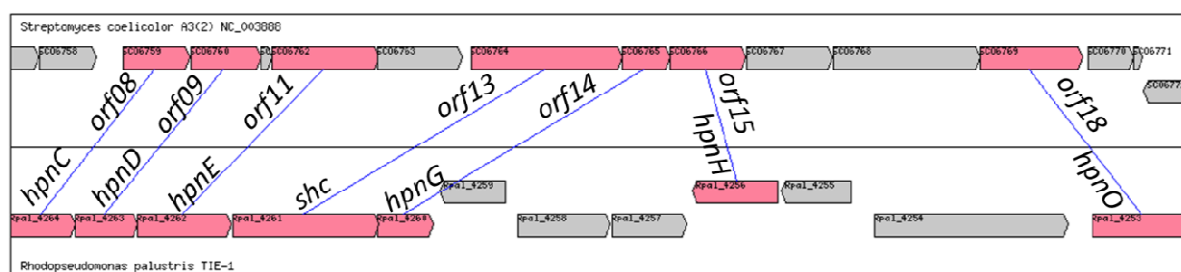
Fig. I-11. Consistent synteny patterns in pairwise representation between *S. coelicolor* and *R. palustris.*

Given these information, the genes probably involved in hopanoid biosynthesis in *S. coelicolor* are summarized in table I-3 with putative functions

Table I-3. Genes hypothetically involved in hopanoid biosynthesis in *S. coelicolor*. Annotation was given according to the Genome Project, Poralla *et al.* (2000) and our work.

orf	SCO locus	Homologs	Annotation	Hypothetical or known function
08	6759	*hpnC*	Squalene/phytoene synthase	Synthesis of squalene
09	6760	*hpnD*	Squalene/phytoene synthase	Synthesis of squalene
11	6761	*hpnE*	Squalene-associated dehydrogenase	Synthesis of squalene
13	6764	*shc*	Squalene-hopene cyclase	Formation of hopanoid cyclic backbone
14	6765	*hpnG*	Hopanoid biosynthesis associated phosphorylase	Cleavage of adenine from side chain
15	6766	*hpnH*	Hopanoid biosynthesis associated radical SAM protein	Addition of adenosyl group to isopropyl hopane side chain
18	6769	*hpnO*	Ornithine-oxo-acid transaminase	aminobacteriohopanetriol biosynthesis

I.3.   Conclusion

Deletion mutation of two genes, *orf14* and *orf18*, in *Streptomyces coelicolor* A3(2) produced strains with two distinct hopanoid profiles that differed from those found in the wild-type strain. This work provides evidence for linking the genes *orf14* and *orf18* to specific reactions of hopanoid side chain biosynthesis. The *orf14* gene is involved in the formation of ribosylhopane from adenosylhopane. The homologs of *orf14* gene were present in the majority of hopanoid producing organisms, suggesting the central roles of adenosylhopane and ribosylhopane, which was identified for the first time in a bacterium, in the formation of hopanoid side chain. The *orf18* gene is required for aminobacteriohopanetriol biosynthesis. Examination of the nucleotide sequences of *orf18* gene in bacteria might have the potential to predict the production of terminal aminoBHPs. Characterization of the *orf14* and *orf18* genes in *S. coelicolor* helps us to better elucidate the pathway of hopanoid side-chain biosynthesis.

I.4.   Experimental Part

I.4.1. Bacteria and Culture conditions

Wild-type strain used in this study is *Streptomyces coelicolor* A3(2). The Δ*orf 14* and Δ*orf18* mutants were obtained from Dr. E. Kannenberg and Dr. T. Härtner (University of Tübingen). The strains used in complementation of Δ*orf18* deletion mutant are obtained from Prof. E. Takano (University of Groningen). All cultures on agar solid medium R2YE (Poralla *et al*. 2000) were cultivated on cellophane discs at 30 °C in Petri dishes. Cellophane was placed above the solid medium, and cultures were grown on the surface of cellophane without direct contact with the agar medium. At the end of the cultures, they were harvested with the cellophane paper together for subsequent extraction of lipids. The growing time of different strain varies: 3 days for wild-type strain, 7~8 days for the Δ*orf18* strain, 16 days for the strains in complementation experiment and 8~10 days for the Δ*orf14* strain.

R2YE medium used in the cultivation of all *S. coelicolor* A3(2) strains:

Yeast extract	4 g/L
Malt extract	10 g/L
Glucose	4 g/L
Agar	20 g/L
pH = 7.5	

Apramycin	50 μg/mL (for Δ*orf 14* and Δ*orf18* strains and complementation experiment)
Hygromycine	50 μg/mL (only for the complementation experiment)

I.4.2. Identification of bacteriohopanoids from *S. coelicolor*

I.4.2.1. Aminobacteriohopanetriol tetraacetate from wild-type *S. coelicolor*

35-Amino-(22R,32R,33R,34S)-bacteriohopanetriol tetraacetate
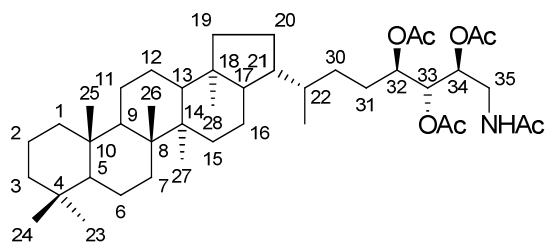
The lyophilized cells collected from 36 Petri dishes were extracted with MeOH/CHCl$_3$ (1:2, v/v, 150 mL) under reflux for 45 min for three times. The combined extract was concentrated and dried under vacuum overnight. The residue was acetylated with acetic anhydride in pyridine (1:2, v/v, 1 mL) at room temperature overnight and then evaporated to dryness. The directly acetylated cell-extracts were first purified by FCC (EtOAc/DCM, 1:4). The fractions containing hopanoids were further purified by preparative TLC using MeOH/CH$_2$Cl$_2$ (5:95, v/v) as the eluent, and afforded aminobacteriohopanetriol tetraacetate (0.14 mg) (R$_f$=0.54) (Neunlist *et al.*, 1988).

^{1}H-NMR (300MHz, CDCl$_3$): δ/ppm = 6.069 (1H, t, J = 6.2 Hz, -N*H*Ac), 5.091 (1H, dd, J = 6.2, 4.0 Hz, 33-H), 4.996 (1H, ddd, J = 6.3, 6.2, 3 Hz, 34-H), 4.913 (1H, ddd, J = 9.6, 3.9, 3.5 Hz, 32-H), 3.584 (1H, ddd, J = 14.7, 6.2, 3.1 Hz, 35-H$_b$), 3.295 (1H, dt, J = 14.6, 6.3Hz, 35-H$_a$), 2.014 (3H, s, C*H*$_3$COO-), 1.989 (3H, s, C*H*$_3$COO-), 1,961 (3H, s, C*H*$_3$COO-), 1.877 (3H, s, C*H*$_3$CONH-), 0.867 (6H, s, 8β and 14α-Me), 0.825 (3H, d, *J*= 6.4 Hz, *22R*-Me), 0.767 (3H, s, 10β-Me), 0.734 (3H, s, 4α-Me), 0.712 (3H, s, 4β-Me), 0.603 (3H, s, 18α-Me).

^{13}C-NMR (75MHz, CDCl$_3$): δ/ppm = 170.4 (CH$_3$*C*O-), 170.2 (CH$_3$*C*O-), 169.9 (2 CH$_3$*C*O-), 71.8 (C-32), 71.5 (C-33), 70.5 (C-34), 55.9 (C-5), 54.2 (C-17), 50.2 (C-9), 49.1 (C-13), 45.7 (C-21), 44.1 (C-18), 41.9 (C-3), 41.6 and 41.5 (C-8 and C-14), 41.4 (C-19), 40.1 (C-1), 38.8 (C-35), 37.2 (C-10), 35.8 (C-22), 33.5 (C-15), 33.2 (C-23), 33.1 (C-7), 33.0 (C-4), 30.7 (C-30), 27.3 (C-20), 25.5 (C-31), 23.8 (C-12), 22.9 (CH$_3$CONH-), 22.7 (C-16), 21.4 (C-24), 20.8 and 20.6 (3 *C*H$_3$COO-), 19.6 (C-29), 18.5 (C-2 and C-6), 16.4 and 16.3 (C-26 and C-27), 15.7 and 15.6 (C-25 and C-28).

EI-MS spectrum (direct-inlet): *m/z* = 713 (M$^+$, 9%), 698 (M$^+$-Me, 4%), 653 (M$^+$-AcOH, 25%), 638 (M$^+$-Me-AcOH, 6%), 492 (ring C cleavage, 100%) (Budzikiewicz *et al.*, 1963), 432 (ring C cleavage-AcOH, 19%), 369 (M$^+$-side-chain, 21%), 312 (ring C cleavage-3AcOH, 26%),

253 (ring C cleavage-3AcOH-AcNH, 46%), 191 (ring C cleavage, 86%)

I.4.2.2. Ribosylhopane triacetate and bacteriohopanetetrol tetraacetate from Δ*orf18* strain

The lyophilized cells collected from 340 Petri dishes were extracted with MeOH/CHCl$_3$ (1:2, v/v, 500 mL) under reflux for 45 min for three times. The combined extract (1.4 g) was concentrated and then acetylated with AcO$_2$/Py (1/2, v/v, 6 mL). The acetylated extract was fractionated by flash chromatography using CH$_2$Cl$_2$ (60 mL) and then AcOEt/DCM (2:8, v/v, 60 mL) to give pink/orange fractions containing hopanoids. The proper fractions were collected, concentrated and then further purified by a TLC method on silica gel (AcOEt/hexane, 1:5, v/v) (Schaeffer *et al.*, 2008). Lipids were visualized on preparative TLC under UV light (366 nm) using rhodamine as revelator.

Further purification by RP-HPLC (MeOH/iPrOH/H$_2$O, 33/16/1 by C$_{18}$ Polaris Varian, 250×20 nm, 5 μm, 1 mL min^{-1}) of fraction R$_f$ 0.23 afforded bacteriohopanetetrol tetraacetate (2.5 mg), of fraction R$_f$ 0.14 afforded 35α-ribosylhopane triacetate (0.5 mg) and of fraction R$_f$ 0.32 afforded 35β-ribosylhopane triacetate (1 mg).

35β-Ribosylhopane triacetate
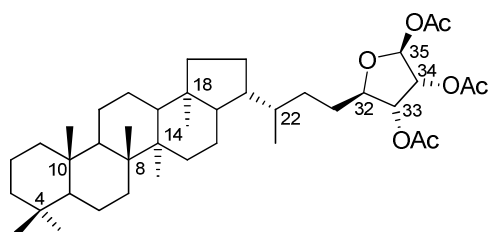
^{1}H NMR (500 MHz, CDCl$_3$): δ/ppm = 6.121(1H, br.s, 35β-H); 5.318 (1H, br.dd, *J* = 5.0 Hz, 34-H), 5.181 (1H, dd, *J* = 6.4, 5.0 Hz, 33-H), 4.123 (1H, m, 32-H), 2.111 (3H, s, -COC*H*$_3$), 2.077 (3H, s, -COC*H*$_3$), 2.064 (3H, s, -COC*H*$_3$); 0.945 (6H, s, 8β and 14α-Me), 0.925 (3H, d, *J*= 6.4 Hz, *22R*-Me), 0.842 (3H, s, 4α-Me), 0.810 (3H, s, 10β-Me), 0.788 (3H, s, 4β-Me), 0.690 (3H, s, 18α-Me).

^{13}C NMR (125 MHz, CDCl3): δ/ppm = 170.0, 169.7, 169.5, 98.3, 82.3, 74.8, 73.8, 56.1, 54.3, 50.3, 49.2, 45.9, 44.4, 42.1, 41.8, 41.6, 41.5, 40.3, 37.4, 36.4, 33.6, 33.4, 33.3, 33.2, 31.0, 30.8, 27.5, 23.9, 22.7, 21.6, 21.2, 20.9, 20.7 (×2), 20.0, 18.7, 16.6, 16.5, 15.9 (×2).

EI-MS spectrum (direct inlet): m/z = 670 (M$^+$, 2%), 610 (M$^+$–AcOH, 50%), 595 (M$^+$–AcOH–Me, 19%), 550 (M$^+$–2AcOH, 2%), 449 (ring C cleavage, 7%) (Budzikiewicz *et al.*, 1963), 435 (17%), 389 (ring C cleavage–AcOH, 87%), 369 (M$^+$–side chain, 25%), 329 (10%), 287 (11%), 269 (15%), 191 (ring C cleavage, 100%).

35α-Ribosylhopane triacetate
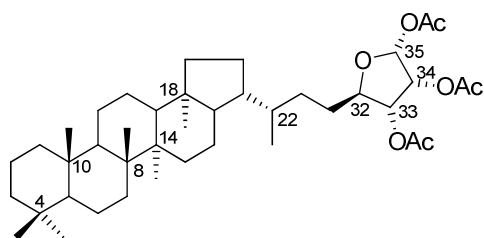
^{1}H NMR (500MHz, CDCl$_3$): δ/ppm = 6.362 (1H, d, J = 4.5 Hz, 35β-H), 5.207 (1H, dd, J = 6.8, 4.5 Hz, 34-H), 5.041 (1H, dd, J = 6.8, 3.6 Hz, 33-H), 4.193 (1H, m, 32-H), 2.114 (3H, s, -COCH_3), 2.103 (3H, s, -COCH_3), 2.058 (3H, s, -COCH_3), 0.945 (6H, s, 8β and 14α-Me), 0.922 (3H, d, J = 6.4 Hz, *22R*-Me), 0.842 (3H, s, 4α-Me), 0.811 (3H, s, 10β-Me), 0.788 (3H, s, 4β-Me); 0.687 (3H, s, 18α-Me).

EI-MS spectrum (direct inlet): m/z = 670 (M$^+$, 2%), 610 (M$^+$-AcOH, 27%), 595 (M$^+$-AcOH-Me, 9%), 550 (M$^+$–2AcOH, 1%), 449 (ring C cleavage, 29%) (Budzikiewicz *et al.*, 1963), 389 (ring C cleavage-AcOH, 67%), 369 (M$^+$–side chain, 26%), 329 (7%), 287 (7%), 269 (14%), 191 (ring C cleavage, 100%).

(22*R*,32*R*,33*R*,34*S*)-Bacteriohopanetetrol tetraacetate
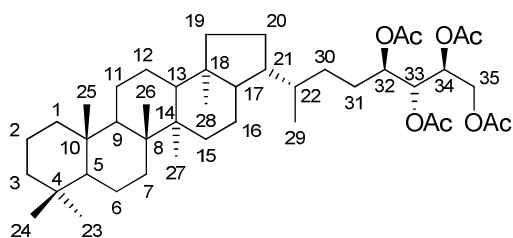
^{1}H NMR (500MHz, CDCl$_3$): δ/ppm = 5.259 (1H, ddd, J = 6.6, 5.6, 2.3 Hz, 34-H), 5.218 (1H, dd, J = 5.6, 4.4 Hz, 33-H), 5.020 (1H, ddd, J = 9.6, 4.3, 3.4 Hz, 32-H), 4.376 (1H, dd, J = 12.2, 2.5 Hz, 35-H$_a$), 4.139 (1H, dd, J = 12.1, 6.6 Hz, 35-H$_b$), 2.083 (3H, s, -COCH_3), 2.077 (3H, s, -COCH_3), 2.070 (3H, s, -COCH_3), 2.050 (3H, s, -COCH_3), 0.926 (6H, s, 8β and

14α-Me), 0.891 (3H, d, J = 6.4 Hz, *22R*-Me), 0.832 (3H, s, 4α-Me), 0.795 (3H, s, 10β-Me), 0.775 (3H, s, 4β-Me), 0.665 (3H, s, 18α-Me).

^{13}C NMR (125 MHz, CDCl$_3$): δ/ppm = 170.8 (-*C*OCH$_3$), 170.5 (-*C*OCH$_3$), 170.1 (-*C*OCH$_3$), 169.8 (-*C*OCH$_3$), 71.8 (C-34), 71.5 (C-33), 69.4 (C-32), 62.1 (C-35), 56.0 (C-5), 54.2 (C-17), 50.3 (C-9), 49.1 (C-13), 45.8 (C-21), 44.3 (C-18), 42.0 (C-3), 41.7 and 41.6 (C-8 and C-14), 41.5 (C-19), 40.2 (C-1), 37.3 (C-10), 36.0 (C-22), 33.6 (C-15), 33.4 (C-23), 33.2 and 33.1 (C-4, C-23 and C-7), 30.8 (C-30), 27.5 (C-20), 26.0 (C-31), 23.9 (C-12), 22.7 (C-16), 21.6 (C-24), 21.0 (-CO*C*H$_3$), 21.0 (-CO*C*H$_3$×2), 20.8 (-CO*C*H$_3$×2 and C-11), 19.8 (C-29), 18.6 (C-2 and C-6), 16.5 and16.4 (C-26 and C-27), 15.9 and15.8 (C-25 and C-28)

EI-MS spectrum (direct-inlet): m/z = 699 (M[+]-Me, 2%), 654 (M[+]-AcOH, 2%), 594 (M[+]-2AcOH, 1%), 493 (ring C cleavage, 82%) (Budzikiewicz *et al.*, 1963), 433 (ring C cleavage-AcOH, 10%), 369 (M[+]-side-chain, 21%), 253 (ring C cleavage -4AcOH, 31%), 191 (ring C cleavage, 100%).

I.4.2.3 Adenosylhopane triacetate from Δ*orf14* strain

Adenosylhopane triacetate
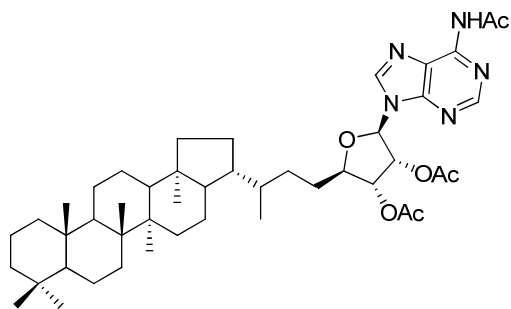
The freeze-dried cells from 35 petri dishes were extracted and acetylated as for aminobacteriohopanetriol tetraacetate. The total acetylated lipid extracts were analyzed following methods previously established, using a Thermo Surveyor LC interfaced to an LTQ-MS. Adenosylhopane was identified by comparison of retention times and mass spectra to published information (Talbot *et al.* 2007a).

ACPI-MS[2] of the molecular ion peak m/z 788 [M+H][+]: m/z = 611 ([M+H–*N*-acetyl adenine][+], 100%), 551 ([M+H–*N*-acetyl adenine–AcOH][+], 4%), 509 ([M+H–*N*-acetyl

adenine–AcOH–CH$_2$CO]$^+$, 2%), 491 ([M+H–*N*-acetyl adenine–2AcOH]$^+$, 4%), 191 (ring C cleavage, 1%), 178 ([*N*-acetyl adenine+H]$^+$, 27%)

Chapter II

Hemisynthesis of adenosylhopane and of a deuteriated isotopomer

II.1. Introduction

(22*R*)-Adenosylhopane has been found in fairly large amounts in a few species of bacteria (Neunlist and Rohmer, 1985b; Seemann *et al.*, 1999; Bravo *et al.*, 2001) and in trace amounts in many hopanoid producing bacteria (Talbot *et al.*, 2007a). It possesses a carbon-carbon linkage between the C-30 carbon atom of the hopane moiety and the C-5' carbon atom of adenosine. The commonly occurring configuration of adenosylhopane was determined by circular dichroism and high-field NMR spectroscopy, and was indicated as 22*R*, 32*R*, 33*R*, 34*R* and 35*R* (Neunlist and Rohmer, 1985b). Trace amount of (22*S*)-adenosylhopane as the minor isomer was also reported from *Rhodopseudomonas acidophila* (Neunlist *et al.*, 1988). Chemical conversion of adenosylhopane into bacteriohopanetetrol (BHT) permitted the determination of the stereochemistry of all asymmetric centers of the side-chain of BHT as 22*R*, 32*R*, 33*R* and 34*S* (Neunlist *et al.*, 1988). Later syntheses of the eight possible diastereomers of BHT with different chirality at C-32, C-33 and C-34 confirmed that the absolute configuration of the C_5 unit was identical to that of a D-ribitol linked via its C-5 carbon atom to the hopane skeleton (Bisseret and Rohmer, 1989). The same configuration was also found for 35-aminobacteriohopanetriol via chemical correlation with BHT (Neunlist and Rohmer, 1988), as well as in other complex bacteriohopanoids (*e.g.* BHT glycoside **16** and BHT cyclitol ether **18**) (Renoux and Rohmer, 1985; Flesch and Rohmer, 1989). The consistent side-chain configuration further supported the hypothesis deduced from the labeling experiments that the C_5 units of the elongated bacteriohopanoids originated from a D-ribose derivative (see general introduction and/or chapter I). Adenosylhopane was consequently considered as a possible intermediate in the biosynthesis of the C_{35} hopanoids, leading to BHT **6** and aminobacteriohopanetriol **7** (Flesch and Rohmer, 1988b; Rohmer *et al.*, 1989).

In the purpose of elucidating the side-chain biosynthesis of bacteriohopanoids, a sufficient amount of adenosylhopane is necessary for future enzyme tests. In principle, there are two distinct methods to produce complex hopanoids: fermentation and appropriate chemical hemisynthesis. The obvious limitations of fermentation for complex hopanoids come from their poor solubility in most solvents and their amphiphilic character, which makes their extraction largely troublesome. Moreover, fermentation is only appropriate for a few of them because many complex hopanoids are produced by bacteria in only trace amounts.

Chemical synthesis, on the other hand, allows the access to a broad range of naturally occurring hopanoids in sufficient amounts. Many efforts have been invested to synthesize ribosylhopane, BHT and many other related structures (Bisseret and Rohmer, 1989; Stampf, 1992; Duvold, 1997; Pan, 2005). Some synthetic strategies are quite successful with excellent stereochemistry control and good overall yields. However, adenosylhopane has not been successfully synthesized with the reported methodologies, mostly due to the huge hindrance introduced by the adenosine moiety and the pentacyclic triterpene structure. We therefore attempted to look for an alternative synthetic pathway for adenosylhopane, which could also be easily applied to the preparation of other naturally occurring hopanoids or even non-natural analogues. Moreover, considering the needs of isotopic labeled hopanoids for future biochemical investigation, this strategy should be able to introduce isotopes, such as deuterium, into the hopanoid structure conveniently and economically.

II.2. Review of the reported syntheses of adenosylhopane and hopanoids in related stuctures

Adenosylhopane **25**, ribosylhopane **23** and its lactone analogue **24** are the only reported biohopanoids with cyclic side chains. Considering the structural resemblance between adenosylhopane and ribosylhopane, as well as the limited examples of adenosylhopane synthesis, some of the reported synthetic strategies for ribosylhopane derivatives are also reviewed in this section.

Chemical synthesis of hopanoids has gained more and more attention since the access to hydroxyhopanone **56**, the universal starting material, was allowed (Dunstan *et al.*, 1957). Approaches on preparation of adenosylhopane and of hopanoids with related stuctures were mainly based on two routes. The first strategy is inspired by the supposed biosynthesis of bacteriohopanoid side chains, coupling thus a triterpene moiety and an appropriate chiral building block of C_5 side chain. In the case of the synthesis of adenosylhopane or ribosylhopane, an appropriately protected adenosine or D-ribose derivative was used for the side chain extension. In the other approach, adenosylhopane is derived from adenine and a ribosylhopane derivative via adenylation. The main problems encountered by these methodologies are always the poor yields obtained for the coupling reaction between the triterpene moiety and the D-ribose derived moiety.

II.2.1. Coupling between hopane skeleton and a side-chain building block

Carbon/carbon linkage between a C_{30} triterpene and a D-ribose derivative was postulated for the biosynthesis of the C_{35} bacterial hopanoids two decades ago (Flesch and Rohmer, 1988b; Rohmer, 1993). On the one hand, a biomimetic protocol using an adenosine derivative as a chiral source for the C_5 side chain seems therefore to be a convenient and direct way to synthesize adenosylhopane. On the other hand, a chiron approach is widely employed in the syntheses of natural products (Henessian, 1983 and reference cited therein). Carbohydrates and terpenes are widely used as enantiomerically pure synthons. This strategy offers obvious advantages: numbers of reactions are usually limited, and stereochemistry control is often excellent, since most of the chiral centers are already fixed within the building blocks.

II.2.1.1. Coupling via Wittig-type reactions

Ribosylhopane derivatives **32** and **33** were synthesized via a chiron approach involving a Wittig condensation between the phosphonium salt **29** and the methyl riboside **30** (Francis *et al*. 1991; Stampf, 1992). The phosphonium salt **29** was prepared from 29-iodohopane, which was prepared from hopan-29-ol **28** by Rydon's iodination, via a solvent-free reaction with an excess of molten triphenylphosphine (Bisseret and Rohmer, 1989). Although the yield of the Wittig coupling could be improved from 17% to 36% by using LiHMDS as base instead of *n*-BuLi, it is still not satisfying. The subsequent catalytic hydrogenation afforded the protected ribosylhopane **32** (Fig. II-1). Because of the troublesome deprotection of the methoxy group on the ribose ring, benzyl riboside **33** was employed as an alternative chiron for the synthesis of ribosylhopane, involving the LiHMDS promoted Wittig condensation (Duvold, 1997). The resulting yield was, however, lower (10-15%). The decreased condensation yield was explained by the increased steric hindrance introduced by the benzyl group of riboside **31**, compared to the methoxy group of riboside **30** (Fig. II-1).
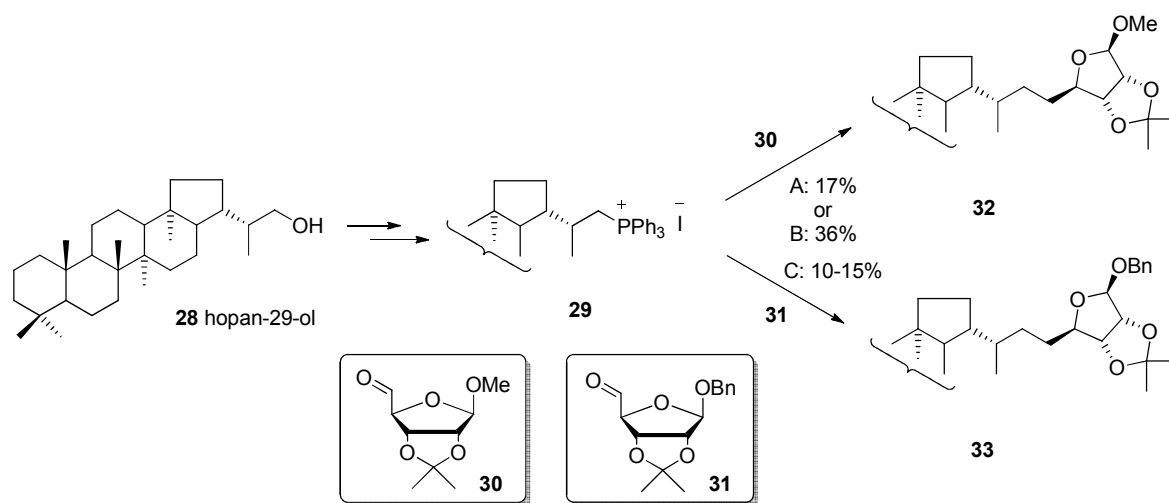
Conditions: A. 1) *n*-BuLi; 2) H_2, PtO_2. B. 1) LiHMDS; 2) H_2, PtO_2. C. 1) LiHMDS; 2) H_2, Pd/C

Fig. II-1. Synthesis of protected ribosylhopane derivatives **32** and **33** by Wittig condensation using different bases (Stampf, 1992; Duvold, 1997).

Another strategy for the coupling between the hopane skeleton and a ribose moiety was developed by Stampf (1992): a Wittig-Horner type reaction using a more stabilized and more reactive hopanyldiphenylphophine oxide **34**. The isolated yield of the coupling between oxide **34** and riboside **30** rose to 62% in the best case. The subsequent elimination of PPh_2O_2H and

the following catalytic hydrogenation were achieved in good yields. Clean deprotection of methoxy group turned out to be troublesome. Heating 35-*O*-methyl ribosylhopane **32** in aqueous dioxane with HCl afforded the fully deprotected product in moderate yield, even after prolonged reaction time. Without further purification, subsequent acetylation of deprotected ribosylhopane was achieved by utilizing Ac$_2$O/Py and afforded ribosylhopane peracetate **37**. Ribosylhopane **37** was synthesized for the first time by this work with modest overall yield (23%) starting from oxide **34** (Fig. II-2).
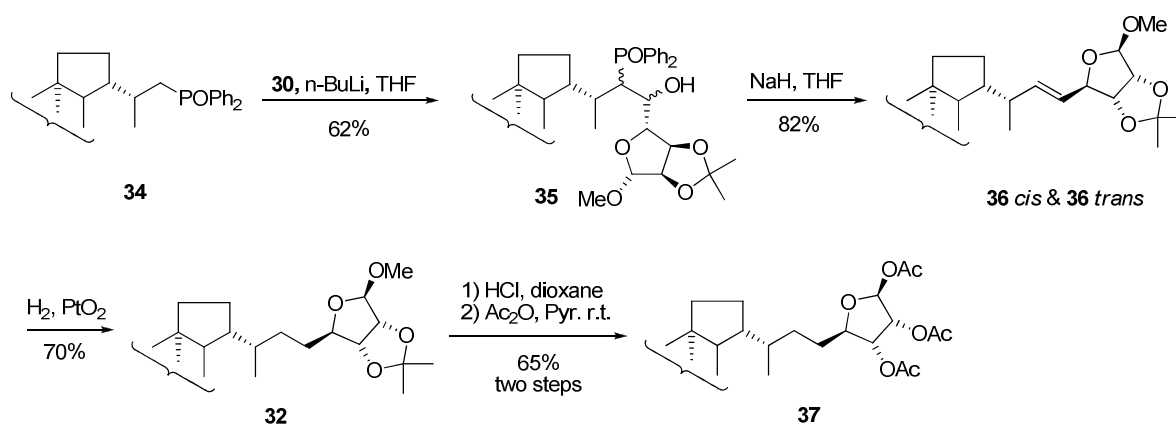
Fig. II-2. Synthesis of ribosylhopane triacetate **37** via Wittig-Horner reaction (Stampf, 1992).

An attempt to synthesize (22*S*)-adenosylhopane was further performed by Stampf (1992) via a similar Wittig-Horner condensation (Fig. II-3). The protected 5'-deoxy adenosine 5'-aldehyde **39** was used as the chiral building block of the side chain. Disappointing yields were obtained not only for the coupling step, but also for the subsequent catalytic hydrogenation with Pt$_2$O to afford (22*S*)-33,34-*O*-isopropylidene adenosylhopane (22*S*)-**40**. Because of the tiny amount of synthetic adenosylhopane derivative obtained, the structure was only verified by ^{1}H-NMR and mass spectrometry. The poor overall yield was attributed to the increased steric hindrance introduced by the adenine moiety of adenosine-5'-aldehyde **39** (as compared to the methoxy group of riboside **30**). The main advantage of this methodology is that the aldehyde **39** was not exposed to the strong bases required for the generation of non-stabilized phosphorane Wittig reagents resulting in consequent decomposition (Kjer *et al.*, 1986; Wnuk and Robins, 1991). The stabilized ylide resulting from diphenylphosphine oxide (22*S*)-**34** was, however, not as reactive as the non-stabilized ones. This reduced reactivity might be another factor leading to the poor yield of the coupling step. Nevertheless, as the first report on adenosylhopane synthesis, it provided, on the one hand, valuable experimental

data, and on the other hand, pointed out the main difficulty in the synthesis of adenosylhopane – the steric hindrance resulting from the bulky hopane skeleton and adenosine moiety.
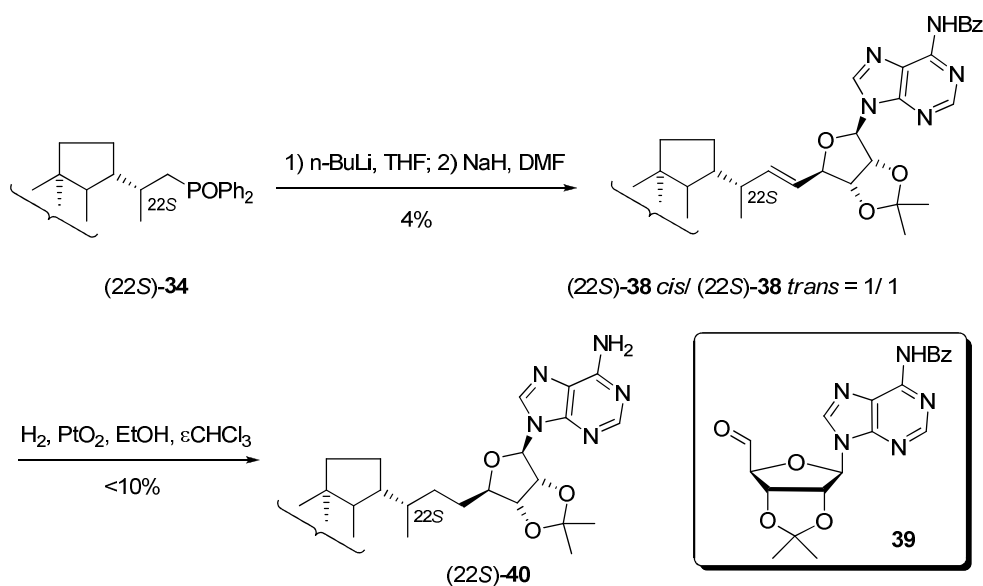
Fig. II-3. Tentative synthesis of (22*S*)-adenosylhopane via Wittig-Horner reaction (Stampf, 1992).

II.2.1.2. Coupling via Julia olefination

Tentative studies on the synthesis of ribosylhopane by using Julia olefination was fully unsuccessful (Fig. II-4) (Stampf, 1992). The poor reactivity of the 29-hopanyl phenyl sulfone **41** probably also originates from the steric hindrance of the bulky hopane framework.
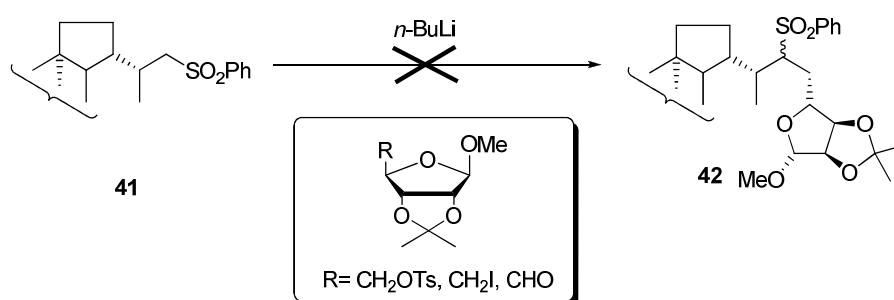
Fig. II-4. Unsuccessful tentative synthesis of ribosylhopane via Julia coupling reaction

II.2.1.3. Coupling via an organolithium mediated cross-coupling strategy

Considering the high reactivity and low steric hindrance demand of organometallic

reagents, a novel [$C_{30}+C_5$] strategy was developed by Pan *et al.* to synthesize ribosylhopane and other bacteriohopanepolyols (Pan *et al.*, 2007). This methodology was based on the metallation of hopanyl phenyl sulfide **43** and its efficient coupling to an aldehyde derived from D-ribose.

Fig. II-5 shows the organolithium assisted coupling reactions in the synthesis of ribosylhopane. 29-Phenylthiohopane **43** was easily prepared from hopan-29-ol **28**. 31-Hydroxy ribosylhopanes **45** and **46** were prepared via a two-steps one-pot reaction. Reductive lithiation of **43** was achieved by using lithium 4,4'-di-*tert*-butylbiphenylide (LiDBB), which is very efficient for the cleavage of C-S bond. Riboside **30** or **31** was added subsequently in one pot, due to the high reactivity of the metallated hopane intermediate. Best yield (81%) of coupling between 29-phenylthiohopane **43** and **30** was obtained by optimizing Cohen's procedure (Cohen and Doubleday, 1990). Unfortunately, the use of benzyl riboside **31** under the same optimized conditions resulted only in a lower yield ($<$ 8-10%), while giving hopane **44** as the major product. This is probably due to the interaction between the bulky hopane skeleton and the bulkier benzyloxy group in **31** as compared to the methoxy group in **30**.

aldehyde	adducts	yields
30	45	81%
31	46	12%
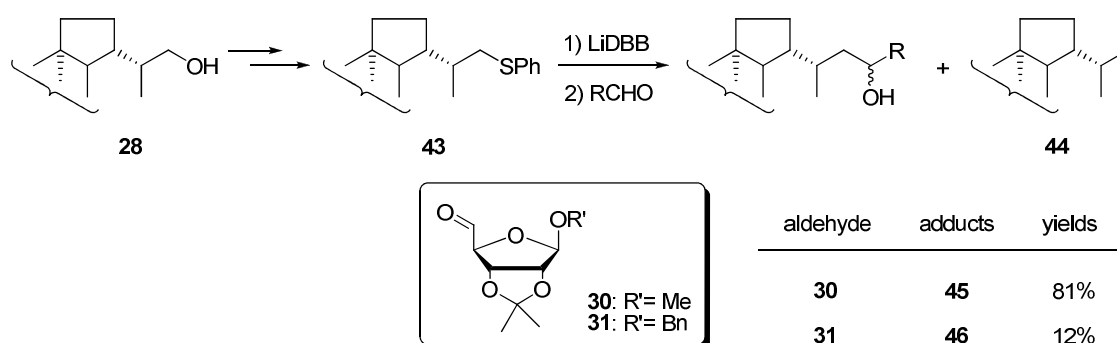
Fig. II-5. Coupling between hopane and riboside through a lithiated hopane intermediate (Pan *et al.* 2007).

Following deoxygenation of the additional hydroxy group at C-31 position and further derivatization of the desired product **32** gave ribosylhopane triacetate **37** in high yields (Fig. II-6).
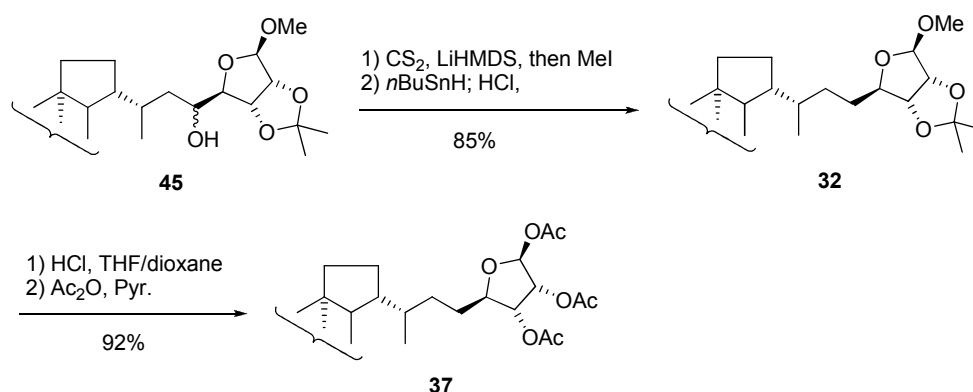
Fig. II-6. Deoxygenation and deprotection of 31-hydroxyribosylhopane **45** (Pan *et al.*, 2007).

This LiDBB promoted hopane-riboside coupling was much more efficient than the reported Wittig-type strategies. However, the steric hindrance resulting from hopane skeleton and some bulky substitution group at C-1′ position of ribose still remained a severe problem.

I.2.2. Direct adenylation on ribosylhopane derivative

With all the knowledge gathered about ribosylhopane synthesis and the well-discribed methods for building a glycosidic bond, adenosylhopane may be theoretically prepared from linkage of the N-7 nitrogen atom of adenine to the C-35 carbon atom of ribosylhopane. Stampf (1992) attempted the glycosydic coupling of ribosylhopane triacetate **37** to free adenine **47** in the presence of SnCl₄ as a Lewis acid (Fig. II-7). However, no (22*R*)-adenosylhopane **25** was obtained, but instead its 35α isomer **48** with a poor yield (<10%). Compound **49** was the major product. Treatment of (22*S*)-ribosylhopane triacetates (22*S*)-**37** with adenine and SnCl₄ led to the formation of compound **50**, without trace amount of coupling product. The poor solubility of adenine **47** and ribosylhopane peracetate **37** in acetonitrile was considered as the main reason why the side reactions were promoted. Moreover, the coupling position of adenine **47** to the C-35 position of ribosylhopane **37** could not be determined by ^{13}C-NMR spectroscopy due to the insufficient amount of adenosylhopane isomer **48**. Last but not least, the application of this methodology is also limited considering the many synthetic steps required to reach ribosylhopane.
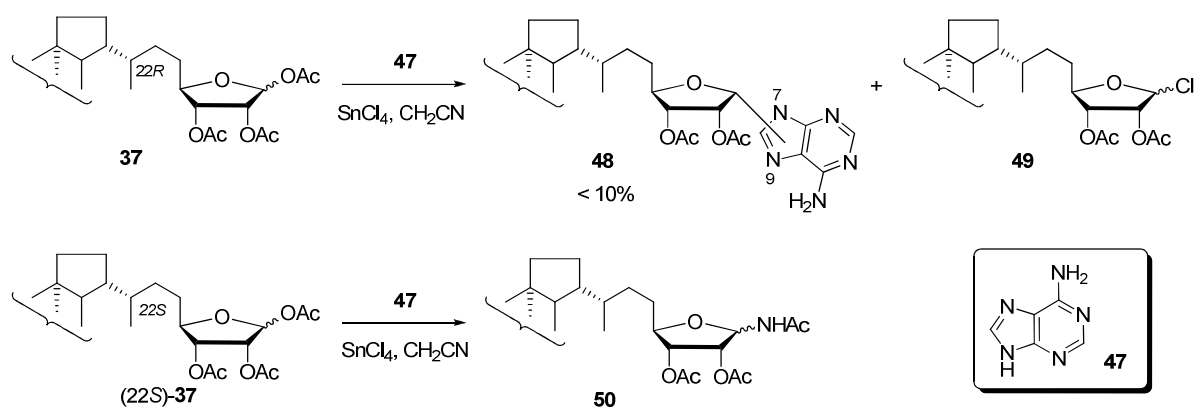
Fig. II-7. Tentative synthesis of adenosylhopane via glycosydic coupling reactions (Stampf, 1992).

II.3. Syntheses of (22*R*)-adenosylhopane and of a deuteriated isotopomer

II.3.1. Introduction

The goal of this project is to develop a concise and flexible approach for the synthesis of adenosylhopane with good yields and excellent stereochemical control of all asymmetric centers, starting from easily available starting materials. This approach should be readily applied to the preparation of other natural or unnatural bacteriohopanepolyols with potential biochemical interest. Moreover, it should also allow an easy access into the introduction of isotopes into hopanoid structure to meet the needs of future biochemical investigation. From the atom-economic point of view, isotopes should be introduced in the final steps of the synthesis.

According to the previous studies on the synthesis of adenosylhopane and ribosylhopane derivatives, the cross coupling strategy according to a biomimetic (C_{30} + C_5) sequence is the most direct way. The major difficulties we might encounter are the steric hindrance induced by the hopane skeleton and the instability of adenosine substrates under harsh reaction conditions. To our knowledge, a coupling strategy based on olefin cross-metathesis (CM) would be promising because of its efficiency (catalytic reactions with usually high yield in relatively short reaction times), mildness (no other reagents are required for pre-activation of the C atoms on the coupling sites, and reactions are typically performed under mild temperature) as well as high tolerance towards various functional groups and bulky structures (*e.g.* tri- or tetrasubstituted olefins that present high steric hindrance). Moreover, the desired olefin product is suitable for further structural elaboration. The subsequent hydrogenation of the carbon-carbon double bond will enable us to introduce deuterium easily and economically. Although no report involving CM reactions in the preparation of triterpenoids of the hopane series was given, this novel type of reactions has been widely employed in the synthesis of many other natural compounds, including carbohydrates (Aljarilla *et al.*, 2010), nucleosides (Amblard *et al.*, 2005) and steroids (Morzycki, 2011). Therefore, it is plausible to explore the use of CM for the synthesis of adenosylhopane.

II.3.2. Olefin cross metathesis

Olefin cross metathesis has been proved to be an efficient way to build an intermolecular carbon-carbon bond. A general mechanistic scheme for the CM reaction of two symmetrically substituted olefins (in practice, this is quite difficult) is presented in Fig. II-8 (Hérisson and Chauvin, 1971). The first step in the catalytic cycle (after the first catalyst turnover to produce **A**) is a [2+2] cycloaddition reaction between olefin **B** and a transition-metal carbene **A** to give a metallacyclobutane **C**. The latter undergoes subsequent collapse in a productive fashion to afford a new olefin product **D** and a new metal carbene (alkylidene) **E**, which carries the alkylidene fragment R_1. Similarly, **E** can react with a molecule of **F** via **G** to yield **D** and **A**, which then re-enters the catalytic cycle. The net result is that **D** is formed from **B** and **F** with **A** and **E** as catalytic intermediates (Connon and Blechert, 2003).
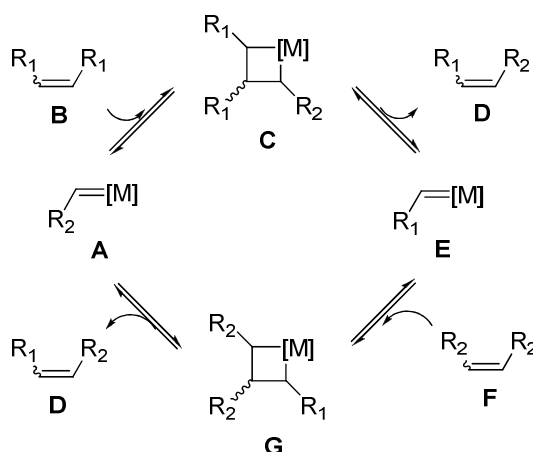
Fig. II-8. Mechanism of olefin metathesis (Connon and Blechert, 2003).

II.3.2.1 Efficiency and selectivity of CM reactions

As it is the case with most transformations, the two important questions concerning any CM reactions are those concerning efficiency and selectivity. The goal of a successful CM reaction is to achieve high yield of the CM product with minimal amounts of competing dimerization (self-methathesis) products. If two olefins of similar reactivity are subjected to CM condition, assuming full conversion, 10 equivalents of one coupling partner must be used to achieve a synthetically efficient yield of 90%. In the meantime, the yield of homodimer from the other coupling substrate is reduced from 25% to 10% (Chatterjee *et al.*, 2003). The stereoselectivity of product formation is another critical issue for CM. Although the *E* olefin

is usually thermodynamically favored as the major cross-product, when the energy difference between the *E* and *Z* isomers is small, the *E/Z* selectivity would be largely attenuated.

CM of two identical olefins eliminates the question of cross product selectivity. Kranusz and co-workers were able to dimerize various 3'-allyl nucleosides through CM promoted by the biphosphane catalyst, Grubbs' catalyst 1st generation (G-I) (10%-20%) (Batoux *et al.*, 2001) (Fig. II-9). Yields were moderate ($\leq$ 45%) and the reaction was largely unselective with regard to olefin geometry. The author cited the inhibition effect of the N atom present in pyrimidines on ruthenium catalyst to interpret why such large amounts of catalyst are required to achieve acceptable CM yields (Fürstner and Langemann, 1997). And indeed, metathesis with N containing products, for example nucleosides, afforded lower yields compared to those obtained from metathesis dimerization of sugar derivatives (Huang and Herdewijn, 2011).

B = thymine, uracil or acetylcytosine; R = TBDPS
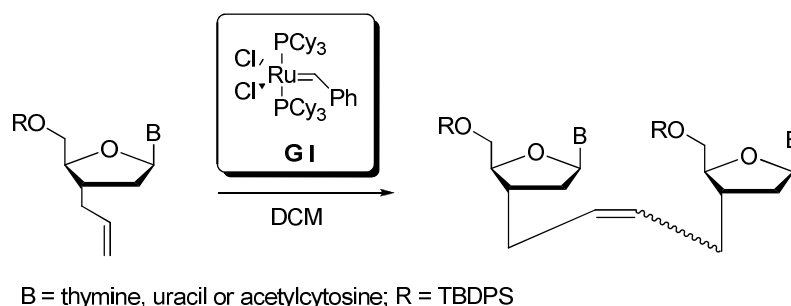
Fig. II-9. Homodimerization of nucleotides (Batoux *et al.*, 2001).

CM of two different olefins has the inevitable challenge of competing homodimerization. The mechanism of metathesis allows equilibration, and the product distribution of a metathesis reaction is governed by the relative energies of product olefins: the most thermodynamically stable isomer is favored (Smith *et al.*, 2001). A general observation that has been made is that the activation energy barriers for electronically deactivated and sterically hindered olefin are high, often resulting in diminished reactivity towards metathesis. If the desired olefin product is kinetically trapped and does not undergo a secondary metathesis, a higher yield can be anticipated as long as undesired products undergo secondary metathesis. A selectivity model for CM was proposed concerning the functionalized olefin reactivity, categorizing olefins into four groups (Chatterjee *et al.*, 2003). In general, a reactivity gradient exists from most active type (Type I olefin) to least active type (Type IV olefin), with sterically unhindered, electron-rich olefins categorized as type I and increasingly sterically hindered and/or electron-deficient olefins falling into typeII through IV.

- Type I olefins undergo rapid dimerization and the resulting homodimers will participate in secondary metathesis.
- Type II olefins homodimerize and the homodimers are Type IV olefins.
- Type III olefins are active in metathesis but do not homodimerize.
- Type IV olefins are not reactive towards metathesis.

As summarized in Fig. II-10, CM between two Type I olefins gives a statistical distribution of hetero- and homodimers, in which case the yield of the reaction can be improved by increasing the equivalents of one olefin in CM while decreasing the formation of homodimer of the other olefin. Higher selectivity of CM can be facilitated by coupling olefins of different types. Good CM yields can then be achieved with low stoichiometric ratios of two olefins (Chatterjee *et al.*, 2003 and references cited therein).

	Type I	Type II	Type III	Type IV
Type IV	No Reaction	No Reaction	No Reaction	No Reaction
Type III	Selective	Low Reaction	Non-selective	
Type II	Selective	Non-selective		
Type I	Statistical			

Fig. II-10. CM mode of selectivity.

It should be noted that different catalysts require different definitions of olefin types and the model of CM selectivity does not apply in all cases. Besides electron deficiency, steric bulk and sometimes chelation effect on ruthenium play as deactivating factors for CM. Indeed, CM is known to be more difficult than dimerization, ring closing or ring opening metathesis due to the loss of advantages from statistics, entropy and ring tension relief respectively. Despite of the relatively low yields and unpredictable reaction scope, CM is more and more employed as a key step into multistep procedures and into the synthesis of natural products (Prunet, 2005), such as nucleoside analogues and steroids (Morzycki, 2011), which show great structural similarity with our target molecule adenosylhopane.

II.3.2.2. Olefin cross metathesis in the synthesis of natural products

A CM coupling with phosphorylated thymidine derivative highlighted the superiority of Grubbs' 2nd generation catalyst (G II) over G I in terms of both activity and functional-group

tolerance, and its potential for CM modification of biologically important molecules. Moreover, the intramolecular chelation of the nucleotides to ruthenium was cited as the reason of the large amounts of catalyst consumed (20%) (Lera and Hayes, 2001) (Fig. II-11).
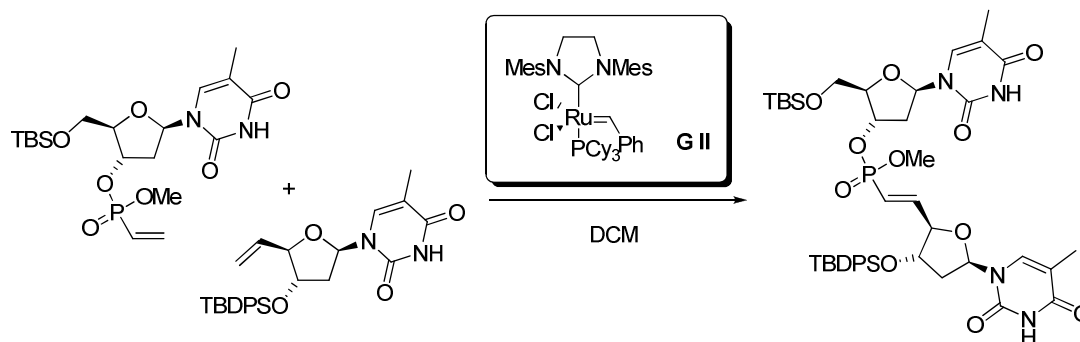
Fig. II-11. Coupling of nucleotides by CM (Lera and Hayes, 2001).

However, a similar strategy was not successful when it was applied to the synthesis of 3'-phosphonoalkenyl adenosine analogues (Huang and Herdewijn, 2011) (Fig. II-12). CM of allylphosphonate with adenosine derivative did not give the desired coupling product, but the CM with a sugar moiety afforded the CM product quantitatively. This result was in accord with the observed decreased reactivity of nitrogen containing substrates towards CM, which are more often the nucleotides, compared to that of a sugar substrate. Although no interpretation was given by the authors, steric hindrance seemed a likely explanation.
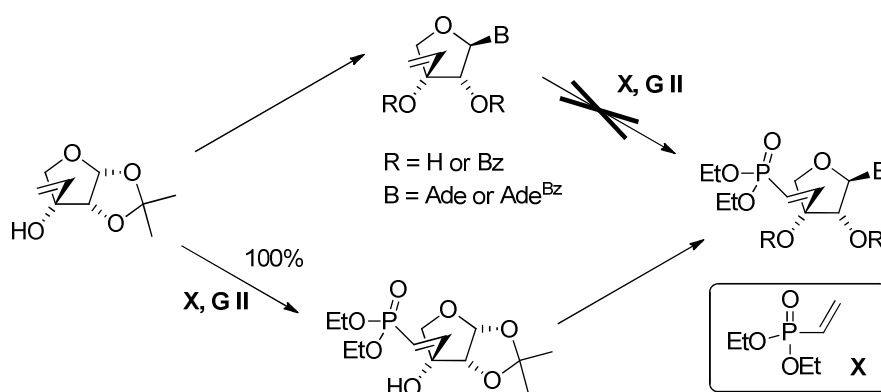
Fig. II-12. CM in the synthesis of modified nucleoside phosphonate (Huang and Herdewijn, 2011).

Successful CM was reported to couple the protected 5'-deoxy-5'-methyleneadenosine or uridine analogues with six-carbon amino acids (homoallylglycines) in the presence of

Hoveyda-Grubbs catalyst 2nd generation (H II) or Grubbs catalyst G II respectively, giving nucleoside analogues with a C5'-C6' double bond (Wnuk and Robins, 1993; Andrei and Wnuk, 2006) (Fig. II-13). It is worth to mention that protection of the amino group at C-6 position of the adenosyl coupling partner was necessary to facilitate CM reactions. CM failed with the adenosyl substrate containing a free amino group, while the 6-*N*-benzoyl derivative afforded good yields for CM products, and the di-protected derivative even better yields, which is consistent with the observed deactivation of ruthenium catalyst in the presence of an amino group (Batoux *et al.*, 2001). Furthermore, an interesting protocol was developed by the authors to perform CM under pressure, which proved efficient when the activation energy barrier of the metallacyclic transition state is probably too high to achieve under classical thermal conditions.

B = Uri, Ade, Ade[Bz] or Ade[Bz2]
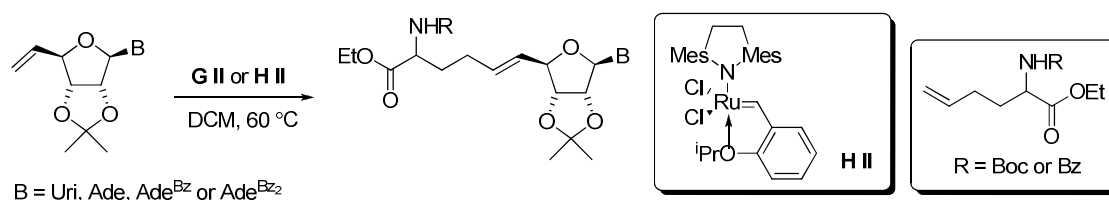
Fig. II-13. Coupling of nucleosides with amino acids by CM (Wnuk and Robins, 1993; Andrei and Wnuk, 2006).

In the field of steroid chemistry, ruthenium-mediated metathesis is largly employed in total synthesis and hemisynthesis of these polycyclic natural products (Morzycki, 2011). However, limited examples were documented using CM for the modification of the steroid side chain. CM reaction of steroidal terminal olefins with two-fold excess of 3-perfluoroalkyl propene reagent **51** catalyzed by ruthenium carbine H II afforded the desired products in good yield (Fig II-14). Interestingly, reactions of the steroidal olefin with the shorter side chain (n = 0) were completely *E*-stereoselective, while substrate with the longer one (n = 2) afforded diastereomeric mixtures with the *E* olefin prevailing. The unexpected stereoselectivity might be explained by the huge steric bulk present in the metallacyclobutane intermediate corresponding to the *Z* isomer (Eignerová *et al.*, 2008).
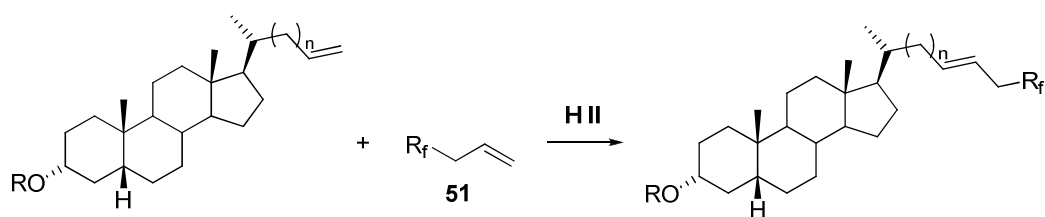
R = TBS or THP; n = 0 or 2; R_f = n-C6F13, n-C3F7 or i-C3F$_7$

Fig. II-14. CM between steroid and perfluoroalkyl propene **51** (Eignerová *et al.*, 2008).

However, without the help of inductive effects of the perfluoroalkyl group, CM of Δ^{22}-steroid **52**, catalyzed by H II catalyst, with excess of simple alkenes **53** are rather sluggish and low-yielding (*e.g.* 12% yield achieved for the Δ^{22}-cholesterol derivative) or do not occur at all (Fig. II-15). All attempts to apply stigmasterol (with an additional 24β-ethyl group) derivatives in metathesis reaction (CM or RCM) failed, probably due to steric reasons (Czajkowska and Morzycki, 2009).

R = H, Me, i-Bu,
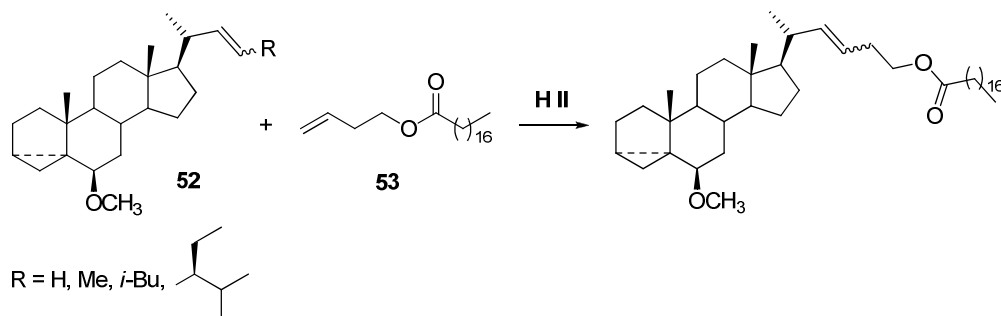
Fig. II-15. CM between Δ^{22}-steroid **52** and 3-butenyl stearate **53** (Czajkowska and Morzycki, 2009).

Steric hindrance remains an important factor in the studies on CM of steroids, especially for the dimerization of steroidal olefins. Successful examples for steroid dimerization were reported by Edelsztein *et al.* (2009) only under the assistant of microwave heating.

II.3.2.3. Applying CM into the synthesis of adenosylhopane

To date, among the few works using ruthenium-mediated metathesis for the synthesis of triterpenes, only ring-closing metathesis has been employed to construct the polycyclic skeleton (Srikrishna *et al.*, 2010). Therefore, our work will be the first report of a side chain elongation in the hopane series by CM. According to the present knowledge on metathesis

involving nucleosides or steroid-like structures, several precautions should be taken into account in order to facilitate CM for the coupling between an adenosine derivative and the hopane moiety.

Theoretically, there are three ways to perform the coupling via CM from different starting materials (see Paths A, B and C, Fig. II-16). Path A requires diploptene **3** as a coupling substrate: the bulky pentacyclic skeleton represents a huge steric hindrance and is usually inert to chemical derivatization. Path C involves 5'-deoxy-4',5'-didehydroadenosine **54**, which is an enol ether with an activated C/C double bond due to the electron-donating effect from the adjacent oxygen atom, and thus presents high reactivity towards CM reactions according to the general selectivity model (Chatterjee *et al.*, 2003). However, using adenosine derivative **54** as a starting material might cause epimerization on C-4' position of adenosine due to the *E/Z* stereoselectivity of CM and further hydrogenation. Therefore, coupling between homohop-30-ene **55** and a 5'-vinyl adenosine derivative (path B) seems a promising choice.
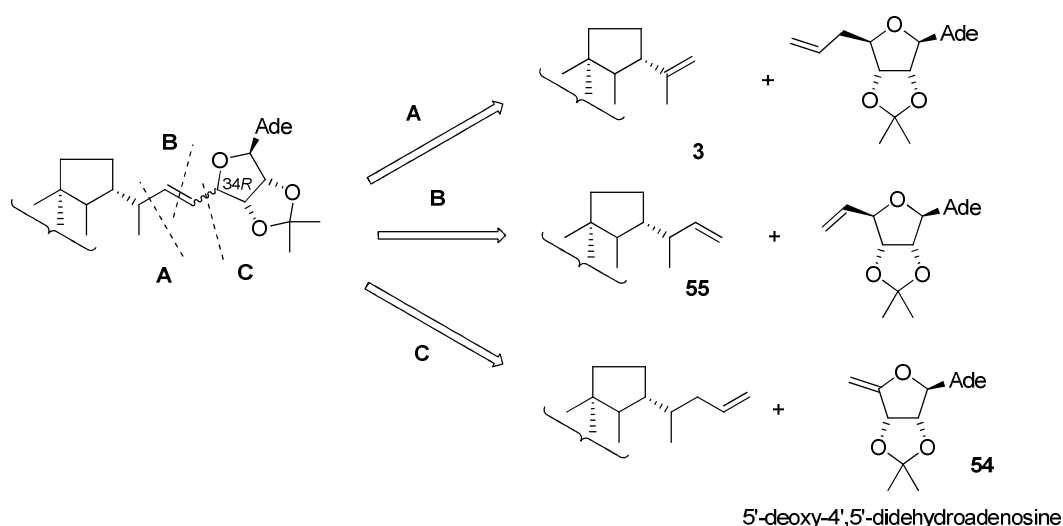
Fig. II-16. Three possible ways for CM reaction between the hopane skeleton and an adenosine moiety.

Although metathesis usually presents high tolerance towards functional groups, appropriate protection of the 6-NH$_2$ of the adenosine moiety is required, probably because of the chelation to ruthenium by amino group, which weakens the reactivity of the catalysts. Higher reactivity was reported for a 6-*N,N'*-dibenzoyl adenosine substrate towards CM reactions (Andrei and Wnuk, 2006). The increased steric hindrance caused by the second benzoyl group may, however, disfavor the coupling to the bulky hopane skeleton. Furthermore, oxidation of 6-*N,N'*-dibenzoyl adenosine to the corresponding 5'-aldehyde

analogue, the precursor of 5'-methylene adenosine, proved to be much more difficult than that of its mono-protected or unprotected analogs (Craig *et al.*, 1986). For these reasons, we shall use 6-*N*-benzoyl-5'-deoxy-5'-methylene-2',3′-*O*-isopropylideneadenosine **62** for the coupling.

The advent of the catalysts G II (Huang *et al.*, 1999; Trnka and Grubbs, 2001) and H II (Garber *et al.*, 2000; Gessler *et al.*, 2000) had a tremendous impact on the CM reaction. These ruthenium alkylidenes contain nonlabile, sterically hindered *N*-heterocyclic carbene ligands with strong σ-donor and poor π-acceptor properties, which help to stabilize the 14-electron ruthenium intermediates during metathesis (Connon and Blechert, 2003). They display a functional-group tolerance akin to that of bisphosphane-based catalyst G I, but have a reactivity closer to that of the highly active yet oxophilic molybdenum catalyst, and are thus by far superior to G I catalyst in terms of reactivity. Recently, a novel ruthenium catalyst, Zhan-1B, with 5-aminosulfonyl substituted 2-isoprenoxy styrene ligand has been reported to be more stable and highly active towards metathesis reactions, including CM (Zhan, 2007). We thus found these three catalysts of great interest for the synthesis of adenosylhopane.

II.3.3. Retrosynthetic analysis

The synthetic strategy toward adenosylhopane was designed based on the advantage of the coupling of an appropriate protected 5'-methyleneadenosine substrate and a triterpene moiety possessing a terminal C-C double bond at C-30 and C-31 position via cross-metathesis. Then the desired carbon-carbon double bond could be reduced to afford saturated adenosylhopane and, when necessary, two deuterium atoms may be introduced by hydrogenation into the product. The hopane moiety was obtained in a few steps from hydroxyhopanone **56**. The starting material of adenosine moiety **57** is commercially available.
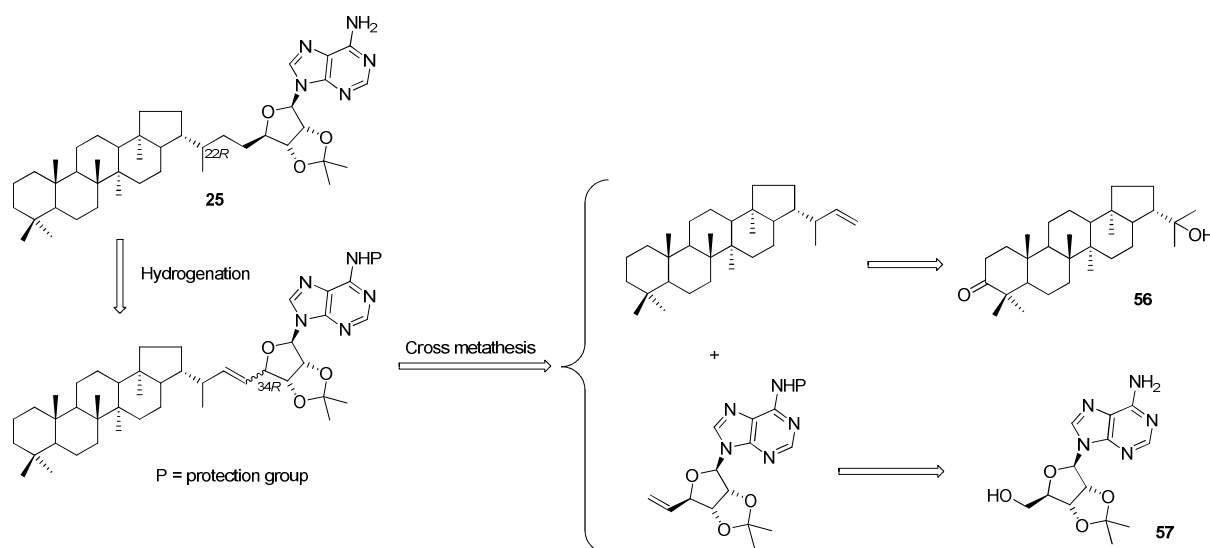
Fig. II-17. Retrosynthetic analysis for the hemisynthesis of adenosylhopane **25**

II.3.4. Preparation of functionalized hopane and adenosine derivatives

II.3.4.1. Preparation of hopane derivative

Hydroxyhopanone **56** was extracted from commercially available Dammar resin and purified by crystallization (Dunstan *et al*., 1957) with a yield of ca. 5.5 g/kg (Fig. II-18). Subsequent Wolff-Kishner reduction afforded diplopterol **2** in a 90% yield. Key point to obtain this high yield is to remove extra hydrazine monohydrate and water as much as possible before KOH powder is added in. The following reaction could reach a temperature above 200 ^{o}C to facilitate the successive deprotonations of the hydrazone intermediate. Otherwise the total yield would be affected.
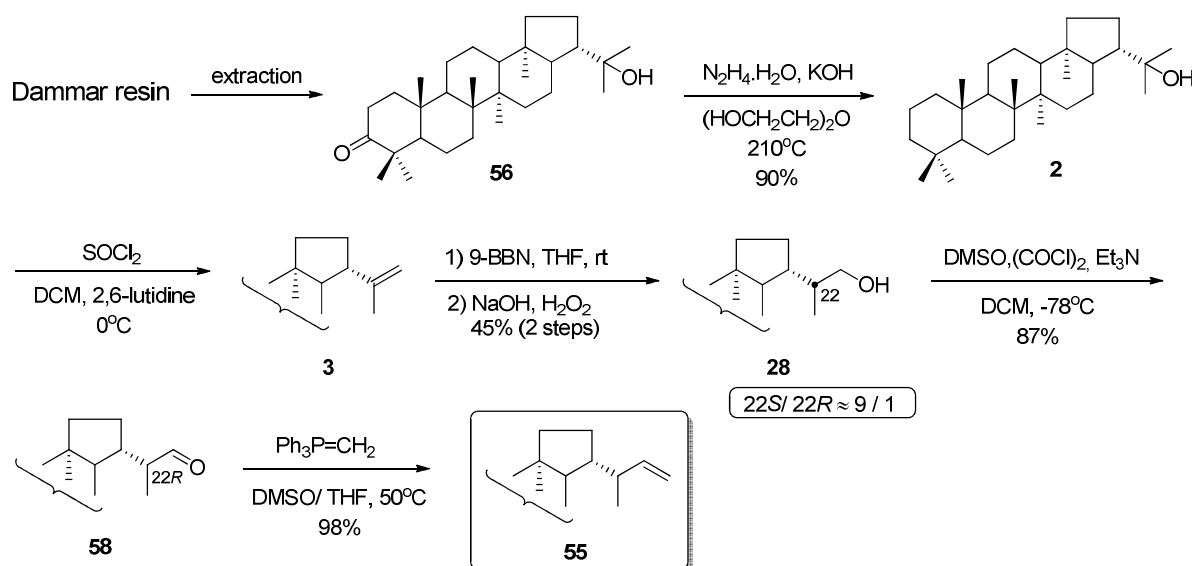
Fig. II-18. Preparation of homohop-30-ene **55**.

Diplopterol **2** was then dehydrated in the presence of $SOCl_2$ to give diploptene **3** as the major product accompanied by hop-21-ene **59** in a 3.3:1 ratio, which was determined by ^{1}H-NMR spectroscopy (Fig. II-19). 2,6-Lutidine was chosen as the base, for its hindered nitrogen atom improved the regioselectivity of the elimination (Pan, 2005).
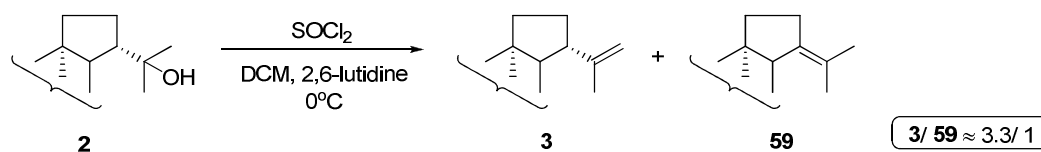
Fig. II-19. Regioselectivity of dehydration of diplopterol **2**.

The mixture of diploptene **3** and its isomer **59** was directly engaged in the next step without further purification. Hydroboration/oxidation of the terminal olefin **3** (Stampf, 1992) majorily afforded (22*S*)-hopan-29-ol **28** with the C-22 configuration of the natural biohopanoids with isolated yield of 45% starting from diplopterol **2** (Fig. II-18). The (22*S*)-epimer could be easily separated from 22*R* epimer by ordinary silica gel chromatography. Hopan-30-al **58** was obtained via Swern oxidation (Duvold, 1997) from primary alcohol **28**. Then aldehyde **58** was treated with a Wittig reagent to afford hop-30-ene **55** in high yield (Ensminger, 1974) (Fig. II-18).

II.3.4.2. Preparation of adenosine derivative

In the synthesis of 5'-vinyladenosine **62**, adenosine-5'-adehyde **39** was an important intermediate. Protection of the 6-amino group of the adenine ring is necessary, otherwise the yield of the following cross-metathesis would be largely affected (Andrei and Wnuk, 2006). According to Moffatt and co-workers (Ranganathan *et al.*, 1974), 6-*N*-benzoyladenosine-5'-adehyde **39** is synthesized from compound **60** via Moffatt oxidation, subsequent protection of the resulting crude aldehyde, liberation of the hydrate **39•H₂O** and dehydration of the aldehyde hydrate to yield aldehyde **39** (Fig. II-20).
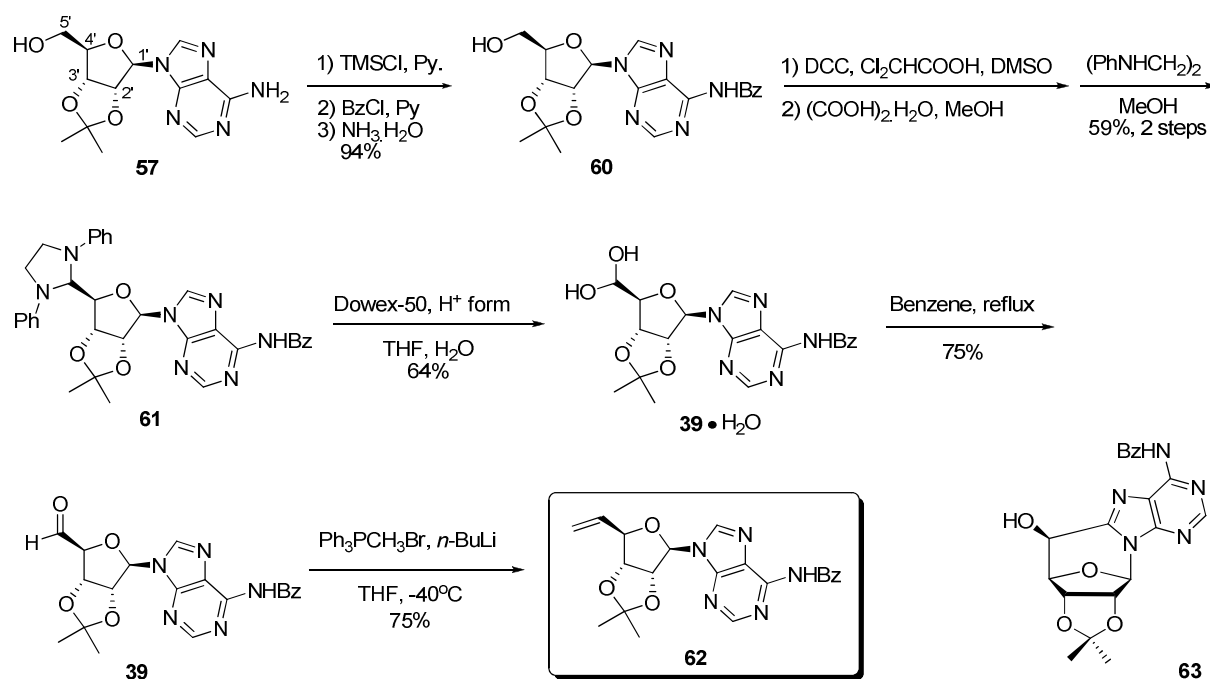
Fig. II-20. Preparation of adenosine derivative **62**

The parent nucleoside 6-*N*-benzoyl-2',3'-*O*-isopropylideneadenosine **60** was prepared from commercially available compound **57** via a one-pot reaction (McLaughlin *et al.*, 1985). Oxidation of **60** was conveniently achieved by treatment with DMSO and *N,N'*-dicyclohexylcarbodiimide (DCC) in the presence of dichloroacetic acid. However, the resulting crude aldehyde can not be purified via flash chromatography, because such aldehydes readily epimerize at C-4' or eliminate the acetonide function, giving 3',4'-unsaturated aldehydes upon attempted chromatography (Jones, 1969; Kjer *et al.*, 1986). Therefore, the crude aldehyde was directly protected with *N,N'*-diphenylethylenediamine. The corresponding derivative **61** was easily crystallized from EtOH. In order to obtain the useful but quite sensitive aldehyde **39**, the *N,N'*-diphenylimidazolidine **61** must be carefully recrystallized. Sometimes quick flash chromatography was necessary in order to remove most of the impurities from the crude mixture before recrystallization. It is worth to mention that the protected compound **61** may also epimerize at C-4' after prolonged or repeated purification by flash chromatography on silica gel (Fig. II-20).

Treatment of the crystalline **61** with Dowex 50 (H$^+$) resin in aqueous THF at room temperature readily regenerated the aldehyde as its pure and stable hydrate **39**•H$_2$O in 75% yield. Prolonged stirring with Dowex 50 (H$^+$) resin could lead to the appearance of 2',3'-*O*-deprotected product. After careful washing with water and pre-drying under vacuum overnight, **39**•H$_2$O was dehydrated by azeotropic distillation with benzene using a Dean-Stark trap to afford the free aldehyde **39**. However, care should be taken since cyclonucleoside **63**, a less polar, benzene-insoluble side product could be easily obtained by prolonged distillation. 5'-Deoxy-5'-methyleneadenosine **62** was further derived via a Wittig reaction from aldehyde **39** (Fig. II-20).

II.3.4.3. Coupling of homohop-30-ene 55 and the 5-vinyl adenosine derivative 62

CM reactions between homohop-30-ene **55** and 5-vinyl adenosine derivative **62** were tested under different conditions (Fig. II-21 and Table II-1). Initial attempts with alkene **62** and one equivalent of homohopene **55** in the presence of H II catalyst failed to give the desired product **38** under reflux conditions (Table II-1, entry 1). This lack of reactivity resulted probably from the highly steric hindered metallacyclobutanyl transition state during CM, together with an activation energy barrier too high to be overcome under classical thermal conditions. However, we were pleased to see that **38** could be isolated with an up to 13% yield when the same reaction was performed under microwave irradiation. Dimer **64** was

also isolated in 43% yield, resulting from the self-metathesis of the nucleoside substrate **62**. The rest corresponded to starting materials **55** and **62**, which were found unreacted (Table II-1, entry 2).

Ruthenium catalyst G II could also promote CM between **55** and **62**, but the yield of the cross product **38** was lower (Table II-1, entry 4), suggesting higher efficiency of H II catalyst than that of G II in the presence of an adenosyl moiety. Finally, the *N,N*-dimethylaminosulfonyl group containing Hoveyda–Grubbs-type complex catalyst, Zhan-1B, was almost as active as H II for this CM reaction, and similar yields of the coupling product and dimer were obtained (Table II-1, entry 3).
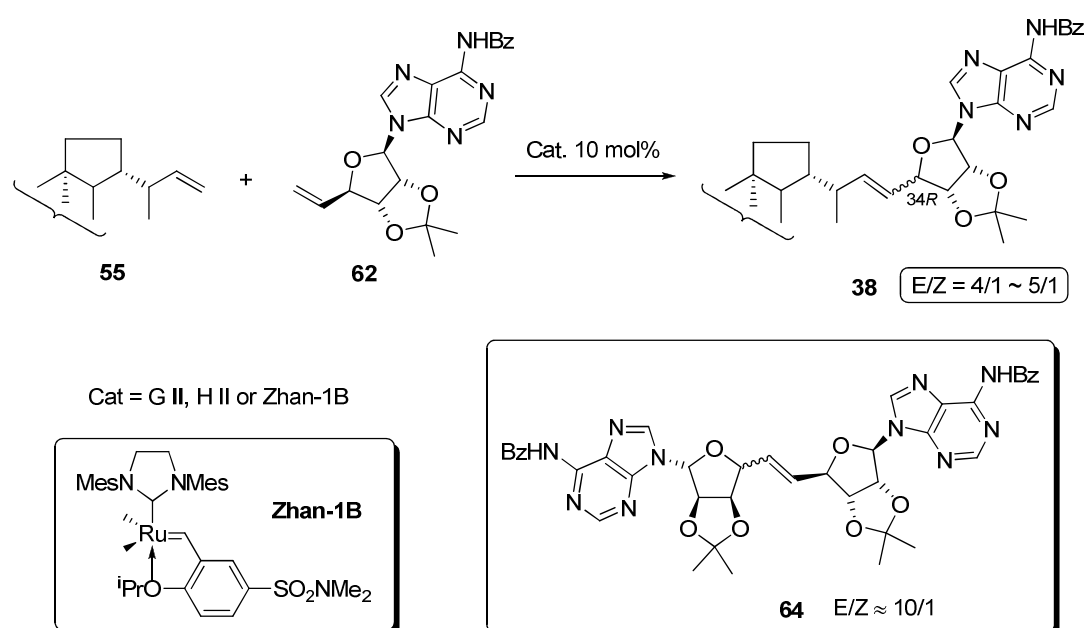
Fig. II-21. CM reaction of homohop-30ene **55** and 5'-vinyl adenosine derivative **62**.

On the one hand, dimerization of homohopene **55** was not observed, suggesting that it might belong to type III olefins for CM reactions (Fig. II-10). On the other hand, the adenosine derivative **62** seemed to act like a type II olefin (Fig. II-10), undergoing homodimerization slowly. Furthermore, the corresponding product **64** was proved essentially inactive to secondary CM, because the attempted CM reactions between homohopene **55** and dimer **64** under microwave irradiation at 75 °C did not lead to the formation of adenosylhopene **38**, but allowed us to recover the two starting reagents. Given these features, the crucial point to obtain higher yields for the coupling compound **38** is to maintain a low concentration of adenosine derivative as compared to that of homohopene, minimizing

thereby the amount of dimerization. Stoichiometric excess (10 eq.) of the less reactive homohopene **55** was thus introduced, and, as expected, the yield of adenosylhopene **38** rose from 13% to 59% in the presence of Zhan-1B catalyst under microwave irradiation (Table II-1, entry 5). However, the CM yield was only moderate, probably due to the low reactivity of homohopene **55**. Adenosine substrate **62** was fully consumed under these conditions, resulting in 40% of dimer **64**. A prolonged reaction time failed to increase the yield in **38**, further supporting that dimer **64** was indeed unable to undergo a secondary hetero-metathesis with excess homohop-30-ene **55**. The inability of compound **55** to homodimerize, probably due to a strong steric hindrance induced by the hopane ring system and the pseudo-axial position of the side chain, allowed us to recycle the large excess of **55**.

Table II-1. Optimization of reaction conditions for cross-metathesis between homohopene **55** and adenosine derivative **62**.

	Catalyst[a]	Condition	**55/62** ratio	Products
1	H II	40°C, DCM, 24 h[b]	1/1	No reaction
2	H II	MW[d], 75 °C, DCM, 3 h	1/1	**38** (13%), **64** (43%)
3	Zhan-1B	MW, 75 °C, DCM, 3 h	1/1	**38** (12%), **64** (45%)
4	G II	MW, 75 °C, DCM, 3 h	1/1	**38** (6%)[c]
5	Zhan-1B	MW, 75 °C, DCM, 3 h	10/1	**38** (59%), **64** (40%)
6	H II	In sealed tubes, DCM, 75 °C, overnight	10/1	**38** (51%), **64** (46%)
7	Zhan-1B	In sealed tubes, DCM, 75 °C, overnight	10/1	**38** (52%), **64** (43%)
8	H II	MW, 75 °C, perfluorobenzene, 3 h	1/1	**38** (6%), **64** (78%)

[a] 10 mol% of catalyst was used. [b] Reaction was conducted under reflux, ambient pressure. [c] Yield of **64** was not measured. [d] MW is abbreviation of microwave irradiation.

The same reactions were performed in sealed tubes to mimic the rapid heating effect under microwave conditions (Table II-1, entry 6 and 7). A night long reaction time was required to reach an even slightly lower CM yield, indicating that the highly beneficial effect of microwave irradiation did not only arise from the rapid heating allowed in the microwave oven (purely thermal/kinetic effect), but also some specific thermal microwave effect, such as wall effect and the selective heating of strongly microwave absorbing heterogeneous catalysts in less polar reaction medium.

Furthermore, polar solvent (*e.g.* DCM) is required to enhance the heating effect of microwave. Although perfluorobenzene was reported being capable of increasing activity of

CM catalysts (Samojlowicz *et al.*, 2008), its apolar character led to less efficient heating by microwave and probably thus resulted in a lower yield of **38** in comparison to that obtained with the use of DCM (table II-1, entry 2 and 8).

The cross-metathesis product **38** was found to be predominantly in the *E* configuration. Based on the integration of the 32-H and 33-H signals of both (*E*)- and (*Z*)-adenosylhopene **38** in the ^{1}H-NMR spectrum [(*E*)-32-H 4.74 ppm, (*Z*)-32-H 5.03 ppm, (*E*)-33-H 4.96 ppm, (*Z*)-33-H 4.85 ppm], the proportion of *E* isomer varied from 75% to 80%. Energy calculation of *E* and *Z* isomers using MMFF molecular mechanics by Spartan only showed a slightly lower energy for the (*E*)-adenosylhopene **38**. (876.92 kJ/mol for *E*-**38** and 895.09 kJ/mol for *Z*-**38**.) Therefore, the *E* selective CM reaction might be explained by the fact that the metallacyclic transition state corresponding to the *E*-**38** was less hindered than that of the Z isomer.

II.3.4.4. Carbon/carbon double bond reduction and reductive labeling of adenosylhopene 38

Reduction of the C-C double bond of **38** turned out to be more challenging than expected. Catalytic hydrogenation of **38** afforded disappointing yields even under pressure in the presence of various metallic catalysts, such as Pd/C (<10%), Adam's catalyst (Voorhees and Adams, 1922; Stampf, 1992) (<10%), Wilkinson's catalyst (Osborn *et al.*, 1966) (0%) and Crabtree's catalyst (Crabtree, 1979) (0%), probably due to the steric hindrance of the molecule allowing only restricted access of the catalyst to the double bond. This difficult accessibility to the olefin was circumvented by the use of the small sized diimide, which is a short-lived reagent and can be implicated in the reduction of nonpolar multiple bonds. A concerted mechanism concerning the reduction of a symmetrical C/C double bond by *cis*-diimide has been proposed (Spears and Hutchinson, 1988). Diimide is converted into N_2 via a six-center cyclic transition state, which is formed by the *syn* addition of dihydrogene to the double bond (Fig. II-22).
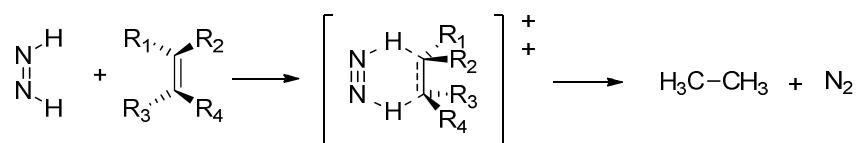
Fig. II-22. Mechanism of diimide reduction on a carbon/carbon double bond (Miller, 1965).

Diimide is typically generated through the oxidation of hydrazine, through the decarboxylation of potassium azodicarboxylate (PADA) or through thermal decomposition of sulfonylhydrazides. A recently developed one-pot protocol for the formation of 2-*N*-benzenesulfonylhydrazide (NBSH) and subsequent diimide alkene reduction was proved equally efficient (Marsh and Carbery, 2009). However, considering the future labeling reduction with deuterium, the acid promoted diimide generation from PADA would be of great interest. Furthermore, acid catalysis may speed up equilibration of the *trans-* and *cis*-diimide, favoring thus the hydrogen transfer from the *cis*-isomer to the alkene.

Direct treatment of **38** with PADA and acetic acid led to partial deprotection of 6'-*N*-benzoyl group. This protecting group was therefore removed before diimide reduction by a mixture of saturated methanolic ammonia solution and dichloromethane to afford compound **65**. Diimide reduction of the C30-C31 double bond of adenosylhopene **65** was then achieved by a continuous addition of PADA and acetic acid for 36 h, and afforded the desired product **40** with a good yield of 73%. This reaction required a large excess of diimide and long reaction time, probably because of the highly crowded substitution patterns of the double bond resulting into the relatively low reaction rate in comparison to that of the disproportionation of diimide to nitrogen gas and hydrazine, the major competing process that can significantly consume the reducing agent. In order to suppress this disproportionation as much as possible, PADA was added into the reaction mixture in small portions, and a drop of anhydrous acetic acid was added only when the nitrogen evolution had stopped, thus keeping a low concentration of diimide. On the other hand, water should be avoided in this case, because it has been reported as a very powerful inhibitor of diimide reductions in aprotic solvents, such as pyridine (Hamersma and Snyder, 1965). The presence of oxygen was not found to be deleterious, but in the present experiments the reaction mixture was flushed with nitrogen to avoid possible complications.
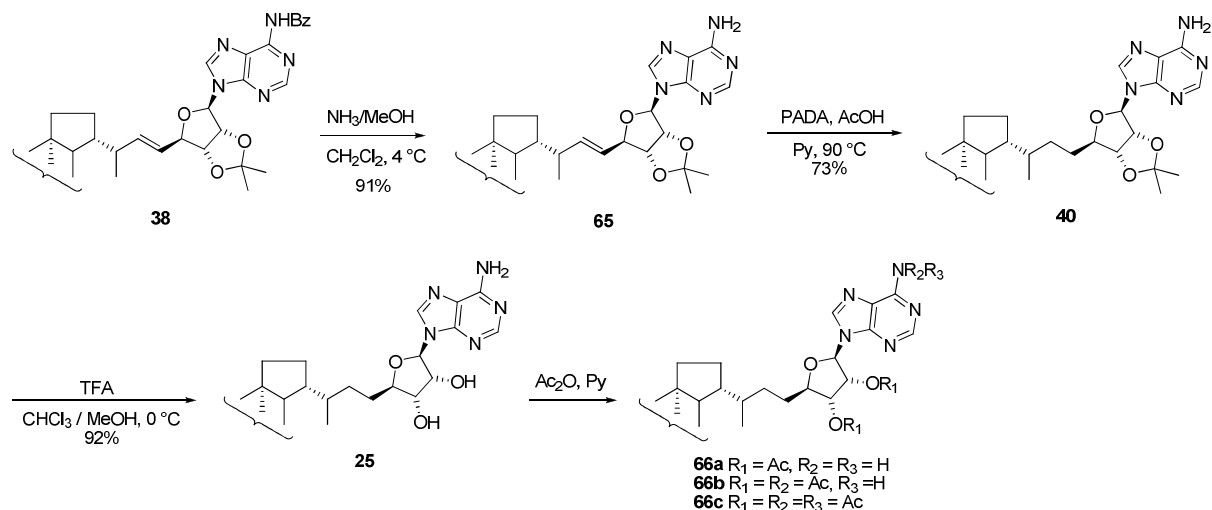
Fig. II-23. Preparation of adenosylhopane **25** from compound **38**.

Only minor changes were necessary to get the deuterium labeled adenosylhopane **25-D**. Compound **65** was first treated first with CH$_3$OD for H-D exchange to avoid introduction of extra protons from the amino group. Deuterated acetic acid CH$_3$COOD (98 atom% D) was adopted as deuterium source to generate dideuteriodiimide *in situ* (Fig. II-24). Reduction of **65-D** with dideuteriodiimide was much slower than reduction with diimide due to a primary deuterium kinetic isotope effect. The relative slow reaction afforded decreased yield (60%) of **40-D** as compared to that of natural abundance **40**, but allowed us to recover unreacted adenosylhopene **65** after 36 h treatment with PADA and AcOD. ^{1}H-NMR spectrum of the recycled starting material **65** showed that the *E/Z* ratio had decreased from 5/1 (before diimide reduction) to 1/1 (after diimide reduction), indicating a faster rate of hydrogenation of the *trans* olefin over that of the *cis* olefin. This phenomenon has been frequently observed in diimide reduction, and was attributed to the more cluttered transition state in the case of the *trans* olefin (Miller, 1965).
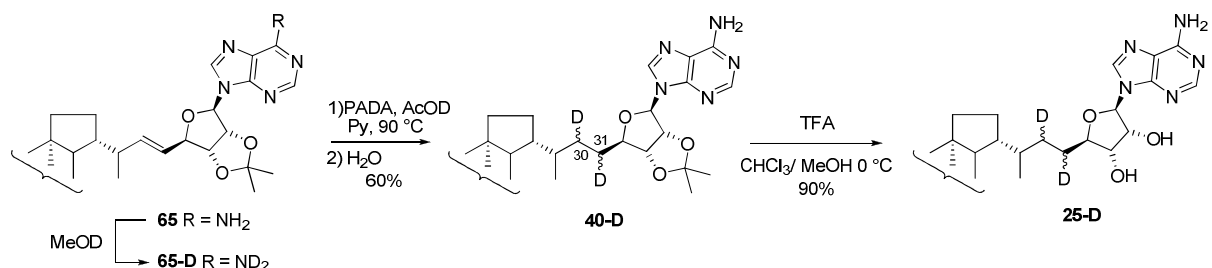
Fig. II-24. Preparation of deuteriated adenosylhopane **25-D.**

^{2}H/(^{2}H + ^{1}H) isotopic abundance of **40-D** was determined by mass spectrometry. In spite

of careful precaution against contamination by water, deuterium content was modest: 60% [30,31-^{2}H$_2$]adenosylhopane and 32% [30-^{2}H]- and [31-^{2}H]adenosylhopane accompanied by 8% natural abundance adenosylhopane. This incomplete labeling was due to the large excess of only 98% labeled CH$_3$COOD (60 eq.) and a primary deuterium kinetic effect favoring sufficiently the protonation by the low amounts of protons, thus leading to a mixture of N$_2$H$_2$, N$_2$HD and N$_2$D$_2$. The labeling ratio can be probably improved by using CH$_3$COOD with higher deuterium enrichment, but the obtained labeling was largely efficient to perform the future incorporation experiments.

II.3.4.5. Deprotection of adenosylhopane and its deuteriated isotopomers

Acid-catalyzed isopropylidene deprotection of **40** and **40-D** with a methanolic solution of TFA gave respectively adenosylhopane **25** and **25-D** in high yields (Fig. II-23 and Fig. II-24). This reaction was conducted at 0 °C on a rotary evaporator, in order to remove the 2,2-dimethoxypropane continuously and shift the reaction equilibrium. Purification of the desired adenosylhopane **25** proved, however, tricky, due to the amphiphilic character of the molecule and its poor solubility in polar solvents, such as acetonitrile, methanol and water, preventing purification by reversed phase HPLC or ion exchange chromatography. A successful purification was finally achieved via silica gel (0.063-0.200 mm) chromatography (DCM/MeOH/NH$_3$•H$_2$O 100:7.5:0.5) under gravity.

II.3.4.6. Configuration of adenosylhopane and of its deuteriated isotopomers

To confirm the structure, the synthesized adenosylhopane **25** was acetylated (Fig. II-23). The spectroscopic data of adenosylhopane acetates **66a-c** (Fig. II-23) were compared with those of natural acetylated adenosylhopane (Neunlist and Rohmer, 1985b; Neunlist *et al.*, 1988). All the analytical data of **66a-c** were consistent with those described previously. The assignments of the ^{1}H- and ^{13}C-NMR signals were made with the help of 2D NMR spectra (^{1}H-^{1}H COSY, HMBC and HSQC) by comparison with those obtained from previously performed work (Pan, 2005; Toulouse, 2011).

The structure of deuteriated adenosylhopane **25-D** was confirmed by comparing its ^{1}H-NMR and ^{13}C-NMR spectra with those of natural abundance adenosylhopane **25** (Table II-3). Four different configurations at C-30 and C-31 of adenosylhopane **25-D** were obtained

after dideuteriodiimide reduction. Given that diimide reacts faster with (*E*)-adenosylhopene, which is the dominant isomer, the major products resulting from *syn*-addition of diimide to the *trans* double bond should be [30*R*,31*R*-^{2}H$_2$]- and [30*S*,31*S*-^{2}H$_2$]adenosylhopane. The [30*R*,31*S*-^{2}H$_2$]- and [30*S*,31*R*-^{2}H$_2$]adenosylhopane diastereomers would be generated by the attack of diimide to the (*Z*)-adenosylhopene from different faces. (Fig. II-25).
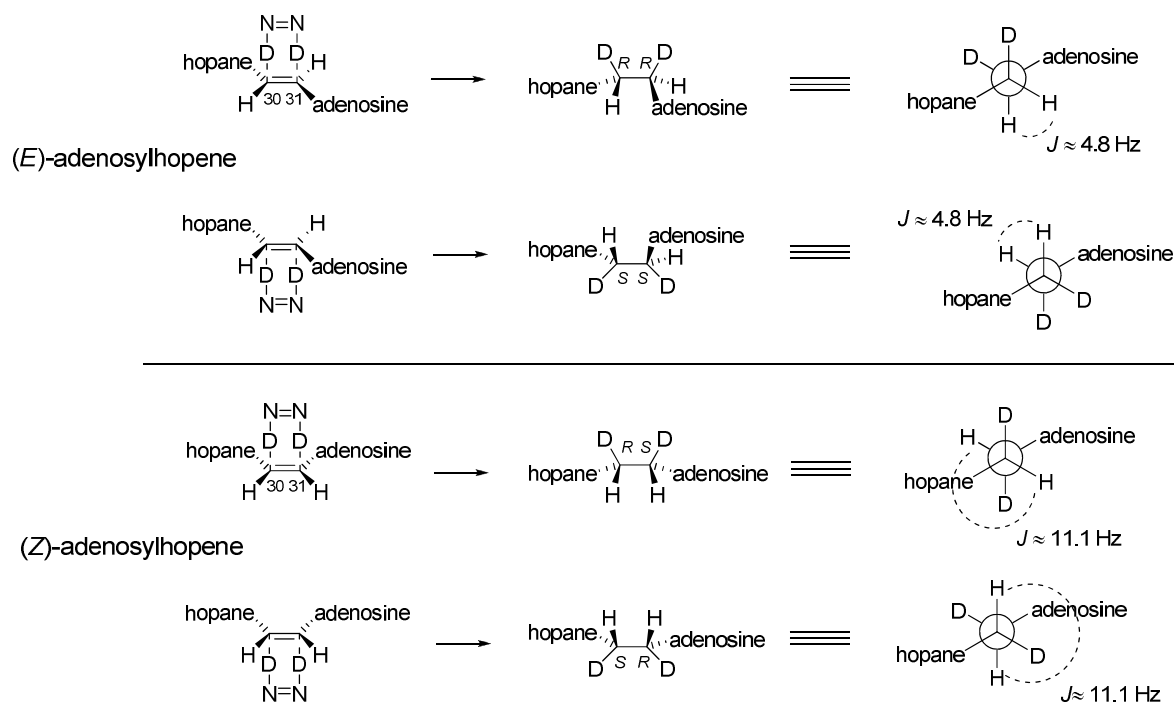
Fig. II-25. The four different diastereomers of [30,31-^{2}H$_2$]adenosylhopane resulting from diimide reduction of (*E*)- and (*Z*)-adenosylhopene **40**.

For natural abundance adenosylhopane **25**, the two protons at C-31 (31-H$_a$ and 31-H$_b$) are magnetically non-equivalent because of the chiral center at C-32. A similar situation was found for 30-H$_a$ and 30-H$_b$, which are adjacent to the asymmetric center at C-22. Assuming a straggled conformation of the side chain of adenosylhopane **25**, four different *J-J* coupling constants observed from the splitting of ^{1}H-NMR signals of 31-H$_a$ were interpreted as follows (Table II-3).

- A coupling constant of 13.7 Hz is attributed to the geminal coupling between 31-H$_a$ and 31-H$_b$. The same value was also observed for 31-H$_b$.

- A value of 8.4 Hz, which characterizes the signal splitting of 32-H signal as well results from the coupling between 31-H$_a$ and 32-H.

- The coupling constant J_{anti} =11.1 Hz originates from the coupling between 30-H$_a$ and 30-H$_b$ in the *anti* spatial relationship, which leads to a configuration with a dihedral angle

close to 180°. Therefore, the last constant (J_{gauche} = 4.8 Hz) characterizes a *J-J* coupling between 30-H_b and 31-H_a when the two adjacent C–H bonds are in *gauche* relative position. The dihedral angle between those *gauche* protons is around 60°, resulting thus in a smaller value for the corresponding coupling constant (Fig. II-25).

A similar interpretation can be applied to the signal-splitting for 31-H_b (Table II-3).

Two largest coupling constant (J_{gem} and J_{anti}) apparently disappears in the ^{1}H-NMR spectrum of deuteriated adenosylhopane **25-D** and the shape of the peaks turned into a dd from a dddd. Absence of J_{gem} indicated that there was one and only one deuterium at C-31 position. The apparent disappearance of J_{anti} between 30-H and 31-H can be explained by the reason that 30-H and 31-H are always in the *gauche* form, which was in accord with the supposed major configurations ([30*R*,31*R*-[2]H$_2$]- and [30*S*,31*S*-[2]H$_2$]adenosylhopane) originating from (*E*)-adenosylhopane. Presence of [30*R*,31*S*-[2]H$_2$]- and [30*S*,31*R*-[2]H$_2$]adenosylhopane can not be proven from ^{1}H-NMR, because the protons from the minor products, including the mono-deuteriated isotopomer and natural abundance adenosylhopane, which are generated from the incomplete labeling of adenosylhopene **65**, can not be differentiated due to their low intensity and their nearly identical chemical shifts.

The only partial deuteriation and the occurrence of four bisdeuteriated diastereomers resulted in difficulties to interpret the ^{13}C-NMR spectrum of **25-D**. The disappearance of the two singlets for carbons C-30 and C-31 pointed out the presence of two deuterium atoms in these positions. The rough α+β shifts of carbon C-30 and carbon C-31 were found from edited HSQC spectrum as -430 ppb and -410 ppb respectively. The signals of carbons C-32, C-22 and C-21 became more complex due to the deuterium atoms at C-30 and/or C-31 positions. However, values of the β or γ shifts resulting from each configuration could not be determined.

Table II-2. ^{1}H- and ^{13}C-NMR of the acetonide of (22*R*)- and (22*S*)-adenosylhopane **40** and of the bisdeuteriated (22*R*)-isotopomer **40-D**.

Proton	(22*R*)-**40** [a]	(22*R*)-**40-D** [b]	(22*S*)-**40** [c]
2'-H	8.35 (1H, s)	8.35 (1H, s)	8.736 (1H, s)
8'-H	7.89 (1H, s)	7.90 (1H, s)	8.036 (1H, s)
35-H	6.03 (1H, dd, $J_{34,35} = 2.4$ Hz)	6.03 (1H, dd, $J_{34,35} = 2.4$ Hz)	6.076 (1H, dd, $J_{34,35} = 2.2$ Hz)
-NH$_2$	5.85 (2H, s,)	5.92 (2H, s,)	—
34-H	5.51 (1H, dd, $J_{33,34} = 6.5$ Hz, $J_{34,35} = 2.4$ Hz)	5.51 (1H, ddd, $J_{33,34} = 6.4$ Hz, $J_{34,35} = 2.4$ Hz, $J_{32,34} = 1.2$ Hz)	5.547 (1H, dd, $J_{33,34} = 6.4$ Hz, $J_{34,35} = 2.2$ Hz)
33-H	4.80 (1H, dd, $J_{33,34} = 6.5$ Hz, $J_{32,33} = 3.5$Hz)	4.80 (1H, ddd, $J_{33,34} = 6.4$ Hz, $J_{32,33} = 3.5$, $J_{31,33} = 1.2$ Hz Hz)	4.835 (1H, dd, $J_{33,34} = 6.4$ Hz, $J_{32,33} = 3.1$Hz)
32-H	4.15 (1H, ddd, $J_{31a,32} = 7.4$ Hz, $J_{31b,32} = 6.5$ Hz, $J_{32,33} = 3.5$ Hz)	4.15 (1H, br dd, $J_{31,32} = 7.3$, $J_{32,33} = 3.5$ Hz, 32-H)	4.202 (1H, m)
Me$_2$C	1.60 and 1.38 (6H, 2s)	1.60 and 1.38 (6H, 2s)	1.613 &1.399 (6H, 2s)
8β-Me	0.928 (3H, s)	0.927 (3H, s)	0.952
14α-Me	0.921 (3H, s)	0.920 (3H, s)	0.938
22-Me	0.83 (3H, d, $J = 6.2$ Hz)	0.838-0.827 (6H, m)	0.732
4α-Me	0.834 (3H, s)		0.849
10β-Me	0.800 (3H, s)	0.798 (3H, s)	0.812
4β-Me	0.779 (3H, s)	0.778 (3H, s)	0.793
18α-Me	0.656 (3H, s)	0.655 (3H, s)	0.612

Carbon	(22*R*)-**40** [a]	(22*R*)-**40-D** [b]	Carbon	(22*R*)-**40** [a]	(22*R*)-**40-D** [b]
C-1	40.3	40.3	C-22	36.38	36.35, 36.28 and 36.25
C-2	18.7	18.7	C-23	33.4	33.4
C-3	42.1	42.1	C-24	21.6	21.6
C-4	33.3 or 33.2	33.3 or 33.2	C-25	15.9 or 15.8	15.9 or 15.8
C-5	56.1	56.1	C-26	16.6 or 16.5	16.6 or 16.5
C-6	18.7	18.7	C-27	16.6 or 16.5	16.6 or 16.5
C-7	33.3 or 33.2	33.3 or 33.2	C-28	15.9 or 15.8	15.9 or 15.8
C-8	41.7	41.6	C-29	20.0	20.0
C-9	50.4	50.4	C-30	31.4	—
C-10	37.4	37.4	C-31	30.0	—
C-11	20.9	20.9	C-32	87.67	87.63 and 87.60
C-12	23.9	23.9	C-33	84.0	84.0
C-13	49.3	49.2	C-34	84.3	84.3
C-14	41.8	41.8	C-35	90.5	90.5
C-15	33.6	33.6	C-2'	153.0	152.9
C-16	22.7	22.7	C-4'	149.4	149.4
C-17	54.4	54.3	C-5'	120.3	120.3
C-18	44.3	44.3	C-6'	155.4	155.5
C-19	41.5	41.5	C-8'	139.8	139.8
C-20	27.5	27.5	-*C*Me$_2$	114.4	114.4
C-21	45.74	45.70	-C(*C*H$_3$)$_2$	27.1 &25.4	27.1 and 25.4

[a] (CDCl$_3$, 75 MHz). [b] (CDCl$_3$, 150 MHz). [c] (CDCl$_3$, 250 MHz) (Stampf, 1992)

Table II-3. ^{1}H- and ^{13}C-NMR of deprotected (22R)-adenosylhopane **25** and of the bisdeuteriated isotopomer **25-D**.

Proton	25 [a]	25-D [a]
2'-H	8.77 (1H, s)	8.72 (1H, s)
8'-H	8.61 (1H, s)	8.60 (1H, s)
-NH$_2$	8.29 (2H, s)	8.28 (2H, s)
34-OH	7.74 (1H, d, $J_{34,34\text{-OH}}$ = 5.5 Hz)	7.73 (1H, d, $J_{34,34\text{-OH}}$ = 5.1 Hz,)
33-OH	7.04 (1H, d, $J_{33,33\text{-OH}}$ = 5.8 Hz)	7.03 (1H, d, $J_{33,33\text{-OH}}$ = 5.6 Hz)
35-H	6.72 (1H, d, $J_{34,35}$ = 4.4 Hz)	6.72 (1H, d, $J_{34,35}$ = 4.4 Hz)
34-H	5.43 (1H, *pseudo* q, J = 4.7 Hz)	5.43 (1H, *pseudo* td, J = 4.8, 3.9 Hz,)
33-H	4.77 (1H, *pseudo* q, J = 5.2 Hz)	4.77 (1H, *pseudo* q, J = 5.0 Hz)
32-H	4.56 (1H, *pseudo* dt, J = 8.4, 4.8 Hz)	4.57-4.54 (1H, m)
31-H$_a$	2.13 (1H, dddd, J_{gem} = 13.7 Hz, $J_{30a,31a}$ = 11.1 Hz, $J_{31a,32}$ = 8.4 Hz, $J_{30b,31a}$ = 4.7 Hz)	2.11 (1H, dd, $J_{31a,32}$ = 8.3 Hz, $J_{30b,31a}$ = 4.6 Hz)
31-H$_b$	1.99-1.92 (1H, dddd, J_{gem} = 13.7 Hz, $J_{30b,31b}$ = 11.3 Hz, $J_{31b,32}$ = $J_{30a,31b}$ = 5.0 Hz)	1.93 (1H, br. dd, $J_{31b,32}$ = $J_{30a,31b}$ = 4.9 Hz)
30-H$_a$ and 20-H$_a$	1.82-1.76 (2H, m)	1.82-1.71 (3H, m)
21-H	1.75-1.72 (1H, m)	
22-Me	0.994 (3H, d, J = 6.3 Hz)	0.993 (3H, d, J = 6.3 Hz)
8β-Me	0.959 (3H, s)	0.961 (3H, s)
14α-Me	0.948 (3H, s)	0.949 (3H, s)
4α-Me	0.882 (3H, s,	0.883 (3H, s)
4β-Me	0.819 (3H, s)	0.820 (3H, s)
10β-Me	0.815 (3H, s)	0.816 (3H, s)
18α-Me	0.665 (3H, s)	0.667 (3H, s)

Carbon	25 [b]	25-D [b]	Carbon	25 [b]	25-D [b]
C-1	40.5	40.5	C-21	46.37	46.34
C-2	19.0	19.0	C-22	36.94	36.90, 36.86 and 36.81
C-3	42.3	42.3	C-23	33.6	33.6
C-4	33.4	33.4	C-24	21.8	21.8
C-5	56.4	56.4	C-25	16.0 or 16.1	16.0 or 16.1
C-6	19.0	19.0	C-26	16.8 or 16.7	16.8 or 16.7
C-7	33.6	33.6	C-27	16.8 or 16.7	16.8 or 16.7
C-8	41.9	41.9	C-28	16.0 or 16.1	16.1 or 16.0
C-9	50.7	50.7	C-29	20.4	20.3
C-10	37.6	37.6	C-30	32.3	—
C-11	21.2	21.2	C-31	31.0	—
C-12	24.2	24.2	C-32	85.23	85.20 and 85.15
C-13	49.6	49.6	C-33 and C-34	75.24 and 75.16	75.21 and 75.15
C-14	42.0	42.0	C-35	90.0	90.0
C-15	33.9	33.9	C-2'	153.8	153.8
C-16	23.0	23.0	C-4'	150.6	150.6
C-17	54.6	54.6	C-5'	121.3	121.3
C-18	44.5	44.5	C-6'	157.6	157.6
C-19	41.8	41.8	C-8'	140.0	140.0
C-20	27.9	27.9			

[a] (pyridine-D5, 600 MHz). [b] (pyridine-D5, 150 MHz)

II.4. Conclusion

A concise and flexible approach has been developed for the hemisynthesis of adenosylhopane with excellent stereochemical control at all asymmetric centers. It includes as key steps, a cross metathesis between two olefins containing either the hopane moiety or a protected adenosine derivative and a subsequent diimide reduction of the resulting olefin (Fig. II-26). This strategy also allowed the access to deuteriated adenosylhopane isotopomers via the reduction step.
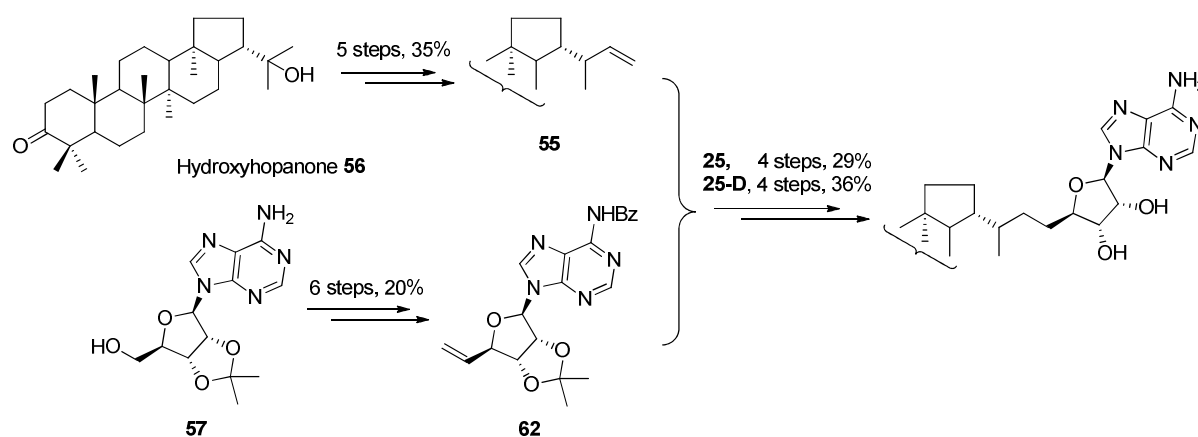
Fig. II-26. Schematic summary for the synthesis of adenosylhopane **25** and its isotopomer **25-D**.

The synthetic protocol described here is of general utility because it might also give access to tritiated adenosylhopane and to other elongated hopanoids via cross metathesis between homohopene **55** and a proper methylene derived partner. It represents a versatile tool to access to diverse/many complex bacterial hopanoids for biosynthetic studies. Adenosylhopane **25** seems indeed to be the most difficult natural hopanoid isolated to date to synthesize, because of the proximity of the triterpene skeleton and adenine. Once again, we were impressed to see that nature has succeeded in the difficult task of joining such hindered pieces by a carbon-carbon bond, with the help of a close preorganized environment in the active site, and thus giving rise to plenty of varied structures.

II.5. Experimental Part

Hydroxyhopanone 56
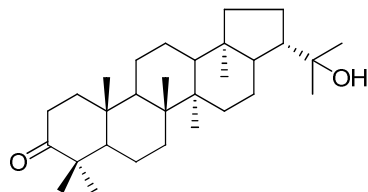
Finely ground resin (1 kg) was extracted with methanol (4 L) by simmering for 1 hr. After the mixture had stood overnight, the undissolved material was filtered off and the extract evaporated under reduced pressure. The residue, in 100 g batches, was dissolved in ether (450 mL) and the dammar acids removed by shaking with KOH solution (5%, 250 mL) and then with water. The ethereal solution was dried with Na_2SO_4 and its volume adjusted to 4.5 mL per 1 g of extract used. The solution was kept at 0 °C for several days and was then decanted from the solid which separated and which generally firmly adhered to the sides of the flask. The solid was washed with ether and crystallized from acetone or isopropyl acohol to give hydroxyhopanenone as white needles (5.5 g per 1 kg of resin).

(This procedure has been described by Dunstan *et al.*, 1957)

Diplopterol 2
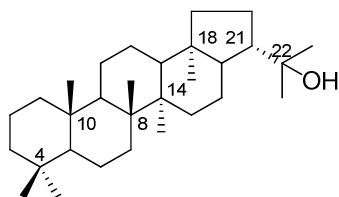
To a suspension of hydroxyhopanone **56** (1 g, 2.5 mmol) in diethylene glycol (100 mL) was added hydrazine monohydrate (12 mL, 0.25 mol). The mixture was vigorously stirred. The reaction mixture was refluxed at 170 °C for 2 h, after which time, the flask was cooled down to room temperature. Hydrazine and water were distilled off under reduced pressure (33 °C, 9 mmHg) before KOH powder (2.5 g) was added and the reaction mixture was refluxed overnight at 210 °C. The mixture was allowed to reach room temperature before water and Et_2O were added. The two phases were separated, and the aqueous layer was

extracted twice with Et$_2$O. The combined organic phases were dried over anhydrous Na$_2$SO$_4$ and filtered through cotton. The filtrates were evaporated to dryness providing a crystalline product **2**, which was further purified by FCC (PE/EtOAc 14:1) (0.87 g, 90%).

(This molecule has been previously described in the literature: Stampf, 1992).

^{1}H NMR (300 MHz, CDCl$_3$): δ/ppm = 2.22 (1H, dt, J = 9, 10.4 Hz, 21-H), 1.91 (1H, m), 1.205 and 1.176 (6H, 2s, 22-Me), 0.953 (6H, s, 8β and 14α-Me), 0.842 (3H, s, 4α-Me), 0.811 (3H, s, 10β-Me), 0.789 (3H, s, 4β-Me), 0.758 (3H, s, 18α-Me).

^{13}C NMR (75 MHz, CDCl$_3$): δ/ppm = 73.9, 56.1, 53.9, 51.1, 50.3, 49.8, 44.1, 42.1, 41.9, 41.8, 41.2, 40.3, 37.4, 34.4, 33.4, 33.2 (2C), 30.8, 28.7, 26.6, 24.1, 22.0, 21.6, 20.9, 18.7 (2C), 17.0, 16.7, 16.1, 15.8.

MS (EI, direct inlet, positive mode 70 eV): m/z = 428 (M$^+$, 3%), 410 (M$^+$-H$_2$O, 14%), 395 (M$^+$-CH$_3$, 7%), 367 (M$^+$-side chain-2H, 17%), 341 (6%), 299 (4%), 231 (17%), 207 (ring C cleavage, 19%), 191 (ring C cleavage, 100%), 189 (72%), 149 (56%), 121 (26%).

(22*S*)- and (22*R*)-Hopan-29-ol   28

A solution of diplopterol **2** (812 mg, 1.89 mmol) in dry DCM/2,6-lutidine (35 mL/8.8 mL) was cooled down to 0 °C under Ar. Then freshly distilled SOCl$_2$ (1.4 mL, 19 mmol) was added dropwise to this mixture. After 20 min of stirring at this temperature, the reaction mixture was quenched with a saturated solution of Na$_2$CO$_3$ and extracted twice with DCM. The combined organic phases were dried over anhydrous Na$_2$SO$_4$ and filtered through cotton. The solvents were evaporated *in vacuo*. After drying overnight under vacuum, the crude mixture (diploptene/hop-21-ene, ca. 3/1, mol/mol) was dissolved in dry THF (45 mL) under Ar. Then a solution of 9-BBN in THF (0.5 M, 43 mL, 21.5 mmol) was added at 0 °C. The reaction mixture was stirred for 24 h at room temperature. An aqueous solution of NaOH (3 M, 30 mL) was added to the stirred reaction mixture at 0 °C, followed by 30% H$_2$O$_2$ (30 mL). The two phases were separated after being vigorously stirred for 1 h at 40 °C. The aqueous phase was extracted twice with Et$_2$O. The combined organic phases were dried over anhydrous NaSO$_4$ and filtered through cotton. The solvents were evaporated under reduced

pressure. The crude product was purified by FCC (PE/EtOAc, 8:1) to yield alcohol epimers at C-22 **28$_S$** (36mg, 4.5%) and **28$_R$** (357 mg, 44%) as colorless crystals.

(These molecules have been previously described in the literature: Stampf, 1992; Duvold and Rohmer, 1999; Pan, 2005)

(*22S*)-Hopan-29-ol   28$_S$:
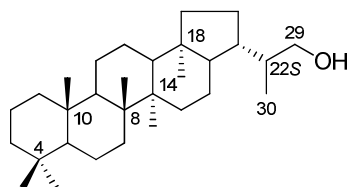
R$_f$ 0.34 (toluene/EtOAc, 9 :1)

M.p. 209-210 °C (Lit: 209-210 °C, Duvold and Rohmer 1999).

^{1}H NMR (300 MHz, CDCl$_3$): δ/ppm = 3.63 (1H, dd, $J_{22, 29b}$= 3.1Hz, $J_{29a, 29b}$= 10.6 Hz, 29-H$_b$), 3.38 (1H, dd, $J_{22, 29a}$= 6.7 Hz, $J_{29a, 29b}$= 10.6 Hz, 29-H$_a$), 1.05 (3H, d, $J_{22, 30}$= 6.4Hz, 22*S*-CH$_3$), 0.953 (6H, s, 8β and 14α-CH$_3$), 0.845 (3H, s, 4α-CH$_3$), 0.813 (3H, s, 10β-CH$_3$), 0.790 (3H, s, 4β-CH$_3$), 0.721 (3H, s, 18α-CH$_3$).

^{13}C NMR (75 MHz, CDCl$_3$): δ/ppm = 67.76, 56.13, 54.26, 50.42, 49.26, 44.39, 42.57, 42.10, 41.81, 41.72, 41.66, 40.32, 39.60, 37.38, 33.63, 33.40, 33.28, 33.24, 27.17, 23.97, 22.64, 21.58, 20.93, 18.69 (2C), 18.15, 16.60, 16.51, 15.90, 15.76.

MS (EI, direct inlet, positive mode 70 eV): m/z = 428 (M$^+$, 5%), 369 (M$^+$-side chain, 7%), 207 (ring C cleavage, 100%), 191 (ring C cleavage, 70%), 149 (55%), 121 (16%).

(*22R*)-Hopan-29-ol   28$_R$
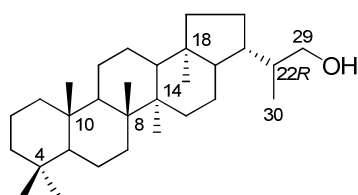
R_f 0.40 (toluene/EtOAc, 9 :1)

M. p. 190-192 °C.

^{1}H NMR (300 MHz, CDCl$_3$): δ/ppm = 3.74 (1H, dd, $J_{22,\,29b}$ = 3.0Hz, J_{gem} = 10.6 Hz, 29-H$_b$), 3.34 (1H, dd, $J_{22,\,29a}$ = 7.3 Hz, J_{gem} = 10.6 Hz, 29-H$_a$), 0.948 (6H, s, 8β and 14α-CH$_3$), 0.930 (3H, d, $J_{22,\,30}$ = 6.7Hz, 22R-CH$_3$), 0.843 (3H, s, 4α-CH$_3$), 0.812 (3H, s, 10β-CH$_3$), 0.789 (3H, s, 4β-CH$_3$), 0.710 (3H, s, 18α-CH$_3$).

(22S)-Hopan-30-al   58
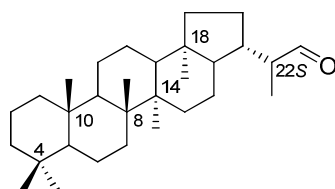
A solution of (COCl)$_2$ (1.1 mL, 12 mmol) in dry DCM (10 mL) was cooled down at -78 °C under Ar, and dry DMSO (1.1 mL, 15 mmol) in dry DCM (1 mL) was added slowly. The alcohol **28$_S$** (644 mg, 1.5 mmol) in dry DCM (120 mL) was added slowly, and the reaction mixture was stirred at –78 °C for 3 h. After this time the reaction was quenched with triethylamine (5.2 mL) at –78 °C, and then the mixture was allowed to attain room temperature and stirred for additional 1 h. The reaction mixture was poured into water and extracted with DCM twice. The combined organic phases were dried over anhydrous Na$_2$SO$_4$ and filtered through cotton. The solvents were evaporated under reduced pressure. The crude product was purified by FCC (PE/EtOAc 35:1) to yield a crystalline product (600 mg, 94%) (This molecule has been previously described in the literature: Duvold and Rohmer, 1999)

M.p. 179-180 °C (Lit: 180-181 °C, Duvold and Rohmer 1999).

^{1}H NMR (300 MHz, CDCl$_3$): δ/ppm = 9.42 (1H, d, $J_{22,\,29}$ = 4.4 Hz, -CHO), 2.54-2.43 (1H, m, 22S-H), 2.24-2.12 (1H, m), 1.20-1.89 (1H, m), 1.101 (3H, d, $J_{22,\,30}$ = 6.7 Hz, 22S-CH$_3$), 0.956 (6H, s, 8β and 14α-CH$_3$), 0.845 (3H, s, 4α-CH$_3$), 0.813 (3H, s, 10β-CH$_3$), 0.790 (3H, s, 4β-CH$_3$), 0.730 (3H, s, 18α-CH$_3$).

^{13}C NMR (75 MHz, CDCl$_3$): δ/ppm = 205.07, 56.08, 53.89, 50.52, 50.34, 49.19, 44.51, 42.06, 41.83, 41.80, 41.60, 40.88, 40.29, 37.37, 33.45, 33.38, 33.26, 33.22, 27.73, 23.91, 21.97, 21.57, 20.86, 18.66, 16.60, 15.86, 15.77, 14.90.

MS (EI, direct inlet, positive mode 70 eV): m/z = 426 (M$^+$, 7%), 369 (M$^+$-side chain, 8%), 368 (M$^+$-C$_3$H$_6$O), 206 (ring C cleavage, 18%), 205 (100%), 191 (ring C cleavage, 85%), 149 (25%)

(22*S*)-Homohop-30-ene   55
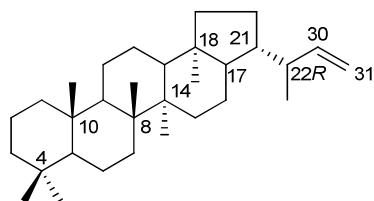
A suspension of NaH (126 mg, 5 mmol) in DMSO (2.5 mL) was stirred at 75 °C for 50 min. The light green suspension was cooled down to room temperature, added into a solution of PPh$_3$CH$_3$Br (1.9 g, 5.4 mmol) in DMSO (27 mL) and stirred at room temperature for 20 min to afford a light green-grey suspension. The resulted mixture was then added into a solution of aldehyde **58** (297 mg, 0.70 mmol) in THF (20 mL) and stirred overnight at 50 °C. The reaction was quenched with water, and extracted three times with pentane. The combined organic phases were dried over anhydrous Na$_2$SO$_4$, filtered through cotton, and evaporated to dryness *in vacuo* to give an almost pure crystalline product, which was further purified by FCC (petroleum ether) to yield the terminal olefin **55** (290 mg, 98%). R$_f$ 0.67 (petroleum ether/EtOAc 20:1).

M.p. 203-205 °C

^{1}H-NMR (600 MHz, CDCl$_3$): δ/ppm = 5.53 (1H, ddd, $J_{30,31a}$ = 17.8 Hz, $J_{30,31b}$ = 9.5 Hz, $J_{22,30}$ = 9.1 Hz, 30-H), 4.85 (1H, ddd, $J_{30,31a}$ = 17.8 Hz, J_{gem} = 2.0 Hz, J_{22-31a} = 0.5 Hz, 31-H$_a$), 4.85 (1H, dd, $J_{30,31b}$ = 9.5 Hz, J_{gem} = 2.0 Hz, 31-H$_b$), 2.21 (1H, ddq, $J_{21,22}$ = 9.7 Hz, $J_{22,30}$ = 9.1 Hz, $J_{22,29}$ = 6.5 Hz, 22-H), 1.8 (1H, tdd, $J_{21,22}$ = 9.7 Hz, $J_{20,21}$ = $J_{17,21}$ = 4.8 Hz, 21-H), 1.01 (3H, d,

$J_{22,29}$ = 6.5 H, 22R-Me), 0.960 (6H, s, 8β-Me and 14α-Me), 0.851 (3H, s, 4α-Me), 0.818 (3H, s, 10β-Me), 0.796 (3H, s, 4β-Me), 0.710 (3H, s, 18α-Me).

^{13}C-NMR (150 MHz, CDCl$_3$): δ/ppm = 145.3, 112.0, 56.1, 54.1, 50.4, 49.2, 45.0, 44.4, 42.2, 42.1, 41.9, 41.8, 41.7, 40.3, 37.4, 33.5, 33.4, 33.3, 33.2, 27.6, 24.0, 22.3, 22.0, 21.6, 20.9, 18.7, 16.6, 15.9.

MS (EI, direct inlet, positive mode 70 eV): m/z = 424 (M$^+$, 19%), 409 (M$^+$–CH$_3$, 5%), 369 (M$^+$–side chain, 20%), 203 (ring C cleavage, 100%), 191 (ring C cleavage, 88%).

6-N-benzoyl-2',3'-O-isopropylideneadenosine   60
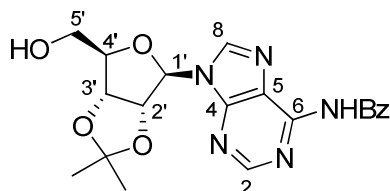
To 2',3'-O-isopropylideneadenosine **57** (1.4 g, 4.7 mmol) in freshly distilled pyridine (35 mL) is added TMSCl (4.7 mL, 37 mmol), and the mixture was stirred at ambient temperature overnight. After adding benzoyl chloride (1.1 mL, 9.3 mmol) at 0 °C, the mixture was allowed to warm up to room temperature and stirred for an additional 2 h. The reaction was stopped by adding water (10 mL) at 0 °C with stirring. After stirring 5 min at 0 °C and another 5 min at room temperature, 30% aqueous ammonia (20 mL) is added. After stirring an additional 30 min the mixture is partitioned between equal volumes (40 mL) of DCM and phosphate buffer (pH = 7). The organic phase was washed with water (3×10 mL), dried with anhydrous Na$_2$SO$_4$ and evaporated to dryness. The crude compound was purified by FCC (DCM/ MeOH 100:3, 100:4, 100:4.5) to yield crystalline product **60** (1.8 g, 94%).

(This molecule has been described in the literature: McLaughlin *et al.*, 1985)

M.p. 147-149 °C (Lit: 148-150 °C, Stampf 1992)

^{1}H NMR (300 MHz, CDCl$_3$): δ/ppm = 9.37 (1H, br., -NH) 8.74 (1H, s, 2-H), 8.10 (1H, s, 8-H), 8.03-8.00 (2H, m, arom. H), 7.62-7.47 (3H, m, arom. H), 5.96 (1H, d, J = 4.6 Hz, 1'-H), 5.21

(1H, dd, J = 5.9, 4.6 Hz, 2'-H), 5.09 (1H, dd, J = 5.9, 1.3 Hz), 4.52 (1H, m, 4'-H), 3.96 (1H, dd, J = 12.6, 1.7 Hz, 5'$_b$-H), 3.79 (1H, dd, J = 12.6, 2.2 Hz, 5'$_a$-H), 1.63 and 1.37 (3H, s, Me$_2$C).

^{13}C NMR (75 MHz, CDCl$_3$): δ/ppm = 164.7 (C=O), 152.2 (2-C), 150.5 (6-C), 150.3 (4-C), 142.5 (8-C), 133.4, 132.9, 128.8, 128.0, 124.2 (5-C), 114.2 (Me$_2$C), 94.0 (1'-C), 86.3 (4'-C), 83.2 (2'-C), 81.5 (3'-C), 63.2 (5'-C), 27.5 (Me$_2$C), 25.2 (Me$_2$C).

MS (ESI): m/z = 434 [M+Na]$^+$.

6-N-Benzyol-5'-deoxy-2',3'-O-isopropylidene-5',5'-(N,N'-diphenylethylenediamino)adenosine   61
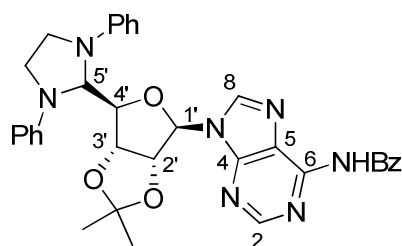
To a solution of 6-N-benzoyl-2',3'-O-isopropylidene adenosine **60** (1.8 g, 4.38 mmol) and N,N'-dicyclohexylcarbodiimide (2.7 g, 13.1 mmol) in dry DMSO (14 mL) was added dropwise dichloroacetic acid (0.18 mL, 2.2 mmol) in DMSO (1.5 mL) at 0 °C. After stirring for 2.5 h at ambient temperature, a solution of oxalic acid dihydrate (1.1 g, 8.8 mmol) in methanol (4.5 mL) was added slowly. The mixture was then stirred for another 30 min and then filtered. The crystalline residue of dicyclohexylurea was washed with ice-cold methanol. N,N'-Diphenylethylenediamine (975 mg, 4.6 mmol) was added to the combined filtrate and washings and the resulting solution was stirred at room temperature overnight. The mixture was diluted with EtOAc after being concentrated under vacuum, and washed with water three times. After evaporating the solvent, the crude compound was purified by FCC (DCM/MeOH, 100:1.5). Proper fractions were collected, concentrated and then recrystallized in EtOH to give N,N'-diphenylimidazolidine **61** as light brown crystals (2.0 g, 76%).

(This molecule has been described in the literature: Eppacher *et al*., 2004.)

M.p. 133-135 °C (Lit: 131-133 °C, Stampf 1992).

^{1}H NMR (300 MHz, CDCl$_3$): δ/ppm = 9.19 (1H, br. s, -NH), 8.73 (1H, s, 2-H), 8.04-8.02 (2H, m, arom. H) 7.81 (1H, s, 8-H), 7.63-7.50 (3H, m, arom. H), 7.23-7.14 (4H, m, arom. H), 6.82-6.70 (6H, m, arom. H), 6.17 (1H, d, J = 2.2 Hz, 1'-H), 5.75 (1H, d, J = 2.6 Hz, 5'-H), 5.21 (1H, dd, J = 6.2, 4.6 Hz, 3'-H), 5.17 (1H, dd, J= 6.2, 2.2 Hz, 2'-H), 4.63 (1H, dd, J = 4.6, 2.6 Hz, 4'-H), 3.74-3.57 (4H, m, CH$_2$CH$_2$), 1.49 & 1.33 (6H, 2s, Me$_2$C).

^{13}C NMR (75 MHz, CDCl$_3$): δ/ppm = 164.6 (C=O), 152.8 (2-C), 151.2 (6-C), 149.5 (4-C), 146.4, 141.6 (8-C), 133.6, 132.7, 129.3, 129.1, 128.8, 127.9, 122.9 (5-C), 118.3, 118.2, 115.0, 113.5, 113.4, 88.4 (1'-C), 86.9 (4'-C), 83.7 (2'-C), 80.1 (3'-C), 73.3 (5'-C), 58.3, 47.7, 46.8, 27.3, 25.7.

MS (ESI): m/z = 604 [M+H$^+$].

6-N-Benzoyl-9-(2,3-O-isopropylidene-β-D-ribo-pentodialdo-1,5-furanosyl)adenine Hydrate   39•H$_2$O
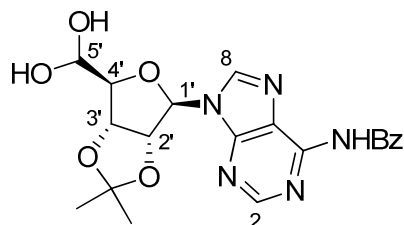
Dowex 50 (H$^+$) resin (3 g) was added to a solution of **60** (2.8 g 4.6 mmol) dissolved in THF/H$_2$O 1:1 (240 mL) and stirred for 4 h at room temperature. The resin was removed by filtration and washed with THF (5×10 mL). The combined filtrates were concentrated to *ca.* ½ of the volume and the resulting white, amorphous solid was removed, washed with water, and dried *in vacuo* to afford **39•H$_2$O** (1.3 g, 67%) as a stable hydrate.

(This molecule has been described in the literature: Eppacher *et al*., 2004.)

^{1}H NMR (300 MHz, DMSO-D6): δ/ppm = 11.21 (1H, br. s, -NH), 8.76 (1H, s, 2-H), 8.64 (1H, s, 8-H), 8.06-8.03 (2H, m, arom. H), 7.68-7.53 (3H, m, arom. H), 6.32 (1H, d, J = 5.8 Hz, -OH), 6.27 (1H, d, J = 2.6 Hz, 1'-H), 6.20 (1H, d, J = 6.1Hz, -OH), 5.37(1H, dd, J = 2.7, 6.1

Hz, 2'-H), 5.07 (1H, dd, J = 1.7, 6.1 Hz, 3'-H) 4.85 (1H, ddd, J = 4.9, 5.7, 6.1 Hz, 5'-H), 4.08 (1H, dd, J = 1.7, 4.8 Hz, 4'-H), 1.56 & 1.35 (6H, 2s, Me$_2$C)

MS (ESI): m/z = 450 [M+Na]$^+$.

Adenosine derivatives aldehyde 39 and cyclonucleoside 63

A suspension of hydrated aldehyde **39**•H$_2$O (1.3 g, 3.1 mmol) in benzene (75 mL) was heated under reflux for 2 h using a Dean-Stark condenser and evaporated. The residue was dried *in vacuo* to afford aldehyde **39** (1.1 g, 85%) and cyclonucleoside **63** (190 mg, 15%) as an inseparable mixture.

6-*N*-Benzoyl-2', 3'-*O*-isopropyldieneadenosine-5'-aldehyde   39
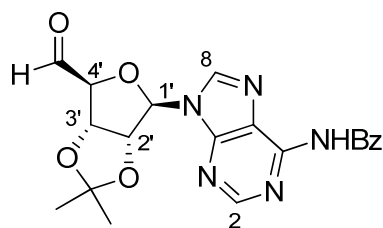
(Aldehyde **39** has been described in the literature: Ranganathan *et at.*, 1974 and Eppacher *et al.*, 2004.)

^{1}H NMR (300 MHz, DMSO-D6): δ/ppm = 11.24 (1H, br. s, -NH), 9.33 (1H, s, CHO), 8.63 (1H, s, 2-H), 8.60 (1H, s, 8-H), 8.06-8.03 (2H, m, arom. H) 7.68-7.53 (3H, m, arom. H), 6.58 (1H, s, 1'-H), 5.51 (1H, dd, J = 1.7, 6.0 Hz, 3'-H), 5.43 (1H, d, J = 6.0 Hz, 2'-H), 4.8 (1H, d, J = 1.6 Hz, 4'-H), 1.55 & 1.37 (6H, 2s, Me$_2$C).

MS (ESI): m/z = 432 [M+Na]$^+$.

(5'*S*)-6-*N*-Benzoyl-8,5'-cyclo-2',3'-*O*-isopropyldieneadenosine-5'-aldehyde   63
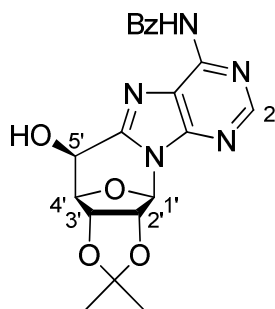
(This molecule has been described in the literature: Eppacher *et al*., 2004.)

^{1}H NMR (300 MHz, CDCl$_3$): δ/ppm = 9.23 (1H, br. s, -NH), 8.75 (1H, s, 2-H), 8.02-8.00 (2H, m, arom. H), 7.72-7.45 (3H, m, arom. H), 6.31 (1H, s, 1'-H), 5.39 (1H, dd, *J* = 2.1, 6.4 Hz, 5'-H), 5.08 (1H, d, *J* = 5.7Hz, 3'-H), 4.54 (1H, d, *J* = 5.7 Hz, 2'-H), 4.49 (1H, d, *J* = 6.4 Hz, 4'-H), 1.51 & 1.27 (6H, 2s, Me$_2$C).

MS (ESI): *m/z* = 410 [M+H]$^+$.

6-*N*-Benzoyl-5'-methylene-2',3'-*O*-isopropylidene adenosine   62
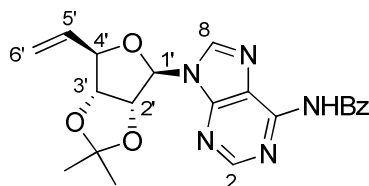
To a stirred suspension of methyltriphenylphosphonium bromide (1.8 g, 5 mmol) in dry THF (80 mL) under Ar was added a solution of *t*-BuLi in THF (3.1 mL, 2.1 mmol) at –40 °C. The bright yellow solution was warmed up to 0 °C and stirred for another 1 h before being cooled to –40 °C again. The mixture of aldehyde **39** and cyclonucleoside **63** (880 mg, 85/15, mol/mol) in anhydrous THF (40 mL) was added slowly and stirring continued at –40 °C for 2 h and overnight at 0 °C. A saturated NH$_4$Cl/H$_2$O (60 mL) was added. The layers were separated. The aqueous layer was extracted twice with EtOAc. The two organic fractions were combined and washed with NaHCO$_3$/H$_2$O and brine. After drying over anhydrous NaSO$_4$, the residue was evaporated to dryness *in vacuo* and purified by FCC (DCM/MeOH 100:4) to give terminal olefin **62** as a colorless solid foam (588 mg, 67%).

^{1}H NMR (300 MHz, CDCl$_3$): δ/ppm = 8.78 (1H, s, 2-H), 8.08 (1H, s, 8-H), 8.02-8.7.99 (2H, m, arom. H), 7.60-7.46 (3H, m, arom. H), 6.17 (1H, d, J = 2.0 Hz, 1'-H), 5.88 (1H, ddd, J = 17.2, 10.5, 6.8 Hz, 5'-H), 5.54 (1H, dd, J = 6.2, 2.0 Hz, 2'-H), 5.24 (1H, ddd apparent dt, J = 17.2, 1.3 Hz, 6'-H$_a$), 5.13 (1H, ddd apparent like dt, J = 10.5, 1.1 Hz, 6'-H$_b$), 5.01 (1H, dd, J = 6.2, 3.3 Hz, 3'-H), 4.71 (1H, dd, J = 6.8, 3.3 Hz, 4'-H), 1.62 & 1.40 (6H, 2s, Me$_2$C).

^{13}C NMR (75 MHz, CDCl$_3$): δ/ppm = 164.7, 152.6, 151.3, 149.7, 142.2, 134.7, 133.5, 132.7, 128.8, 127.8, 123.5, 118.4, 114.5, 90.7, 88.4, 84.4, 84.2, 27.0, 25.3.
MS (ESI): m/z = 408 [M+H]$^+$.

(*E*)-33,34-*O*-Isopropylidene-6'-*N*-benzoyl adenosylhop-30-ene   (*E*)-38
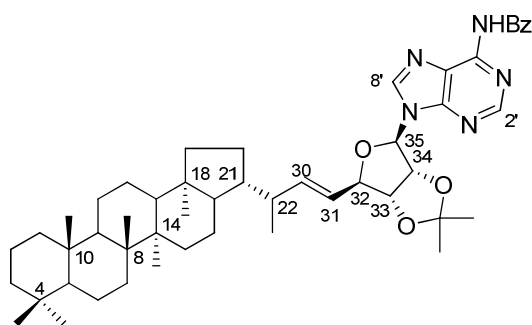
(*Z*)-33,34-*O*-Isopropylidene-6'-*N*-benzoyl adenosylhop-30-ene   (*Z*)-38
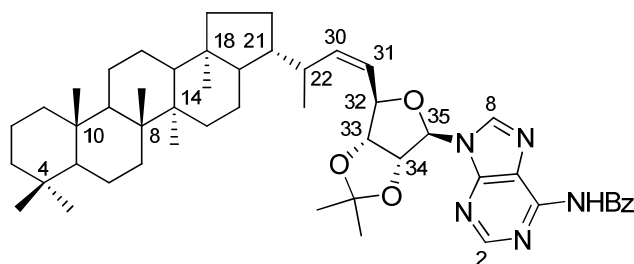
Procedure A. Compounds **55** (156 mg, 0.37 mmol), **62** (15 mg, 0.037mmol) and Ru-catalyst (10 mol%) were dissolved in dry DCM (3.6 mL) at ambient temperature under an atmosphere of Ar and the resulting solution was heated overnight at 75 °C (oil bath) in a pressure tube (Ace glass). Volatiles were evaporated and the residue was purified by flash chromatography (DCM to DCM/MeOH 100:3) to afford compound **38** (15 mg, 52%, *E/Z* ~ 5/1) as a mixture of

two isomers which was used in the next step without further purification and dimer **64** (6 mg, 43%) as a by-product.

Procedure B. Compound **55** (210 mg, 0.49 mmol), **62** (20 mg, 0.049 mmol) and Ru-catalyst (10 mol%) were dissolved in dry DCM (5 mL) in a sealed tube equipped with a Teflon-coated stirrer bar and heated under microwave irradiation at 75 °C for 3 h (Power: 40~60 W; Pressure: 1.5~2 Bar). The mixture was then evaporated to dryness *in vacuo* and purified by flash chromatography (DCM to DCM/MeOH 100:3) to afford compound **38** (23 mg, 59%, E/Z ~ 5:1) and dimer **64** (7.5 mg, 40%). Compound **38** was isolated as a colorless solid as a mixture of the E/Z isomers that were not separated. R_f 0.47 (DCM/MeOH 100:3).

^{1}H-NMR (300 MHz, CDCl$_3$) for (*E*)-**38** and (*Z*)-**38**: δ/ppm = 9.29 (6H, br. s, -NHC=O), 8.82 (5H, s, 2'-H$_{trans}$), 8.11 (5H, s, 8'-H$_{trans}$), 8.13 (1H, s, 8'-H$_{cis}$), 8.04-8.01 (12H, m, Ar-H), 7.63-7.51 (18H, m, Ar-H), 6.14 (6H, d, $J_{34,35}$ = 1.9 Hz, 35-H$_{cis}$ and35-H$_{trans}$), 5.57 (5H, dd, $J_{33,34}$ = 6.2 Hz, $J_{34,35}$ = 1.9 Hz, 34-H$_{trans}$), 5.53 (1H, dd, $J_{33,34}$ = 6.1 Hz, $J_{34,35}$ = 1.8 Hz, 34-H$_{cis}$), 5.47 (5H, dd, $J_{30,31}$ = 15.4 Hz, $J_{22,30}$ = 8.9 Hz, 30-H$_{trans}$), 5.38 (1H, dd, $J_{30,31}$ = 11.0 Hz, $J_{22,30}$ = 9.9 Hz, 30-H$_{cis}$), 5.37 (5H, dd, $J_{30,31}$ = 15.4 Hz, $J_{31,32}$ = 7.4 Hz, 31-H$_{trans}$), 5.28 (1H, dd, $J_{30,31}$ = 11.0 Hz, $J_{31,32}$ = 8.7 Hz, 31-H$_{cis}$), 5.03 (1H, dd, $J_{31,32}$ = 8.7 Hz, $J_{32,33}$ = 3.0 Hz, 32-H$_{cis}$), 4.96 (5H, dd, $J_{33,34}$ = 6.2 Hz, $J_{32,33}$ = 3.0 Hz, 33-H$_{trans}$), 4.85 (1H, dd, $J_{33,34}$ = 6.0 Hz, $J_{32,33}$ = 3.0 Hz, 33-H$_{cis}$), 4.74 (5H, dd, $J_{31,32}$ = 7.3 Hz, $J_{32,33}$ = 2.8 Hz, 32-H$_{trans}$), 2.71-2.65 (1H, m, 22-H$_{cis}$), 2.17-2.11 (5H, m, 22-H$_{trans}$), 1.65 and 1.41 (36H, 2s, Me$_2$C), 1.01 (3H, d, $J_{22,29}$ = 6.2 Hz, 22*R*-Me$_{cis}$), 0.97 and 0.95 (6H, 2s, 8β-Me$_{cis}$ and 14α-Me$_{cis}$), 0.93 and 0.92 (30H, 2s, 8β-Me$_{trans}$ and 14α-Me$_{trans}$), 0.89 (15H, d, $J_{22,29}$ = 6.4 Hz, 22*R*-Me$_{trans}$), 0.84 (18H, s, 4α-Me), 0.80 (18H, s, 10β-Me), 0.781 (18H, s, 4β-Me), 0.64 (18H, s, 18α-Me).
(Subscript "*cis*" characterizes the ^{1}H-NMR signals of (*Z*)-**38**, and "*trans*" for (*E*)-**38**.)

^{13}C-NMR (75 MHz, CDCl$_3$) for (*E*)-**38**: δ/ppm = 164.5, 152.6, 151.1, 149.6, 142.1, 133.6, 132.7, 128.7, 127.8, 124.5, 123.5, 114.3, 91.2, 88.6, 84.8, 84.4, 56.0, 54.0, 50.3, 49.1, 44.8, 44.3, 42.0, 41.8, 41.7, 41.5, 40.5, 40.2, 37.3, 33.4, 33.3, 33.2, 33.2, 27.5, 27.0, 25.4, 23.9, 21.9, 21.7, 21.5, 20.9, 18.6, 16.5, 15.9, 15.8.

HRMS (ESI): *m/z* [M+Na]$^+$, calcd for C$_{50}$H$_{69}$N$_5$NaO$_4^+$: 826.525, found: 826.524.

Homodimer of 5'-methylene adenosine   64
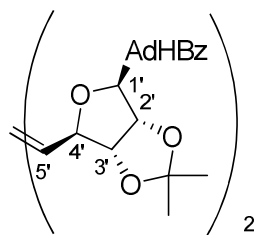
Dimer **64** was isolated as a solid mixture of two isomers (~10:3). R_f 0.16 (DCM/MeOH 100:3).

^{1}H-NMR (300 MHz, CDCl$_3$): δ/ppm = 9.24 (7H, br. s, -NHBz), 9.11 (2H, br. s, -NHBz*), 8.79 (2H, br. s, 2-H*), 8.63 (7H, br. s, 2-H), 8.10 (2H, s, 8-H*), 8.04-8.02 (22H, m, Ar-H), 7.95 (2H, s, 8-H), 7.64-7.44 (26H, m, Ar-H), 6.15 (2H, d, $J_{1',2'}$ = 1.5 Hz, 1'-H*), 6.06 (7H, d, $J_{1',2'}$ = 1.7 Hz, 1'-H), 5.72 (7H, dd, J = 3.4, 1.5 Hz, 5'-H), 5.63 (2H, dd, J = 5.5, 1.3 Hz, 5'-H*), 5.56 (2H, dd, $J_{2',3'}$ = 6.1 Hz, $J_{1',2'}$ = 1.5 Hz, 2'-H*), 5.44 (7H, dd, $J_{2',3'}$ = 6.3 Hz, $J_{1',2'}$ = 1.7 Hz, 2'-H), 5.14-5.11 (2H, m, 3'-H*), 4.94 (7H, dd, $J_{2',3'}$ = 6.3, $J_{3',4'}$ = 3.3 Hz, 3'-H), 4.69-4.67 (2H, m, 4'-H*), 4.63 (7H, m, 4'-H), 1.63 and 1.38 (12H, 2s, Me$_2$C*), 1.59 and 1.36 (42H, 2s, Me$_2$C).

^{13}C-NMR (75 MHz, CDCl$_3$): δ/ppm = 164.7, 152.7*, 152.4, 150.9, 149.8*, 149.7, 142.4*, 142.3, 133.5, 133.4*, 132.8*, 132.7, 131.2*, 130.0, 128.9*, 128.7, 128.0, 127.9*, 123.6, 114.6*, 114.5, 91.1*, 90.7, 87.3, 85.4*, 84.5, 84.3*, 84.0, 83.5*, 27.0, 27.0*, 25.3*, 25.2. (Superscript "*" characterizes the NMR signals for the minor isomer of dimer **64**)

HRMS (ESI): *m/z* [M+Na]$^+$, calcd for C$_{40}$H$_{38}$N$_{10}$NaO$_8$$^+$: 809.277, found: 809.277.

(*E*)-33,34-*O*-Isopropylidene adenosylhop-30-ene   (*E*)-65

(Z)-33,34-O-Isopropylidene adenosylhop-30-ene (Z)-65

To a mixture of compounds (E)-**38** and (Z)-**38** (150 mg, 0.19 mmol) in DCM (5 mL) was added a solution of ammonia in MeOH (7N, 20 mL) at 0 °C, and the mixture was stirred at 5 °C for 5 days. The volatiles were evaporated and the residue was purified via flash chromatography (DCM to DCM/MeOH 100:2) to give a mixture of (E)-**65** and (Z)-**65** (120 mg, 0.17 mmol, 91%) as a colorless solid which was used in the next step without further purification. R_f 0.36 (DCM/MeOH 100:5).

^{1}H-NMR (300 MHz, CDCl$_3$) for (E)-**65** and (Z)-**65**: δ/ppm = 8.36 (1H, s, 2'-H$_{cis}$), 8.35 (4H, s, 2'-H$_{trans}$), 7.91 (1H, s, 8'-H$_{cis}$), 7.89 (4H, s, 8'-H$_{trans}$), 6.07 (4H, d, $J_{34,35}$ = 1.8 Hz, 35-H$_{cis}$ and 35-H$_{trans}$), 5.90 (10H, br. s, -NH$_2$), 5.54 (4H, dd, $J_{33,34}$ = 6.2 Hz, $J_{34,35}$ = 1.9 Hz, 34-H$_{trans}$), 5.50 (1H, dd, $J_{33,34}$ = 6.2 Hz, $J_{34,35}$ = 1.9 Hz, 34-H$_{cis}$), 5.45 (4H, dd, $J_{30,31}$ = 15.3 Hz, $J_{22,30}$ = 8.1 Hz, 30-H$_{trans}$), 5.36 (4H, dd, $J_{30,31}$ = 15.3 Hz, $J_{31,32}$ = 6.8 Hz, 31-H$_{trans}$), 5.31-5.29 (2H, m, 31-H and 30-H$_{cis}$), 4.97 (1H, dd, $J_{31,32}$ = 4.7 Hz, $J_{32,33}$ = 2.9 Hz, 32-H$_{cis}$), 4.94 (4H, dd, $J_{33,34}$ = 6.3 Hz, $J_{32,33}$ = 3.1 Hz, 33-H$_{trans}$), 4.83 (1H, dd, $J_{33,34}$ = 6.3 Hz, $J_{32,33}$ = 3.1 Hz, 33-H$_{cis}$), 4.69 (4H, dd, $J_{31,32}$ = 6.8 Hz, $J_{32,33}$ = 2.9 Hz, 32-H$_{trans}$), 2.72-2.63 (1H, m, 22-H$_{cis}$), 2.17-2.09 (4H, m, 22-H$_{trans}$), 1.63 (3H, s, Me$_2$C$_{cis}$), 1.61(12H, s, Me$_2$C$_{trans}$), 1.40 (15H, s, Me$_2$C), 1.00 (3H, d, $J_{22,29}$ = 6.4 Hz, 22R-Me$_{cis}$), 0.96 and 0.94 (6H, 2s, 8β-Me$_{cis}$ and 14α-Me$_{cis}$), 0.93 (12H, s, 8β-Me$_{trans}$), 0.92 (12H, s, 14α-Me$_{trans}$), 0.89 (12H, d, $J_{22,29}$ = 6.4 Hz, 22R-Me$_{trans}$), 0.834 (15H, s, 4α-Me), 0.799 (15H, s, 10β-Me), 0.779 (15H, s, 4β-Me), 0.640 (15H, s, 18α-Me). (Subscript "*cis*" characterizes the ^{1}H-NMR signals of (Z)-**65**, and "*trans*" for (E)-**65**).

^{13}C-NMR (75 MHz, CDCl$_3$) for (E)-**65**: δ/ppm = 155.5, 153.0, 149.4, 141.7, 139.8, 124.8, 120.3, 114.2, 90.8, 88.4, 85.0, 84.4, 56.1, 54.1, 50.4, 49.1, 44.9, 44.3, 42.1, 41.8, 41.7, 41.6, 40.5, 40.3, 37.4, 33.5, 33.4, 33.3, 33.2, 27.5, 27.1, 25.4, 23.9, 22.1, 22.0, 21.7, 21.6, 20.9, 18.8, 18.7, 16.6, 15.9.

HRMS (ESI): m/z [M+H]$^+$, calcd for C$_{43}$H$_{65}$N$_5$NaO$_3$$^+$: 722.499, found: 722.498.

Preparation of dipotassium azodicarboxylate (PADA)

To a vigorously stirred cold water solution of KOH (40%, 60 mL) was added azodicarbonamide (1 g, 8.6 mmol) portion wise during 2 h at 0 °C. After the addition was complete the mixture was stirred for an additional hour at room temperature. The bright yellow salt was filtered through a sintered glass and washed with cold anhydrous methanol (8×4 mL), and dried over P$_2$O$_5$ under vacuum for 24 h. The salt, which was used for the deuteriation, was gently ground to a powder under dry N$_2$ atmosphere and treated with equal weight of methanol-d4. The slurry was left overnight at 5 °C under N$_2$. Methanol was removed under reduced pressure, and the residue was stored under vacuum in the presence of P$_2$O$_5$.

33,34-*O*-Isopropylidene adenosylhopane   40
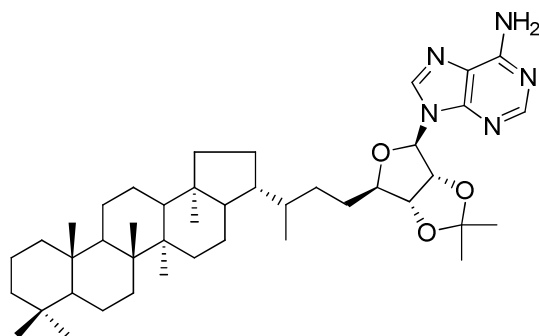
Procedure C. To a stirred slurry of PADA (90 mg, 0.46 mmol) in pyridine (1 mL) in a two-neck round bottom flask equipped with a condenser under N$_2$ atmosphere was added a solution of **65** (32 mg, 0.046 mmol) in pyridine (3 mL). The mixture was heated to reflux, and a solution of anhydrous acetic acid (0.030 mL, 0.55 mmol) in pyridine (0.1 mL) was carefully added dropwise. Each drop of acetic acid solution was added after the end of N$_2$ evolution. The mixture was left under reflux until the yellow color vanished. Another five portions of PADA and subsequent acetic acid were necessary to increase the conversion. The reaction was quenched with water, and extracted with dichloromethane three times. The combined organic

phases were washed with brine and dried over anhydrous Na_2SO_4, filtered through cotton, and evaporated to dryness *in vacuo*. The crude product was further purified by flash chromatography (DCM/MeOH 100:1 to 100:2) to yield the saturated product **40** (23 mg, 73%). Compound **40** was isolated as a colorless solid. R_f 0.38 (DCM/MeOH 100:5).

M.p. 256-257 °C.

$[\alpha]^{20}_D$ +34 (*c* 0.35, CHCl$_3$).

^{1}H- and ^{13}C-NMR data see Table II-2.

HRMS (ESI): *m/z* [M+H]$^+$, calcd for C$_{43}$H$_{67}$N$_5$NaO$_3$$^+$: 724.514, found: 724.514.

[30,31-^{2}H$_2$]- 33,34-*O*-Isoproplylidene adenosylhopane 40-D

Compound **65** (51 mg, 0.073 mmol) was dissolved in a mixture of CH$_3$OD/CDCl$_3$ (1:2) under an atmosphere of N$_2$ for H-D exchange. After 5 min standing, the solvents were carefully evaporated under vacuum. The same procedure was repeated three times, and the labeled intermediate **65-D** was carefully dried overnight under vacuum in the presence of P$_2$O$_5$. **40-D** was prepared following procedure **C** using PADA (850 mg, 43.8 mmol) and AcOD (98 atom%, 3.3 mL, 56.9 mmol) to generate deuteriated diimide *in situ*. Compound **40-D** (31 mg, 60%) was isolated as a colorless solid with unreacted starting material **65** (8.6 mg, 17%). Compound **40-D** has R_f 0.38 (DCM/MeOH, 100:5). Deuterium content of **40-D** was calculated from HRMS (ES) spectrum by evaluating the relative intensities of the *m/z* 724, 725 and 726 peaks corresponding to each isotopomer: natural abundance adenosylhopane 8%;

monodeuteriated adenosylhopane 32%; bisdeuteriated adenosylhopane 60%; trisdeuteriated adenosylhopane 0%. This corresponds to an average of 1.52 deuterium per molecule.

NMR data see Table II-2.

HRMS (ESI): m/z [M+H]$^+$, calcd for $C_{43}H_{65}D_2N_5NaO_3^+$: 726.527, found: 726.526.

Adenosylhopane   25

Procedure D. A solution of **40** (6.3 mg, 9 µmol) and TFA (2 mL) in $CHCl_3$/MeOH (2:1, 5 mL) in a round bottom flask was shacken under reduced pressure (450~500 mbar) at 0 °C for 2h30 (rotary evaporator). When starting material could no more be detected by TLC, the reaction mixture was evaporated to dryness and the residue was purified by column chromatography on silica gel (63-200 µm) ($CHCl_3$/MeOH/NH_4OH, 100:2:0.5 to 100:5:0.5 to 100:7.5:0.5) to afford adenosylhopane **25** as a colorless solid (5.3 mg, 8 µmol 90%). R_f 0.09 (DCM/MeOH 100:5).

$[\alpha]^{20}_D$ +34 (*c* 0.3, THF).

NMR data see table II-3.

HRMS (ESI): m/z [M+H]$^+$, calcd for $C_{40}H_{64}N_5O_3$+: 662.501, found: 662.500.

[30,31-^{2}H$_2$]Adenosylhopane 25-D

Deprotection of **40-D** (9.3 mg, 13.2 µmol) by TFA (3 mL) in CHCl$_3$/MeOH (2:1, 7 mL) following procedure D afforded deuteriated adenosylhopane **25-D** (7.7 mg, 11.6 µmol, 90%). R$_f$ 0.09 (DCM/MeOH 100:5). Deuterium content of **25-D** was calculated from HRMS (ES) spectrum: natural abundance adenosylhopane 8%; monodeuteriated adenosylhopane 32%; bisdeuteriated adenosylhopane 60%; trisdeuteriated adenosylhopane 0%.

NMR data see table II-3.

HRMS (ESI): m/z [M+H]$^+$, calcd for C$_{40}$H$_{62}$D$_2$N$_5$O$_3^+$: 664.513, found: 664.513.

Adenosylhopane acetates 66a-c

Adenosylhopane **25** (1.8 mg) was acetylated overnight at room temperature in the mixture of acetic anhydride and pyridine (0.3 mL, v/v, 1/2). Solvent and reagent were removed under vacuum afterwards. The resulting residue was purified by preparative thin layer chromatography (CH$_2$Cl$_2$/MeOH, 100:5) to afford adenosylhopane diacetate **66a** (0.042 mg) (Neunlist *et al.*, 1988), triacetate **66b** (0.62 mg) (Neunlist and Rohmer, 1985b; Neunlist *et al.*, 1988) and tetraacetate **66c** (0.79 mg).

Adenosylhopane diacetate 66a

R_f 0.30 (DCM/MeOH 100:5).

^{1}H-NMR (300 MHz, CDCl$_3$): δ/ppm = 8.30 and 7.95 (2×1H, 2s, 2'-H and 8'-H), 6.68 (2H, br.s, -NH$_2$), 6.14 (1H, d, J = 5.5 Hz, 35-H), 5.87 (1H, dd, J = 5.7, 5.5 Hz, 34-H), 5.38 (1H, dd, J = 5.5, 4.5 Hz, 33-H), 4.15 (1H, td, J = 8.4, 4.3 Hz, 32-H), 2.14 (3H, s, CH_3COO-), 2.06 (3H, s, CH_3COO-), 0.94 (9H, m, 8β-Me, 14α-Me and 22R-Me), 0.84 (3H, s, 4α-Me), 0.81 (3H, s, 10β-Me), 0.79 (3H, s, 4β-Me), 0.68 (3H, s, 18α-Me).

MS (EI, direct inlet, positive mode 70 eV): m/z = 746 (M$^+$, 9%), 686 (M$^+$–AcOH, 6%), 626 (M$^+$–2AcOH, 24%), 595 (6%), 538 (15%), 491 (5%), 389 (17%), 367 (M$^+$–CH$_2$CO–side chain, 9%), 191 (ring C cleavage, 10%), 136 (adenine–H, 100%).

Adenosylhopane triaacetate 66b

R_f 0.38 (DCM/MeOH 100:5).

^{1}H-NMR (300 MHz, CDCl$_3$): δ/ppm = 8.87 (1H, s, NHCOCH$_3$), 8.69 and 8.06 (2×1H, 2s,

2'-H and 8'-H), 6.14 (2H, d, J = 5.5 Hz, 35-H), 5.94 (1H, dd, $J = J$ = 5.5 Hz, 34-H), 5.42 (1H, dd, J = 5.5, 4.5 Hz, 33-H), 4.17 (1H, td, J = 8.4, 4.3 Hz, 32-H), 2.60 (3H, s, CH_3CONH-), 2.15 (3H, s, CH_3COO-), 2.06 (3H, s, CH_3COO-), 0.94 (9H, m, 8β-Me, 14α-Me and 22R-Me), 0.84 (3H, s, 4α-Me), 0.81 (3H, s, 10β-Me), 0.79 (3H, s, 4β-Me), 0.68 (3H, s, 18α-Me).

MS (EI, direct inlet, positive mode 70 eV): m/z = 788 (M$^+$, 2%), 610 (M$^+$–N,N-acetyladenine, 4%), 595 (ring C cleavage, 2%), 491 (1%), 389 (6%), 367 (M$^+$–CH$_2$CO–side chain, 4%), 191 (ring C cleavage, 11%), 178 (N-acetyladenine–H, 100%).

Adenosylhopane tetraacetate 66c

R$_f$ 0.66 (DCM/MeOH 100:5).

^{1}H-NMR (300 MHz, CDCl$_3$): δ/ppm = 88.97 and 8.21 (2×1H, 2s, 2'-H and 8'-H), 6.18 (2H, d, J = 5.5 Hz, 35-H), 5.96 (1H, dd, $J = J$ = 5.5 Hz, 34-H), 5.42 (1H, dd, J = 5.5, 4.5 Hz, 33-H), 4.21-4.17 (1H, m, 32-H), 2.37 (6H, s, 2×CH_3CONH-), 2.16 (3H, s, CH_3COO-), 2.09 (3H, s, CH_3COO-), 0.94 (6H, br. s, 8β-Me and 14α-Me), 0.94 (3H, d, J = 6.1 Hz, 22R-Me), 0.84 (3H, s, 4α-Me), 0.81 (3H, s, 10β-Me), 0.79 (3H, s, 4β-Me), 0.69 (3H, s, 18α-Me).

MS (EI, direct inlet, positive mode 70 eV): m/z = 830 (M$^+$, 0.3%), 788 (M$^+$–CH$_2$CO), 662 (1%), 610 (M$^+$–CH$_2$CO–N,N-acetyladenine, 8%), 595 (ring C cleavage–CH$_2$CO, 5%), 491 (3%), 389 (16%), 367 (M$^+$–CH$_2$CO–side chain, 8%), 191 (ring C cleavage, 20%), 178 (N-acetyladenine–H, 100%).

Chapter III

Incorporation of deuteriated adenosylhopane into bacteriohopanetetrol by a cell-free system from *Methylobacterium organophilum*

III.1. Introduction

Bacteria of the genus *Methylobacterium* are well-studied examples of facultative methylotrophs. These bacteria are classified as α-proteobacteria and are capable of growth on methanol, methylamine and a variety of C_2, C_3, and C_4 carbon sources. They are non-motile rod-shaped and are obligatory aerobic. Because of their distinctive pink pigmentation, they are sometimes referred to as PPFMs (pink-pigmented facultative methylotrophs). *Methylobacterium* strains are commonly found in soils, as well as on the surface of leaves of numerous plants (Corpe *et al.*, 1986).

III.1.1 Hopanoid production in *Methylobacterium*

Several species of *Methylobacterium* have been shown to produce a number of hopanoids in abundant quantities to date (Renoux and Rohmer, 1985; Knani et al., 1994, Bradley *et al.* 2010). Diploptene **3**, diplopterol **2**, 2β-methyldiplopterol and BHT **6** are present in all the examined strains (Fig. III-1). 2β-Methyldiplopterol is always produced in large amount, but its relative content depends on the growth conditions and the nature of the culture (Bisseret et al., 1985; Renoux and Rohmer, 1985). The presence of 2α-methyldiplopterol was only reported in *Methylobacterium organophilum* (Stampf *et al.*, 1991). Three complex hopanoids were found in most of the *Methylobacterium* strains, including glucosaminyl BHT **16**, BHT cyclitol ether **18** and guanidine-substituted BHT cyclitol ether **19** (Fig. III-1). One of the two former bacteriohopanepolyols (BHPs) is normally the main product. The presence of a guanidinium group on the carbapseudopentose moiety of the BHT ether **19** seems presently to be restricted to the genus *Methylobacterium*.

Fig. III-1. Hopanoids produced by *Methylobacterium* spp.

III.1.2. Hopanoid biosynthesis in *Methylobacterium*

Given that *Methylobacterium* spp. produce many types of hopanoids in important amounts and that they can grow on a variety of carbon sources, they represent ideal model strains for the study of bacteriohopanoid biosynthesis. Labeling experiments with *M. organophilum* with L-[methyl-^{3}H,^{14}C]methionine or L-[methyl-^{2}H$_3$]methionine indicated that this amino acid is the actual methyl donor for the 2β-methyl group of 2-methylhopanoids, probably via *S*-adenosylmethionine (Zundel and Rohmer, 1985b). This argument was recently further supported by the characterization of the *hpnP* gene from *Rhodopseudomonas palustris* TIE-1 (Appendix 1) (Welander *et al.* 2010). This gene was suggested to encode for a SAM radical enzyme required for the methylation at C-2 of the bacteriohopanoids.

Incorporation of ^{13}C-labelled acetate into hopanoids of *M. organophilum* not only led to the discovery of the MEP pathway for the biosynthesis of isoprene units, but also showed that the BHPs are derived from a unique carbon/carbon linkage between the triterpenic hopane moiety and the C-5 carbon atom of a D-ribose derivative, which arises from the non-oxidative pentose phosphate pathway (Flesch and Rohmer, 1988b).

While we were performing this work, investigations on the elucidation of bacteriohopanoid biosynthesis at genetic level have been reported by other groups. The genome of *Methylobacterium extorquens* AM1 has been partially sequenced. It contains open reading frames with significant similarity to genes formerly supported to be involved in the biosynthesis of hopanoids (Vuilleumier *et al.*, 2009; Bradley *et al.*, 2010). The *hpnA-F* and *hpnP* genes were suggested to be involved in the construction of hopanoid cyclic backbone.

Another three genes, *hpnG*, *hpnH* and *hpnI*, were characterized from *M. extorquens* and are suggested to be necessary in the side-chain biosynthesis for bacteriohopanoids (Appendix 1).

Protein HpnH belongs to the radical *S*-adenosylmethionine (SAM) superfamily of enzymes that utilizes an iron-sulfur redox cluster and SAM to carry out diverse radical mediated reactions. The deletion of *hpnH* gene in *Methylobacterium* results in the absence of C_{35} hopanoids; only diploptene and diplopterol were produced (Bradley *et al.*, 2010). Accordingly, the radical SAM protein was presumed to serve as the possible adenosyl donor to the double bond of diploptene, leading to the formation of adenosylhopane.

The sequence of *hpnG* from *Methylobacterium* indicates that it might encode for a purine nucleoside phosphorylase (PNP) homolog (Bradley, 2010). The activity of PNPs is to cleave adenine (or guanine) from the corresponding nucleoside and results in phosphate addition to the ribose. The cleavage reaction is believed to proceed through an S_N1 mechanism with an oxocarbenium intermediate with ordered substrate binding and with product release as the rate-limiting step (Fig. III-2) (Bennett *et al.*, 2003 ; Kline and Schramm, 1995; Erion *et al.*, 1997). An acidic amino acid residue (*e.g.* the active site Asp 240 of the *Escherichia coli* PNP) is proved to participate in the catalytic mechanism, promoting the cleavage of the glycoside bond by protonating the N-7 nitrogen atom of the purine moiety. The phosphorolysis is accomplished with an inversion of the configuration at C-1 of ribose moiety.

Morover, deletion of the *hpnG* gene led to the accumulation of adenosylhopane as the single extended hopanoid. This observation means that further modification on the side chain probably requires the loss of the adenine moiety, and suggests that ribosylhopane 35-phosphate could be the possible intermediate (Bradley *et al.*, 2010).

Fig. III-2. S_N1 mechanism for a *E. coli* PNP catalyzed phosphorolysis reaction (Bennett *et al.*, 2003).

The next step of hopanoid biosynthesis in *Methylobacterium* might involve the loss of the phosphate group to give ribosylhopane. The corresponding gene(s) is(are) yet unknown (Fig. III-3). This hypothesis is supported by our discovery of ribosylhopane in a *Streptomyces coelicolor* mutant (see Chapter I) and our work in which ribosylhopane has been proved to be reduced into BHT in a crude cell-free system of *M. organophilum* in the presence of NAD(P)H (Bodlenner, unpublished work).

A reduction step is involved in the further transformation from ribosylhopane to BHT, requiring NAD(P)H as a cofactor (Charon, 2000; Bodlenner, unpublished work) (Fig. III-3). Incorporation of $[1\text{-}^2\text{H}]$glucose into BHT derived hopanoids in *Zymomonas mobilis* pointed out that a $\text{NAD(P)}^2\text{H}$ dependent reduction happens on a carbonyl group located at the C-35 position (Charon, 2000). The putative substrate is most likely to be the open aldehyde form of ribosylhopane, which is normally present like for all the aldehydes in equilibrium with the two furanose isomers (35α- and 35β-ribosylhopane).

Last but not least, the *hpnI* gene, located upstream of *hpnH*, was annotated as a glycosyltranferase and was suggested to be engaged in the production of glucosaminyl BHT **16** and BHT ethers **18** and **19** (Fig. 2) in *Methylobacterium* (Bradley *et al.*, 2010). A bioinformatic search for homologs of the *hpnI* gene in InterPro database shows that they are also present in other reported microbial producers of BHT ether, such as *Zymomonas mobilis, Frateuria aurantia* and *Acetobacter* spp. Glycosyltranferases catalyse the transfer of monosaccharide moieties from the glycosyl donor, usually an activated nucleotide sugar, to a glycosyl acceptor molecule, usually an alcohol. This annotation of the *hpnI* gene is consistent with previous studies on the biosynthesis of glucosaminyl BHT **16** and BHT ether **18** in *Z. mobilis* (Vincent *et al.*, 2003): A *N*-acetyl-D-glucosamine (GlcNAc) derivative probably obtained from the enzymatic co-factor UDP-GlcNAc is likely a precursor of the sugar ring of glycoside **16**. The resulting glycoside **16** may be further transferred into ether **18** via an oxidative *endo* opening of the sugar ring.

Fig. III-3. Hypothetical biosynthetic scheme for the biosynthesis of hopanoids in *Methylobacterium*.

The identification of the *hpnG* and *hpnH* genes represents a major progress in the elucidation of the side-chain biosynthesis of bacteriohopanoids at the genetic level. The role of adenosylhopane as a crucial intermediate is well supported. However, no direct molecular proof is given that adenosylhopane is enzymatically converted into elongated C_{35} bacteriohopanoids (*e.g.* BHT). Therefore, an incorporation experiment of deuteriated labeled adenosylhopane into C_{35} hopanoids is of great interest.

III.2. Incorporation of deuteriated adenosylhopane into bacteriohopanetetrol by a cell-free system from *Methylobacterium organophilum*

Incorporation experiments of deuteriated adenosylhopane into BHT were conducted with a cell-free system from *M. organophilum*. A cell-free system is an *in vitro* tool widely used to study biological reactions that happen within cells while reducing the complex interactions found in a whole cell. Subcellular fractions can be derived via cell lysis and isolated by ultracentrifugation to provide the molecular machinery required for the side-chain modification of bacteriohopanoids, while many of the other cellular components are removed.

M. organophilum is known as good hopanoid source, for it is easy to grow and it produces hopanoids in large amounts within a relatively short time. The total amount of bacteriohopane derivatives could reach up to 13 mg/g dry cells within 24 h incubation (Renoux and Rohmer, 1985). More importantly, *M. organophilum* is ideal for the incorporation experiment performed in a crude cell system, because it can produce BHT but never as a major compound. Accordingly, the dilution of [^{2}H]BHT, which is synthesized *de novo* from the introduced [^{2}H]adenosylhopane by the cell free system, by endogenous natural abundance BHT produced during the culture should be significantly minimized. For these reasons, *M. organophilum* DSM 760 was chosen as the model microorganism for our investigation.

According to the hypothetical biogenetic pathway for the side-chain biosynthesis in *Methylobacterium*, the presence of inorganic phosphate may be required to promote the cleavage of adenosyl group under catalysis of a PNP. The crude extract was therefore prepared by ultrasonic cell breaking in a phosphate buffer (50 mM, pH=7.5) and subsequent ultracentrifugation, in order to eliminate unbroken cells and large cell debris containing natural abundance BHT and hence to diminish isotopic dilution of the analyzed BHT. For the reduction of ribosylhopane into BHT, NADPH was proven to be a preferred cofactor in *M. organophilum* (Bodlenner, unpublished work) and was thus added in the cell-free system. Insolubility of adenosylhopane in water is a problem for enzymatic reactions, which require an aqueous environment. Adenosylhopane was therefore first dissolved in THF (10% volume

of the crude extract) and then added into the cell extracts (Siirola *et al.*, 2011).

After 24 h incubation at 30 °C, BHT was isolated as a tetraacetylated derivative via a standard procedure (Renoux and Rohmer, 1985). The sample was analyzed by GC/EI-MS for isotopic abundance measurements of the corresponding fragments. Incorporation ratio was calculated from the isotope distribution of the labeled ions of [^{2}H]BHT tetraacetate in comparison to that of the corresponding ions of natural isotopic abundance. Evidence for intense labeling of acetylated BHT was observed as the intensity of *m/z*+1 and *m/z*+2 signals of the fragments containing the side chain [*m/z* 714 (M$^+$), 699 (M$^+$-CH$_3$), 654 (M$^+$-AcOH) and 493 (ring C cleavage)] increased, but not for the fragments *m/z* 369 (M$^+$-side chain) or 191 (ring C cleavage), indicating that the ^{2}H-labeling only occurred on the C$_5$ side chain (for fragmentation of BHT by EIMS, see general experimental part).

In order to minimize the influence of background noise, incorporation percentage was calculated only for the fragments *m/z* 191 and 493, which have the highest intensities among all fragments (Table III-2). An adjusted value of *m/z*+1 or *m/z*+2 intensity for each fragment in natural abundance is given as: $X_i = x_i \pm 2 \times S_i$ (with deviation of 95%). S_i is the sample standard deviation that was calculated by the following equation:

$$S_i = \sqrt{\frac{\sum_{i=1}^{n}(x_i - \bar{x})^2}{n-1}}$$

where x_i is the observed values of the sample items and $\bar{x}$ is the mean value of these observations, while n stands for the size of the sample. The adjusted value Xi of the natural abundance fragments in Table III-2 was calculated from the data obtained from six independent experiments.

Table III-1. [2]H isotope distribution of fragments m/z 191 and m/z 493 from BHT tetraacetate.[a]

	Conditions[b]	Fragment m/z 191		Fragment m/z 493	
		% of M+1 to M	% of M+2 to M	% of M+1 to M	% of M+2 to M
1	Natural[c]	20±4	5±2	28±3	6±1
2	A	19	4	47	47
3	B	21	4	36	18
4	C	24	1[d]	29	6
5	D	19	2	28	6

[a] Fragments are analyzed via GC/MS. Isotopic patterns of the samples were measured according to the the signal intensities observed for ion current m/z, m/z+1 and m/z+2.

[b] All the incorporation experiments were performed at 30 °C for 24 h.

  A. Deuteriated adenosylhopane with cell-free extract in phosphate buffer.

  B. Deuteriated adenosylhopane with cell-free extract in TEA buffer.

  C. Decomposed deuteriated adenosylhopane after 24 h in phosphate buffer and then incubated with the cell-free extract.

  D. Deuteriated adenosylhopane with inactivated cell-free extract in phosphate buffer.

[c] Reference: BHT tetraacetate isolated from the cell pellets apart from the supernatant in the same experiment.

[d] High signal/noise ratio.

In order to check the influence of inorganic phosphate on the bioconversion of adenosylhopane into BHT, an incorporation experiment was also performed with a triethylamine (TEA) buffer (50 mM, pH=7.5). Decreased m/z+1 and m/z +2 intensities for fragment m/z 493 were observed in the absence of phosphate supplementation in TEA buffer (Table III-1, entry 2), in comparison to that obtained from phosphate buffer (Table III-1, entry 3). Although we can not exclude some inhibiting effect of TEA on the conversion of adenosylhopane into BHT, we observed that a sufficient amount of phosphate salt apparently increases the activity of the enzymes. This observation is, to a certain degree, inherent with the involvement of a PNP in adenine cleavage (Bradley *et al.*, 2010).

Given that the introduced [2]H-labeled adenosylhopane is in fact a mixture of mono- and bisdeuteriated isotopomers ($d_1/d_2 \approx 1/1.9$), the same ratio should be found in [^{2}H]BHT after bioconversion. Incorporation percentage from [[2]H$_1$]- or [[2]H$_2$]adenosylhopane respectively was determined by dividing the amount of [[2]H$_1$]BHT or [[2]H$_2$]BHT with the total amount of molecules:

Amount of [^{2}H$_1$]BHT: $\mathcal{R} = x_i - x_{nat}$

Amount of [^{2}H$_2$]BHT: $\mathcal{R}' = y_i - y_{nat} - y'$

Total amount of molecules: $1 + \mathcal{R} + \mathcal{R}'$

where x corresponds to the intensity of *m/z*+1 signal (relative to natural abundance), y corresponds to the intensity of *m/z*+2 signal (relative to natural abundance), subscript "i" corresponds to the observed value, subscript "nat" to natural abundance and superscript " ' " is to indicate the value derived from [^{2}H$_2$]BHT.

Accordingly, molar percents [^{2}H$_2$]- and [^{2}H$_1$]BHT were determined as 23% and 12% from phosphate buffer ($d_2/d_1 \approx 1.9/1$), and 9% and 5% from TEA buffer ($d_2/d_1 \approx 1.8/1$). This ratio is consistent with that of the incubated ^{2}H labeled adenosylhopane and indicates that the incubated [^{2}H]adenoyslhopane is the only deuterium source, and that there is no isotopic kinetic effect in the enzymatic reaction(s), which is plausible since the side-chain modifications do not happen on the ^{2}H labeled C-30 and/or C-31 positions.

In order to confirm that the conversion of adenosylhopane into BHT is enzymatic, [^{2}H]adenosylhopane was incubated in a boiled inactivated cell free system. No ^{2}H labeling was found in BHT tetraacetate (Table III-2). The possible chemical degradation of adenosylhopane into another possible BHT precursor was also checked by leaving adenosylhopane in phosphate buffer with 10% THF at 30 °C for 3 days. ^{2}H labeled BHT was not detected, indicating that, as expected, adenosylhopane cannot be spontaneously converted into BHT in a buffer. According to TLC analysis, adenosylhopane seemed to be still present, but incubation of this adenosylhopane sample with a *M. organophilum* cell-free system resulted in no formation of ^{2}H labeled BHT, indicating indeed that most of the ^{2}H-labeled adenosylhopane was decomposed into unknown compounds that can not be converted by the cell-free system into BHT.

III.3. Conclusion

Successful incorporation of deuteriated adenosylhopane into bacteriohopanetetrol was achieved in *Methylobacterium organophilum* via a cell-free system. Although neither ribosylhopane nor phosphoribosylhopane, as putative intermediates, have been detected by GC-MS, there is no doubt that adenosylhopane can be converted into BHT and is thus a likely a precursor in BHT biosynthesis in *M. organophilum*.

Recently, hopanoid side chain biosynthesis was partially revealed in *Rhodopseudomonas palustris* TIE-1 (Welander *et al.*, 2012). The *hpnH* gene was characterized for adenosylhopane biosynthesis as in *M. extorquens*. However, the *hpnG* gene was annotated as a nucleotide hydrolase leading thus to ribosylhopane directly from adenosylhopane. This disagreement does not deny the role of adenosylhopane as the first C_{35} hopanoid intermediate in the biosynthesis of hopanoid side chain, but requires the full identification of the *hpnG* gene product. The next and last step is the identification of the catalytic activity of all gene products supposed to be involved in bacteriohopanoid biosynthesis with the expression of the gene and isolation of the corresponding enzymes. This will probably be more difficult for a HpnG which is a [4Fe-4S] cluster protein and quite sensitive towards O_2, thus needs to be manipulated in a glove box under a strictly anaerobic atmosphere.

III.4. Experimental Part

III.4.1. Bacteria and cultures

Methylobacterium organophilum DSM 760 was grown on a modified medium of Hestrin & Schramm (Hestrin and Schramm, 1954) (6×500 mL) in 2-L conical flasks on a rotator shaker (200 rpm) at 30 °C. The cells were harvested before the end of the exponential growth phase (O.D.~0.6) by centrifugation (8 000 rpm, 10 min), and then washed with buffer (A. sodium phosphate buffer: 50 mM $NaH_2PO_4/Na_2HPO_4^{2-}$, 0.5 mM, $MgCl_2$, 1 mM dithiothreitol, pH 7.5; B. TEA buffer: 0.1 M triethylamine, 0.5 mM $MgCl_2$, 1 mM dithiothreitol, pH 7.5). After centrifugation (8 000 rpm, 10 min), the cells (3 g) were suspended in buffer (15 mL) and sonicated (8×40 s with 3 min pause at 0 °C). The crude cell extract was centrifuged (10 000 rpm, 10 min). The cell pellet was freeze-dried, and the supernatant was used directly for the incubation experiments.

Modified Hestrin & Schramm Medium:

Yeast extract	5 g
Bacteriopeptone	5 g
Glucose	1 g
Citric acid anhydrous	1.04 g
Na_2HPO_4	2.7 g
H_2O	1 L
pH = 6.8	

III.4.2. Isolation of bacteriohopaneterol from *M. organophilum* cells

The freeze-dried cells were extracted with $CHCl_3/CH_3OH$ (2:1, v/v) three times under reflux. The combined extracts were brought to dryness, acetylated with Ac_2O/pyridine (1:2 v/v) and the excess of reagents was evaporated *in vacuo*. The residue was separated by preparative TLC (silica gel, cyclohexane/ethyl acetate 3:7) to give an apolar fraction (Rf > 0.7) containing diploptene, diplopterol, and acetylated bacteriohopanetetrol and ribosylhopane. The mixture was further purified by preparative TLC (silica gel, cyclohexane/ethyl acetate 5:1), yielding pure BHT tetraacetate (0.16 < Rf < 0.20).

III.4.3. Incorporation of deuteriated adenosylhopane into bacteriohopanetetrol

A solution of deuteriated adenosylhopane **25** (200 μg) in THF (500 μL) was added to the supernatant (5 mL) in a glass screw cap vial, followed by a solution of NADPH (1.5 mg) in water (100 μL). Another portion of cofactor solution was added after 4 h incubation. The sample was incubated for another 20 h with shaking at 200 rpm and at 30 °C. It was freeze-dried and directly acetylated overnight at room temperature with Ac_2O/pyridine (1:2 v/v, 3.9 mL). The mixture were filtered over cotton and washed with toluene (3×2 mL) and CH_2Cl_2 (3×2 mL). The combined filtrates were concentrated in vacuum, and the residue was subjected to preparative TLC (silica gel, cyclohexane/ethyl acetate 3:7) to give an apolar fraction (Rf > 0.7) containing diploptene, diplopterol and acetylated bacteriohopanetetrol and ribosylhopane. The latter were further purified by preparative TLC (silica gel, cyclohexane/ethyl acetate 5:1), yielding pure BHT tetraacetate(0.16 < Rf < 0.20), which was analyzed by GC-EIMS.

Chapter IV

Attempts of identification of the origin of the terminal amino group of 35-aminobacteriohopanetriol in *Rhodopseudomonas palustris*

IV.1. Introduction

35-Aminobacteriohopanetriol is one of the most frequently found C_{35} bacteriohopanoids (Ourisson *et al.*, 1987; Rohmer, 1993). The hypothetical biosynthetic pathway for the side-chain biosynthesis of aminobacteriohopanetriol proposes that it is derived directly from ribosylhopane via reductive amination (Rohmer, 1993). This argument was supported by our study on a *Streptomyces coelicolor* mutant, which is deficient in a putative aminotransferase required for the biosynthesis of aminobacteriohopanetriol from ribosylhopane. A Basic Local Alignment Search Tool (BLAST) search of this unexpressed protein showed that it belongs to the acetylornithine aminotransferase family that catalyzes the exchange of the amino group from an amino acid with the carbonyl group from the other substrate. Indeed, deletion of this putative aminotransferase blocked the production of aminobacteriohopanetriol in *S. coelicolor*, and allowed us to isolate trace amount of ribosylhopane for the first time in a bacterium.

The role of ribosylhopane as the possible precursor of aminobacteriohopanetriol is also suggested by Welander *et al.* (2012). Although the authors did not detect ribosylhopane, the *hpnO* gene was characterized from *Rhodopseudomonas palustris* TIE-1as required in the aminobacteriohopanetriol biosynthesis. *R. palustris* strain lacking the *hpnO* gene is not able to produce aminobacteriohopanetriol but BHT as the only C_{35} bacteriohopanoid. The enzyme encoded by the *hpnO* gene is proposed to be a homologue of acetylornithine aminotransferase, ArgD (Welander *et al.*, 2012). ArgD (EC:2.6.1.11) is the enzyme required in the fourth step of arginine biosynthesis, catalyzing the reductive amination of 2-oxoglutarate to yield L-glutamate (Fig. IV-1). *N*-Acetyl-L-ornithine donates its 5-amino group and is converted to *N*-acetyl-L-glutamate 5-semialdehyde (Fig. IV-1).
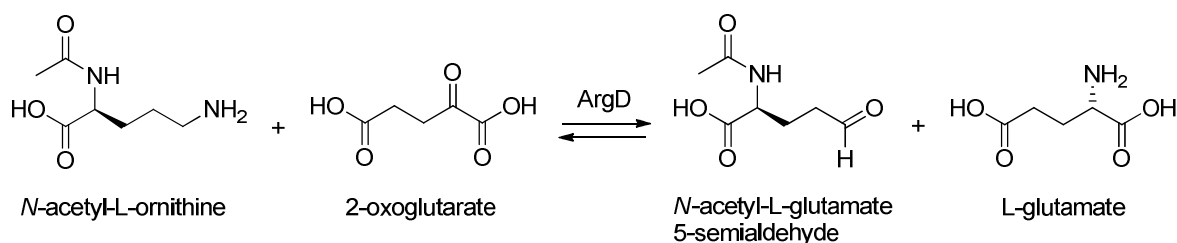
Fig. IV-1. Transamination catalyzed by the ArgD enzyme.

Further elucidation of this reductive amination step would involve the expression and

purification of the responsible enzyme. Identifying the hopane substrate on the one hand and the possible donor for the terminal amino group of aminobacteriohopanetriol, on the other hand, is required to allow enzyme tests in the future. For this reason, we conducted a series of experiments to look at the amino acid candidates, using *R. palustris* as a model microorganism.

IV.1.1. Hopanoid biosynthesis in *Rhodopseudomonas palustris*.

R. palustris is a gram-negative purple non-sulfur bacterium, which has been found to grow in swine waste lagoons, earthworm droppings, marine coastal sediments and pond waters. Young cells of *R. palustris* are very motile. Formation of clusters of cells, which are attached to each other with the flagella, is characteristic for older cultures. The color of the cell can go from translucent white/yellow (chemotrophic growth in the dark) to dark blood red (phototrophic growth).

R. palustris is known as one of the most metabolically versatile bacteria ever described. It has the ability to switch between the four different modes of metabolism that support life (Larimer *et al.*, 2004) (Fig. IV-2):

- Chemoheterotrophic: Energy and carbon from organic compounds.

- Chemoautotrophic: Energy from inorganic compounds and carbon from carbon dioxide.

- Photoheterotrophic: Energy from light and carbon from organic compounds.

- Photoautotrophic: Energy from light and carbon from carbon dioxide.
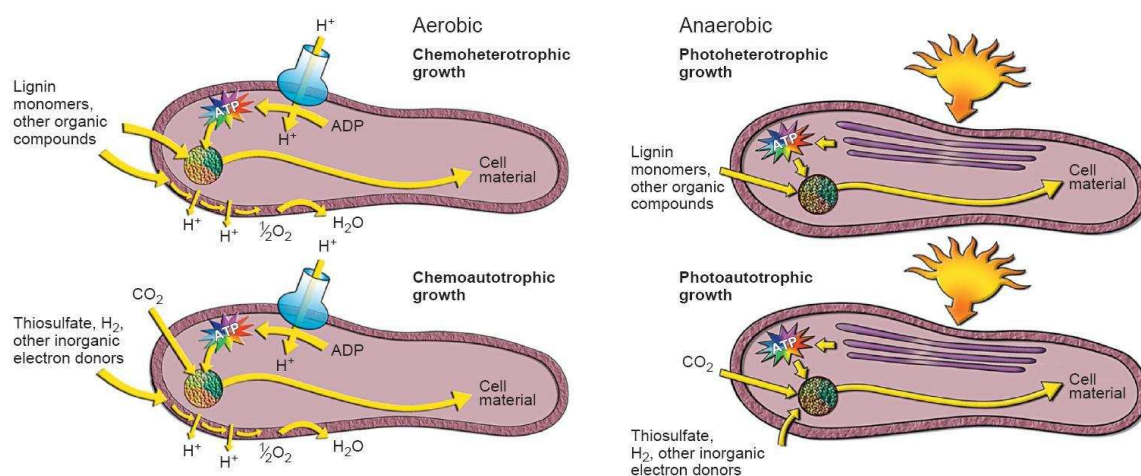
Fig. IV-2. Metabolic modes of *R. palustris* (Larimer *et al.*, 2004).

R. palustris is an attractive model organism for the study of hopanoid biology. *R. palustris*, type strain DSM 123, produces only diploptene **3**, diplopterol **2**, tetrahymanol **5** and aminobacteriohopanetriol **7** as the C_{35} hopanoids (Neunlist *et al.*, 1988; Kleemann *et al.*, 1990). It was chosen for this reason in this study. Strain TIE-1 produces additional 2β-methyldiplopterol and BHT **6** and approximately no tetrahymanol **5** (Welander *et al.* 2009, 2012). Since growth of *R. palustris* does not require hopanoids under all conditions (Welander *et al.*, 2009), harvesting of hopanoids is less dependent on the environment. Furthermore, its versatile metabolic modes allow more accesses to hopanoid accumulation. A group of genes involved in hopanoid biosynthesis has been identified from *R. palustris* (Kleemann *et al.*, 1994; Welander *et al.*, 2010; Doughty *et al.*, 2011; Welander *et al.*, 2012) (Fig. IV-3). The *hpnN* gene was annotated as a putative transporter responsible for movement of hopanoids from the cytoplasmic to the outer membrane (Doughty *et al.*, 2011); the *hpnO* gene was suggested to be engaged in the biosynthesis of aminobacteriohopanetriol (Welander *et al.*, 2012) (For the annotation of other related genes see Appendix 1).
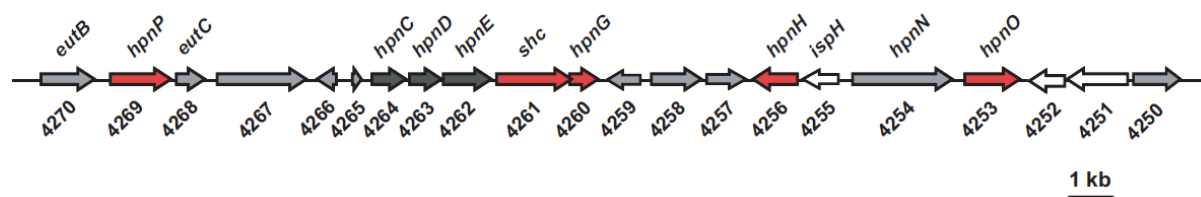
Fig. IV-3. Graphical depiction of the putative hopanoid biosynthetic gene cluster of *R. palustris* TIE-1 (Welander *et al.*, 2012). Red arrows represent genes that were shown to be involved in hopanoid biosynthesis, black arrows represent genes that are expected to be associated with hopanoid production, gray arrows represent genes not involved in hopanoid biosynthesis, and white arrows are genes with putative redundant copies elsewhere on the chromosome. The numbers under the arrows represent the gene numbers corresponding to the genome annotation, while the labels above the arrows are the gene names.

IV.1.2. Catalytic mechanism of the pyridoxal phosphate dependent aminotransferase

The protein encoded by the *hpnO* gene was predicted to belong to the pyridoxal phosphate (PLP)-dependent aspartate aminotransferase superfamily. In the reaction catalyzed by PLP-dependent aminotransferase, a prototropical rearrangement followed by hydrolysis reversibly converts PLP to pyridoxamine 5'-phosphate (PMP). In the subsequent step, the amino group from PMP is transferred to the amino acceptor to regenerate PLP (Fig. IV-4) (Walsh, 1979).

In all the PLP-dependent enzymes yet examined, the coenzyme is bound to the active site via an imine linkage to the ε-amino group of a lysine residue, and this aldimine is the active form of the resting enzyme. For the first half-reaction, the amino group donor **A**, an α-amino acid, enters into imine linkage with the coenzyme in a transaldimination, liberating the active-site lysine amino group. Once this initial imine (aldimine) has formed, the acidity of the α-hydrogen of the donor **A** has been increased because the carbanion, on proton removal, is extensively stabilized by resonance. Thus, the abstraction of that proton is readily accomplished by an active-site base. Subsequent protonation of the carbanion would yield the ketimine product. If the enzyme promotes hydrolysis of the ketimine, the products **B** will be an α-oxo acid and the amine form of the coenzyme, PMP.

The second half-reaction then constitutes the reversal of the steps of the first half-reaction, with PMP oxidized back to pyridoxal level and the product aldimine (derived from PMP and the amino group acceptor C) reduced to the corresponding amino acid. Expulsion of the product D from the product-coenzyme imine is initiated by attack of the active-site lysine's ε-amino group to yield a free amino acid D and regenerates the resting-enzyme-coenzyme aldimine, ready for another catalytic cycle.
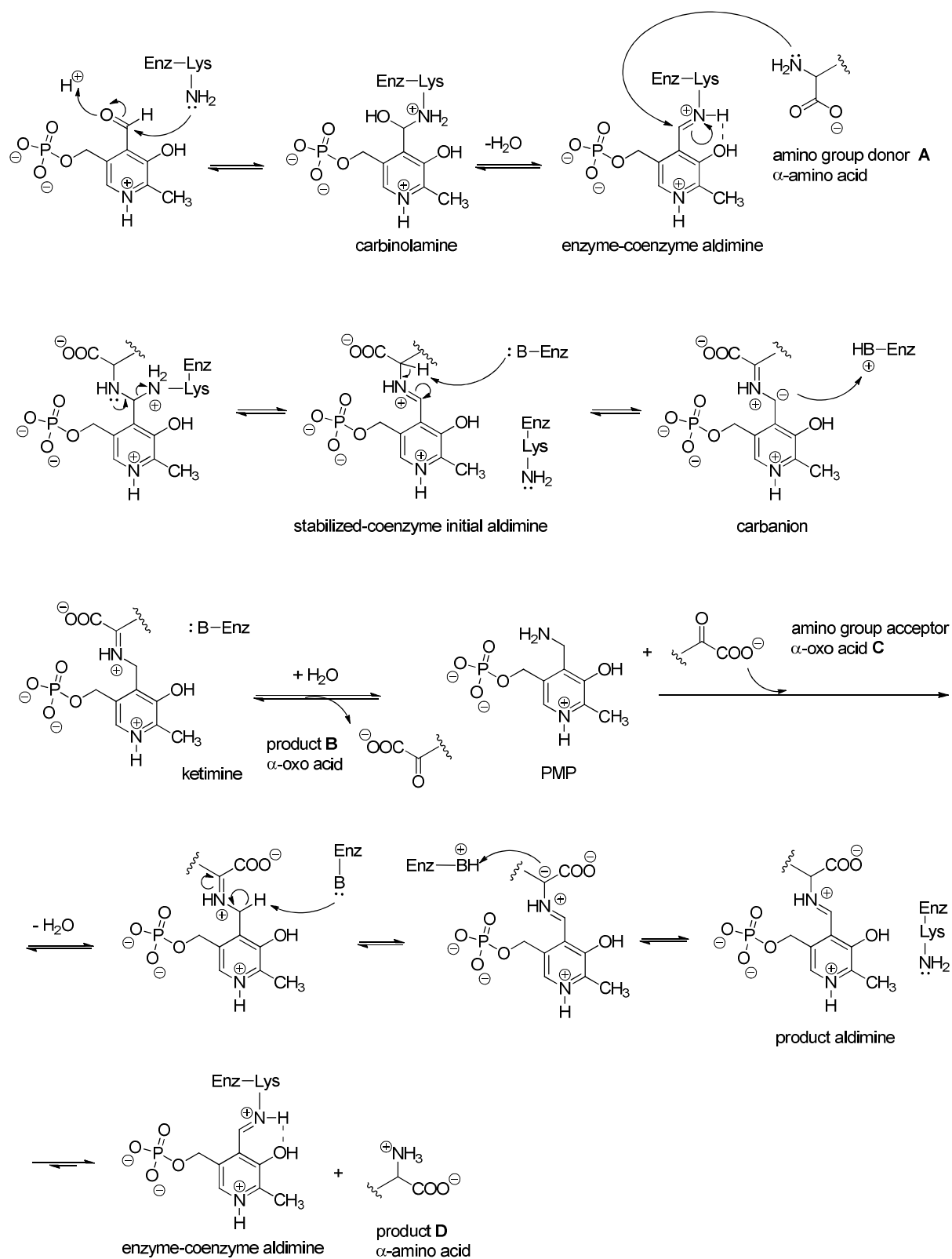
Fig. IV-4. The transfer of an amino group from an amino acid **A** to an α-oxo acid **C** catalyzed by PLP-dependent aminotransferases (Walsh, 1979).

IV.2. Attempts of the identification of the origin of the terminal amino group of aminobacteriohopanetriol

The major enzymes in the acetyl ornithine aminotransferase family correspond to ornithine aminotransferase, acetylornithine aminotransferase, alanine-glyoxylate aminotransferase, dialkylglycine decarboxylase, 4-aminobutyrate aminotransferase, β-alanine-pyruvate aminotransferase, adenosylmethionine-8-amino-7-oxononanoate aminotransferase, and glutamate-1-semialdehyde 2,1-aminomutase. Several possible amino acids, including ornithine, alanine, aspartate, glutamate and glutamine, were hence tested as possible amino donors in order to find out the right candidate.

IV.2.1. Attempted feeding experiments with ^{15}N labeled amino acids on *R. palustris*.

R. palustris can live with or without oxygen, going through different metabolic modes. Its growth rate, however, is severely influenced by growth conditions. When *R. palustris* is grown photoheterotrophically at 30 °C for 5 days on modified *Rhodospirillaceae* medium (http://www.dsmz.de/microorganisms/medium/pdf/DSMZ_Medium27.pdf), ~ca. 0.6 g lyophilized cells were harvested from a 1 L culture; only half of this amount (~0.3 g/L) were obtained when *R. palustris* was incubated under aerobic conditions at the same temperature within the same time. The content of aminobacteriohopanetriol remained, however, unchanged (3.3 mg/g dry weight).

In order to harvest aminobacteriohopanetriol in a relatively short time, the culture of *R. palustris* was incubated under the anaerobic condition and feed with ^{15}N labeled amino acids (2 mM). Yeast extract and ammonia acetate were removed from the original media. Ammonium chloride was left as the only ^{14}N natural abundance nitrogen source, in order to diminish the dilution of ^{15}N from natural abundance nitrogen sources. In the late exponential phase, aminobacteriohopanetriol tetraacetate was isolated and analyzed by EI-MS (direct-inlet).

Intense ^{15}N labeling was observed however in the feeding experiments with ^{15}N labelled

aspartate, alanine, glutamate and glutamine in the fragments containing the side-chain: M^+, M^+–CH_3, M^+–AcOH and the fragments containing rings D, E and side chain derived from ring C cleavage. In contrast, no labeling was found in the fragments m/z 369 (M^+–side chain) and 191 (ring C cleavage) (for the fragmentation of aminobacteriohopanetriol tetraacetat by EIMS, see general experimental part and Table IV-1, entries 2, 3, 4 and 5). The incorporation percentage obtained from these experiments remained as ~20%. It is consistent with the original ratio of ^{15}N (from amino acid)/^{14}N (from NH_4Cl) in the media. These results indicate that the terminal amino group of aminobacteriohopanetriol was successfully labeled, but the possible donor can not be identified since labeling results can't be differentiated from one to another. The possible reasons why all the amino acid candidates were incorporated into aminobacteriohopanetriol are that the aminotransferase is not specific to certain amino acid, or alternatively, that the ^{15}N-labeled amino group was transferred to the right candidate via the amino acid metabolism in *R. palustris* (Fig. IV-5). The α-amino group of aspartate and alanine can be easily transferred into glutamate by the correspongding aminotransferases. Generation of glutamate from 2-oxoglutarate and glutamine is the main pathway for glutamate synthesis in bacteria. And glutamate ubiquitously acts as donor of amino groups for biosynthetic reactions in numerous trasamination reactions.

Table IV-1. M+1/M ratio of different fragments derived from aminobacteriohopanetriol peracetate analyzed by EI-MS.

	Fragments Amino acids	M^+–AcOH[b] 654/653	ring C cleavage 493/492	M^+–side chain[b] 370/369	ring C cleavage 192/191
1	Natural abundance[a]	48	30	30	19
2	^{15}N-Asp	62	49	37	19
3	^{15}N-Ala	66	47	31	19
4	^{15}N-Glu	64	43	32	19
5	^{15}N-Gln	68	48	30	19
6	$^{15}N_2$-ornithine	50	31	29	18

[a] Natural abundance of aminobacteriohopanetriol was obtained from the cells grown on DSM No.27 medium.
[b] High signal/noise ratio.

No obvious labeling on the side chain of aminobacteriohopanetriol was observed when *R. palustris* was grown with extragenous $^{15}N_2$-ornithine, indicating that ornithine or acetyl ornithine is less likely a donor for the terminal amino group of aminobacteriohopanetriol

(table IV-1, entry 6). The fact that the amino groups of $^{15}N_2$-ornithine can not be transferred into glutamate *in vivo* suggested that the additional ornithine may mainly be utilized to synthesize proteingenic amino acid arginine or to supply polyamines in this bacterium (Fig. IV-5).
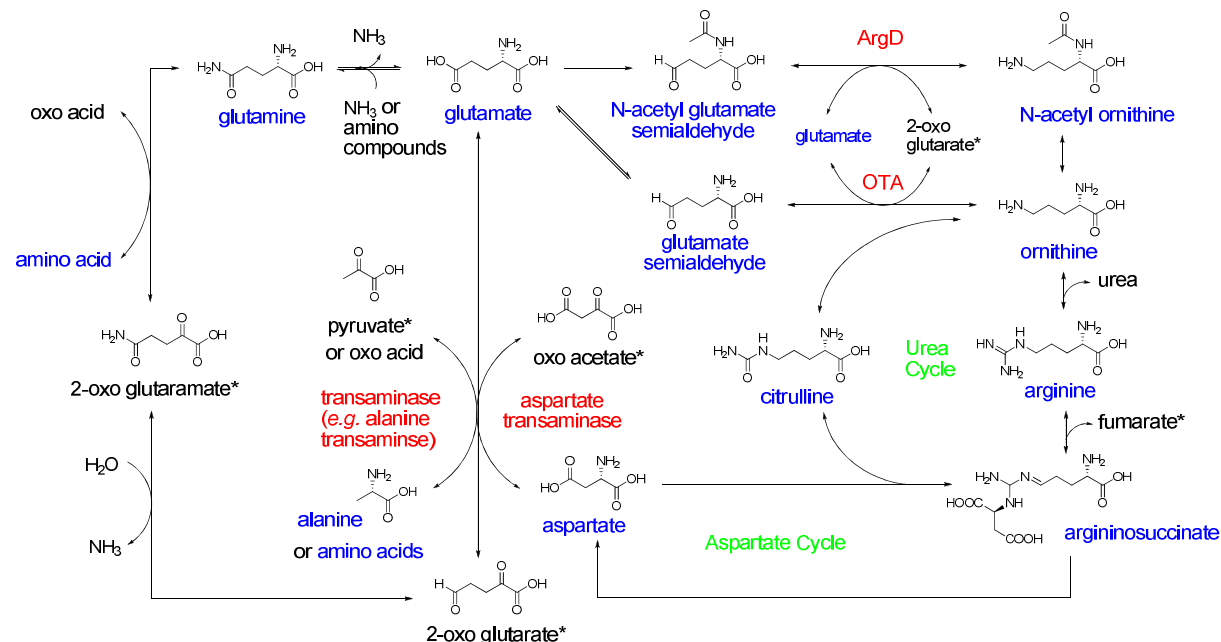
Fig. IV-5. Partial metabolism of glutamate, glutamine, aspartate, alanine, ornithine and related compounds in *R. palustris*. Amino acids are printed in bule, enzymes in red and metabolic pathways in green. Compounds labeled with * are, or can be converted into, intermediates in citrate cycle. Points on both ends of an arrow ↔ indicate noticeable reversibility of this reaction under biological conditions. Double arrows ⇌ are used when interconversion of two compounds proceeds via different reactions in both directions.

IV.2.2. Attempted incorporation of ^{15}N labeled amino group into aminobacteriohopanetriol via a cell-free system of *R. palustris*.

In order to avoid the distribution of ^{15}N from our target amino acids into other metabolites, incorporation experiments with a cell-free system of *R. palustris* were performed. With this methodology, the biosynthesis of amino acids could be largely suppressed, resulting thus in less interferences between the metabolic products.

The cells were harvested before the end of exponential phase. The cell-free system was obtained by sonication in phosphate buffer (50 mM, pH = 7.5) in the presence of PLP as a cofactor. After centrifugation, the supernatant was directly used for the incorporation step.

^{15}N-amino acids were added in the cell extract as well as synthetic [35-^{2}H]ribosylhopane (Bodlenner, unpublished work), the putative substrate of the transamination reaction. After 24 h at 30 °C, the reaction was stopped by freezing, and the samples were lyophilized and acetylated. The fractions containing aminobacteriohopanetriol tetraacetate were analyzed by EI-MS (direct-inlet). Aminobacteriohopanetriol tetraacetate was isolated in small amounts in all cases, and no ^{15}N labeling was detected by mass spectrometry (Table IV-2). Only natural abundance was found in the most intense fragment (*m/z* 492), which is derived from the ring C cleavage and contains ring D, E and the side chain, by analyzing the relative intensities of the most intense *m/z* 492, 493 and 494 signals.

Table IV-2. Incorporation of [35-^{2}H]ribosylhopane and ^{15}N-labeled amino acids into aminobacteriohopanetriol by cell-free system of *R. palustris*.[a]

^{15}N-amino acids Fragment		Natural abundance[b]	[^{15}N]Asp	[^{15}N]Ala	[^{15}N]Glu	[^{15}N]Gln	[^{15}N$_2$]Ornithine	No AA[c]
Fragment *m/z* 492	493/492 (%)	31±1	32	34	30	32	31	33
	494/492 (%)	7.0±0.5	8.5	9.1	7.8	8.4	7.8	10.1[d]

[a] All the samples were analyzed by EI-MS (direct-inlet)

[b] Natural abundance of aminobacteriohopanetriol was obtained from extract of the dry cells and was expressed with sample deviation of 95% (For the calculation, see Section III.2).

[c] No amino acid was introduced, only deuterium labeled ribosylhopane was present.

[d] High signal/noise ratio.

Two possible explanations for the negative labeling results may be proposed. The responsible enzyme is inactive, or the conversion rate of ribosylhopane into aminobacteriohopanetriol is so low that the trace amount of ^{15}N-aminobacteriohopanetriol (if there is any) could not be detected by EI-MS; alternatively, the tested ^{15}N amino acids were not the precursors of the terminal amino group of aminobacteriohopanetriol. The aminobacteriohopanetriol fractions were always accompanied by other pollutants, which can be hardly removed by TLC techniques. As a consequence aminobacteriohopanetriol was present as a minor component in the fractions analyzed by mass spectrometry, accurate measurement of the incorporation percentage was thus impossible due to the high signal/noise ratio, but in any case no high incorporation was obtained. The use of liquid chromatography techniques is a necessity for further purification.

IV.3. Conclusion

The attempts to identify the origin of 35-NH_2 of aminobacteriohopanetriol failed. Incorporation experiments with different ^{15}N-amino acids afforded nearly identical labeling patterns. Feeding experiments in amino acid pools were not suitable for this investigation because of the scrambling of labeling raised by the metabolisms of amino acids. The enzyme tests in cell-free systems barely resulted in any ^{15}N labeling on aminobacteriohopanetriol, either due to the low reactivity of the putative aminotransferase or due to the limited types of amino acids that have been tested. Expression of gene *hpnO* and purification of the corresponding enzyme are required in the future investigation.

IV.4. Experimental Part

IV.4.1. Bacteria and culture

Rhodopseudomonas palustris DSM 123 (DSMZ-Deutsche Sammlung von Mikroorganismen und Zellkulturen GmbH) was grown photoheterotrophically in DSM medium No. 27 at 30 °C for 4-5 days in top-filled stoppered 250 mL flasks and under continuous illumination with a 40-W tungsten lamps (average yield: 0.6 g/L, lyophilized cells).

DSM No. **27** medium

Sodium succinate	1.00 g
KH_2PO_4	0.50 g
$MgSO_4 \times 7H_2O$	0.40 g
NaCl	0.40 g
NH_4Cl	0.40 g
$CaCl_2 \times 2H_2O$	0.05 g
Yeast extracts	0.30 g
(NH_4)-acetate	0.50 g
EtOH	0.50 mL

Fe (III) citrate solution (0.1% in H_2O)	5.00 mL
Vitamin B_{12} solution (1 mg in 10 mL H_2O)	0.40 mL
Trace element solution SL-6	1.00 mL
Distilled Water	1050.00 mL
pH = 6.8	

IV.4.2. General procedure for feeding experiments with ^{15}N amino acids

R. palustris cultures for feeding experiments were grown on a modified DSM No. 27 medium. Yeast extract and ammonia acetate were replaced by sodium acetate (0.53 g/L) and ^{15}N-amino acids (2 mM). ^{15}N amino acids (^{15}N L-aspartate, ^{15}N L-alanine, ^{15}N L-glutamate, ^{15}N L-glutamine and $^{15}N_2$ L-ornithine) were purchased from Eurisotope and used as delivered. The bacterial cells were harvested at the end of the exponential growth phase by

centrifugation (10 000 rpm, 4 °C, 10 min), freeze-dried and extracted under reflux with $CHCl_3/CH_3OH$ (2:1, v/v). The combined extracts were taken to dryness, acetylated with Ac_2O/Py and then separated by flash chromatography (DCM/EtOAc 1:1 to EtOAc). The fractions were monitored by analytic TLC. The proper fraction containing aminobacteriohopanetriol tetraacetate was further purified by preparative TLC (DCM/MeOH 100:4) and afforded aminobacteriohopanetriol tetraacetate (R_f = 0.33). The resulting compound was analyzed by EI-mass spectrometry.

EI-MS spectrum of natural abundance aminobacteriohopanetriol tetraacetate (direct-inlet): m/z = 713 (M^+, 9%), 698 (M^+-Me, 4%), 653 (M^+-AcOH, 25%), 638 (M^+-Me-AcOH, 6%), 492 (ring C cleavage, 100%) (Budzikiewicz *et al.*, 1963), 432 (ring C cleavage-AcOH, 19%), 369 (M^+-side-chain, 21%), 312 (ring C cleavage-3AcOH, 26%), 253 (ring C cleavage-3AcOH-AcNH, 46%), 191 (ring C cleavage, 86%)

IV.4.3. General procedure for ^{15}N labeled amino acids and [35-^2H]ribosylhopane incorporation experiments in cell-free systems of *R. palustris*

A *R. palustris* culture grown on DSM medium No. 27 was harvested before the end of the exponential growth phase (O.D.~0.6) by centrifugation (10 000 rpm, 10 min), and then washed with sodium phosphate buffer (50 mM, $MgCl_2$ 0.5 mM, dithiothreitol 1 mM, PLP 0.1 mM, pH 7.5). After centrifugation (10 000 rpm, 10 min), the cells were suspended in the buffer (0.6 g/ 10 mL) and sonicated (8×40 s with 3 min pause at 0 °C). The crude cell extract was centrifuged (10 000 rpm, 10 min). The cell pellet was freeze-dried, and the supernatant was used directly for the incubation experiments.

A solution of deuteriated ribosylhopane (200 μg) in THF (400 μL) was added to the supernatant (4 mL) in a glass screw cap vial, followed by a solution of ^{15}N amino acid (30 eq. to ribosylhopane) in water (0.5~1 mL). The sample was incubated for 24 h with shaking at 200 rpm at 30 °C. It was freeze-dried and acetylated overnight with Ac_2O/pyridine (1:2, v/v, 3.9 mL). The mixture was filtered over cotton and washed with toluene (3×2 mL) and CH_2Cl_2 (3×2 mL). The combined filtrates were concentrited under reduced pressure. The residue was subjected to preparative TLC (DCM/MeOH 100:4) and afforded aminobacteriohopanetriol tetraacetate (R_f = 0.33), which was analyzed by direct-inlet EI-mass spectrometry.

General conclusion

Ultimate target of this study is to elucidate the formation of the C_5 side-chain bacterial triterpenoids of the hopane series. To understand the enzymatic reactions involved in this pathway, relevant genes were characterized and biosynthetic intermediates were identified.

Hopanoid production by two *Streptomyces coelicolor* A3(2) mutants defective in the *orf14* and *orf18* genes respectively was analyzed via various chromatography techniques and mass spectrometry (FCC, GC, HPLC, EI-MS, GC/MS, APCI-LC/MS^n). The different hopanoid profiles allowed characterization of the *orf14* and *orf18* genes, whose putative functions were further supported by bioinformatics analysis.

i) ORF14, which was annotated as a lipoprotein, was proved to be required in hopanoid biosynthesis in *S. coelicolor*, because the strain lacking *orf14* gene only accumulated adenosylhopane as the extended hopanoid. The ORF14 protein shows significant similarities to the enzymes HpnG protein and MTA/AdoHcy nucleosidases, suggesting that it possibly catalyzes the hydrolysis of adenosylhopane into ribosylhopane.

ii) Deletion of the *orf18* gene from *S. coelicolor* blocked the production of aminobacteriohopanetriol, but allowed us to detect those hopanoids that were generally not seen in the wild-type strain, including adenosylhopane, ribosylhopane and bacteriohopanetetrol. The putative intermediate ribosylhopane was isolated for the first time from a living organism and its structure was confirmed by NMR spectroscopy. The unique hopanoid phenotype, as well as the annotation of ORF18 protein as an aminotransferase, indicated its hypothetical function of transferring an amino group to the C-35 position of ribosylhopane and generating aminobacteriohopanetriol.

iii) The cluster of genes associated with hopanoid biosynthesis in *S. coelicolor* was compared with other microbial genomes that contain the genes required for aminobacteriohopanetriol production. The relative location of the homologous genes is well preserved, indicating the homologous traits of these microorganisms in term of hopanoid production. This analysis also suggested that the gene *orf15* is probably engaged in the side-chain formation as a radical SAM enzyme, catalyzing the production of adenosylhopane from diploptene and a 5'-deoxyadenosyl radical.

The conclusions above are in total agreement with the hypothetical biosynthetic pathway for hopanoid side-chain formation. Adenosylhopane serves as a precursor of ribosylhopane, which could lead to the formation of BHT and aminobacteriohopanetriol via reduction and

reductive amination respectivly.

To meet the needs of future biochemical investigation, adenosylhopane and a deuteriated isotopomer were synthesized from hydroxyhopanone and adenosine via a concise approach. Cross-metathesis and diimide reduction were employed in this convergent synthesis as the key steps (Fig. 16). The huge steric hindrance caused by the bulky hopane skeleton and the adenosyl group was consequently circumvented within good to moderate yields. This methodology presents a general utility for the preparation of functionalized bacteriohopanoids. Replacement of the adenosyl moiety with other acyclic or cyclic synthons would allow the access to a vast array of hopanoid structures.
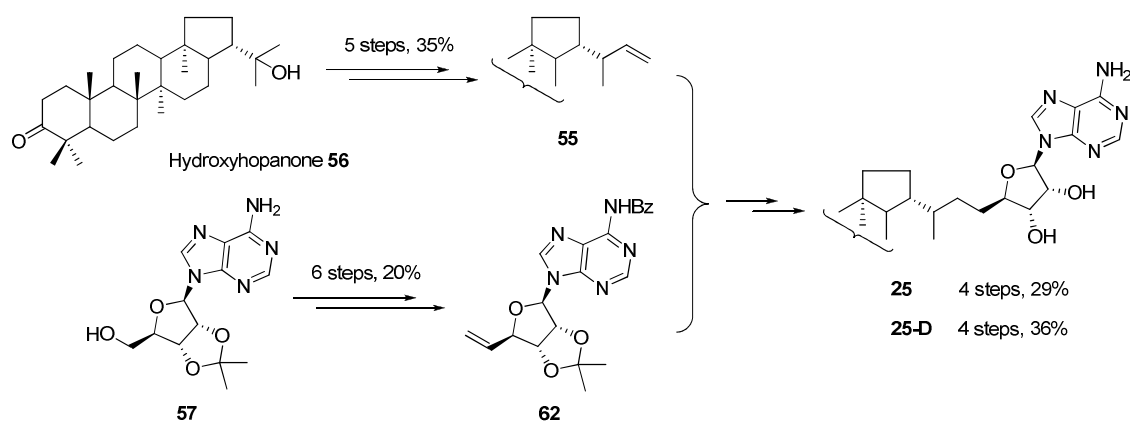
Fig. 16. Hemisynthesis of adenosylhopane and of a deuteriated isotopomer.

The role of adenosylhopane as an intermediate in the side-chain formation of bacteriohopanoids was further confirmed by the enzyme tests conducted with a cell-free system of *Methylobacterium organophilum*. Deuteriated adenosylhopane was successfully converted into deuteriated BHT via enzymatic reaction. NADPH is required as a reducing co-factor.

The last aspect of the project concerns the determination of the origin of the terminal amino group of aminobacteriohopanetriol and was not successful. Feeding experiments in vivo with *Rhodopseudomonas palustris* and enzyme tests with a cell-free system from the same bacteria with ^{15}N-amino acids gave no valuable information. Purification of the corresponding aminotransferase is probably necessary to elucidate the enzymatic reaction

leading to aminobacteriohopanetriol from ribosylhopane.

This Ph D thesis sheds light on the side-chain biosynthesis of bacteriohopanoids. Many questions are, however, still remaining:

i) Although a SAM enzyme was suggested as the 5'-deoxyadenosyl radical donor to promote the production of adenosylhopane from diploptene, such function of a SAM protein has not been reported. Generally, the 5'-deoxy adenosyl radical serves as an oxidizing reagent to generate other radicals, rather than being consumed as a real substrate. How does this enzyme work in the biosynthesis of adenosylhopane? Does it take diploptene or squalene as the substrate? Are there other co-enzymes involved?

ii) Ribosylhopane was derived from adenosylhopane, but we presently can not prove whether the responsible HpnG enzyme is a nucleosidase or purine nucleophosphorylase. Therefore there is a possibility that ribosylhopane 35-phosphate might be involved in the side-chain formation.

iii) The reductase required in the production of BHT from ribosylhopane has not been documented.

iv) Origin of the terminal amino group of aminobacteriohopanepolyols is unknown.

Deep understanding of these enzymatic reactions definitely requires purification and characterization of the corresponding enzymes.

General experimental part

Reagents and solvents

Reagents were purchased from Sigma-Aldrich, Acros, Alfa Aaesar, Roth Carl. Their purity was more than 98% in all cases. Thionyl chloride was distilled immediately before use. 2-Hydroxyhopanone was extracted from Dammar resin according to reported method (Dunstan *et al.*, 1957). *N,N'*-Dicyclohexylcarbodiimide was purified by distillation under reduced pressure (b.p. 122 °C at 6 mmHg), and then stored at 5 °C. Dowex 50 (H$^+$) resin was purchased from Aldrich and was activated right before use with 10% HCl solution in water.

All solvents were distilled before use. Dry solvents used in moisture sensitive reactions were obtained as follows: THF was freshly distilled from sodium benzophenone ketyl before use. CH_2Cl_2 was distilled over P_2O_5. Pyridine was distilled over KOH and then stored over molecular sieves (4Å). DMSO was purchased from Aldrich (sure sealed) and used directly.

TLC analysis

The progress of reactions was monitored by analytical thin layer chromatography using aluminum-coated Merck 60 F_{254} silica plates. UV visible spots were directly visualized under UV light at $\lambda = 254$ nm. Compounds containing the hopane skeleton could be revealed on TLC plate by UV light ($\lambda = 366$ nm) after spraying with berberine hydrochloride solution in EtOH (1 %).

Purification techniques

Most products were purified by flash column chromatography (FCC) using Merck 60 230-400 mesh silica gel and appropriate eluents. Adenosylhopane **25** and **25-D** were purified by FCC using Merck 60 63-200 µm silica gel under gravity.

Compounds in the amount of less than 10 mg were purified via preparative thin layer chromatography using Merck 60 F_{254} silica gel plates (0.25 mm layer thichness).

Melting Points

Melting points were measured with a BIBBY SMP3 apparatus and are corrected with

benzophenone (m.p. 48±1.5 °C).

Optical rotations

Optical rotations were measured at 20±2 °C using a cell of 10 cm in length 1 mL in volume.

Cell lysis

The bacterial cells were disrupted by sonication using SONIFIER B-30. Duty cycle: 60%, output control: 6, pulsed.

Optical density measurements

Optical densities of the bacterial cultures were measured on spectrophotometer Genesys 10UV, using photometer cuvettes of 1 cm in length and 1 mL in volume. The light wavelength is 595 nm for *Methylobacterium organophilum* cultures and 660 nm for *Rhodopseudomonas palustris* cultures.

Spectroscopic analysis

^{1}H-NMR and ^{13}C-NMR were performed on BRUKER Avance 600 spectrometer (600 MHz for ^{1}H, 150 MHz for ^{13}C), Bruker Biospin 500 spectrometer (500 MHz for ^{1}H, 125 MHz for ^{13}C) and BRUKER Avance 300 spectrometer (300 MHz for ^{1}H, 75 MHz for ^{13}C). Most of the measurements were carried out using $CDCl_3$ as solvent and with $CDCl_3$ ($\delta = 7.26$ ppm) as internal standard for ^{1}H-NMR and $CDCl_3$ ($\delta = 77.0$ ppm) as internal standard for ^{13}C-NMR. NMR spectra of adenosylhopane **25** and **25-D** were recorded in pyridine-D5 as solvent and with pyridine-D5 ($\delta = 8.73$, 7.58 and 7.21 ppm) as internal standard for ^{1}H-NMR and pyridine-D5 ($\delta = 149.9$, 135.5 and 123.5 ppm) as internal standard for ^{13}C-NMR. NMR spectra of adenosine 5'-aldehyde **39•H$_2$O** and **39** were derived using DMSO-D6 as the solvent and with DMSO-D6 ($\delta = 2.50$ ppm) as internal standard for ^{1}H-NMR and DMSO-D6 ($\delta =$

39.52 ppm) as internal standard for ^{13}C-NMR.

The abbreviations represent the multiplicity of the NMR signals:

s   singlet

d   doublet

t   triplet

q   quadruplet

m   multiplet

dd   doublet of doublet

ddd   doublet of doublet of doublet

dddd   doublet of doublet of doublet of doublet

arom   aromatic

br   broad

^{13}C-NMR assignments of known hopanoids were based on earlier assignments (Stampf, 1992; Pan, 2005) and were supported by additional experiments including DEPT, HSQC and HMBC techniques. Assignments of new synthetic compounds were based on earlier assignments (Pan, 2005; Toulouse, 2011) of structurally related compounds and supported by additional DEPT and 2D NMR spectroscopy. [13]C shift values of the carbon atoms in the hopanoid skeleton did not depend significantly on the nature of the side-chain and remained virtually unchanged after introduction of new carbon atoms or functional groups in the C_5 side-chain. Numbering of adenosylhopane skeleton is shown in Fig. 17. The hopane skeletons and C_5 side chains of all the complex hopanoids follow the same order.
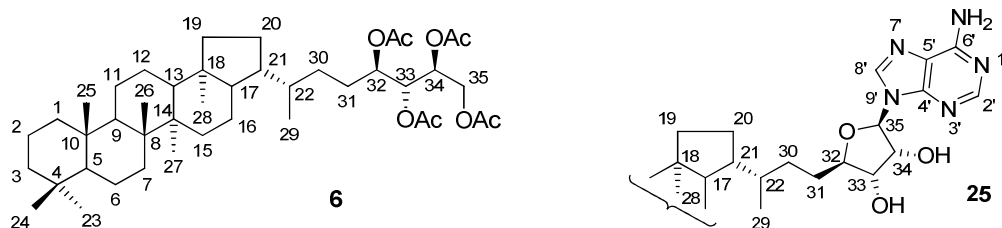
Fig. 17. Molecule numbering pattern of BHT **6** and adenosylhopane **25**.

GC-MS spectra were acquired on a Thermo TSQ Quantum mass spectrometer connected to a Thermo Trace GC ultra gas chromatograph (PTV injector, HP-5 MS column, 30 m, 0.25 mm i.d., 0.25 μm film thichness). Helium (constant flow 1 mL/min) was used as carrier gas.

The temperature program for GC analysis was: 3 min at 55 °C; from 55 °C to 320 °C at 10 °C/min; 50 min at 320 °C.

Mass spectra were produced a Thermo TSQ Quantum mass spectrometer at 70 eV in the electron ionization mode (EIMS) over a mass range of 50-800 Da (cycle time 0.5s). The source temperature was set at 230 °C. Compounds were characterized by their parent ion and by the typical fragmentation patterns of hopanoids (Fig. 18).

m/z 369

side-chain cleavage

ring C cleavage

m/z 191

m/z 492 for aminobacteriohopanetriol tetraacetate
m/z 493 for BHT tetraacetate

Fig. 18. Typical hopanoids fragments observed by mass-spectrometry under EI mode.

APPENDIX

Appendix 1. Genes hypothetically involved in the biosynthesis of bacteriohopanoids

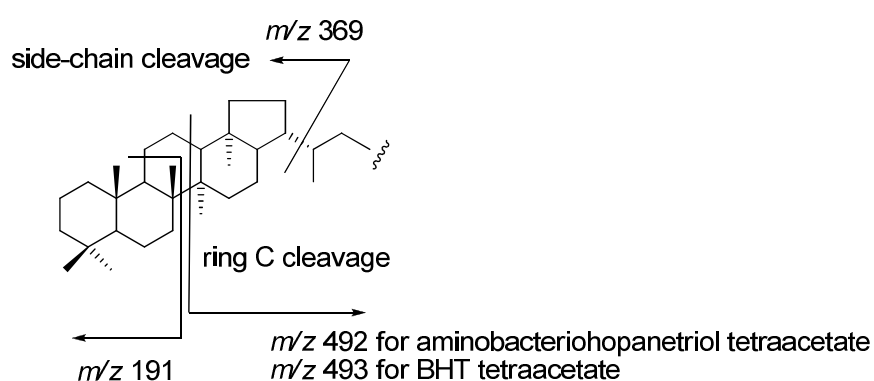| Gene	Annotation	Hypothesized or known function	References
hpnA	Hopanoid associated sugar epimersase	Involved in side chain formation	1
hpnB	Putative glycosyltransferase	Involved in side chain formation	1
hpnC	Squalene synthase	Synthesis of squalene	1
hpnD	Squalene/phytoene synthase	Synthesis of squalene—alternative patheway	1
hpnE	Squalene-associated FAD-dependent desaturase	Synthesis of squalene—alternative patheway	1
hpnF	Squalene-hopene cyclase	Formation of hopanoid cyclic backbone	2
hpnG	Hopanoid biosynthesis associated phosphorylase	Cleavage of adenine from side chain	3,4
hpnH	Hopanoid biosynthesis associated radical SAM protein	Addition of adenosyl group to side chain	3
hpnI	Glycosyltransferase	Possibly involved in side chain formation	5
hpnJ	Hopanoid biosynthesis associated radical SAM protein	Possibly involved in side chain formation	5
hpnK	Hopanoid biosynthesis associated protein (ydjC)	Possibly involved in side chain formation	5
hpnL	Conserved hypothetical protein	Possibly involved in side chain formation	5
hpnM	Hopanoid biosynthesis associated protein (Ttg2D)	Possibly involved in side chain formation	5
hpnN	RND superfamily exporter	Probable hopanoid transporter, similar to eukaryotic Ptc	6
hpnO	Ornithine-oxo-acid transaminase	Production of aminobacteriohopantriol	4
hpnP	Hopanoid A-ring methylase	Methylates A ring at C-2	7
hpnR	Hopanoid A-ring methylase	Methylates A ring at C-3	8

References indicated the publication in which each gene's function was demonstrated or hypothesized. 1. Perzl *et al.* (1998); 2. Reipen *et al.* (1995); 3. Bradley *et al.* (2010); 4. Welander *et al.* (2012); 5. Hypothesized function; 6. Doughty *et al.*, (2011); 7. Welander *et al.*, (2010); 8. Welander and Summons (2012)

Appendix 2. EI-MS spectrum (direct-inlet) of chemically synthesized ribosylhopane (a mixture of 35α- and 35β anomers)
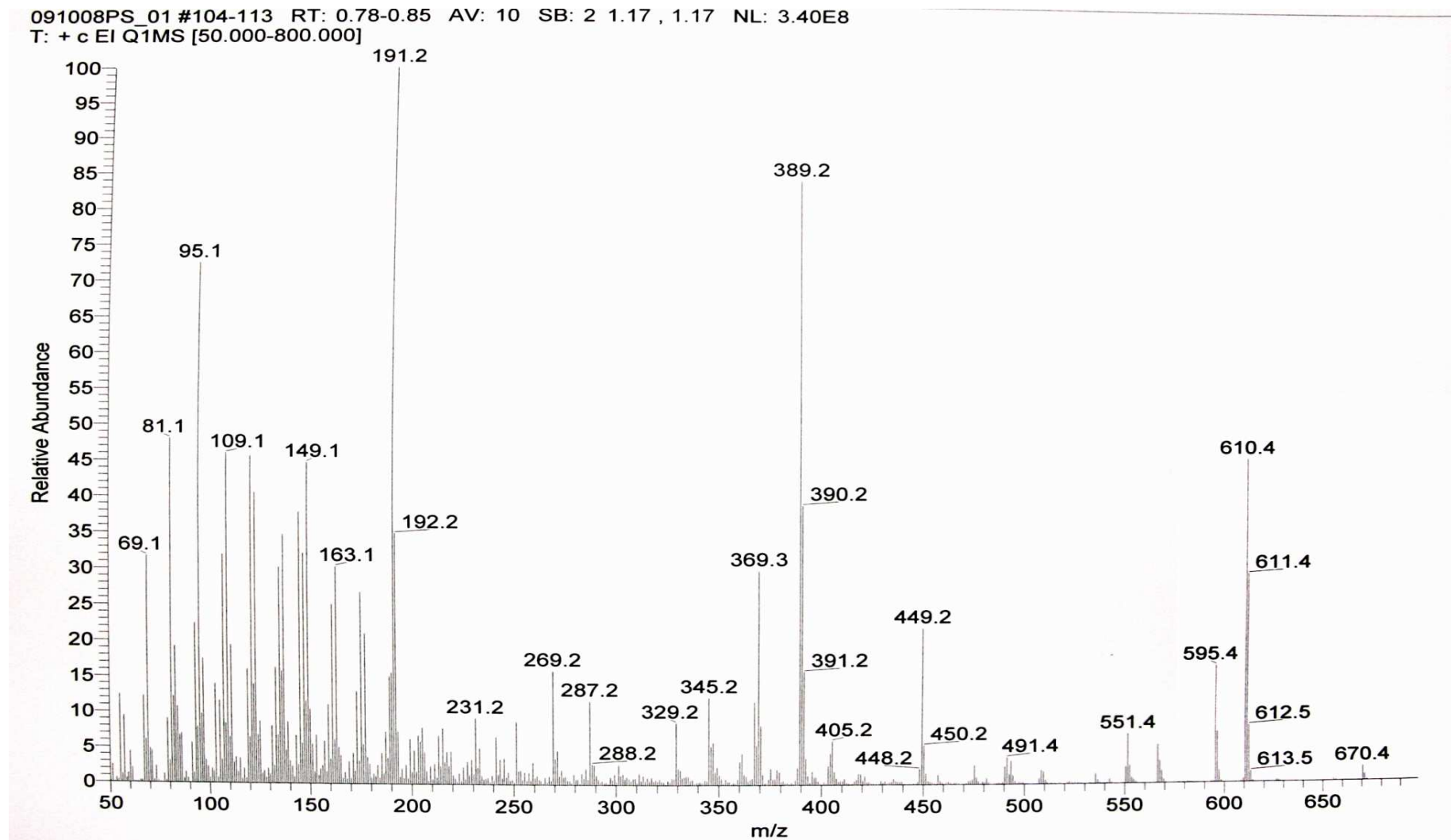
Appendix 3. EI-MS spectrum (direct-inlet) of 35α-ribosylhopane isolated from Δ*orf18* mutant of *S. coelicolor*

091008PS_02 #68-71 RT: 0.52-0.54 AV: 4 SB: 8 0.74-0.75 , 0.36-0.39 NL: 3.42E8
T: + c EI Q1MS [50.000-800.000]
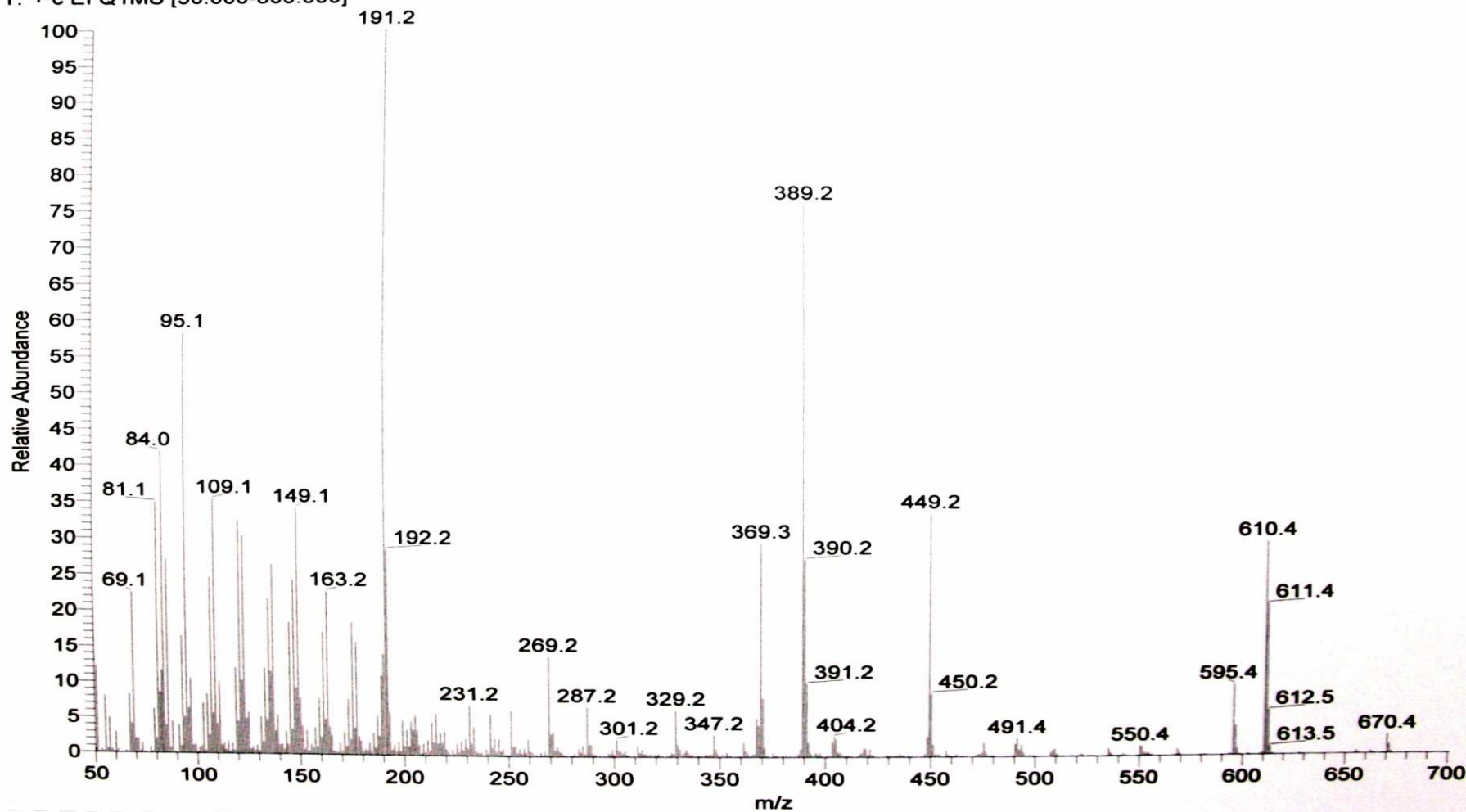
Appendix 4. GC/EI-MS spectrum of 35α-ribosylhopane isolated from Δ*orf18* mutant of *S. coelicolor*

~ 179 ~

Appendix 5. EI-MS spectrum (direct-inlet) of 35β-ribosylhopane isolated from Δ*orf18* mutant of *S. coelicolor*
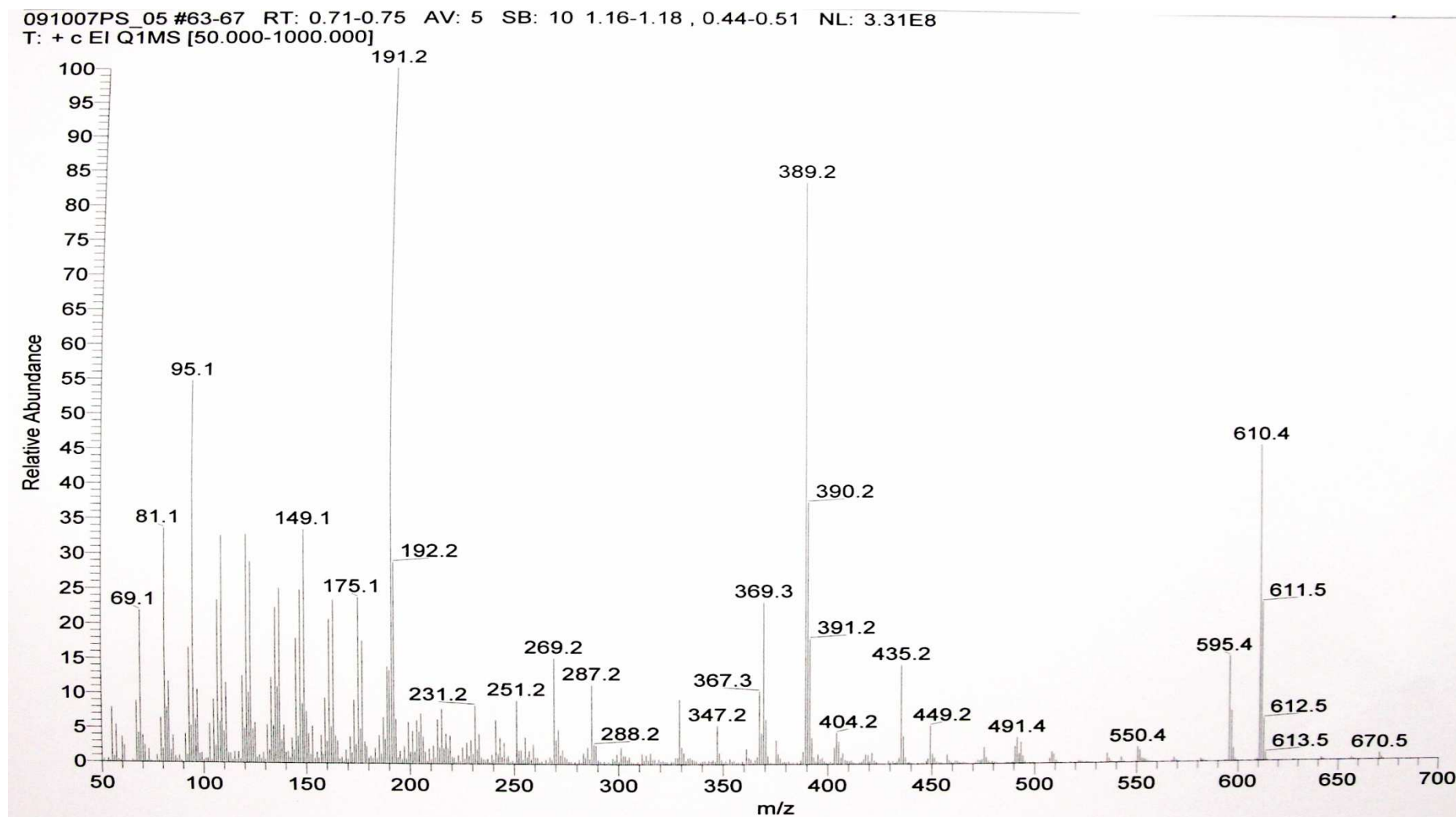
091007PS_05 #63-67 RT: 0.71-0.75 AV: 5 SB: 10 1.16-1.18 , 0.44-0.51 NL: 3.31E8
T: + c EI Q1MS [50.000-1000.000]

Appendix 6. GC/EI-MS spectrum of 35β-ribosylhopane isolated from Δ*orf18* mutant of *S. coelicolor*

090416PS06 #862-958 RT: 40.53-41.70 AV: 97 SB: 185 46.52-47.82 , 38.99-39.92 NL: 4.25E7
T: + c EI Q1MS [50.000-800.000]
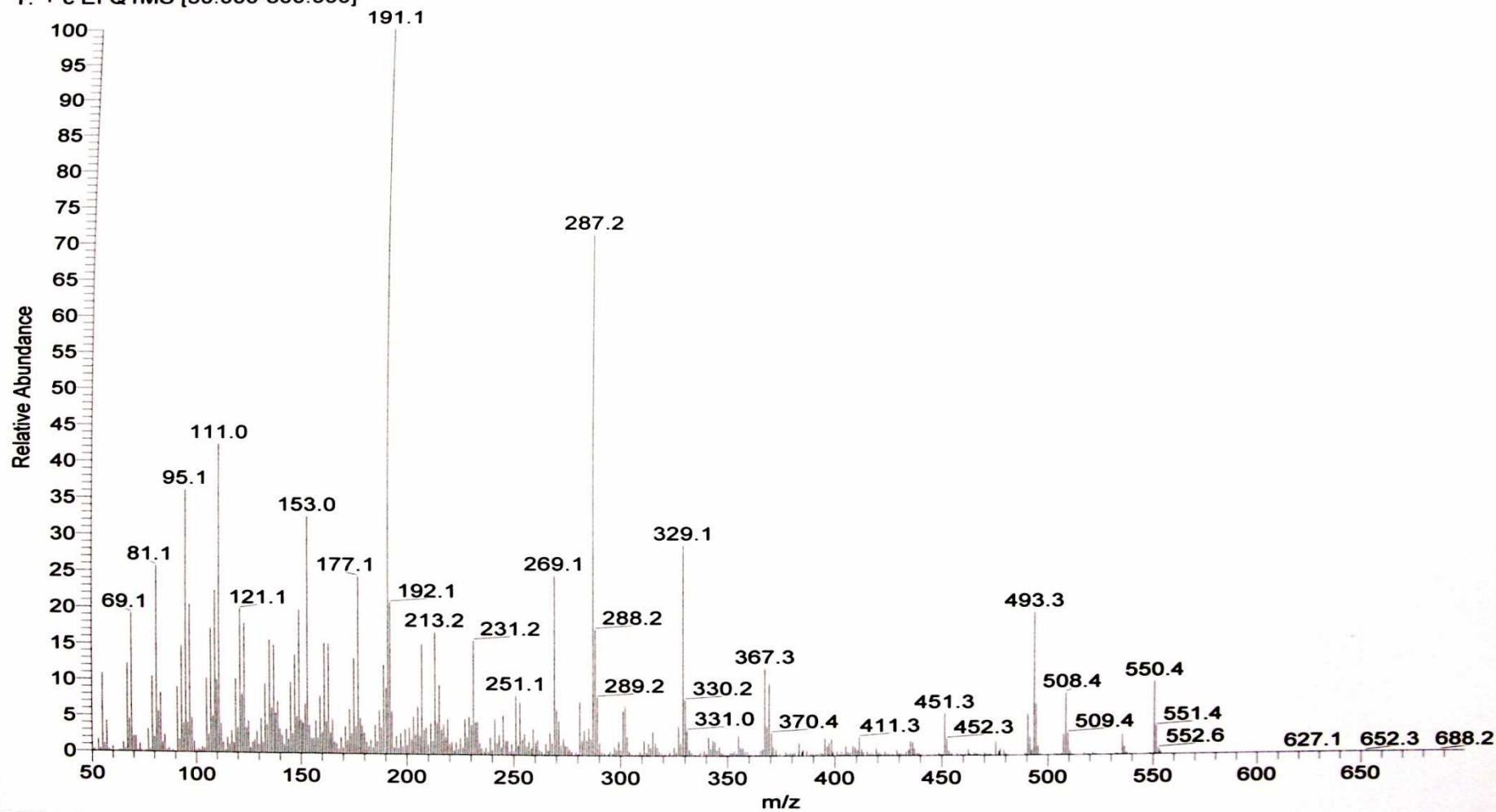
References

Abe, I. (2007) Enzymatic synthesis of cyclic triterpenes. *Nat. Prod. Rep.* **24**, 1311.

Aljarilla, A.; Lopez, J. C. and Plumet, J. (2010) Metathesis reactions of carbohydrates: Recent highlights in cross metathesis. *Eur. J. Org. Chem.*, 6123.

Amblard, F.; Nolan, S. P. and Agrofoglio, L. A. (2005) Metathesis strategy in nucleoside chemistry. *Tetrahedron* **61**, 7067.

Anding, C.; Rohmer, M. and Ourisson, G. (1976) Nonspecific biosynthesis of hopane triterpenes in a cell-free system from *Acetobacter rancens*. *J. Am. Chem. Soc.* **98**, 1274.

Andrei, D. and Wnuk, S. F. (2006) *S*-Adenosylhomocysteine analogues with the carbon-5' and sulfur atoms replaced by a vinyl unit. *Org. Lett.* **8**, 5093.

Batoux, N.; Benhaddou-Zerrouki, R.; Bressolier, P.; Granet, R.; Laumont, G.; Aubertin, A. M. and Krausz, P. (2001) Nucleoside homodimerisation by cross metathesis. *Tetrahedron Lett.* **42**, 1491.

Bennett, E. M.; Li, C.; Allan, P. W.; Parker, W. B. and Ealick, S. E. (2003) Structural basis for substrate specificity of *Escherichia coli* purine nucleoside phosphorylase. *J. Biol. Chem.* **278**, 47110.

Bentley, S. D.; Chater, K. F.; Cerdeno-Tarraga, A. M.; Challis, G. L.; Thomson, N. R.; James, K. D.; Harris, D. E.; Quail, M. A.; Kieser, H.; Harper, D.; Bateman, A.; Brown, S.; Chandra, G.; Chen, C. W.; Collins, M.; Cronin, A.; Fraser, A.; Goble, A.; Hidalgo, J.; Hornsby, T.; Howarth, S.; Huang, C. H.; Kieser, T.; Larke, L.; Murphy, L.; Oliver, K.; O'Neil, S.; Rabbinowitsch, E.; Rajandream, M. A.; Rutherford, K.; Rutter, S.; Seeger, K.; Saunders, D.; Sharp, S.; Squares, R.; Squares, S.; Taylor, K.; Warren, T.; Wietzorrek, A.; Woodward, J.; Barrell, B. G.; Parkhill, J. and Hopwood, D. A. (2002) Complete genome sequence of the model actinomycete *Streptomyces coelicolor* A3(2). *Nature* **417**, 141.

Bird, C. W.; Lynch, J. M.; Pirt, S. J. and Reid, W. W. (1971) The identification of hop-22(29)-ene in prokaryotic organisms. *Tetrahedron Lett.* **12**, 3189.

Bisseret, P. and Rohmer, M. (1989) Bacterial sterol surrogates – determination of the absolute-configuration of bacteriohopanetetrol side-chain by hemisynthesis of its diastereoisomers. *J. Org. Chem.* **54**, 2958.

Bisseret, P. and Rohmer, M. (1993) Heating of hop-17(21)-ene in molten sulfur – a route to new sedimentary biomarkers of the hopane series. *Tetrahedron Lett.* **34**, 5295.

Bisseret, P.; Zundel, M. and Rohmer, M. (1985) Prokaryotic triterpenoids. 2. 2β-methylhopanoids from *Methylobacterium organophilum* and *Nostoc muscorum*, a new series of prokaryotic triterpenoids. *Eur. J. Biochem.* **150**, 29.

Blumenberg, M.; Kruger, M.; Nauhaus, K.; Talbot, H. M.; Oppermann, B. I.; Seifert, R.; Pape, T. and Michaelis, W. (2006) Biosynthesis of hopanoids by sulfate-reducing bacteria (genus *Desulfovibrio*). *Environ. Microbiol.* **8**, 1220.

Bradley, A. S.; Pearson, A.; Saenz, J. P. and Marx, C. J. (2010) Adenosylhopane: The first intermediate in hopanoid side chain biosynthesis. *Org. Geochem.* **41**, 1075.

Bravo, J. M.; Perzl, M.; Hartner, T.; Kannenberg, E. L. and Rohmer, M. (2001) Novel methylated triterpenoids of the gammacerane series from the nitrogen-fixing bacterium *Bradyrhizobium japonicum* USDA 110. *Eur. J. Biochem.* **268**, 1323.

Budzikiewicz, H.; Wilson, J. M. and Djerassi, C. (1963) Mass spectrometry in structural and

stereochemical problems. XXXII.1 Pentacyclic triterpenes. *J. Am. Chem. Soc.* **85**, 3688.

Charon, L. (2000) Biosynthèse des isoprénoïdes : Origine des protons du diphosphate d'isopentényle dans la voie du 2-*C*-méthyl-D-érythritol 4-phosphate. Université de Strasbourg, Strasbourg, France.

Chatterjee, A. K.; Choi, T. L.; Sanders, D. P. and Grubbs, R. H. (2003) A general model for selectivity in olefin cross metathesis. *J. Am. Chem. Soc.* **125**, 11360.

Cohen, T. and Doubleday, M. D. (1990) A simple method for producing cycloalkenyllithiums from cycloalkanones via reductive lithiation of enol phenyl thioethers. *J. Org. Chem.* **55**, 4784.

Connon, S. J. and Blechert, S. (2003) Recent developments in olefin cross metathesis. *Angew. Chem. Int. Edit.* **42**, 1900.

Cooke, M. P.; Talbot, H. M. and Wagner, T. (2008) Tracking soil organic carbon transport to continental margin sediments using soil-specific hopanoid biomarkers: A case study from the congo fan (odp site 1075). *Org. Geochem.* **39**, 965.

Corpe, W. A.; Jensen, T. E. and Baxter, M. (1986) Fine structure of cytoplasmic inclusions of some methylotrophic bacteria from plant surfaces. *Arch. Microbiol.* **145**, 107.

Costantino, V.; Della Sala, G.; Mangoni, A.; Perinu, C. and Teta, R. (2012) Blurring the boundary between bio- and geohopanoids: Plakohopanoid, a C_{32} biohopanoid ester from *Plakortis* cf. *lita. Eur. J. Org. Chem.* **2012**, 5171.

Costantino, V.; Fattorusso, E.; Imperatore, C. and Mangoni, A. (2000) The first 12-methylhopanoid: 12-methylbacteriohopanetetrol from the marine sponge *Plakortis simplex. Tetrahedron* **56**, 3781.

Crabtree, R. (1979) Iridium compounds in catalysis. *Acc. Chem. Res.* **12**, 331.

Craig, G. W.; Sternberg, E. D.; Jones, G. H. and Moffatt, J. G. (1986) Synthesis of 9-[5-(alkylthio)-5-deoxy-β-D-erythro-pent-4-enofuranosyl)adenines as potential inhibitors of transmethylation. *J. Org. Chem.* **51**, 1258.

Cvejic, J. H.; Bodrossy, L.; Kovacs, K. L. and Rohmer, M. (2000a) Bacterial triterpenoids of the hopane series from the methanotrophic bacteria *Methylocaldum* spp.: Phylogenetic implications and first evidence for an unsaturated aminobacteriopanepolyol. *FEMS Microbiol. Lett.* **182**, 361.

Cvejic, J. H.; Putra, S. R.; El-Beltagy, A.; Hattori, R.; Hattori, T. and Rohmer, M. (2000b) Bacterial triterpenoids of the hopane series as biomarkers for the chemotaxonomy of *Burkholderia*, *Pseudomonas* and *Ralstonia* spp. *FEMS Microbiol. Lett.* **183**, 295.

Czajkowska, D. and Morzycki, J. W. (2009) Metathesis reactions of Δ(22)-steroids. *Tetrahedron Lett.* **50**, 2904.

Sinninghe Damsté, J. S.; Rijpstra, W. I. C.; Schouten, S.; Fuerst, J. A.; Jetten, M. S. M. and Strous, M. (2004) The occurrence of hopanoids in planctomycetes: Implications for the sedimentary biomarker record. *Org. Geochem.* **35**, 561.

De Rosa, M.; Gambacorta, A. and Minale, L. (1971) Bacterial triterpenes. *J. Chem. Soc. Chem. Commun.*, 619.

Doughty, D. M.; Hunter, R. C.; Summons, R. E. and Newman, D. K. (2009) 2-Methylhopanoids are maximally produced in akinetes of *Nostoc punctiforme*:

Geobiological implications. *Geobiology* **7**, 524

Doughty, D. M.; Coleman, M. L.; Hunter, R. C.; Sessions, A. L.; Summons, R. E. and Newman, D. K. (2011) The RND-family transporter, HpnN, is required for hopanoid localization to the outer membrane of rhodopseudomonas palustris tie-1. *Proc. Natl. Acad. Sci. USA* **108**, E1045.

Dunstan, W. J. F., H.; Halsall, T. G.; Jones, E. R. (1957) The chemistry of the triterpenes and related compounds. Part XXXII. The chemistry of hydroxyhopanone. *Croat. Chim. Acta* **29**, 173.

Duvold, T. (1997) Chemistry and biochemistry of bacterial isoprenoids. Université Louis Pasteur, Strasbourg, France.

Duvold, T.; Bravo, J. M.; Pale-Grosdemange, C. and Rohmer, M. (1997a) Biosynthesis of 2-*C*-methyl-D-erythritol, a putative C_5 intermediate in the mevalonate independent pathway for isoprenoid biosynthesis. *Tetrahedron Lett.* **38**, 4769.

Duvold, T.; Cali, P.; Bravo, J. M. and Rohmer, M. (1997b) Incorporation of 2-*C*-methyl-D-erythritol, a putative isoprenoid precursor in the mevalonate-independent pathway, into ubiquinone and menaquinone of *Escherichia coli*. *Tetrahedron Lett.* **38**, 6181.

Duvold, T. and Rohmer, M. (1999) Synthesis of ribosylhopane, the putative biosynthetic precursor of bacterial triterpenoids of the hopane series. *Tetrahedron* **55**, 9847.

Edelsztein, V. C.; Di Chenna, P. H. and Burton, G. (2009) Synthesis of C–C bonded dimeric steroids by olefin metathesis. *Tetrahedron* **65**, 3615.

Eignerová, B.; Dračínský, M. and Kotora, M. (2008) Perfluoroalkylation through cross metathesis between alkenes and (perfluoroalkyl)propenes. *Eur. J. Org. Chem.* **2008**, 4493.

Eklund, H.; Eriksson, M.; Uhlin, U.; Nordlund, P. and Logan, D. (1997) Ribonucleotide reductase – structural studies of a radical enzyme. *Biol. Chem.* **378**, 821.

Ensminger, A. (1974) Triterpénoïdes du schiste de Messel. Université Louis Pasteur de Strasbourg, France.

Eppacher, S.; Bhardwaj, P. K.; Bernet, B.; Gala, J. L. B.; Knopfel, T. and Vasella, A. (2004) Oligonucleosides with a nucleobase-including backbone – part 12 – synthesis of mixed ethynylene-linked uridine- and adenosine-derived tetramers. *Helv. Chim. Acta* **87**, 2969.

Erion, M. D.; Takabayashi, K.; Smith, H. B.; Kessi, J.; Wagner, S.; Hönger, S.; Shames, S. L. and Ealick, S. E. (1997) Purine nucleoside phosphorylase. 1. Structure−function studies†. *Biochemistry* **36**, 11725.

Fischer, W. W. and Pearson, A. (2007) Hypotheses for the origin and early evolution of triterpenoid cyclases. *Geobiology* **5**, 19.

Flesch, G. and Rohmer, M. (1988a) Biosynthesis of a carbocyclic pentose analog linked to bacteriohopanetetrol from the bacterium *Methylobacterium organophilum*. *J. Chem. Soc., Chem. Commun.*, 868.

Flesch, G. and Rohmer, M. (1988b) Prokaryotic hopanoids – the biosynthesis of the bacteriohopane skeleton – formation of isoprenic units from two distinct acetate pools and a novel type of carbon carbon linkage between a triterpene and D-ribose. *Eur. J. Biochem.* **175**, 405.

Flesch, G. and Rohmer, M. (1989) Prokaryotic triterpenoids – a novel hopanoid from the ethanol-producing bacterium *Zymomonas mobilis*. *Biochem. J.* **262**, 673.

Forster, H. J.; Biemann, K.; Haigh, W. G.; Tattrie, N. H. and Colvin, J. R. (1973) The structure of novel C_{35} pentacyclic terpenes from *Acetobacter xylinum*. *Biochem. J.* **135**, 133.

Francis, G. W.; Papaioannou, D.; Aksnes, D. W.; Brekke, T.; Maartmannmoe, K. and Taelnes, N. (1991) Approaches to the synthesis of terpenyl carbohydrates. *Acta. Chem. Scand.* **45**, 652.

Fürstner, A. and Langemann, K. (1997) Macrocycles by ring-closing metathesis. *Synthesis* **1997**, 792.

Garber, S. B.; Kingsbury, J. S.; Gray, B. L. and Hoveyda, A. H. (2000) Efficient and recyclable monomeric and dendritic Ru-based metathesis catalysts. *J. Am. Chem. Soc.* **122**, 8168.

Gelpi, E.; Schneider, H.; Mann, J. and Oro, J. (1970) Hydrocarbons of geochemical significance in microscopic algae. *Phytochemistry* **9**, 603.

Gessler, S.; Randl, S. and Blechert, S. (2000) Synthesis and metathesis reactions of a phosphine-free dihydroimidazole carbene ruthenium complex. *Tetrahedron Lett.* **41**, 9973.

Hamersma, J. W. and Snyder, E. I. (1965) Diimide reductions using potassium azodicarboxylate. *J. Org. Chem.* **30**, 3985.

Haigh, W. G.; Forster, H. J.; Biemann, K.; Tattrie, N. H. and Colvin, J. R. (1973) Induction of orientation of bacterial cellulose microfibrils by a novel terpenoid from *Acetobacter xylinum*. *Biochem. J.* **135**, 145.

Handley, L.; Talbot, H. M.; Cooke, M. P.; Anderson, K. E. and Wagner, T. (2010) Bacteriohopanepolyols as tracers for continental and marine organic matter supply and phases of enhanced nitrogen cycling on the late quaternary congo deep sea fan. *Org. Geochem.* **41**, 910.

Härtner, T.; Straub, K. L. and Kannenberg, E. (2005) Occurrence of hopanoid lipids in anaerobic *Geobacter* species. *FEMS Microbiol. Lett.* **243**, 59.

Henessian, S., Ed. (1983). Total synthesis of natural products: The chiron approach, Oxford.

Hermans, M. A. F.; Neuss, B. and Sahm, H. (1991) Content and composition of hopanoids in *Zymomonas mobilis* under various growth conditions. *J. Bacteriol.* **173**, 5592.

Herrmann, D.; Bisseret, P.; Connan, J. and Rohmer, M. (1996) Relative configurations of carbapseudopentose moieties of hopanoids of the bacterium *Zymomonas mobilis* and the cyanobacterium '*Anacystis montana*'. *Tetrahedron Lett.* **37**, 1791.

Hestrin, S. and Schramm, M. (1954) Synthesis of cellulose by *Acetobacter xylinum*. II. Preparation of freeze-dried cells capable of polymerizing glucose to cellulose. *Biochem. J.* **58**, 345.

Hirsch, G. (2004) Triterpénoïdes bactériens de la série du hopane: structure, biosynthèse et mise au point d'inhibiteurs. Université Louis Pasteur. Strasbourg, France.

Hoshino, T.; Kouda, M.; Abe, T. and Ohashi, S. (1999) New cyclization mechanism for squalene: A ring-expansion step for the five-membered C-ring intermediate in hopene biosynthesis. *Biosci. Biotech. Bioch.* **63**, 2038.

Huang, J. K.; Stevens, E. D.; Nolan, S. P. and Petersen, J. L. (1999) Olefin metathesis-active ruthenium complexes bearing a nucleophilic carbene ligand. *J. Am. Chem. Soc.* **121**, 2674.

Huang, Q. Y. and Herdewijn, P. (2011) Synthesis of (*E*)-3'-phosphonoalkenyl modified nucleoside phosphonates via a highly stereoselective olefin cross metathesis reaction. *J. Org. Chem.* **76**, 3742.

Hugenholtz, P. and Pace, N. R. (1996) Identifying microbial diversity in the natural environment: A molecular phylogenetic approach. *Trends Biotechnol.* **14**, 190.

Jahnke, L. L.; Stan-lotter, H.; Kato, K. and Hochstein, L. I. (1992) Presence of methyl sterol and bacteriohopanepolyol in an outer-membrane preparation from *Methylococcus capsulatus* (BATH). *J. Gen. Microbiol.* **138**, 1759.

Jean-Louis Hérisson, P. and Chauvin, Y. (1971) Catalyse de transformation des oléfines par les complexes du tungstène. II. Télomérisation des oléfines cycliques en présence d'oléfines acycliques. *Makromo. Chem.* **141**, 161.

Joyeux, C.; Fouchard, S.; Llopiz, P. and Neunlist, S. (2004) Influence of the temperature and the growth phase on the hopanoids and fatty acids content of *Frateuria aurantia* (DSMZ 6220). *FEMS Microbiol. Ecol.* **47**, 371.

Jürgens, U. J.; Simonin, P. and Rohmer, M. (1992) Localization and distribution of hopanoids in membrane systems of the cyanobacterium *Synechocystis* PCC-6714. *FEMS Microbiol. Lett.* **92**, 285.

Kannenberg, E. L. and Poralla, K. (1999) Hopanoid biosynthesis and function in bacteria. *Naturwissenschaften* **86**, 168.

Kjer, A.; Kjer, D. and Skrydstrup, T. (1986) Synthesis and properties of some stereoisomeric long-chain 1,2,3,4-tetrols. *Tetrahedron* **42**, 1439.

Kleemann, G.; Poralla, K.; Englert, G.; Kjosen, H.; Liaaen-Jensen, S.; Neunlist, S. and Rohmer, M. (1990) Tetrahymanol from the phototrophic bacterium *Rhodopseudomonas Palustris*–1st report of a gammacerane triterpene from a prokaryote. *J. Gen. Microbiol.* **136**, 2551.

Kleemann, G.; Kellner, R. and Poralla, K. (1994) Purification and properties of the squalene-hopene cyclase from *Rhodopseudomonas palustris*, a purple nonsulfur bacterium producing hopanoids and tetrahymanol. *Biochim. Biophys. Acta, Lipids Lipid Metab.* **1210**, 317.

Kline, P. C. and Schramm, V. L. (1995) Pre-steady-state transition-state analysis of the hydrolytic reaction catalyzed by purine nucleoside phosphorylase. *Biochemistry* **34**, 1153.

Knani, M. H.; Corpe, W. A. and Rohmer, M. (1994) Bacterial hopanoids from pink-pigmented facultative methylotrophs (PPFMs) and from green plant surfaces. *Microbiology* **140**, 2755.

Langworthy, T. A.; Mayberry, W. R. and Smith, P. F. (1976) A sulfonolipid and novel glucosamidyl glycolipids from the extreme thermoacidophile *Bacillus acidocaldarius*. *Biochim. Biophys. Acta, Lipids Lipid Metab.* **431**, 550.

Larimer, F. W.; Chain, P.; Hauser, L.; Lamerdin, J.; Malfatti, S.; Do, L.; Land, M. L.; Pelletier, D. A.; Beatty, J. T.; Lang, A. S.; Tabita, F. R.; Gibson, J. L.; Hanson, T. E.; Bobst, C.;

Torres, J. L. T. y.; Peres, C.; Harrison, F. H.; Gibson, J. and Harwood, C. S. (2004) Complete genome sequence of the metabolically versatile photosynthetic bacterium *Rhodopseudomonas palustris*. *Nat. Biotechnol.* **22**, 55.

Lee, J. E.; Cornell, K. A.; Riscoe, M. K. and Howell, P. L. (2003) Structure of *Escherichia coli* 5′-methylthioadenosine/*S*-adenosylhomocysteine nucleosidase inhibitor complexes provide insight into the conformational changes required for substrate binding and catalysis. *J. Biol. Chem.* **278**, 8761.

Lera, M. and Hayes, C. J. (2001) An olefin cross metathesis approach to vinylphosphonate-linked nucleic acids. *Org. Lett.* **3**, 2765.

Lidstrom, M. E. and Chistoserdova, L. (2002) Plants in the pink: Cytokinin production by *Methylobacterium*. *J. Bacteriol.* **184**, 1818.

Llopiz, P.; Neunlist, S. and Rohmer, M. (1992) Prokaryotic triterpenoids: *O*-α-D-glucuronopyranosyl bacteriohopanetetrol, a novel hopanoid from the bacterium *Rhodospirillum rubrum*. *Biochem. J.* **287**, 159.

Marchler-Bauer, A.; Anderson, J. B.; Chitsaz, F.; Derbyshire, M. K.; De Weese-Scott, C.; Fong, J. H.; Geer, L. Y.; Geer, R. C.; Gonzales, N. R.; Gwadz, M.; He, S.; Hurwitz, D. I.; Jackson, J. D.; Ke, Z.; Lanczycki, C. J.; Liebert, C. A.; Liu, C.; Lu, F.; Lu, S.; Marchler, G. H.; Mullokandov, M.; Song, J. S.; Tasneem, A.; Thanki, N.; Yamashita, R. A.; Zhang, D.; Zhang, N. and Bryant, S. H. (2009) CDD: Specific functional annotation with the conserved domain database. *Nucleic Acids Res.* **37**, D205.

Marsh, B. J. and Carbery, D. R. (2009) One-pot *O*-nitrobenzenesulfonylhydrazide (NBSH) formation – diimide alkene reduction protocol. *J. Org. Chem.* **74**, 3186.

Marsh, E. N. G.; Patterson, D. P. and Li, L. (2010) Adenosyl radical: Reagent and catalyst in enzyme reactions. *ChemBioChem* **11**, 604.

McLaughlin, L. W.; Piel, N. and Hellmann, T. (1985) Preparation of protected ribonucleosides suitable for chemical oligoribonucleotide synthesis. *Synthesis-Stuttgart*, 322.

Miller, C. E. (1965) Hydrogenation with diimide. *J. Chem. Educ.* **42**, 254.

Mills, J. S. and Werner, A. E. A. (1955) The chemistry of dammar resin. *J. Chem. Soc.*, 3132.

Moreau, R. A.; Powell, M. J.; Fett, W. F. and Whitaker, B. D. (1997) The effect of ethanol and oxygen on the growth of *Zymomonas mobilis* and the levels of hopanoids and other membrane lipids. *Curr. Microbiol.* **35**, 124.

Moreau, R. A.; Powell, M. J.; Osman, S. F.; Whitaker, B. D.; Fett, W. F.; Roth, L. and O'Brien, D. J. (1995) Analysis of intact hopanoids and other lipids from the bacterium *Zymomonas mobilis* by high-performance liquid chromatography. *Anal. Biochem.* **224**, 293.

Morzycki, J. W. (2011) Application of olefin metathesis in the synthesis of steroids. *Steroids* **76**, 949.

Mulliez, E.; Padovani, D.; Atta, M.; Alcouffe, C. and Fontecave, M. (2001) Activation of class III ribonucleotide reductase by flavodoxin: A protein radical-driven electron transfer to the iron – sulfur center. *Biochemistry* **40**, 3730.

Nalin, R.; Putra, S. R.; Domenach, A. M.; Rohmer, M.; Gourbiere, F. and Berry, A. M. (2000) High hopanoid/total lipids ratio in *Frankia* mycelia is not related to the nitrogen status. *Microbiology* **146** (**Pt 11**), 3013.

Neunlist, S.; Bisseret, P. and Rohmer, M. (1988) The hopanoids of the purple non-sulfur bacteria *Rhodopseudomonas palustris* and *Rhodopseudomonas acidophila* and the absolute configuration of bacteriohopanetetrol. *Eur. J. Biochem.* **171**, 245.

Neunlist, S.; Holst, O. and Rohmer, M. (1985) Prokaryotic triterpenoids – the hopanoids of the purple non-sulfur bacterium *Rhodomicrobium vannielii* – an aminotriol and its aminoacyl derivatives, *N*-tryptophanyl and *N*-ornithinyl aminotriol. *Eur. J. Biochem.* **147**, 561.

Neunlist, S. and Rohmer, M. (1985a) The hopanoids of *Methylosinus trichosporium* – aminobacteriohopanetriol and aminobacteriohopanetetrol. *J. Gen. Microbiol.* **131**, 1363.

Neunlist, S. and Rohmer, M. (1985b) A novel hopanoid, 30-(5'-adenosyl)hopane, from the purple non-sulfur bacterium *Rhodopseudomonas acidophila*, with possible DNA interactions. *Biochem. J.* **228**, 769.

Neunlist, S. and Rohmer, M. (1985c) Novel hopanoids from the methylotrophic bacteria *Methylococcus capsulatus* and *Methylomonas methanica* ─ (22*S*)-35-aminobacteriohopane-30,31,32,33,34-pentol and (22*S*)-35-amino-3-β-methylbacteriohopane-30,31,32,33,34-pentol. *Biochem. J.* **231**, 635.

Neunlist, S. and Rohmer, M. (1988) A convenient route to an acetylenic C$_{35}$ hopanoid and the absolute configuration of the side-chain of aminobacteriohopanetriol. *J. Chem. Soc., Chem. Commun.*, 830.

Ochs, D.; Kaletta, C.; Entian, K. D.; Beck-Sickinger, A. and Poralla, K. (1992) Cloning, expression, and sequencing of squalene-hopene cyclase, a key enzyme in triterpenoid metabolism. *J. Bacteriol.* **174**, 298.

Ochs, D.; Tappe, C. H.; Gartner, P.; Kellner, R. and Poralla, K. (1990) Properties of purified squalene-hopene cyclase from *Bacillus acidocaldarius*. *Eur. J. Biochem.* **194**, 75

Osborn, J. A.; Jardine, F. H.; Young, J. F. and Wilkinson, G. (1966) The preparation and properties of tris(triphenylphosphine)halogenorhodium(I) and some reactions their including catalytic homogeneous hydrogenation of olefins and acetylenes and their derivatives. *J. Chem. Soc. A*, 1711.

Ourisson, G. and Albrecht, P. (1992) Hopanoids.1. Geohapanoids – the most abundant natural products on earth. *Acc. Chem. Res.* **25**, 398.

Ourisson, G.; Albrecht, P. and Rohmer, M. (1979) Hopanoids – palaeochemistry and biochemistry of a group of natural products. *Pure Appl.Chem.* **51**, 709.

Ourisson, G.; Rohmer, M. and Poralla, K. (1987) Prokaryotic hopanoids and other polyterpenoid sterol surrogates. *Annu. Rev. Microbiol.* **41**, 301.

Pan, W. (2005) Development of a general method for the synthesis of natural and labelled biohopanoids as tools for biosynthetic investigations. Université de Paris VI, Paris, France.

Pan, W. D.; Sung, C.; Zhang, Y. M.; Liang, G. Y.; Sinaÿ, P. and Vincent, S. P. (2007) Complex biohopanoids synthesis: Efficient anchoring of ribosyl subunits onto a C$_{30}$ hopane. *Chem. Eur. J.* **13**, 1471.

Pearson, A.; Flood Page, S. R.; Jorgenson, T. L.; Fischer, W. W. and Higgins, M. B. (2007) Novel hopanoid cyclases from the environment. *Environ. Microbiol.* **9**, 2175.

Pearson, A.; Leavitt, W. D.; Saenz, J. P.; Summons, R. E.; Tam, M. C. and Close, H. G. (2009) Diversity of hopanoids and squalene-hopene cyclases across a tropical land-sea gradient. *Environ. Microbiol.* **11**, 1208.

Pearson, A. and Rusch, D. B. (2009) Distribution of microbial terpenoid lipid cyclases in the global ocean metagenome. *ISME J.* **3**, 352.

Peiseler, B. and Rohmer, M. (1992) Prokaryotic triterpenoids of the hopane series – bacteriohopanetetrols of new side-chain configuration from *Acetobacter* species. *J. Chem. Res. (S).*, 298.

Perzl, M.; Reipen, I. G.; Schmitz, S.; Poralla, K.; Sahm, H.; Sprenger, G. A. and Kannenberg, E. L. (1998) Cloning of conserved genes from *Zymomonas mobilis* and *Bradyrhizobium japonicum* that function in the biosynthesis of hopanoid lipids. *Biochim. Biophys. Acta, Lipids Lipid Metab.* **1393**, 108.

Poralla, K.; Hartner, T. and Kannenberg, E. (1984) Effect of temperature and pH on the hopanoid content of *Bacillus acidocaldarius*. *FEMS Microbiol. Lett.* **23**, 253.

Poralla, K.; Muth, G. and Hartner, T. (2000) Hopanoids are formed during transition from substrate to aerial hyphae in *Streptomyces coelicolor* A3(2). *FEMS Microbiol. Lett.* **189**, 93.

Rappe, M. S. and Giovannoni, S. J. (2003) The uncultured microbial majority. *Annu. Rev. Microbiol.* **57**, 369.

Prunet, J. (2005) Application of olefin cross metathesis to the synthesis of biologically active natural products. *Curr. Top. Med. Chem.* **5**, 1559.

Ranganathan, R. S.; Jones, G. H. and Moffatt, J. G. (1974) Novel analogs of nucleoside 3',5'-cyclic phosphates. I. 5'-mono- and dimethyl analogs of adenosine 3',5'-cyclic phosphate. *J. Org. Chem.* **39**, 290.

Rashby, S. E.; Sessions, A. L.; Summons, R. E. and Newman, D. K. (2007) Biosynthesis of 2-methylbacteriohopanepolyols by an anoxygenic phototroph. *Proc. Natl. Acad. Sci. USA* **104**, 15099.

Rattray, J. E.; van de Vossenberg, J.; Hopmans, E. C.; Kartal, B.; van Niftrik, L.; Rijpstra, W. I. C.; Strous, M.; Jetten, M. S. M.; Schouten, S. and Sinninghe Damsté, J. S. (2008) Ladderane lipid distribution in four genera of anammox bacteria. *Arch. Microbiol.* **190**, 51.

Reipen, I. G.; Poralla, K.; Sahm, H. and Sprenger, G. A. (1995) *Zymomonas mobilis* squalene-hopene cyclase gene (*shc*): Cloning, DNA sequence analysis, and expression in *Escherichia coli. Microbiology* **141 (Pt 1)**, 155.

Renoux, J. M. and Rohmer, M. (1985) Prokaryotic triterpenoids – new bacteriohopanetetrol cyclitol ethers from the methylotrophic bacterium *Methylobacterium organophilum*. *Eur. J. Biochem.* **151**, 405.

Rohmer, M. (1993) The biosynthesis of triterpenoids of the hopane series in the eubacteria – a mine of new enzyme reactions. *Pure Appl. Chem.* **65**, 1293.

Rohmer, M. (1999) The discovery of a mevalonate-independent pathway for isoprenoid biosynthesis in bacteria, algae and higher plants. *Nat. Prod. Rep.* **16**, 565.

Rohmer, M. (2007) Diversity in isoprene unit biosynthesis: The methylerythritol phosphate

pathway in bacteria and plastids. *Pure Appl. Chem.* **79**, 739.

Rohmer, M. (2008) From molecular fossils of bacterial hopanoids to the formation of isoprene units: Discovery and elucidation of the methylerythritol phosphate pathway. *Lipids* **43**, 1095

Rohmer, M.; Bouvier, P. and Ourisson, G. (1979) Molecular evolution of biomembranes: Structural equivalents and phylogenetic precursors of sterols. *Proc. Natl. Acad. Sci. USA* **76**, 847.

Rohmer, M.; Bouvier-Nave, P. and Ourisson, G. (1984) Distribution of hopanoid triterpenes in prokaryotes. *J. Gen. Microbiol.* **130**, 1137.

Rohmer, M.; Knani, M.; Simonin, P.; Sutter, B. and Sahm, H. (1993) Isoprenoid biosynthesis in bacteria – a novel pathway for the early steps leading to isopentenyl diphosphate. *Biochem. J.* **295**, 517.

Rohmer, M. and Ourisson, G. (1976a) Methylhopanes from *Acetobacter xylinum* and *Acetobacter rancens* – new family of triterpene compounds. *Tetrahedron Lett.*, 3641.

Rohmer, M. and Ourisson, G. (1976b) Structure des bactériohopanetétrols d'*Acetobacter xylinum*. *Tetrahedron Lett.* **17**, 3633.

Rohmer, M. and Ourisson, G. (1986) Unsaturated bacteriohopanepolyols from *Acetobacter aceti* ssp. *xylinum*. *J. Chem. Res., Synop.* **10**, 356.

Rohmer, M.; Seemann, M.; Horbach, S.; BringerMeyer, S. and Sahm, H. (1996) Glyceraldehyde 3-phosphate and pyruvate as precursors of isoprenic units in an alternative non-mevalonate pathway for terpenoid biosynthesis. *J. Am. Chem. Soc.* **118**, 2564.

Rohmer, M.; Sutter, B. and Sahm, H. (1989) Bacterial sterol surrogates – biosynthesis of the side-chain of bacteriohopanetetrol and of a carbocyclic pseudopentose from ^{13}C-labeled glucose in *Zymomonas mobilis*. *J. Chem. Soc., Chem. Commun.*, 1471.

Rosa-Putra, S.; Nalin, R.; Domenach, A. M. and Rohmer, M. (2001) Novel hopanoids from *Frankia* spp. and related soil bacteria – squalene cyclization and significance of geological biomarkers revisited. *Eur. J. Biochem.* **268**, 4300.

Roth, L. H.; Moreau, R. A.; Powell, M. J. and Obrien, D. J. (1995) Semipreparative separation of intact hopanoids from *Zymomonas mobilis*. *Anal. Biochem.* **224**, 302.

Sahm, H.; Rohmer, M.; Bringermeyer, S.; Sprenger, G. A. and Welle, R. (1993) Biochemistry and physiology of hopanoids in bacteria. *Adv. Micr. Physiol.* **35**, 247.

Samojlowicz, C.; Bieniek, M.; Zarecki, A.; Kadyrov, R. and Grela, K. (2008) The doping effect of fluorinated aromatic hydrocarbon solvents on the performance of common olefin metathesis catalysts: Application in the preparation of biologically active compounds. *J. Chem. Soc. Chem. Commun.*, 6282.

Schaeffer, P.; Schmitt, G.; Adam, P. and Rohmer, M. (2008) Acid-catalyzed formation of 32,35-anhydrobacteriohopanetetrol from bacteriohopanetetrol. *Org. Geochem.* **39**, 1479.

Seckler, B. and Poralla, K. (1986) Characterization and partial purification of squalene-hopene cyclase from *Bacillus acidocaldarius*. *Biochim. Biophys. Acta* **881**, 356.

Seemann, M.; Bisseret, P.; Tritz, J. P.; Hooper, A. B. and Rohmer, M. (1999) Novel bacterial triterpenoids of the hopane series from *Nitrosomonas europaea* and their significance for

the formation of the C$_{35}$ bacteriohopane skeleton. *Tetrahedron Lett.* **40**, 1681.

Siedenburg, G. and Jendrossek, D. (2011) Squalene-hopene cyclases. *Appl. Environ. Microbiol.* **77**, 3905.

Siirola, E.; Grischek, B.; Clay, D.; Frank, A.; Grogan, G. and Kroutil, W. (2011) Tolerance of β-diketone hydrolases as representatives of the crotonase superfamily towards organic solvents. *Biotechnol. Bioeng.* **108**, 2815.

Simonin, P.; Jürgens, U. J. and Rohmer, M. (1996) Bacterial triterpenoids of the hopane series from the prochlorophyte *Prochlorothrix hollandica* and their intracellular localization. *Eur. J. Biochem.* **241**, 865.

Simonin, P.; Tindall, B. and Rohmer, M. (1994) Structure elucidation and biosynthesis of 31-methylhopanoids from *Acetobacter europaeus*. Studies on a new series of bacterial triterpenoids. *Eur. J. Biochem.* **225**, 765.

Smith, A. B.; Adams, C. M.; Kozmin, S. A. and Paone, D. V. (2001) Total synthesis of (−)-cylindrocyclophanes a and f exploiting the reversible nature of the olefin cross metathesis reaction. *J. Am. Chem. Soc.* **123**, 5925.

Spears, J. L. G. and Hutchinson, J. S. (1988) Classical dynamics of trans-diimide: Intramolecular vibrational relaxation involving an active torsion. *J. Chem. Phy.* **88**, 240.

Srikrishna, A.; Babu, R. R. and Beeraiah, B. (2010) Enantiospecific synthesis of ABC-ring system of A-nor and abeo 4(3→2) tetra and pentacyclic triterpenes. *Tetrahedron* **66**, 852.

Stampf, P. (1992) Hemisynthèse de triterpénoïdes bactériens en série hopane. Université de Haute Alsace, Mulhouse, France.

Stampf, P.; Herrmann, D.; Bisseret, P. and Rohmer, M. (1991) 2-α-Methylhopanoids – 1st recognition in the bacterium *Methylobacterium organophilum* and obtention via sulfur induced isomerization of 2-β-methylhopanoids – an account for their presence in sediments. *Tetrahedron* **47**, 7081.

Štefanić, Z.; Narczyk, M.; Mikleušević, G.; Wielgus-Kutrowska, B.; Bzowska, A. and Luić, M. (2012) New phosphate binding sites in the crystal structure of *Escherichia coli* purine nucleoside phosphorylase complexed with phosphate and formycin A. *FEBS Lett.* **586**, 967

Summons, R. E.; Jahnke, L. L.; Hope, J. M. and Logan, G. A. (1999) 2-Methylhopanoids as biomarkers for cyanobacterial oxygenic photosynthesis. *Nature* **400**, 554.

Sutter, B. (1991) Biosynthèse isoprénique chez les prokaryotes: Un modèle innovateur *Zymomonas mobilis*. Université de Haut Alsace, Mulhouse, France.

Talbot, H. M. and Farrimond, P. (2007) Bacterial populations recorded in diverse sedimentary biohopanoid distributions. *Org. Geochem.* **38**, 1212.

Talbot, H. M.; Rohmer, M. and Farrimond, P. (2007a) Rapid structural elucidation of composite bacterial hopanoids by atmospheric pressure chemical ionisation liquid chromatography/ion trap mass spectrometry. *Rapid Commun. Mass Spectrom.* **21**, 880.

Talbot, H. M.; Rohmer, M. and Farrimond, P. (2007b) Structural characterisation of unsaturated bacterial hopanoids by atmospheric pressure chemical ionisation liquid chromatography/ion trap mass spectrometry. *Rapid Commun. Mass Spectrom.* **21**, 1613.

Talbot, H. M.; Squier, A. H.; Keely, B. J. and Farrimond, P. (2003a) Atmospheric pressure

chemical ionisation reversed-phase liquid chromatography/ion trap mass spectrometry of intact bacteriohopanepolyols. *Rapid Commun. Mass Spectrom.* **17**, 728.

Talbot, H. M.; Summons, R.; Jahnke, L. and Farrimond, P. (2003b) Characteristic fragmentation of bacteriohopanepolyols during atmospheric pressure chemical ionisation liquid chromatography/ion trap mass spectrometry. *Rapid Commun. Mass Spectrom.* **17**, 2788.

Talbot, H. M.; Summons, R. E.; Jahnke, L. L.; Cockell, C. S.; Rohmer, M. and Farrimond, P. (2008) Cyanobacterial bacteriohopanepolyol signatures from cultures and natural environmental settings. *Org. Geochem.* **39**, 232.

Talbot, H. M.; Watson, D. F.; Murrell, J. C.; Carter, J. F. and Farrimond, P. (2001) Analysis of intact bacteriohopanepolyols from methanotrophic bacteria by reversed-phase high-performance liquid chromatography-atmospheric pressure chemical ionisation mass spectrometry. *J. Chromatogr. A* **921**, 175.

Thiel, V.; Blumenberg, M.; Pape, T.; Seifert, R. and Michaelis, W. (2003) Unexpected occurrence of hopanoids at gas seeps in the black sea. *Org. Geochem.* **34**, 81.

Toulouse, J. (2011) Biosynthèse des isoprénoïdes bactériens: Inhibiteurs potentiels de la désoxyxylulose phosphate synthase et caractérisation des étapes de réduction dans la formation des hopanoïdes. Université de Strasbourg, Strasbourg, France.

Trnka, T. M. and Grubbs, R. H. (2001) The development of L2X2Ru = CHR olefin metathesis catalysts: An organometallic success story. *Acc. Chem. Res.* **34**, 18.

van Winden, J. F.; Talbot, H. M.; Kip, N.; Reichart, G. J.; Pol, A.; McNamara, N. P.; Jetten, M. S. M.; den Camp, H. J. M. O. and Sinninghe Damsté, J. S. (2012) Bacteriohopanepolyol signatures as markers for methanotrophic bacteria in peat moss. *Geochim. Cosmochim. Acta.* **77**, 52.

Vilcheze, C.; Llopiz, P.; Neunlist, S.; Poralla, K. and Rohmer, M. (1994) Prokaryotic triterpenoids: New hopanoids from the nitrogen-fixing bacteria *Azotobacter vinelandii*, *Beijerinckia indica* and *Beijerinckia mobilis*. *Microbiology* **140**, 2749.

Vincent, S. P.; Sinaÿ, P.; Rohmer, M. (2003) Composite hopanoid biosynthesis in *Zymomonas mobilis*: *N*-acetyl-D-glucosamine as precursor for the cyclopentane ring linked to bacteriohopanetetrol. *Chem. Commun.* 782.

Voorhees, V. and Adams, R. (1922) The use of the oxides of platinum for the catalytic reduction of organic compounds. I. *J. Am. Chem. Soc.* **44**, 1397.

Vuilleumier, S.; Chistoserdova, L.; Lee, M.-C.; Bringel, F.; Lajus, A.; Zhou, Y.; Gourion, B.; Barbe, V.; Chang, J.; Cruveiller, S.; Dossat, C.; Gillett, W.; Gruffaz, C.; Haugen, E.; Hourcade, E.; Levy, R.; Mangenot, S.; Muller, E.; Nadalig, T.; Pagni, M.; Penny, C.; Peyraud, R.; Robinson, D. G.; Roche, D.; Rouy, Z.; Saenampechek, C.; Salvignol, G.; Vallenet, D.; Wu, Z.; Marx, C. J.; Vorholt, J. A.; Olson, M. V.; Kaul, R.; Weissenbach, J.; Médigue, C. and Lidstrom, M. E. (2009) *Methylobacterium* genome sequences: A reference blueprint to investigate microbial metabolism of C1 compounds from natural and industrial sources. *PLoS ONE* **4**, e5584.

Walsh, C. (1979) Enzymatic reaction mechanisms. W. H. Freeman, San Francisco, USA

Welander, P. V.; Coleman, M. L.; Sessions, A. L.; Summons, R. E. and Newman, D. K. (2010)

Identification of a methylase required for 2-methylhopanoid production and implications for the interpretation of sedimentary hopanes. *Proc. Natl. Acad. Sci. U.S.A.* **107**, 8537.

Welander, P. V., Doughty, D. M., Wu, C.-H., Mehay, S., Summons, R. E., Newman, D. K. (2012) Identification and characterization of rhodopseudomonas palustris TIE-1 hopanoid biosynthesis mutants. *Geobiology* **10**, 15.

Welander, P. V.; Hunter, R. C.; Zhang, L.; Sessions, A. L.; Summons, R. E. and Newman, D. K. (2009) Hopanoids play a role in membrane integrity and pH homeostasis in *Rhodopseudomonas palustris* TIE-1. *J. Bacteriol.* **191**, 6145.

Welander, P. V. and Summons, R. E. (2012) Discovery, taxonomic distribution, and phenotypic characterization of a gene required for 3-methylhopanoid production. *Proc. Natl Acad. Sci. USA* **109**, 12905.

Wnuk, S. F. and Robins, M. J. (1991) Nucleic acid related compounds. 63. Synthesis of 5'-deoxy-5'-methyleneadenosine and related Wittig-extended nucleosides. *Can. J. Chem.* **69**, 334.

Wnuk, S. F. and Robins, M. J. (1993) Nucleic acid related compounds.78. Stereocontrolled syntheses of 6'(*E* and *Z*)-halovinyl analogs from uridine-derived vinylsulfones via vinyltin intermediates. *Can. J. Chem.* **71**, 192.

Zhan, Z.-Y. J. (2007) US20070043180.

Zhao, N.; Berova, N.; Nakanishi, K.; Rohmer, M.; Mougenot, P. and Jürgens, U. J. (1996) Structures of two bacteriohopanoids with acyclic pentol side chains from the cyanobacterium *Nostoc* PCC 6720. *Tetrahedron* **52**, 2777.

Zundel, M. and Rohmer, M. (1985a) Prokaryotic triterpenoids.1. 3β-Methylhopanoids from *Acetobacter* species and *Methylococcus capsulatus*. *Eur. J. Biochem.* **150**, 23.

Zundel, M. and Rohmer, M. (1985b) Prokaryotic triterpenoids. 3. The biosynthesis of 2β-methylhopanoids and 3β-methylhopanoids of *Methylobacterium organophilum* and *Acetobacter pasteurianus* ssp. *pasteurianus*. *Eur. J. Biochem.* **150**, 35.

Wenjun Liu

Triterpénoïdes bactériens de série hopane en C$_{35}$: biosynthèse de la chaîne latérale

Les bactériohopanepolyols (BHPs) en C$_{35}$ sont les principaux hopanoïdes trouvés chez les bactéries. Ces composés présentent une chaîne latérale polyhydroxylée en C$_5$ liée par une liaison carbone/carbone au groupement isopropyle du squelette hopane. Ils présentent de nombreuses variations structurales au niveau de la chaîne latérale qui apporte des informations taxonomiques et physiologiques. Le bactériohopanetétrol (BHT) et l'aminobactériohopanetriol sont les composés majoritaires. En outre, ces deux BHPs seront les parents de la plupart des BHPs complexes. L'élucidation de la biosynthèse de la chaîne latérale en C$_5$ des hopanoïdes s'est donc très intéressante pour une meilleure compréhension de la distribution phylogénétique et la signification biologique de BHPs.

Au cours de ce travail, le ribosylhopane a été isolé pour la premier fois chez une bactérie. Cette découverte est une preuve solide confirmant le rôle du ribosylhopane comme intermédiaire dans la biosynthèse des hopanoïdes. En outre, deux gènes impliqués dans la formation de la chaîne latérale des BHPs chez *Streptomyces coelicolor* ont été caractérisé. L'adenosylhopane serait converti par une phosphorylase en ribosylhopane; une aminotransférase est nécessaire pour la formation de l'aminobactériohopanetriol du ribosylhopane. De plus, nous avons développé des synthèses consices de l'adénosylhopane et d'un isotopomère bisdeutérié. L'analogue marqué a par la suite été incorporé dans le BHT par un système acellulaire de *Methylobacterium organophilum*, et le suivi du marquage nous a permis de démontrer l'implication de l'adénosylhopane dans la biosynthèse des hopanoïdes en C$_{35}$.

Mots-clés: bactériohopanetétrol, aminobactériohopanetriol, ribosylhopane, adenosylhopane, deutériation, biosynthèse.

C$_{35}$ Bacteriohopanoids represent the majority of hopanoids produced by bacteria. They bear an additional C$_5$ side chain linked by a carbon/carbon bond to the isopropyl group of the hopane skeleton. The C$_5$ side chains present an impressive structural diversity and carry taxonomic and physiological information. The most common C$_{35}$ bacteriohopanoids are bacteriohopanetetrol (BHT) and aminobacteriohopanetriol. Moreover, these two compounds are proposed as the parents of most complex bacteriohopanoids. Therefore, elucidation of the biosynthesis of hopanoid side chains is in great interest for a better understanding of the physiological distribution and biological importance of bacteriohopanoids.

In this work, ribosylhopane was isolated for the first time from a bacterium. This discovery is a solid proof for the role of ribosylhopane as an intermediate in the biosynthesis of hopanoid side chain. In addition, two genes involved in the hopanoid production in *Streptomyces coelicolor* have been characterized. Adnosylhopane may be converted into ribosylhopane by a phosphorylase; and an aminotransferase is required for the formation of aminobacteriohopantriol from ribosylhopane. Moreover, we have developed a concise strategy for the hemisynthesis of adenosylhopane and a deuteriated isotopmer. The subsequent incorporation of the deuteriated adenosylhopane into BHT by a cell-free system in *Methylobacterium organophilum* proved that adenosylhopane is indeed a precursor of C$_{35}$ bacteriohopanoids.

Key words: bacteriohopanetetrol, aminobacteriohopanetriol, ribosylhopane, adenosylhopane, deuteriation, biosynthese.